Pharmacological Targets for Gene Therapy in Lung Inflammation

Submitted by

Hanan Sayed Mohamed Farghaly

A thesis submitted for the degree of Doctor of Philosophy

University of Bath

Department of Pharmacy and Pharmacology

November 2008

Copyright

Attention is drawn to the fact that the copyright of this thesis rests its author. This copy of the thesis has been supplied on the condition that anyone who consults it is understood to recognise that its copyright rests with author and that no quotation from the thesis and no information derived from it may be published without the prior written consent of the author. This thesis may be made available for consultation within the University Library and may be photocopied or lent to other libraries for the purpose of consultation.

Signed: ……

Table of contents

Acknowledgements

I express my sincere thanks to my supervisor Dr. Malcolm L. Watson for his critical guidance and help throughout the course of this study. I also would like to thank my supervisor Dr. Ian S. Blagbrough. My gratitude goes to Kevin Smith, Catherine Hobbs, Adam Webb and Dr. David A. Medina-Tato for their continuous support. Special thanks and love must go to my husband Anwar and my two children Mohamed and Zeinab for their support and understanding to accomplish my PhD. They have been a great motivator for me. Many people have given me their support to finish this work, but special mention must go to my friends Soad Bayoumi and Mohammed El-Awady for problem-solving guidance. I would like to thank Dr. David Tosh and Dr. Pauline Wood for their aids in immunohistochemistry studies. I also would like to thank Dr. Klaus Okkenhaug (Babraham Institute, Cambridge, UK) for permission to use tissue from $p110^{D910A/D910A}$ and matched DO11.10 control mice. Special mention goes to all Egyptian families who helped me to make my time at Bath very special and who encouraged me through these 4-years of my life. Finally, I would also like to thank the Egyptian Government for their financial support.

Publications

Paper

Farghaly HS, Blagbrough IS, Medina-Tato DA, Watson ML (2008). Interleukin-13 Increases Contractility of Murine Tracheal Smooth Muscle by a Phosphoinositide 3-kinase p110δ Dependent Mechanism. Mol Pharmacol, **73:** 1530-1537. Copy of the paper is included in the appendix

Conference Abstracts

Farghaly HS, Blagbrough IS, Watson ML. Airway Epithelium Modulates Interleukin-13 Induced Murine Tracheal Smooth Muscle Hyperresponsiveness (won Bath postgraduate best poster prize). Bath, U.K. 6 June 2007.

Hanan S.M. Farghaly, Ian S. Blagbrough, and Malcolm L. Watson. Phosphoinositide 3-kinase p110δ isoform mediates interleukin 13-induced hyperresponsiveness of murine tracheal smooth muscle. British Pharmacological Society poster presentation (5th James Black Conference, "Cutting Edge Concepts in Lung Pharmacology" Perthshire, Scotland from 9–11 October 2007.

Hanan S.M. Farghaly, Ben Causton, Ian S. Blagbrough and Malcolm L. Watson (2008). The effect of PI3K inhibition on IL-13-induced arginase I expression in mice tracheal segments. Fundamental & Clinical Pharmacology, Suppl. 2 **22:** 14.

Hanan S.M. Farghaly, Ben Causton, Ian S. Blagbrough and Malcolm L. Watson (2008). The effect of PI3K inhibition on IL-13-induced arginase I expression in mice tracheal segments. International Workshop on Methods in Cardiovascular Pharmacology 18–19 July Manchester, U.K (won best poster 1st prize).

Abstract

Interleukin-13 (IL-13) has been implicated as a critical inducer of a number of features of allergy and asthma including the induction of nonspecific airway hyperresponsiveness (AHR), eosinophilic inflammatory response, eotaxin production, excess mucus formation, and fibrosis. Determining the mechanism(s) of AHR, a hallmark of asthma, is crucial to our understanding of both the pathogenesis and successful treatment of asthma. After carrying out initial experiments to determine the effect of IL-13-induced AHR on murine and rat tracheal rings, mice tissues were chosen for subsequent experiments due to their consistent results and the fact that the mouse genetic map was completed in 1996, which will enable subsequent gene therapy work. Human and mouse share a high percentage of their genes with an average of 85 percent homology. Numerous IL-13 signalling studies have concentrated on the JAK/STAT6 pathway. IL-13 also activates phosphoinositide 3-kinase (PI3K) and downstream effector molecules. In experiments presented in this thesis pharmacological and genetic approaches implicate the involvement of PI3K and its individual isoform PI3Kδ in IL-13 induced AHR *in vitro* and this involvement was confirmed using a small interference RNA (siRNA) technology approach. However, IL-13 induced an early activation of PI3K, whereas increased responsiveness was not observed until overnight incubation. Arginase I induction was demonstrated to be another PI3K-dependent potential mechanism of IL-13-induced hyperresponsiveness. The epithelium is also implicated in IL-13-induced hyperresponsiveness, however, the induction of arginase I was demonstrated in both intact and denuded epithelium tracheal rings. The siRNA approach was also employed in 9HTEo-, A549 and BEAS-2B cell lines using different transfecting agents. From these findings, it is concluded that class IA p110δ could be a useful target for the treatment of asthma by preventing IL-13-induced airway smooth muscle hyperresponsiveness and also that arginase I may be involved in IL-13-induced hyperresponsiveness through PI3K- and epithelial-dependent pathways.

List of Figures

List of Tables

Abbreviations

ABH	2(*S*)-Amino-6-boronohexanoic acid
ACh	Acetylcholine
AHR	Airway hyperresponsiveness
ASM	Airway smooth muscle
ATP	Adenosine triphosphate
BAL	Bronchoalveolar lavage
BEC	*S*-(2-Boronoethyl)-L-cysteine-HCl
BSA	Bovine serum albumin
BTK	Bruton's tyrosine kinase
γc	common-gamma chain
CAT	Cationic amino acid transporter
CCh	Carbachol
CCL	Chemokine ligand
CD	Cluster of differentiation
CF	Cystic fibrosis
CFTR	Cystic fibrosis transmembrane conductance regulator
COPD	Chronic obstructive pulmonary disease
DMEM	Dulbecco's modified Eagle's medium
DMSO	Dimethyl sulfoxide
DNA	Deoxyribonucleic acid
dsRNA	double-stranded RNA
EDTA	Ethylenediamine tetraacetic acid
FBS	Foetal bovine serum
FEV1	Forced expiratory volume in 1 second
GM-CSF	Granulocyte-macrophage colony-stimulating factor
GMP	Guanosine monophosphate
GPCR	G-protein-coupled receptor
Grb	Growth factor receptor-bound protein
GTP	Guanosine triphosphate
h-IL-13	Human interleukin-13
ICAM	Inter-cellular adhesion molecule

IFN	Interferon
Ig	Immunoglobulin
IHC	Immunohistochemistry
IL	Interleukin
IL-13R	Interleukin-13 receptor
IL-4R	Interleukin-4 receptor
JAK	Janus kinases
LPS	Lipopolysaccharides
LTB4	Leukotriene B4
MAP	Mitogen-activated protein
MCP	Monocyte chemoattractant protein
MHC	Major histocompatibility complex
m-IL-13	Murine interleukin-13
MLCK	Myosin light chain kinase
MMP	Matrix metalloproteinases
mRNA	Messenger RNA
NF-κB	nuclear factor-kappa B
NO	Nitric oxide
NOHA	N^{ω}-Hydroxy-L-arginine (NOHA)
Nor-NOHA	N^{ω}-Hydroxy-nor-L-arginine
NOS	Nitric oxide synthase
Nt	Nucleotide
OCT	Optimum Cutting Temperature
PBS	Phosphate buffered saline
PCR	Polymerase chain reaction
PDE	Phosphodiesterase
PDGF	Platelet derived growth factor
PDK	3'-phosphoinositide-dependent kinase
PFA	Paraformaldehyde
PG	Prostaglandin
PI3K	Phosphoinositide 3-kinases
PIAS	Protein inhibitor of activated STAT
PLA	Phospholipase A
PtdIns	Phosphatidylinositol

PtdIns(3,4,5)P_3	Phosphatidylinositol 3,4,5-trisphosphate
PtdIns(4)P	Phosphatidylinositol 4-monophosphate
PtdIns(4,5)P_2	Phosphatidylinositol 4,5-bisphosphate
PTEN	Phosphatase and tensin homolog deleted on chromosome 10
RANTES	Regulated upon Activation, normal T-cell expressed and secreted
r-IL-13	Rat interleukin-13
RISC	RNA-induced silencing complex
RNAi	RNA interference
s.e.m.	Standard error of the mean
SDS	Sodium dodecyl sulphate
SHIP	Src homology 2-containing inositol 5-phosphatase
siRNA	small interfering RNA
SOCS	Suppressor of cytokine signalling
STAT	Signal transducer and activator of transcription
TBS	Tris-buffered saline
TGF	Transforming growth factor
Th	T-cell helper
TNF	Tumour necrosis factor
TYK	Tyrosine kinase
VCAM	Vascular cell adhesion molecule
Vps	Vesicular-protein-sorting protein

Chapter One

Introduction

1.1 Inflammatory lung diseases

Lung diseases are a major cause of disability and death around the world. Respiratory diseases cause a huge economic burden. With one in five deaths due to respiratory diseases (Hubbard, 2006), the UK has one of the highest death rates from such diseases. Additionally, as extensively reviewed by Aït-Khaled *et al*. (2001), most developing countries have no standard protocols for assessing and managing chronic non-communicable respiratory diseases such as chronic obstructive pulmonary disease (COPD) and asthma. These diseases affect 15% of the population in Latin America, 34% in the Arab world, 45% in Sub-Saharan Africa and Southeast Asia (Aït-Khaled *et al.*, 2001). Lung inflammation and its associated disease states are challenging due to their multiple signalling pathways and these, together with the structural features of the lung, make targeting and delivery of therapeutics to the lung a continuing problem in medicine.

Asthma, COPD and cystic fibrosis (CF) together account for more than half of lung disease patients (Figure 1.1), totalling half a billion people worldwide. Much interest has been generated in better understanding the role of inflammatory mediators in the development of inflammatory lung diseases. Such diseases clearly have a large impact on health care worldwide, with COPD affecting 24 million Americans and 2 million Britons. The diagnosis of asthma is increasing in frequency. Moreover, economic costs can be billions of dollars (Donnelly & Rogers, 2008). A differential diagnosis between COPD and asthma is important for subsequent treatment options. The Dutch hypothesis (Sluiter *et al.*, 1991; Orie, 2000) postulates that asthma and COPD share common origin, with overlapping obstructive clinical features. Asthma may evolve into COPD with the development of obstruction depending on inflammation, airway hyperresponsiveness and host hereditary factors, but modulated by exogenous factors. The British hypothesis proposes that asthma and COPD are distinct and generated by distinct mechanisms. Much debate between these theories has been discussed, but the similarities between asthma and COPD favour the Dutch hypothesis (Chang & Mosenifar, 2007). Although the airways obstruction in asthma is largely reversible, it was demonstrated that asthmatics can show irreversible airflow obstruction (Ulrik & Backer, 1999). Also, COPD patients with reversible airways obstruction have been documented (Chanez *et al.*, 1997).

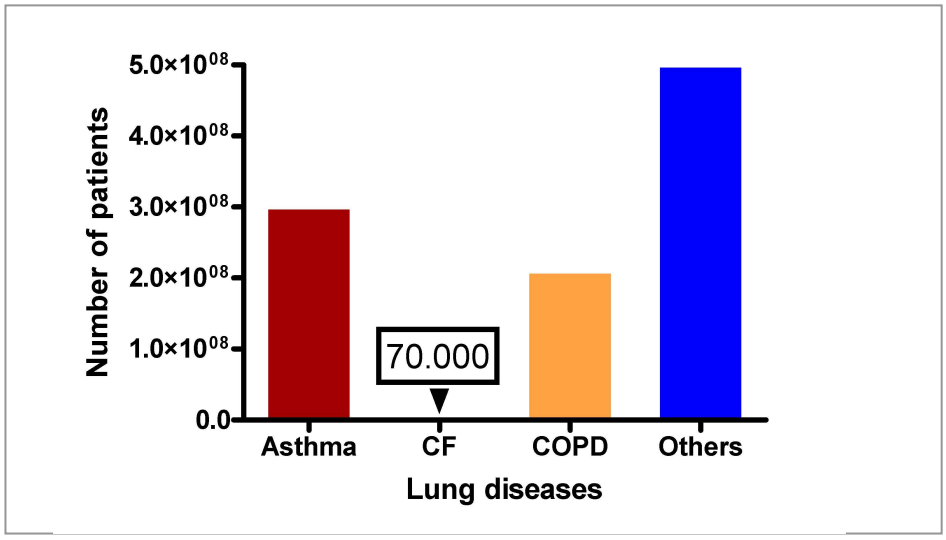

Figure 1.1 Worldwide prevalence of inflammatory and other lung diseases (after Donnelly & Rogers, 2008).

1.1.1 Asthma

Asthma was first recorded in the Ebers Papyrus, one of the most important medical papyri of ancient Egypt of about 1550 BC, which described asthma treatment in the form of inhaled mixture of herbs heated on a brick. Hippocrates, the great Greek physician during 460 - 375 BC was the first to describe asthma spasms and nearly 250 years later Galen, a Greco-Roman doctor attributed the cause of asthma to bronchial obstructions. The name asthma was derived from an ancient Greek meaning gasping or panting to describe the nature of illness (Cohen, 1992). Ancient Chinese used ephedrine thousands of years ago prior to western doctors adopting it as a method of treatment (Chu & Drazen, 2005). Twenty years ago, many parts of the world were experiencing the second peak of asthma deaths of the millennium pointing to needs of alternative treatments for asthma to meet the requirements of all asthmatic patients (Partridge, 2007).

Asthma is defined as a chronic inflammatory disorder of the airways, which causes an associated increase in AHR that leads to recurrent episodes of wheezing, breathlessness, chest tightness, and coughing, particularly at night or in the early morning. These episodes are usually associated with widespread and variable airflow

obstruction that is often reversible either spontaneously or with treatment (Chang & Mosenifar, 2007). The prevalence of asthma in children has dramatically increased in the last decades all over the world (Ronchetti *et al.*, 2001). It is estimated that 300 million people worldwide suffer from asthma, furthermore, there may be an additional 100 million persons with asthma by 2025 (Masoli *et al.*, 2004). According to the World Health Organization, 255,000 died of asthma in 2005 (Bloemen *et al.*, 2007). The exact cause of asthma remains uncertain with several factors influencing the disease, for example genetic factors (e.g. a history of asthma in the family, atopy), environmental factors (e.g. air pollution, occupational exposure, viral infections, allergen exposure) and lifestyle factors (e.g. smoking habits, food) (Bloemen *et al.*, 2007). Asthma can be classified according to its stimuli into allergic and non-allergic asthma (Hurwitz, 1955). Nonallergic asthma is characterized by negative skin tests and no clinical or family history of allergy with normal serum total IgE concentrations. Patients with nonallergic asthma are usually older than their allergic counterparts and have onset of symptoms in later life as reviewed in Humbert *et al.* (1999). Allergic asthma is characterized by:

- Allergen-induced airway obstruction, in which early asthmatic reaction (EAR) develops rapidly and is reversible within 1-2 h. EAR is usually followed by a late phase asthmatic reaction (LAR), which develops after 4-7 h after allergen exposure and can last for up to 24 h after provocation (Booij-Noord *et al.*, 1971).
- The allergic cascade of asthma (Figure 1.2), characterized by infiltration, priming and activation of various inflammatory cells in airway tissues (Holgate & Polosa, 2008).
- Non-specific AHR in asthma might be caused by increased force generation in the smooth muscle itself; due to either increased receptor numbers, increased affinity of ligand-receptor interaction, or modified intracellular contractile signalling pathways (Fernandes *et al.*, 2003).

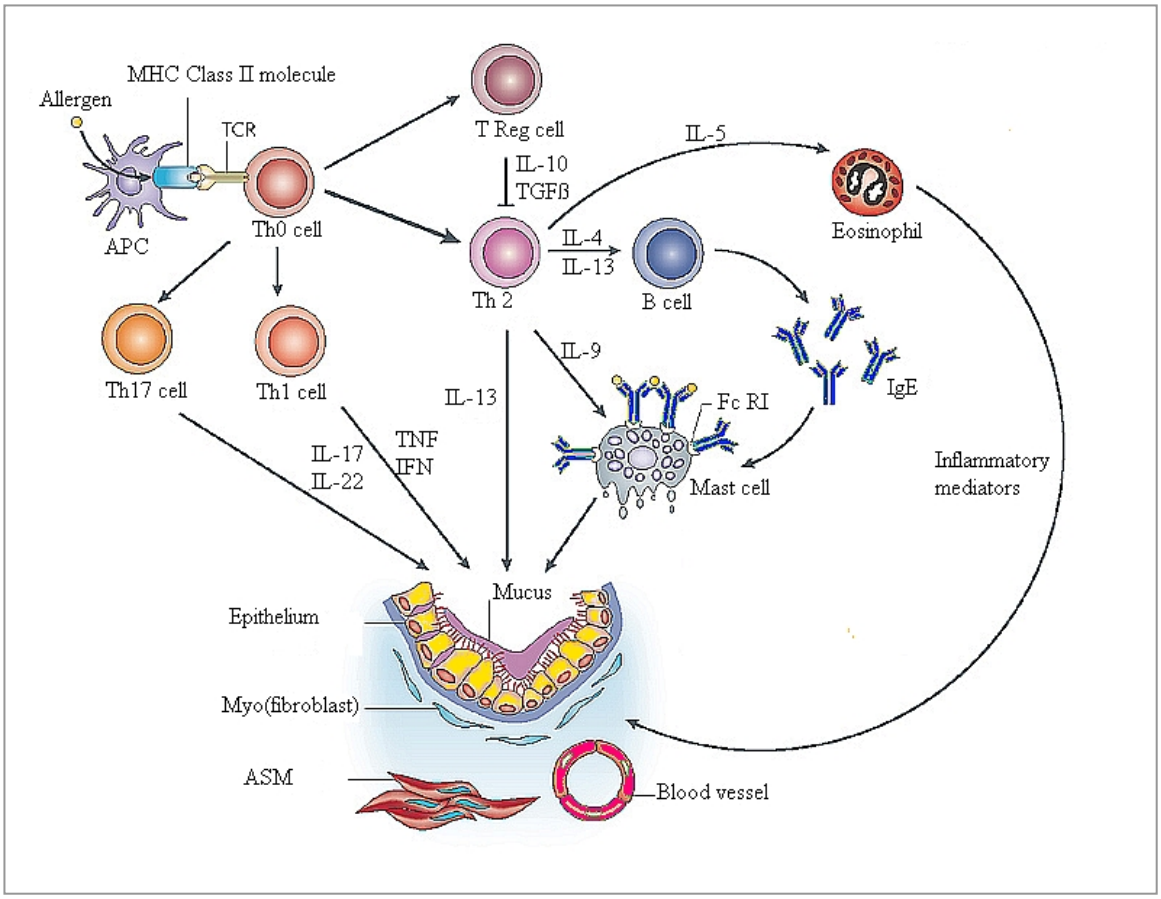

Figure 1.2 Inflammatory and immune cells involved in asthma adapted from Holgate & Polosa (2008).

A challenge of asthma treatment lies in differentiation between asthma cases and COPD and which treatment paradigm to adopt to control asthma symptoms and lung function. Therapy for COPD is directed at relief of symptoms, whereas for asthma the treatment is to reduce inflammation (Stirling & Chung, 2001; Chang & Mosenifar, 2007). Sensitization is fundamental to the development of allergic diseases. Therefore, avoidance of allergens before or after sensitization could be beneficial as primary or secondary prophylaxis (Holgate & Polosa, 2008). Inhaled corticosteroids and β2-adrenoceptor agonists are the mainstay of asthma (Holgate & Polosa, 2008) but there is an increasing finding that many patients with asthma are resistant to conventional bronchodilating and anti-inflammatory therapies. Different terms are used by clinicians to describe complicated cases of asthma such as "chronic severe", "acute severe", "therapy-resistant", "difficult-to-control", "refractory",

"corticosteroid -resistant or -dependent", "near-fatal", and "fatal asthma" (Stirling & Chung, 2001). The need for new asthma treatment is increasing and to identify possible target(s) against which treatment will be directed will be a first step towards asthma management of those cases. Treatment strategies of asthma are summarised in Table 1.1

Table 1.1 Treatments strategies of asthma

Treatment	Comment	Reference(s)
Short-acting β-agonists	First line of treatment	Chang & Mosenifar, 2007; Holgate & Polosa, 2008
Inhaled corticosteroids	Mainstay treatment	Holgate & Polosa, 2008; Barnes, 2008
Immunotherapy e.g. low-dose methotrexate, azathioprine or cyclosporine A	Inconsistent results Common side effect up to anaphylaxis	Holgate & Polosa, 2006
Anti-immunoglobulin E e.g. omalizumab	Used in severe allergic asthma	Babu *et al.*, 2001; Djukanovic *et al.*, 2004; Holgate *et al.*, 2005
Mast cells inhibitors	Nedocromil sodium	Edwards & Howell, 2000
Cytokine-based immunotherapies	Monoclonal antibodies, fusion proteins	Holgate & Polosa, 2008
Leukotriene antagonists e.g. montelukast and zafirlukast	Modest effect	Misson *et al.*, 1999

1.1.2 COPD

COPD is a major global health problem that is expected to be the third most common cause of death in the world by 2020 (Lopez & Murray, 1998). It is characterized by airflow limitation that is not fully reversible. The airflow limitation is usually both progressive and associated with an abnormal inflammatory response of the lungs to noxious particles or gases. Asthma and COPD have differences and similarities (Table 1.2), thus the differentiation between both conditions is essential for subsequent diagnosis and treatment.

Table 1.2 Differential diagnosis between COPD and asthma

	Asthma	COPD	Reference(s)
AHR	Significant	Insignificant	Welte & Groneberg, 2006; Medina-Tato *et al.*, 2006
Airway obstruction	Variable Reversible	Progressive Largely irreversible (about 10 % are reversible)	Barnes, 2008
Location of inflammation	Mainly large airways	Small airways	Chang & Mosenifar, 2007
Inflammatory cells			
Mast cells	Increased	-	Brightling *et al.*, 2002; Barnes, 2008
Eosinophils	Increased	-	Barnes, 2008
Neutrophils	-	Increased	Welte & Groneberg, 2006
Lymphocytes	CD4	CD8	Medina-Tato *et al.*, 2006; Barnes, 2008
Oxidative stress	+	+++	Barnes, 2008
ASM hypertrophy and hyperplasia	Usually found	Not usually increased	Chang & Mosenifar, 2007
Epithelial cells	Friable	Pseudostratification	Barnes, 2008

Table 1.2 Differential diagnosis between COPD and asthma – continued.

Basement membrane	Thickened	-	Barnes, 2008
Fibrosis	Subepithelial	Peribronchiolar	Barnes, 2008
Angiogenesis	Detected	-	Siddiqui *et al.*, 2007
Lung parenchema integrity	-	Destructed	Chang & Mosenifar, 2007
Mediators produced	LTB4, Histamine, IL-4, IL-5, IL-13, Eotaxin, RANTES	LTB4, TNF, IL-8	Barnes, 2000; Elias, 2004
Short-acting β-agonists	First-line of treatment	Needed basis treatment and no advantage to their regular use	Chang & Mosenifar, 2007
Long-acting β-agonists	Uncertain benefit	Used in later stages	Chang & Mosenifar, 2007
Short-acting anticholinergics	Uncertain benefit	Mainstay of treatment	Chang & Mosenifar, 2007
Response to steroid	Present	Variable	Welte & Groneberg, 2006

1.1.3 Cystic fibrosis

CF is an autosomal recessive disease considered to be the most lethal inherited trait among Caucasians affecting the exocrine glands of the lungs, liver, pancreas, and intestines causing progressive multisystem failure. CF is one of the most common life-shortening, childhood-onset inherited diseases. Over 8,000 children, young people and adults in the UK are affected by cystic fibrosis (Harrop, 2007). It is caused by a mutation in a gene called the cystic fibrosis transmembrane conductance regulator (CFTR). The product of this gene is a chloride ion channel important in creating sweat, digestive juices, and mucus (Figure 1.3). The basis of management are proactive treatment of airway infection, and encouragement of good nutrition. Additionally, therapies such as transplantation and gene therapy hold promise therapeutic strategy.

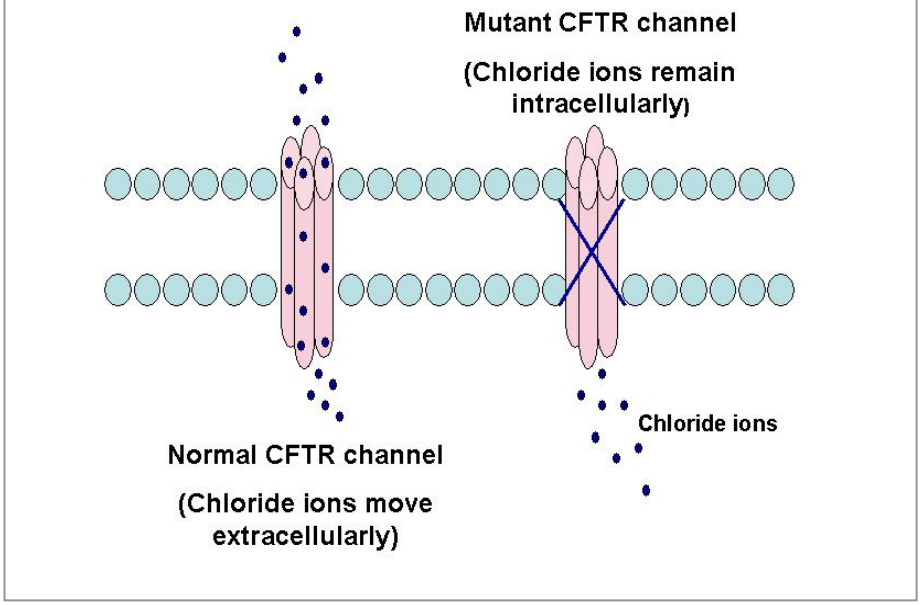

Figure 1.3 Pathogenesis of cystic fibrosis. Cystic fibrosis transmembrane conductance regulator (CFTR) receptor does not operate in CF.

1.2 Cytokine profiles in lung diseases

Professional antigen-presenting cells, including dendritic cells, process exogenous antigens before presentation to T cells. Naive T helper (Th0) cells are activated and differentiate into either Th1 or Th2 cells. Th1 cells are characterised by the production of interferon-γ, and are associated with autoimmune diseases. Th2 cells secrete IL-4, IL-5, IL-9 and IL-13 and are involved in humoral (B cell) responses and IgE production, as well as tissue fibrosis, mastocytosis and eosinophilia. Allergy results from an imbalance in favour of a Th2 response and dysregulation of Th2 responses and is implicated in various atopic diseases (Holgate & Polosa, 2008). In asthma and COPD, cytokines play a critical role in orchestrating and perpetuating inflammation, and several specific cytokine and chemokine inhibitors are in development for treatments of these diseases (Barnes, 2000; Temann *et al.*, 2007). Th2-dominated tissue inflammation is believed to play a central role in asthma pathogenesis. IL-4, IL-5, IL-9, and IL-13 have been extensively reviewed, and increase significantly in the asthmatic airway (Jaffar *et al.*, 1999; Elias, 2004;

Bloemen *et al.*, 2007). The biology of IL-13 and IL-13 receptors is discussed further in section 1.4, in this section its role in allergic diseases is discussed.

The Th2 cytokine IL-4 (Brusselle *et al.*, 1995; Corry *et al.*, 1996) and the closely related cytokine IL-13 (Grunig *et al.*, 1998; Izuhara, 2003; Yang *et al.*, 2004; Yang *et al.*, 2005) have strong associations with allergic disease. IL-4Rα is a unique member of the common-gamma chain (γc) family of receptors (Nelms *et al*., 1999). IL-4 binds IL-4Rα chain with high affinity (K_d 20 to 300 pM) with the ability to signal within IL-4Rα/IL-4Rα, IL-4Rα/γc (Type I) and IL-4Rα/IL-13Rα1 (Type II) receptor complexes (Nelms *et al.*, 1999; Andrews *et al.*, 2006). The type II receptor is a functional receptor for IL-4 as well as IL-13 (Obiri *et al.*, 1995; Hilton *et al.*, 1996) which can explain the overlap of the biological effects between IL-4 and IL-13. Type I receptor complexes can only be formed by IL-4 and are more active in regulating Th2 development. In contrast, the Type II receptor complex formed by either IL-4 or IL-13 is not found on T cells and is more active in regulating cells that mediate airway hypersensitivity and mucus secretion (Andrews *et al.*, 2006).

The role of IL-13 in inflammatory diseases of the lung has been investigated in different disease models including asthma (Grunig *et al.*, 1998; Wills-Karp *et al.*, 1998; Munitz *et al.*, 2008), emphysema (Zheng *et al.*, 2000), anaphylaxis (Fallon *et al.*, 2001) and hyperoxic acute lung injury (Corne *et al.*, 2000). Although IL-4 and IL-13 are capable of inducing an asthma-like phenotype, IL-13 seems to have a superior role during the effector phase of the disease. It is proposed that IL-4 production at the site of inflammation is short lived and that IL-13 may persist or IL-4 is difficult to be measure at the site of inflammation (Kroegel *et al.*, 1996). The biological role of IL-13 in asthma has been intensively studied. Pulmonary expression of IL-13 induces an asthma-like phenotype in mice, including a mononuclear and eosinophilic inflammatory response, mucus cell metaplasia, airway fibrosis, eotaxin production, airways obstruction, and AHR (Zhu *et al.*, 1999). In addition to enhancing polarisation of T-lymphocytes to a Th2 phenotype and promoting B-cell synthesis of IgE (Levy *et al.*, 1997; Hajoui *et al.*, 2004), IL-13 may contribute towards asthma *via* tissue remodelling (Kumar *et al.*, 2002), epithelial activation (Lordan *et al.*, 2002), decreasing β2 adrenoceptor function (Laporte *et al.*, 2001) and enhancing contractility of airway smooth muscle in human and IgG1 in mice.

IFN-γ causes an emphysema like-phenotype. IFN-γ transgenic mice show massive alveolar destruction and pulmonary emphysema associated with neutrophil-rich tissue inflammatory response. Neutrophils, lymphocytes and macrophages (but not eosinophils) are increased in BAL fluid compared with transgene-negative controls. Mucous metaplasia is not a prominent finding in these animals and tissue fibrosis is not detected (Wang *et al.*, 2000). In contrast, the same group demonstrates that IL-13-induced emphysema is associated with eosinophilia, mucus hyperproduction, pulmonary fibrosis and mucous metaplasia with little parenchymal fibrosis and is due to protease-mediated epithelial apoptosis, stimulated matrix metalloproteinases (MMPs), cathepsins, and α1-antitrypsin inhibition (Zheng *et al.*, 2000). They suggested that their finding can explain the British/Dutch hypothesis on the basis that the Th1/TC1 pathway (increases in MMPs and cathepsins, decreases in secretory leukocyte proteinase inhibitor apoptosis-dependent, and apoptosis-independent-alveolar destruction) predominates in patients with definite COPD symptoms (British hypothesis) and that the Th2/TC2 pathway (increases in MMPs and cathepsins, decreases in α1-antitrypsin and increases in adenosine and genetic factors) dominates in patients with features of asthma and emphysema (Dutch hypothesis).

IL-13 plays a key role in asthma pathogenesis. Both *in vivo* and *in vitro* studies demonstrate IL-13 induces IgE production (Grunig *et al.*, 1998; Kuperman *et al.*, 2002; Wills-Karp, 2004; Zheng *et al.*, 2008), mucus production and mucous cell metaplasia (Grunig *et al.*, 1998; Kuperman *et al.*, 2002; Wills-Karp, 2004; Zheng *et al.*, 2008), generation of extracellular matrix proteins (Lanone *et al.*, 2002; Zheng *et al.*, 2008), airway eosinophilia and eotaxin production (Zhu *et al.*, 1999; Kumar *et al.*, 2002; Wills-Karp, 2004), airway fibrosis (Grunig *et al.*, 1998; Kuperman *et al.*, 2002; Wills-Karp, 2004; Zheng *et al.*, 2008), as well as AHR and enhanced contractility of airway smooth muscle cells (Grunig *et al.*, 1998; Kuperman *et al.*, 2002; Foster *et al.*, 2003; Wills-Karp, 2004; Zheng *et al.*, 2008).

IL-12 can suppress IgE production. Th1 cells transferred into IL-12 knockout mice do not inhibit IgE production, but can be inhibited by transfer of bone marrow-derived dendritic cell precursors from IL-12 competent mice as well as transfer of IL-18-competent wild-type bone marrow-derived dendritic cells indicating that both

IL-12 and IL-18 are needed for Th1 mediated immunity (Thomas *et al.*, 2002; Salagianni *et al.*, 2007). These findings are associated with negligible amounts of IFN-γ. In OVA-sensitized BALB/c mice an association of IL-12 with enhanced IL-4, IL-5, and IL-13 production in BAL fluid was demonstrated. When anti-IL-12p35 or anti-IL-12p40 mAb administered to these mice it was demonstrated decreased level of those cytokines with lack of methacholine-induced bronchial hyperresponsiveness and eosinophilia (Meyts *et al.*, 2006). In contrast intranasal mice administration of Lactococcus lactis as a source of IL-12 is associated with elevated IFN-γ and decreased IL-4 (Wu *et al.*, 2006).

The role of IL-5 in eosinophil expansion and priming has been established in many studies. Recently, it was observed that small interfering RNA against IL-5 decreases airway eosinophilia and eotaxin levels in BAL fluid, IL-5 mRNA levels in lungs and hyperresponsiveness to methacholine, but not OVA-specific IgE level in a mouse model of asthma (Huang *et al.*, 2008). In a study using atopic asthmatic patients exposed to humanized anti–IL-5 monoclonal antibody (mepolizumab), it was demonstrated mepolizumab decreased eosinophilia, the expression of tenascin, lumican and procollagen III in the bronchial mucosal biopsy compared with placebo suggesting the mechanism of IL-5 in asthma tissue remodelling is through the deposition of extracellular matrix proteins (Flood-Page *et al.*, 2003). The role of IL-5 in tissue remodelling, and eosinophils as a source of TGF-β, was confirmed in a study conducted using IL-5–deficient mice (Cho *et al.*, 2004). Clinical trials using two humanized monoclonal anti-IL-5 antibodies (mepolizumab and SCH55700) demonstrated that although both sputum and blood eosinophils were reduced to very low levels after intravenous administration of mepolizumab to asthmatic patients, modulation of the late asthmatic reaction or airway hyperresponsiveness to histamine was not detected (Leckie *et al.,* 2000). Similarly SCH55700, adminstered intravenously to difficult-to-treat asthma patients (who were already on inhaled or oral corticosteroid), reduced blood eosinophils but improved FEV1 only with the use of higher dose (Kips *et al.,* 2003). In a recent study to evaluate the efficacy of mepolizumab conducted in more than 300 moderate to severe asthmatic patients a pronounced reduction in blood eosinophils was observed. However, mepolizumab had no significant effect on FEV1 with a nonsignificant 50 % decrease in exacerbation rates which did not add clinical benefit to the patients (Flood-Page *et al.,*

2007). IL-5 and eotaxin-deficient mice do not have tissue eosinophilia or methacholine induced-AHR, which is associated with impaired IL-13 level, corrected by eosinophil transfer to those mice, which suggests that, both IL-5 and eotaxin modulate IL-13 production (Mattes *et al.*, 2002). Targeted deletion of IL-13 prevents expression of AHR in allergen-challenged mice, despite maintenance of elevated IL-4 and IL-5 release (Walter *et al.*, 2001). Likewise, neutralization of IL-13 using IL-13 receptor constructs or antibodies reduces AHR without influencing IL-5 levels (Eum *et al.*, 2005). IL-13-induced hyperresponsiveness can be inhibited by anti-IL-5 antibody in the rabbit trachea (Grunstein *et al.*, 2002). However, overexpression of IL-13 in the mouse lung does not result in IL-5 (or IL-4) up-regulation (Zhu *et al.*, 1999), IL-13-induced *in vivo* AHR is maintained in IL-5 knock-out mice (Yang *et al.*, 2001), and antigen-induced AHR is inhibited by anti-IL-13 but not anti-IL-5 treatment (Grunig *et al.*, 1998).

1.3 Airway hyperresponsiveness

In 1921 Alexander and Paddock observed enhanced bronchoconstriction in asthmatic patients compared to non-asthmatic patients after exposure to pilocarpine. These findings were confirmed by findings that asthmatic subjects develop increased bronchoconstriction and carbon dioxide tension in response to histamine compared to healthy volunteers (reviewed in O'Byrne & Inman, 2003). AHR involves two phenomena, a shift of the constrictor dose-response curves to the left (airway hypersensitivity) and increased slope of the curves with greater maximum degree of induced-constriction (airway hyperreactivity) (Woolcock *et al.*, 1984; Sterk & Bel, 1989). Airway sensitivity can be a result of epithelial damage and malfunction, neural control, and changed inflammatory cell number or activity, while determinants of airway reactivity include ASM contractility, the elastic load on ASM shortening, swelling of the airway wall, and intralumenal exudate and secretions (Niimi *et al.*, 2003).

1.3.1 Indices of airway hyperresponsiveness

AHR can be classified into variable (inducible or episodic) AHR and persistent AHR. The variable AHR may reflect airway inflammation, thus

representing acute aspect of the disease while the baseline persistent AHR likely relates to structural airway changes referred to as airway remodelling and probably reflects chronicity of disease (Cockcroft & Davis, 2006). Direct and indirect stimuli are used to measure airway responsiveness. The direct stimuli act directly on receptors on airway smooth muscle e.g. histamine and methacholine, while the indirect stimuli act through intermediate pathway(s), most commonly acting via release of mediators from inflammatory cells e.g. exercise, cold air and mannitol (Van Schoor *et al.*, 2005).

1.3.2 Mechanisms of airway hyperresponsiveness

The mechanism of airway hyperresponsiveness in asthma remains unclear. Many studies have been performed to determine the correlation of inflammatory cells in BAL fluid with AHR. Although some of these studies detected the correlation it is weak and most often when bronchoconstriction or response to direct stimuli is measured (Boulet *et al.*, 1993; Oddera *et al.*, 1998). Still, both inflammatory mediators and resident airway cells could be involved in the mechanisms of AHR. It is suggested that acute exposure to the inflammatory mediators results in increased ASM responsiveness *in vitro* due to:

- Enhancing contractile agonist-stimulated increases in inositol 1,4,5-trisphosphate and augmentation of peak and sustained intracellular calcium levels (Martin *et al.*, 2000).
- Blunting ASM relaxation, normally induced by β_2-adrenoceptor stimulation, through β_2-adrenoceptor phosphorylation, Gs protein dysfunction, increased prostanoid and peptide leukotriene release.
- Increasing the activity and/or content of smooth muscle MLCK (Jiang *et al.*, 1995; Ammit *et al.*, 2000).

However, growing evidence indicates the crucial role of different resident cells to mediate AHR (Kuperman *et al.*, 2002; Tliba *et al.*, 2003; Syed *et al.*, 2005). Airway epithelium is composed of a heterogenous population of cells, which act more than just a physical barrier, but also possesses a number of diverse functions (Spina & Page, 1992). The integrity of airway epithelium has an important role in defence mechanisms both physically and functionally. In a trial to restore damaged airway

epithelium, asthmatic patients demonstrated elevated epidermal growth factor receptor expression (Puddicombe *et al.*, 2003). For example, AHR was not demonstrated in IL-13-defecient mice exposed to OVA stimulation despite the presence of eosinophilic pulmonary inflammation (Walter *et al.*, 2001). Alternatively, IL-13 may induce AHR via direct effects on airway epithelial cells. Epithelial cells that are devoid of STAT6 are not affected by IL-13-induced AHR, and have reduced mucus production (Kuperman *et al.*, 2002).

ASM releases several inflammatory mediators under various conditions of stimulation indicating the likelihood that they may contribute to chronic inflammatory processes in the airway (Table 1.3). ASM can exhibit various states: a synthetic phase, a proliferative phase as well as a contractile phase. The contractile phenotype of ASM cells under culture is well recognized in enzyme-dissociated cells seeded in primary culture within 24-48 h, with intense immunostaining for muscle specific contractile proteins and with visible contraction to constrictor agonists (reviewed in Hirst, 1996). Serum can affect the phenotype acquired during culture (Chamley-Campbell *et al.*, 1979). Serum deprivation for 10 days in canine isolated tracheal smooth muscle cells allows the acquisition of a subpopulation of myocytes with a morphological and functional contractile phenotype (Halayko *et al.*, 1999). In the presence of proliferating stimuli, such as foetal calf serum, contractile airway smooth muscle changes into a "synthetic" phenotype, characterized by increased mitogenic activity; expression of intracellular organelles associated with synthesis; and a decrease in immunostaining for smooth muscle specific contractile proteins. It was shown in proliferating tracheal smooth muscle cells that the levels of smooth muscle myosin heavy chain are markedly reduced with a reduction in mRNA for this protein and α-actin, (Halayko *et al.*, 1996). The synthetic cells produce extracellular matrix components and also autocrine growth-promoting factors, and these could in turn influence the contractile or synthetic phenotype (Chung, 2000).

ASM is considered a crucial component of AHR (Figure 1.4). As reviewed in Parameswaran *et al.* (2002) increased intracellular calcium is responsible for AHR but it is also documented in studies conducted in asthmatic patients that voltage-dependent calcium channel-blocking drugs do not attenuate AHR, implicating inflammatory process for the studied AHR. The demonstrated hypertrophy and /or

hyperplasia or increased muscle-shortening velocity in asthmatic subjects can explain hyperreactivity but not hypersensitivity. TNFα and IL-13 significantly increased cultured murine tracheal ring contractile responses to carbachol and KCl without affecting changes in receptor affinity, suggesting modulation of ASM responsiveness at a site downstream from receptor activation (Chen *et al.*, 2003; Tliba *et al.*, 2003). Epithelium-denuded rabbit tracheal segments sensitized passively with IgE show enhanced response to ACh and isoproterenol, which is inhibited by the presence of anti-IL-4Rα antibodies. Furthermore, IgE-sensitized cultured human ASM cells exhibit IL-13 mRNA and protein upregulation, whereas IL-4 expression is not detected (Grunstein *et al.*, 2002). Also, human ASM cells show increased CD38 expression associated with enhanced intracellular calcium responses to bradykinin, thrombin, and histamine compared with controls (Deshpande *et al.*, 2004).

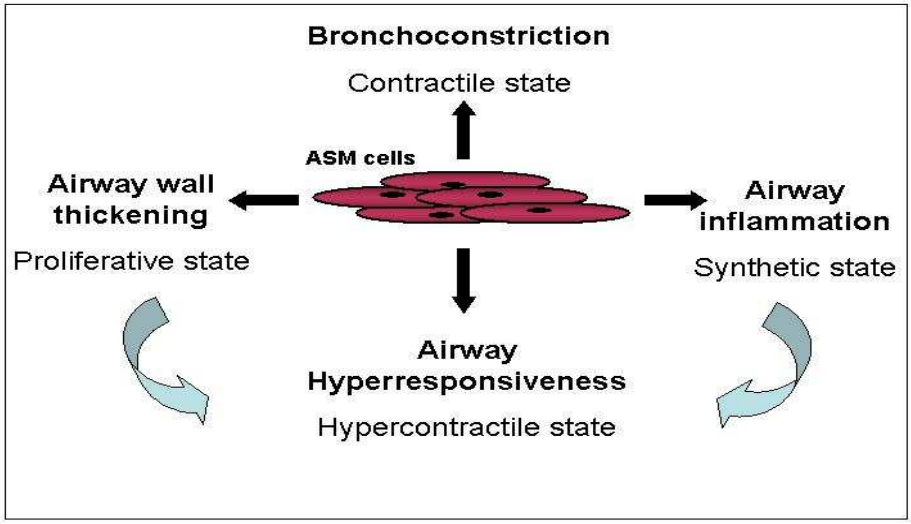

Figure 1.4 Proposed model for the pathological roles of ASM in asthma. Increase ASM number (hyperplasia) and size (hypertrophy) cause elevated muscle mass. This leads to AHR, bronchoconstriction, airway wall thickening (remodelling), and production of several inflammatory mediators (Amrani & Panettieri, 2003).

Table 1.3 Cytokines, mediators enzymes and receptors produced by airway smooth muscle cells in culture (Chung, 2000)

Cytokines/ chemokines	Growth factors	Receptors/ surface molecules	Lipid mediators/ enzymes
MCP-1, 2 & 3	PDGF-BB	IL-2R	PGE_2
RANTES	MMP-1	IL-12R	s-PLA_2
Eotaxin	Stem cell factor	IFNγR	NOS
IL-8		ICAM-1	
GM-CSF		VCAM-1	
IL-6		CD44	
IL-11		CD40	
IL-5		MHC Class 2	
IFNγ			
IL-2			
IL-12			

Fibroblasts also contribute to AHR. Anatomically, they are a hetreogenous group of differentiated cells of mesenchymal origin. They provide both cellular and extracellular stroma for epithelial cell layers (Quan *et al.*, 2004). A main function of fibroblasts is the production and homeostatic maintenance of the extracellular matrix components including collagens, proteoglycans, tenascin, laminin and fibronectin (McAnulty, 2007). Each cell can synthesise approximately 3.5 million procollagen molecules/cell/day (McAnulty *et al.*, 1991). A potential role of fibroblasts is related to wound repair and inflammatory fibrosis (Bucala *et al.*, 1994).

Fibroblasts may convert into elongated cells termed myofibroblasts containing intracellular filaments, irregularly shaped nuclei and filaments. Exposure to IL-4 or IL-13 (100 ng/ml) increases α-smooth muscle actin protein expression indicating that these cytokines are capable of inducing the phenotypic change to myofibroblasts (Hashimoto *et al.*, 2001).

Goblet cells, which are glandular simple columnar epithelial cells situated in the conducting airways and whose function is to secrete mucus, play a pivotal role in protecting the airway surface from inhaled particles which become trapped in the mucus before cleared by the mucociliary mechanism (Rogers, 2004). Goblet cell hyperplasia is a characteristic feature in bronchial asthma and chronic bronchitis causing airway narrowing by changing epithelial barrier function (Kamachi *et al.*, 2001). IL-13 induces mucus production, possibly through induction of soluble TGF-α from lung epithelium (Yoshisue & Hasegawa, 2004). Human airways are innervated by populations of afferent nerves, stimulation of which result in reflex cough and bronchoconstriction. The bronchial hyperresponsiveness seen in asthma might be also explained on the basis of an increase in afferent activity due to the effect of different inflammatory mediators, including prostaglandins, neuropeptides, cytokines and growth factors lead to activation of inflammatory cells and airway wall remodelling (Spina *et al.*, 1998).

1.4 Interleukin-13

1.4.1 IL-13 production

Murine IL-13, previously known as P600, was identified *in vitro* using activated mouse lymphocytes (Cherwinski *et al.*, 1987). Human IL-13 is secreted mainly by Th2 $CD4^+$ T cells was then cloned and shown to be a pleiotropic cytokine produced by a variety of cell types (McKenzie *et al.*, 1993b). In addition to T-cells, IL-13 is also produced by numerous non-T-cell populations that are of particular importance to the allergic response such as mast cells, basophils, and eosinophils. Natural killer T cells may be an important source of IL-13 early in the allergic response (Akbari *et al.*, 2003). In addition IL-13 has been shown to be released from structural cells such as ASM (Grunstein *et al.*, 2002). A number of cytokines and mediators have been implicated in the regulation of IL-13 production including IL-5, IL-9, IL-25, histamine, adenosine, and endothelin-1 (Fort *et al.*, 2001; Wills-Karp, 2004; Temann *et al.*, 2007).

1.4.2 IL-13 protein structure

The IL-13 gene is located on human chromosome 5q31 or mouse chromosome 11 in the cluster of genes encoding IL-3, IL-4, IL-5, IL-9, and granulocyte-macrophage colony-stimulating factor (GM-CSF). The IL-13 gene is located between the GM-CSF and the IL-4 gene, with the IL-13 gene in close vicinity of the IL-4 gene, being 12 kb upsteam difference. Although the IL-13 protein has only about 25% homology with IL-4 (Minty *et al.*, 1993), it shares many structural characteristics and functional properties with IL-4 due to a shared chain in their individual multimeric receptor complexes (Zurawski *et al.*, 1993) or due to the homology in the first and last α-helical regions of IL-4 and IL-13 (Minty *et al.*, 1993). Both mouse and human IL-13 genes are formed by 4 exon : 3 introns (Table 1.4) with intron size 1055, 251, and 345 in the human IL-13 gene and 1258, 576, and 311 in the mouse IL-13 gene (McKenzie *et al.*, 1993b). Transcriptional regulatory sequence motifs in the human and mouse IL-13 genes studies show that a TATA box which is a DNA sequence found in the promoter region of most genes and to which transcription factors or histones bind is located at positions 697-701 and 786-790 of

h- and m-IL-13 genes respectively. The polyadenylation sequence of h-IL-13 gene is found between positions 4055-4060 and between positions 3633-3638 in m-IL13 gene. Sequence homology between h-IL-13 and m-IL-13 cDNA is 66% and after the translation stop codon they have 70% homology. Also both genes show a relatively high degree of nucleotide identity in their 5'-flanking regions (McKenzie *et al.*, 1993b).

IL-13 is secreted mainly as unglycosylated protein of approximately 12 kDa. The mature protein contains 3 (mouse) or 4 (human) potential *N* –glycosylation sites so that minor glycosylation of the protein that results in higher molecular weight can occur (McKenzie *et al.*, 1993a). The cDNA for human IL-13 was cloned approximately 15 years ago by 3 groups (Morgan *et al.*, 1992; Minty *et al.*, 1993; McKenzie *et al.*, 1993a). The nucleotide sequence of IL-13 encodes a protein of 131 (murine) and 132 (human) amino acids (Table 1.4) each containing a putative 20 amino acid signal peptide sequence with approximately 58% sequence homology at the amino acid level (Minty *et al.*, 1993; McKenzie *et al.*, 1993b). Human IL-13 acts on mouse and rat cells but with low affinity for mouse receptors (Cash *et al.*, 1994), while mouse and human IL-13 are equally active on human cells (McKenzie *et al.*, 1993a). A comparison between m- and h-IL-13 is shown in Figure 1.5 & Table 1.4.

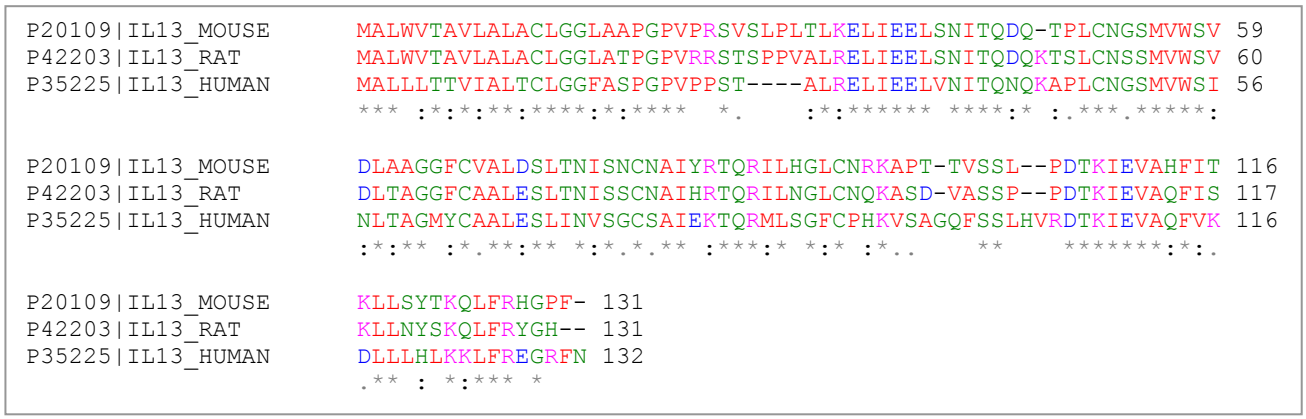

Figure 1.5 Multiple alignment of mouse, rat and human IL-13. * indicates identical sequences between the three species, **:** conserved substitution, **.** semi-conserved substitutions

Table 1.4 Human and murine IL-13 physicochemical properties (Minty, 1997)

	Human	Mouse
Amino acids		
Precursor	132 (146)[a]	131
Signal sequence	20 (34)[a]	18[b]
Mature	112[c]	111[b]
Potential N-glycosylation sites	4	3
Disulfide bonds	28-56 44-70	

[a]Two methionine initiation codons, the most probable initiation codon would give 132 amino acids and a signal peptide of 20 amino acids.

[b]prediction based on homology with human protein without experimental determination.

[c]determined experimentally in recombinant expression system in CHO cells.

1.4.3 IL-13 receptors and signalling

IL-13 mediates its action via a complex receptor system that includes the IL-4Rα chain and at least two other IL-13-binding proteins designated as IL-13Rα1 and IL-13Rα2 (Hilton *et al.*, 1996). It was shown that IL-13R (IL-4Rα/IL-13Rα1) is expressed on both hematopoietic and non-hematopoietic cells for example B cells, monocytes/macrophages, dendritic cells, eosinophils, basophils, fibroblasts, endothelial cells, airway epithelial, and ASM cells (Hershey, 2003). Expression of IL-13 Rα2 has been reported on fibroblasts, airway epithelial cells, ASM cells, B lymphocytes and macrophages cells (Laporte *et al.*, 2001; Daines & Hershey, 2002; Zheng *et al.*, 2003; Yoshikawa *et al.*, 2003).

IL-13Rα1 is expressed as a 60-70 kDa glycosylated protein that binds IL-13 but not IL-4. The cytoplasmic domain of IL-13Rα1 contains a membrane–proximal proline-rich region termed box-1 and two tyrosine residues, Tyr-402 and Tyr-405, with the latter in a YXXQ sequence motif that binds the SH2 domain of STAT3 (Stahl *et al.*, 1995). The proline-rich box region in the intracellular domain is needed for binding of JAK. JAKs are tyrosine kinases that each contains a true catalytic domain and a pseudokinase domain. There are 4 JAKs: JAK1, JAK2, JAK3, and Tyk2. JAK1, JAK2, and Tyk2 are ubiquitously expressed, while JAK3 is expressed mainly in hematopoietic cells. IL-4Rα, γc, and IL-13Rα1 bind JAK1, JAK3, and Tyk2, respectively (reviewed in Leonard & Lin, 2000).

The IL-13Rα2 gene was first cloned in Caki-1 human renal carcinoma cell line (Caput *et al*., 1996) while the murine homologue m-IL-13Rα2 was detected in murine serum and urine (Zhang *et al*., 1997). Comparisons of the h-, m- and r-IL-13Rα2 receptors show that they all have an N-terminal signal sequence, an N-terminal fibronectin type III domain in the extracellular domain, four putative N-glycosylation sites, four conserved cysteine residues and a conserved WSEWS motif (Wu & Low, 2002). The IL-13Rα2 amino acid sequence among rat, human and mouse shows that rat IL-13Rα2 protein is most closely related to that of mouse with 91.2% homologous amino acid residues and the similarity between rat and human is about 54.2% at the amino acid sequence level (McKenzie *et al.*, 1993b; Wu & Low, 2002).

IL-13 binds to IL-13Rα1 first with low affinity (K_d 4 nM) and then recruits IL-4Rα to the complex, generating a high affinity receptor (K_d ~50 pM). Heterodimerization of IL-13Rα1 with IL-4Rα causes activation of JAK, TYK2 and JAK1, constitutively associated with IL-13Rα1 and IL-4R, respectively, followed by activation of STAT6. STAT6 is a transcription factor usually considered critical for IL-13 signals. Activated JAKs results in tyrosine phosphorylation in IL-4Rα, leading to the recruitment of STAT6 to the receptor, which in turn phosphorylates STAT6. The association of STAT6 with tyrosine-phosphorylated regions of cytokine receptors occurs through its SH2 domain. Phosphorylated STAT6 molecules dimerize and activated STAT6 dimers translocate to the nucleus where it activates transcription of downstream genes (Figure 1.6). A study using peritoneal macrophages isolated from STAT6-deficient mice revealed that IL-13 does not decrease nitric oxide production (Takeda *et al.*, 1996) which demonstrates an IL-13/STAT6 dependent pathway.

Binding of ligands to the IL-4 type 1 receptor recruits IRS-1 and IRS-2 to phosphorylated Y497 of IL-4Rα leading to phosphorylation and activation of IRS-1 and IRS-2 (Jiang *et al.*, 2000). Y497 and the surrounding motif are found to be essential for recruitment of IRS-1 (Keegan *et al.*, 1994). Phosphorylated IRS-1 and IRS-2 activate PI3K through an interaction with the p85α subunit (Jiang *et al.*, 2000). The importance of PI3K in IL-13 signalling has been demonstrated in several studies. In the human colonic epithelial cell line HT-29 it was shown that IL-13 increases PtdIns(3,4)P_2 and PtdIns(3,4,5)P_3 as well as lipid kinase activity of p85 immunoprecipitates. Both effects are inhibited by wortmannin and LY294002 (Wright *et al.*, 1997). Using another human colonic epithelium T84 cells it was demonstrated that changes in transepithelial resistance can be still observed after pretreatment with transcription factor decoys which inhibit STAT6 activation but not after pre-treatment with PI3K inhibitors wortmannin or LY294002. GRB-2 is a small SH2- and SH3 domain-containing adapter protein that associates with the mammalian SOS homolog to activate ras during growth factor signalling (Myers, Jr. *et al.*, 1994; White, 1998).

The other IL-13-binding unit, IL-13Rα2, binds IL-13, but not IL-4 with high affinity (K_d 50 pM). It was identified in both human and mice with 59% overall

identity of protein sequence (Donaldson *et al.*, 1998). It thought that the IL-13Rα2 receptor acts usually as a non-signalling "decoy" receptor in which its cytoplasmic tail is short and does not contain any obvious signalling motif, or that it may combine with IL-13Rα1 to facilitate the formation of a high affinity signalling complex (Wills-Karp & Chiaramonte, 2003; Arima *et al.*, 2005). However, the cytoplasmic domains of m-IL-13Rα2 and m-IL-13Rα1 are dissimilar, and the cytoplasmic domains of both the m- and h-IL-13Rα2 are short. In addition co-expression of IL-13Rα2 with IL-4Rα fails to induce a response to IL-13, and its co-expression with IL-4Rα/IL-13Rα1 fails to modify the binding affinity for IL-13. Furthermore, no box 1 or box 2, needed for activation and association with JAK1 respectively, signalling motifs are present, although a putative consensus phosphorylation site at Y_{343}PKM may interact with SH2-containing downstream signalling components (Kawakami *et al.*, 2001b; Usacheva A *et al.,* 2002). IL-13Rα2 was found to modulate IL-13 signalling in the BEAS-2B cell line (Yasunaga *et al.*, 2003). These findings together support the decoy receptor function of IL-13Rα2.

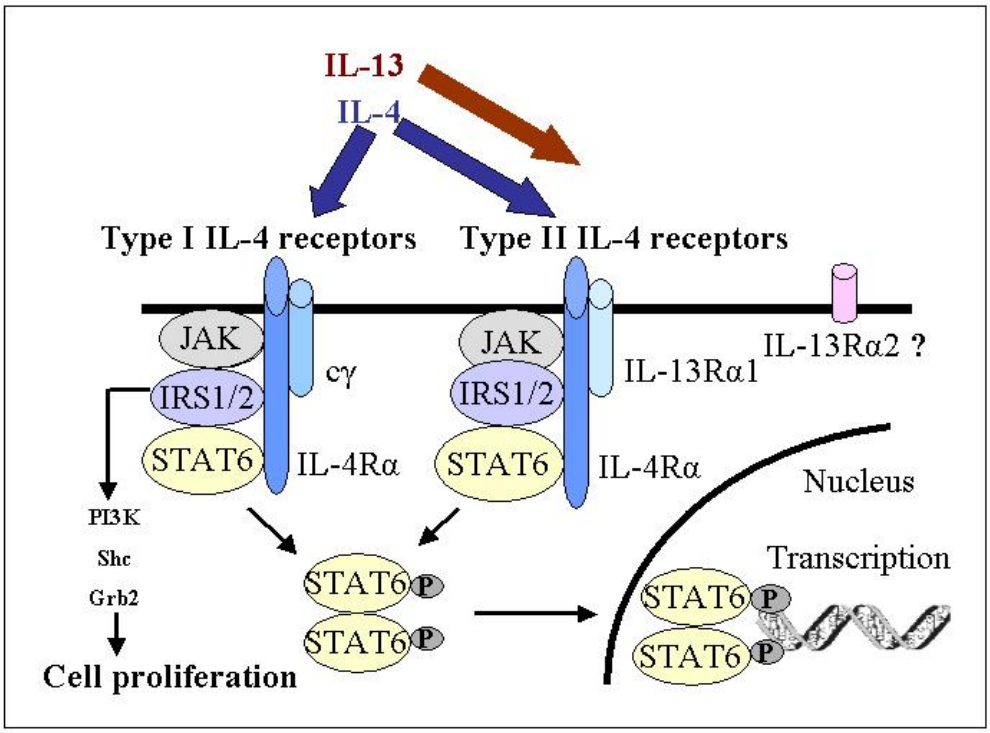

Figure 1.6 IL-13/IL-4 receptor structure and signal transduction pathways. The functional IL-13 receptor consists of a heterodimeric complex composed of the IL-4Rα and IL-13Rα1 chains. IL-13 and IL-4 can induce heterodimerization of the IL-4Rα and IL-13Rα1 chains, and dimerization of both chains induces phosphorylation and activation of Janus kinases (JAK). Activated JAK phosphorylates tyrosine residues of the IL-4Rα chain. Signal transducers and activators of transcription 6 (STAT6) are attached with phosphorylated tyrosine. Phosphorylated STAT6 proteins dimerize and translocate to the nucleus where they bind to specific DNA sequences. IL-4 can also signal through a receptor complex composed of the IL-4Rα and the common γ chain. The IL-13Rα2 chain binds only IL-13, not IL-4, with high affinity. Insulin receptor substrate (IRS) and STAT6 are attached with phosphorylated tyrosine via Src homology domains and phosphorylated by JAK. Phosphorylated IRS1/2 is associated with several signalling molecules, such as phosphoinositide 3 kinase (PI3K), Grb2, and Shc that mediate downstream signals for growth and cell proliferation (adapted from Wills-Karp, 2004).

1.4.4 Regulation of IL-13 signalling

Regulators of IL-13 signalling pathway include many intracellular molecules for example SH2-containing phosphatases (SHP-1), suppressors of cytokine signalling (SOCS), and protein inhibitors of activated STAT (PIAS). SHP-1 is involved in the negative regulation of many cytokine receptors, for example erythropoietin, IL-2, IL-3, CSF, and IL-4Rα (reviewed in Hershey, 2003). Bone marrow-derived macrophages isolated from motheaten mice that express reduced levels of SHP-1 activity show enhanced activation of STAT6 after treatment with IL-4, implicating SHP-1 in the negative regulation of the IL-4/IL-13-activated JAK-STAT pathway (Haque *et al.*, 1998). SHP inhibitory mechanism(s) can be through binding to receptors, or SHP-1 can bind JAK2 directly (Klingmuller *et al.*, 1995; Kashiwada *et al.*, 2001)**.**

SOCS is another regulator of IL-13 signalling. SOCS genes are induced after cytokine stimulation and SOCS proteins form a negative feedback loop to inhibit cytokine signalling. SOCS-1 has been shown to bind and inhibit JAKs (Chen *et al.*, 2000) but this might not be true of all SOCS family members. In an OVA-induced asthma model using SOCS-5 transgenic mice, lung and BAL fliud eosinophilia, increased IL-5 and IL-13 in BAL fluid and enhanced AHR to methacholine were observed compared with wild-type mice (Ohshima *et al.*, 2007). In human primary bronchial epithelial cell cultures, pretreatment with IFN-γ decreases IL-4–induced nuclear- and cytoplasmic phospho-STAT6, induces IL-13Rα2 mRNA expression and does not decrease mRNA for IL-4Rα or IL-13Rα1. All these previous findings were associated with increased mRNA for both SOCS-1 and SOCS-3 (Heller *et al.*, 2004), and using the lung epithelial cell line A549, IL-4 and IL-13 were shown to induce SOCS-1 gene expression (Hebenstreit *et al.*, 2003).

Another important family of proteins involved in the regulation of the JAK/STAT pathway is PIAS. PIAS binds to phosphorylated STAT dimers and prevents them from binding DNA. It is thought that degradation and regulation of STAT6 involved in IL-13 signalling is via proteasomal degradation or dephosphorylation through specific phosphatase because no PIAS has been identified for STAT6 (Hershey, 2003).

1.4.5 IL-13 functions

IL-13 effector functions include a diverse array of biological activities on wide varieties of cells mostly related to allergic disorders (Wynn, 2003). IL-13 promotes proliferation of B-cell and induces class switching to IgE (D'Amato, 2003). It induces expression the low-affinity IgE receptor CD23 (FcεRII) and MHC class II (Defrance *et al.*, 1994; Hart *et al.*, 1999). IL-13 also enhances the expression of many integrin family molecules important in adhesion such as CD11b, CD11c and CD18 (Oyoshi *et al.*, 2008), but in a study using denderitic cells it was demonstrated that IL-13 does not enhance CD11b expression (D'Amico *et al.*, 1998). IL-13 promotes eosinophil chemotaxis (Pope *et al.*, 2001; Pope *et al.*, 2005). The action of IL-13 on nonhematopoietic cells has been extensively studied especially in cells involved in allergic lung diseases (Lee *et al.*, 2001; Laoukili *et al.*, 2001; Akaiwa *et al.*, 2001; Kawakami *et al.*, 2001a; Kondo *et al.*, 2002; Kuperman *et al.*, 2002; Izuhara, 2003). However, the role of IL-13 as an anti-inflammatory mediator can be demonstrated in studies that show that IL-13 inhibits the production of prostaglandins and TNF-α and leukocyte accumulation after OVA stimulation (Endo *et al.*, 1996; Watson *et al.*, 1999).

IL-13 seems to play a critical role in the pathogenesis of asthma (Wills-Karp, 2004). Several mechanisms have been suggested including isotype switching of B-cells to Ig-E synthesis, downregulation of production of pro-inflammatory cytokines (TNF-α and IL-1β), RANTES, IL-12, upregulation of expression of VCAM-1, increase in eosinophil survival, chemotaxis, activation of fibroblasts and stimulation of mucus production (Kips, 2001). Pulmonary expression of IL-13 induces an asthma-like phenotype in mice, including a mononuclear and eosinophilic inflammatory response, mucus cell metaplasia, airway fibrosis, eotaxin production, airway obstruction, and nonspecific AHR (Zhu *et al.*, 1999). In addition it enhances polarization of T lymphocytes to a Th2 phenotype (Levy *et al.*, 1997; Hajoui *et al.*, 2004), and IL-13 may contribute to asthma via tissue remodelling (Kumar *et al.*, 2002), epithelial activation (Lordan *et al.*, 2002), decreasing β2 adrenoceptor function (Laporte *et al.*, 2001), and enhancing contractility of airway smooth muscle (Tliba *et al.*, 2003).

Although several Th2 cytokines have been implicated in antigen-induced AHR, IL-13 seems to play a pre-eminent role. Targeted deletion of IL-13 prevents expression of AHR in allergen-challenged mice, despite maintenance of elevated IL-4 and IL-5 release (Walter *et al.*, 2001). IL-4 expression fails to elicit an asthma phenotype and both wild and IL-4 knock-out Balb/c mice display reduced airway eosinophilia without an effect on AHR, denoting that IL-4 plays a pivotal role in eosinophilic inflammation, but not AHR (Cohn *et al.*, 1998). Likewise, neutralization of IL-13 using IL-13 receptor constructs or antibodies reduces AHR without influencing IL-5 levels (Grunig *et al.*, 1999; Eum *et al.*, 2005). The exact mechanisms by which IL-13 induces airway obstruction or AHR are currently unknown. Several lines of evidence suggest that IL-13 can induce AHR in the absence of inflammatory cells. Although IL-13 is able to direct the recruitment of inflammatory cells into the airways, they are likely not required for induction of AHR. IL-13 may induce AHR via direct effects on resident airway cells (Kuperman *et al.*, 2002).

A cytokine trap is a high affinity blocker consisting of fusions between the constant region of IgG and the extracellular domains of two distinct cytokine receptor components involved in cytokine binding. A trap containing IL-13Rα1 and IL-4R to block both IL-4 and IL-13 has been created and can be used to alleviate experimental asthma in animal models (Economides *et al.*, 2003). Laporte and associates (2001) demonstrated that IL-13, but not IL-4, significantly reduces β adrenoceptor-induced relaxation of cell stiffness of human ASM cells through a MAP kinase-dependent pathway. Studies by Kuperman *et al*. (2002) also provide strong support for a central role of the airway epithelium in IL-13 induced AHR. Specifically, they showed that expression of STAT6 only in the airway epithelium reproduces the allergic phenotype including AHR and mucus hypersecretion. Interestingly, IL-13 transgenic mice expressing STAT6 only in the epithelium do not manifest eosinophilic inflammation suggesting that eosinophils are not required for the development of AHR and that signals from the epithelium are not sufficient to regulate eosinophil recruitment. Epithelial-derived mediators such as TGF-β may also contribute to increases in stiffness of the airway wall. Although the fibrotic changes induced via IL-13 stimulation of epithelium are likely important in chronic disease, Kuperman's data suggest that IL-13-induced AHR is independent of fibrotic

changes in the airways and they also added that IL-13 is known to regulate the production of a number of secreted molecules that alter the contraction or relaxation of ASM cells. Whether IL-13 mediates AHR via these known actions or by as yet undescribed pathways, the epithelium clearly plays an important role in IL-13 mediated AHR. It is probable that AHR arises *via* the combined actions of IL-13 on the epithelium and ASM.and IL-13 could contribute to AHR and eosinophilia in mouse asthma models independently of IL-4 (Wills-Karp *et al.*, 1998; Grunig *et al.*, 1999).

1.4.6 IL-13 genetic variants in asthma

Genetic studies strongly support the role IL-13 genetic variants in the development of asthma. Commonly identified IL-13 variants associated with asthma are 1111C > T (The IL-13 -1055 TT genotype) (van der Pouw Kraan *et al.*, 1999) and +2043G > A (R130Q) (van der Pouw Kraan *et al.*, 1999; Howard *et al.*, 2001). Sequencing of the IL-13 gene and its promoter from various groups originating from East and West Africa, Europe, China and South America demonstrated that R130Q is the only variant detected in these groups (Tarazona-Santos & Tishkoff, 2005). *In vivo* and *in vitro* studies of this variant indicated enhanced IL-13–dependent gene induction. Furthermore, BALB/c mice treated with R130Q IL-13 variant displayed increased AHR (Chen *et al.*, 2004). It is concluded from these studies that allergic asthma and the R130Q polymorphism are associated with increase in the activity of IL-13. A 1111C > T variation is located in the IL-13 promoter region (van der Pouw Kraan *et al.*, 1999), however the associations between -1111C > T and asthma-related phenotypes may be independent of the R130Q polymorphism. It has also been demonstrated in primary bronchial fibroblasts isolated from non-smoker nonatopic asthmatic patients that binding of the R130Q variant to human IL-13Rα1 is not significantly different from wild type binding, but binding to soluble h-IL-13RILα2 is different (Andrews *et al.*, 2007). The IL-13 α1 receptor subunit is involved in the control of IgE production. The promoter and coding region of IL-13Rα1 located on chromosome Xq24 were screened in asthmatic Caucasian families but the two identified polymorphisms (281T>G and 1365A>G) were not associated with asthma susceptibility or severity (Konstantinidis *et al.*, 2007).

1.5 Phosphoinositide 3-kinases (PI3K)

PI3K family plays an important role in inflammatory lung diseases particularly asthma. PI3K control inflammatory cells growth, differentiation, survival, migration, proliferation, and mediator production (reviewed in Finan & Thomas, 2004; Medina-Tato *et al*. 2007; Ito *et al.* 2007). IL-13 binding to IL-13Rα1/IL-4αR can elicit airway hyperreactivity, independently of inflammation, mainly through the Janus kinase/STAT6 pathway (Yang *et al.*, 2001). However, IL-13 binding can also results in inducing intrinsic kinase activities that initiate intracellular signal transduction cascades including the PI3Ks (Ceponis *et al.*, 2000; Hershey, 2003).

The phosphoinositol cycle was uncovered in the 1950s by Lowell and Mabel Hokin (Hokin & Hokin, 1953). The Hokins discovered that phosphatidylinositol (PtdIns) could be sequentially phosphorylated on its myo-inositol ring to generate a phosphatidylinositol bisphosphate that was likely to be phosphatidylinositol 4,5-bisphosphate (PtdIns(4,5)P_2) and was thought to be a precursor to other lipid signalling molecules. It is now clear that PtdIns (4,5)P_2 is widely recognized as a potent messenger itself, and a major mediator of biochemical activities and cellular functions (Heck *et al.*, 2007). PtdIns(4,5)P_2 directly regulates an array of protein interactions and cellular processes, including vesicular trafficking (Wenk & De, 2004), secretion (Martin, 2001), cell motility /cytoskeletal assembly (Janmey, 1994; Yin & Janmey, 2003), ion channels (Suh & Hille, 2005; Delmas *et al.*, 2005), and nuclear signalling pathways (Gonzales & Anderson, 2006).

1.5.1 PI3K family

Phosphoinositide 3-kinases (PI3K) are a family of related enzymes that are capable of phosphorylating the 3 position hydroxyl group of the inositol ring of phosphatidylinositol and the serine residues of certain proteins (Rameh & Cantley, 1999). This family has been linked to an extraordinarily diverse group of cellular functions and disease states. The PI3K family plays a prominent role in various inflammatory conditions by controlling cell growth, differentiation, survival, proliferation, and cytokine production through its downstream components (Duan *et*

al., 2005). The PI3K family has been divided into three classes according to their structure and lipid substrate specificity (Table 1.5). As seen in Table 1.5, class I PI3K comprises four distinct protein species of approximately 110 kDa (p110α, p110β, p110γ and p110δ). Class I PI3K are largely cytosolic in resting cells, but upon stimulation are recruited to membranes via interactions with receptors or adaptor proteins. They are thought to function primarily at the plasma membrane, but there have been reports of class I PI3K associated with vesicular and nuclear membranes (Rameh & Cantley, 1999; Katso *et al.*, 2001). The class I family is further subdivided into two groups on the basis of their regulatory partners and mechanisms of activation.

Table 1.5 Characteristics of the PI3K family (Ito *et al.*, 2007)

PI3K Family	Isoforms	Catalytic Molecule	Regulatory Molecule	*In vitro* Substrate	Distribution
Ia	PI3Kα PI3Kβ PI3Kδ	p110α p110β p110δ	p85 α, p85 β p55γ p85α, p85β	PtdIns PtdIns(4)P PtdIns(4,5)P_2	Ubiquitous Ubiquitous Whole blood, thymus
Ib	PI3Kγ	p110γ	p101 p84/p87^{FIKAP}	PtdIns(4,5)P_2	Whole blood, thymus
II		C2α C2β C2γ	Clathrin Clathrin Clathrin	PtdIns,PtdIns(4)P PtdIns PtdIns	Widely expressed Widely expressed Prostate, Liver, Breast
III		Vps34p	Vps15p (p150) Beclin 1	PtdIns	Ubiquitous Constitutive

Class I PI3K has been widely reported in the literature. Upon activation, class I PI3K converts PtdIns(4,5)P_2 into PtdIns(3,4,5)P_3, a ubiquitous second messenger (Figure 1.7). PtdIns(3,4,5)P_3 then acts as a targeting site for downstream signalling molecules, such as protein serine/threonine kinases (including protein kinase B/Akt). This class is further divided into class IA and class IB PI3K. Structurally, PI3K IA

exists as heterodimeric complexes in which a catalytic p110 subunit (α, β or δ) is in association with particular regulatory subunits (designated p85α, p55α, p50α, p85β or p55γ). The first three regulatory subunits are all splice variants of the same gene (Pik3r1), the other two being expressed by other genes (Pik3r2 and Pik3r3). The most highly expressed regulatory subunit is p85α. All three catalytic subunits are expressed by separate genes (Pik3ca, Pik3cb and Pik3cd for p110α, p110β and p110δ, respectively). p110α and p110β isoforms are ubiquitously expressed, and genetic knockout leads to early embryonic death. Expression of the p110δ was considered to be restricted to the hematopoietic systems, and mice lacking expression of PI3Kδ do not show any overt adverse phenotype. PI3K IA signals downstream of receptor tyrosine kinase and Ras while the single class PI3K Ib consists of the p110γ catalytic subunit complexed to the p101 regulatory subunit and signals downstream of GPCRs and Ras. GPCR can bind a diverse array of peptides and non peptide ligands leading to activation of heterotrimeric $G_{\alpha\beta\gamma}$ protein to exchange the GDP molecule bound to the G_{α} subunit for GTP which leads to the dissociation of the GTP-bound G_{α} subunits from the $G_{\beta\gamma}$ subunits. Free $G_{\beta\gamma}$ subunit binds and activates p110γ which is stimulated by the regulatory subunit, p101 (Stephens *et al.*, 1997; Krugmann *et al.*, 1999). Class Ib PI3K differs from other class Ia members because they are activated by βγ subunits of GPCR. βγ subunits of GPCR could activate p110γ either directly (Stoyanov *et al.*, 1995) or through the binding of regulatory p101 subunit to βγ subunits (Stephens *et al.*, 1997). Class Ib PI3K is abundant in leukocytes and involved in immune system regulation. Gene deletion of Pik3cg responsible for p110γ protein expression displayed different phenotypes i.e lack of neutrophils and macrophages recruitment and reduced ability to produce superoxide production needed for chemoattraction (Li *et al.*, 2000), colorectal cancer (Sasaki *et al.*, 2000). In a study conducted in neutrophils isolated from mice lacking p110γ or p101 or expressing $p110\gamma^{DASAA/DASAA}$ the migration was reduced, and peritoneal neutrophil migration was reduced *in vivo* implicating the associated role of βγ subunits, p101 and Ras in the regulation of PI3Kγ in immune function (Suire *et al.*, 2006).

Class II PI3K predominantly use PtdIns and PtdIns(4)P substrates (Table 1.5). They are mainly associated with the phospholipid membranes and are present in the endoplasmic reticulum and Golgi apparatus (Domin *et al.*, 1997). The class II enzymes

differ significantly from the class I enzymes in their mode of regulation and substrate preference. Three mammalian isoforms, PI3KC2α, PI3KC2β, PI3KC2γ, and one *Drosophilia* homolog are known. They are larger proteins, with a molecular weight of 170 kDa, characterized by the presence of a C-terminal C2 domain which is sufficient and necessary for recruitment of PI3KC2α and PI3KC2β (Arcaro *et al.*, 2000). Deletion of this domain increases the catalytic activity of PI3KC2β implicating its negative regulatory role on the catalytic activity of the enzyme (Arcaro *et al.*, 1998). PI3KC2α and PI3KC2β are widely distributed while PI3KC2γ is less distributed (Ito *et al.*, 2007). Both isoforms can function downstream of several receptors including tyrosine kinases, integrin receptors and cytokine receptors (Turner *et al.*, 1998; Brown *et al.*, 1999), however, a precise function of this class is unclear.

Class III PI3K is the homolog of the yeast vesicular-protein-sorting protein Vps34p (Schu *et al.*, 1993). Both the catalytic subunit, Vps34p and the serine threonine protein kinase, p150, are important for targeting the Vps34p to membranes. The major cellular function of the class III PI3Ks is in intracellular trafficking (Katso *et al.*, 2001). Class III PI3K is reported to be involved in macroautophagy, which is a multistep process responsible for the degradation of long-lived proteins and organelle renewal, and starts with the formation of an autophagosome. This pathway is important in the maintenance of cell function during periods of nutrient deprivation. Class III PI3K uses only membrane PtdIns as a substrate and generates PtdIns(3)P. Cellular levels of PtdIns(3)P are usually maintained at constant levels, suggesting that the class III isoform does not respond to extracellular stimuli (Krymskaya *et al.*, 2001).

1.5.2 PI3K signalling

Termination of PI3K signalling by degradation of PtdIns(3,4,5)P_3 can be mediated by at least two different types of phosphatases, namely Src homology 2-containing inositol 5-phosphatase (SHIP) and phosphatase and tensin homolog deleted on chromosome 10 protein (PTEN) (Koyasu, 2003) (Figure 1.7). PTEN removes the 3-phosphate of PtdIns(3,4,5)P_3 and, thus, directly counteracts all types of PI3K by catalyzing the opposite reaction. It was reported that the PTEN knockout mice is embryonically lethal and PTEN plays a pivotal role in Th2-mediated airway

inflammation and airway responsiveness (Kwak *et al.*, 2003). In addition, PTEN overexpression reduced airway hyperresponsivenss and vascular endothelial growth factor expression in a murine model of asthma (Lee *et al.*, 2006b). In contrast, SHIP removes the 5-phosphate from the inositol ring of PtdIns(3,4,5)P_3 to generate PtdIns(3,4)P_2, and this dephosphorylation of PtdIns(3,4,5)P_3 by SHIP impairs downstream effects of PI3K. Although PtdIns(3,4)P_2, the metabolic product of SHIP, may also mediate PI3K-dependent responses. SHIP knockout mice show increased mast cell degradation, B-cell activation, and increased chemotaxis. These mice also suffer from a lethal accumulation of macrophages and neutrophils in the lungs; therefore, persistent high levels of PtdIns(3,4,5)P_3 and subsequent activation of its downstream effectors might lead to excessive inflammation (Rauh *et al.*, 2003).

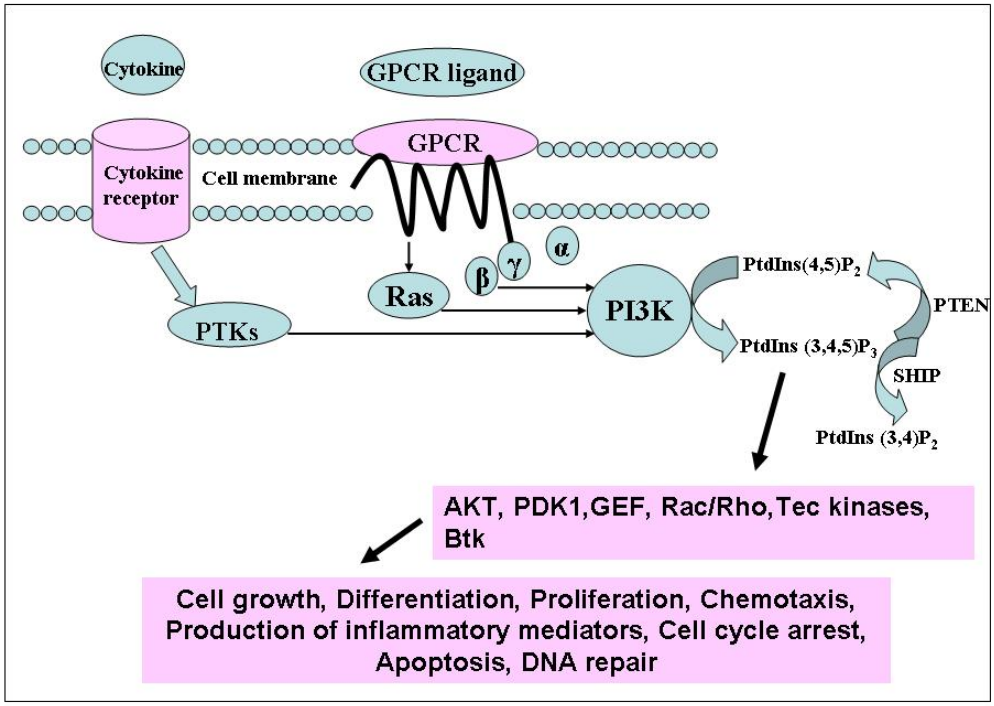

Figure 1.7 PI3K signalling pathway. Activation of PI3K through tyrosine kinase or G-protein coupled receptors (GPCR). PtdIns(4,5)P_2 converts into PtdIns(3,4,5)P_3. Akt, PDK1, guanidine nucleotide factor (GEF), Rac/Rho kinase, Tec kinases and Btk are activated downstream of PI3K to carry out different cell functions e.g. cell growth, metabolism, angiogenesis, glucose uptake, survival, metabolism. PTEN dephosphorylates PtdIns(3,4,5)P_3 and returns it to PtdIns(4,5)P_2. SHIP can also dephosphorylate PtdIns(3,4,5)P_3 to generate PtdIns(3,4)P_2.

1.5.3 PI3K inhibitors

The availability of two PI3K inhibitors, wortmannin, a naturally occurring metabolite of Penicillin funiculosum and an irreversible inhibitor, and LY294002, a reversible inhibitor derived from the broad-spectrum kinase inhibitor quercetin, has contributed greatly to the understanding of the biological role of PI3K and its effector proteins (Ward & Finan, 2003). However, wortmannin and LY294002 have no selectivity for individual PI3K isoforms, and have poor stability, solubility, toxicity, and absorption. In addition, wortmannin and LY294002 exhibit some compound-specific toxicity and possess off-target effects. For example wortmannin inhibits myosin light chain kinase and LY294002 inhibits casein kinase-2 (CK2). ICOS Corporation has described several p110δ inhibitors, including IC87114, a selective p110δ inhibitor, and this has been used to investigate the role of p110δ in allergic airway inflammation and hyperresponsiveness using a mouse asthma model (Lee *et al.*, 2006a). IC87114 significantly reduced the serum levels of total immunoglobulin (IgE), OVA-specific IgE, leukotriene C4 release into the airspace, OVA-induced lung tissue eosinophilia, airway mucus production, and importantly OVA-induced increase in expression of IL-4, IL-5, IL-13, intercellular adhesion molecule-1, vascular cell adhesion molecule-1, CCL5, and CCL11. Furthermore, IC87114 significantly suppressed OVA-induced AHR to inhaled methacholine, and this corresponded with a reduction in OVA-induced Akt serine phosphorylation. These results are supported by the *in vitro* findings that p110δ is involved in B- and T-cell antigen receptor signalling and activation and allergen-IgE-induced mast cell degranulation. There is also evidence from studies in knockout mice that PI3Kp110δ is an important component in the pathogenesis of asthma (Nashed *et al.*, 2007). PI3K inhibitors are illustrated in Figure 1.8 and Table 1.6.

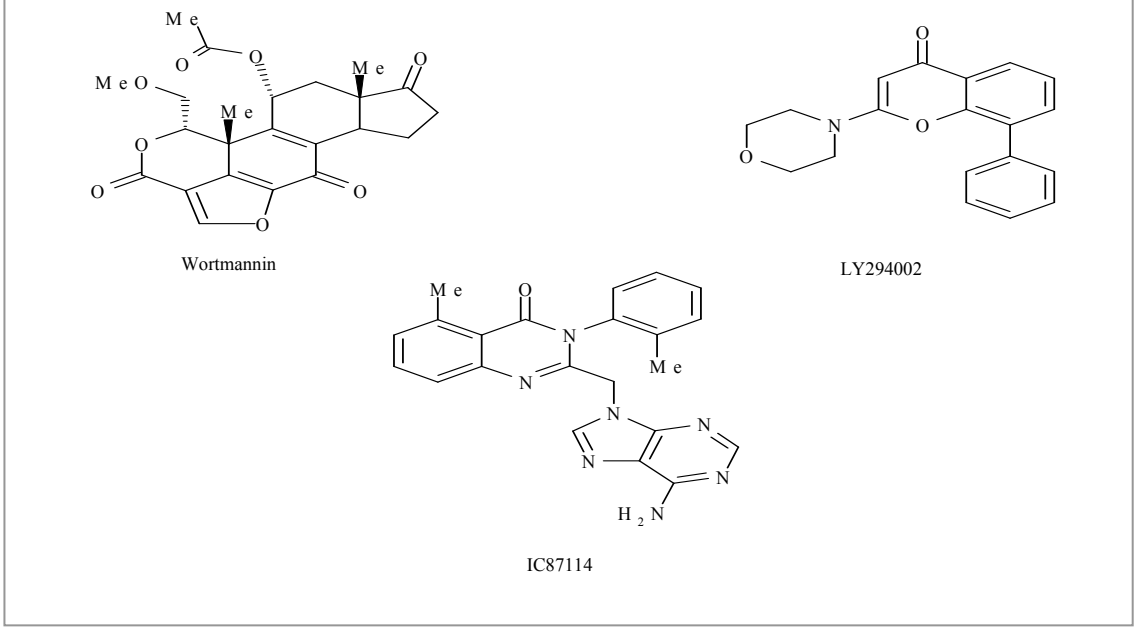

Figure 1.8 Some PI3K inhibitors (Stokoe, 2005).

Table 1.6 Specificity profile of some PI3K inhibitors (Marone *et al.*, 2008)

IC50 (μM) p110α p110β p110γ p110δ	Name	Corporation	Comment
200 16 61 0.13	IC87114/	ICOS	Selective p110δ inhibitor Cell permeable
1–3 1–3 2 ND	LY294002	Lilly	Pan-PI3K inhibitor
~ 0.004 ~ 0.004 ~ 0.004 ~ 0.004	Wortmannin	Wander AG, Lilly	High nM Active against DNA-PK, mTOR, ATR, ATM, PI4K, MLCK

1.5.4 PI3K and inflammatory lung diseases

PI3K may contribute to the pathogenesis of asthma by effecting the recruitment, activation, and apoptosis of inflammatory cells (Medina-Tato *et al.*, 2007). Administration of wortmannin or LY294002, two broad-spectrum inhibitors of PI3K, attenuates inflammation in murine models of allergic asthma (Ezeamuzie *et al.*, 2001; Kwak *et al.*, 2003). Intratracheal administration of LY294002 significantly inhibits most of the pathological characteristics of the mouse asthma model, including increased eosinophil counts and eotaxin, IL-5, and IL-13 levels in bronchoalveolar lavage fluid. Furthermore, lung tissue eosinophilia, airway mucus production, and AHR to inhaled methacholine are all significantly suppressed (Duan *et al.*, 2005). Although these studies with broad-spectrum inhibitors provide good evidence for a role for PI3K in allergic airway dysfunction, these inhibitors do not distinguish among the four class I PI3K isoforms (Davies *et al.*, 2000). The development of isoform selective inhibitors, as well as genetically modified mice, allow the characterization of the different roles of individual PI3K isoforms in airway disease. In addition to contributing to the AHR seen in asthma, airway smooth muscle cells are potentially linked with many other features of asthma, including the production of cytokines and inflammatory mediators involved in tissue remodelling. PI3K signalling and its putative roles in lung disease have been extensively reviewed (Vanhaesebroeck *et al.*, 2001; Medina-Tato *et al.*, 2007; Ito *et al.*, 2007).

1.6 Arginase and Arginine metabolism

Arginase activity is regulated by Th2 cells and their cytokines (Munder *et al.*, 1999). A potential mechanism of IL-13-induced hyperresponsiveness is the induction of arginase, which can compete with nitric oxide synthase (NOS) for the common substrate arginine, and remove the modulatory effects of NO on airway smooth muscle contraction (Meurs *et al.*, 2003). Furthermore, attenuation of IL-13-induced airway hyperresponsiveness was observed *in vivo* using RNA interference towards arginase I (Yang *et al.*, 2006).

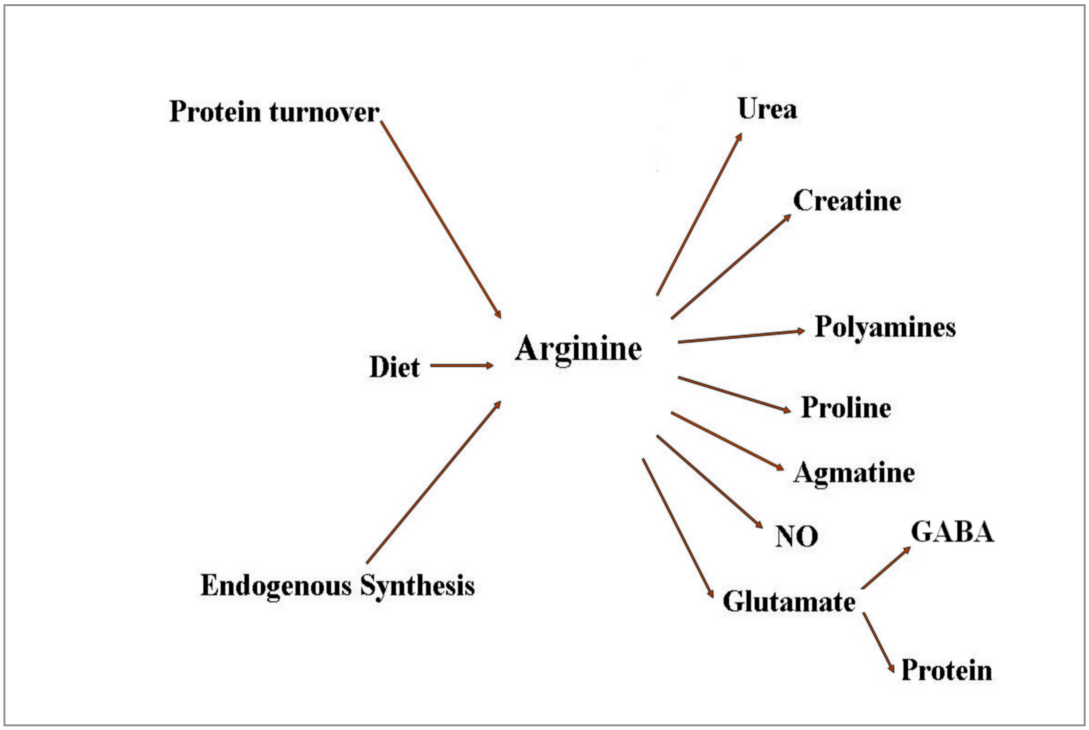

Figure 1.9 Arginine – its source and fates

It was the discovery of the urea cycle by Krebs and Henseleit in 1928 that brought arginine to the focus of many studies. Arginine is classified as semiessential or conditionally essential amino acid because endogenous arginine synthesis cannot fully meet the needs of infants and growing children or adults under catabolic stress, trauma, surgery (Wakabayashi *et al.*, 1994), kidney or small intestine dysfunction, inflammation, or sepsis (Morris, Jr., 2002). L-Arginine is a precursor in protein synthesis (Figure 1.9) and a substrate for a number of enzymes, including nitric oxide synthase (NOS), arginase, arginine:glycine aminotransferase and arginine decarboxylase, yielding nitric oxide (NO) and L-citrulline, L-ornithine and urea, creatine, and agmatine, respectively (Wu & Morris, 1998).

1.6.1 Arginase isozymes

Arginase (also known as L-arginine ureahydrolase, or amidinohydrolase) (Jenkinson *et al.*, 1996) has the highest potential activity of all the urea cycle enzymes in the liver which is responsible for a very low level of arginine liver extractability (0.007 mmol/g wet weight), whereas higher levels of arginine are detected in the gut (0.45), heart (0.13), stomach (0.13), erythrocyte (0.11), muscle (0.11), kidney (0.08) and lung (0.05) (White, 1985). L-Arginine is also the substrate for NOS, which

generates NO. Although the affinity of L-arginine is much higher for purified NOS (K_m ~ 2–20 μM) than for arginase (K_m ~ 1–5 mM), the maximum activity of arginase is more than 1,000 times that of NOS suggesting similar rates of substrate utilization at physiologic L-arginine concentrations (Durante *et al.*, 2007).

Arginase is a 105 kDa homotrimeric enzyme that requires manganese for the hydrolysis of L-arginine to form L-ornithine and urea. It is widely distributed throughout different organisms including bacteria, yeasts, plants, invertebrates and vertebrates (Jenkinson *et al.*, 1996; Ash, 2004). Arginase's active site is extraordinarily specific due to the high number of hydrogen bonds between the substrate and the enzyme, so modifying the substrate structure and/or stereochemistry will markedly lower the kinetic activity of the enzyme. Two genetically distinct isozymes, arginase I and II, have been identified with differing tissue distributions and subcellular locations in mammals (Wu & Morris, 1998). Arginase I and II are encoded by different genes which are located on chromosomes 6q23 and 14q24 respectively (Sparkes *et al.*, 1986; Gotoh *et al.*, 1997). Both isozymes are constitutively expressed in the airways, particularly in the epithelium, endothelium, (myo) fibroblasts and alveolar macrophages (Que *et al.*, 1998; Klasen *et al.*, 2001; Lindemann & Racke, 2003) and share approximately 60% amino acid sequence homology. Arginase I is located predominantly in the liver cytoplasm, where it catalyzes the final step of the urea cycle and is responsible for the generation of ~10 kg of urea per year by the average human adult. However, other studies report a wider distribution of arginase I including airway epithelial cells (Cederbaum *et al.*, 2004; Bergeron *et al.*, 2007). Arginase II is a mitochondrial enzyme being more widely distributed in the kidney, prostate, brain, skeletal muscle, and poorly expressed in the liver (Morris *et al.*, 1997; Durante *et al.*, 2007).

1.6.2 Arginase regulation and inhibitors

The interplay between NO synthases and arginase pathways generated significant interest concerning their regulation through competitive pathways. Arginase activity can effectively inhibit NO-dependent processes for example smooth muscle tone by depleting the substrate pool (arginine) available for NO biosynthesis. In LPS activated macrophages cell line it was demonstrated that arginase II activity has been

increased together with induction of iNOS. These findings have been prevented by IFN-γ (Wang *et al.*, 1995). In cultured rat LPS-treated peritoneal macrophages changes have been demonstrated in iNOS and arginase I mRNAs both *in vivo* and *in vitro* but not in arginase II-mRNA. Moreover, in primary murine bone marrow-derived macrophages arginase activity was increased by Th2 cytokines i.e. IL-4 and IL-10 and PGE_2, while the Th1 cytokine IFN-γ induces NO synthesis in these cells suggesting a Th1/Th2cytokines-dependent cytokines regulatory role of arginase/NO synthesis by intracellular substrate depletion (Corraliza *et al.*, 1995).

Arginase I is induced in rat aortic smooth muscle cells by IL-4 associated with increased cell proliferation and an increase in polyamine (spermidine and spermine) production after 24 h incubation (Ignarro *et al.*, 2001). Intimal hyperplasia was detected in premenopausal human uterine arteries with enhanced arginase activity in both endothelial cells and the smooth muscle layer, and impaired cyclic GMP production in endothelial cells, which suggests a role of arginase in vascular remodelling (Loyaga-Rendon *et al.*, 2005). Different regulators of arginases are shown in Table 1.7. N-Hydroxy-L-arginine an intermediate of NO biosynthesis is an arginase inhibitor; however, 2(*S*)-amino-6-boronohexanoic acid and (*S*)-2-boronoethyl-L-Cysteine-HCl (Figure 1.10), which are boronic acid derivatives, are not inhibitors of NOS. It is possible that these synthetic boronic acid-based arginine analogues inhibit arginase leading to increased arginine availability for NOS (Colleluori & Ash, 2001; Durante *et al.*, 2007). In addition, the arginase product L-ornithine acts as a competitive inhibitor of arginase activity and also inhibits cellular L-arginine transport (Messeri *et al.*, 2000; Cox *et al.*, 2001).

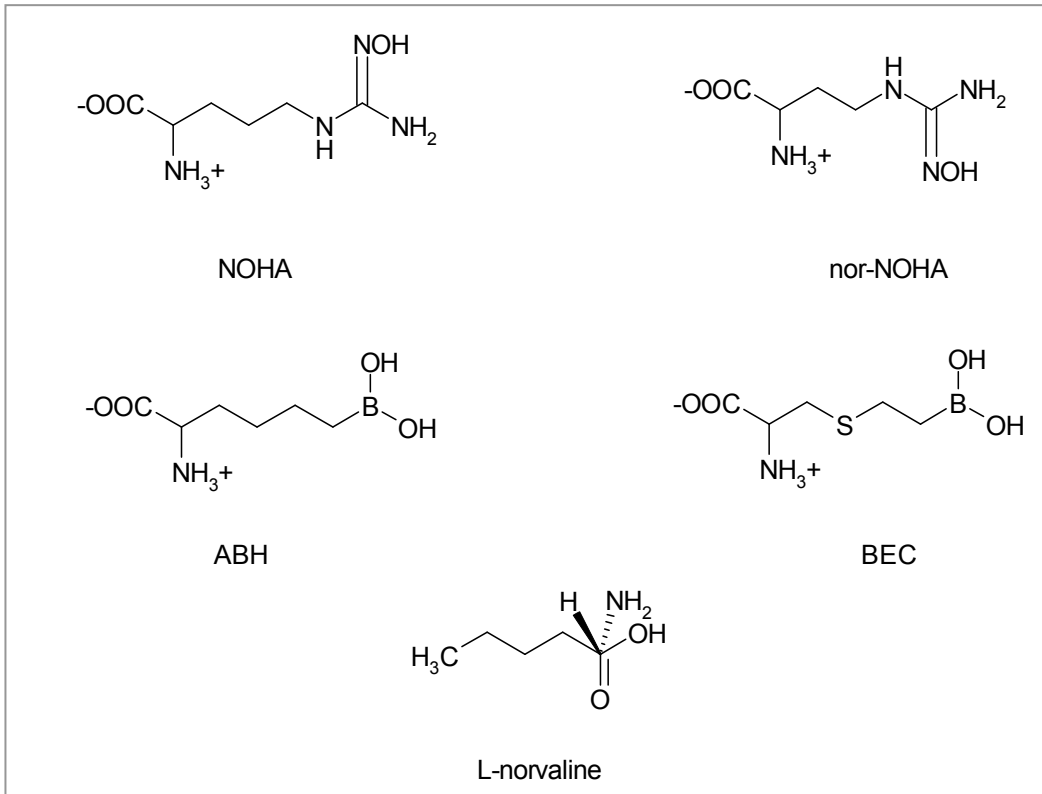

Figure 1.10 Structure of some arginase inhibitors. (Christianson, 2005)
NOHA: *N*-Hydroxy-L-arginine, nor-NOHA: *N*-Hydroxy-nor-L-arginine,
ABH: 2(*S*)-amino-6-boronohexanoic acid,
BEC: (*S*)-2-boronoethyl-L-cysteine-HCl

Table 1.7 Regulation of arginase I and II

Arginase regulator	Model	Reference(s)
IL-4, IL-10, PGE2	Murine macrophages	Modolell *et al.*, 1995; Corraliza *et al.*, 1995; Munder *et al.*, 1999
IL-4, IL-13	Rat airway fibroblasts Murine macrophages Dendritic cells	Munder *et al.*, 1999; Lindemann & Racke, 2003; Barksdale *et al.*, 2004
TGF-β	Rat peritoneal macrophages Murine macrophages Dendritic cells	Boutard *et al.*, 1995
PDE inhibitors	Alveolar macrophages RAW 264.7 cells	Hammermann *et al.*, 2000; Erdely *et al.*, 2006
Oxygen tension	Rat peritoneal macrophages Murine macrophage cell lines	Louis *et al.*, 1998
Cigarette smoke	Asthmatic subjects Airway epithelial cells Smooth muscle BEAS-2B cell line	Bergeron *et al.*, 2007

1.6.3 Arginase and asthma

Changes in L-arginine homeostasis in the airways may contribute to key features of allergic asthma, such as AHR, inflammation and remodelling of the airway wall (de Gouw *et al.*, 1999; Takemoto *et al.*, 2007; Maarsingh *et al.*, 2008b). L-arginine is uptaken intracellularly via specific cationic amino acids transporters (CAT) (reviewed in White, 1985). Arginases transform arginine into ornithine, which gives rise to polyamines and proline (Figure 1.11). Polyamines are essential for cell proliferation and differentiation demonstrated by the failure of Chinese hamster ovary (CHO) cell line, deficient in arginase, to proliferate unless provided with polyamines i.e. putrescine, spermidine or spermine (Holtta & Pohjanpelto, 1982). Overexpression of ornithine decarboxylase, a rate-limiting enzyme in polyamine biosynthesis, in fibroblasts results in increased expression of genes implicated in cell proliferation by promoting histone acetyltransferase activity and chromatin hyperacetylation (Hobbs & Gilmour, 2000).

The role of proline in collagen formation, which might underlies subepithelial fibrosis seen in asthma, was demonstrated as collagen I mRNA, arginase I and II mRNA are induced in a mouse model of bleomycin-induced lung fibrosis (Endo *et al.*, 2003). Arginine is also a substrate for NOS, which generates NO, an essential regulator of airway smooth muscle tone (reviewed in Fischer *et al.*, 2002). The NOS and arginase pathways, through substrate competition, can modulate each other. Th2 cytokines induce arginase expression (Munder *et al.*, 1999; Yang *et al.*, 2006). Increased expression of arginase I subjected to intratracheal adminstration of IL-13 correlates with AHR and mucus overproduction in OVA-sensitised as well as wild-type mice (Yang *et al.*, 2006). Overexpression of arginase I in lung epithelial cells increases basal and cytokine-induced NF-κB activity and is associated with reduced NO production and decreased S-nitrosylation of p50 (Ckless *et al.*, 2007). Lung inflammation in the form of eosinophilia, together with up-regulation of eotaxin-1 and IL-4 is detected in L-arginine transporter (CAT-2) knockout mice and NO production by activated alveolar macrophages is diminished in these animals (Rothenberg *et al*., 2006).

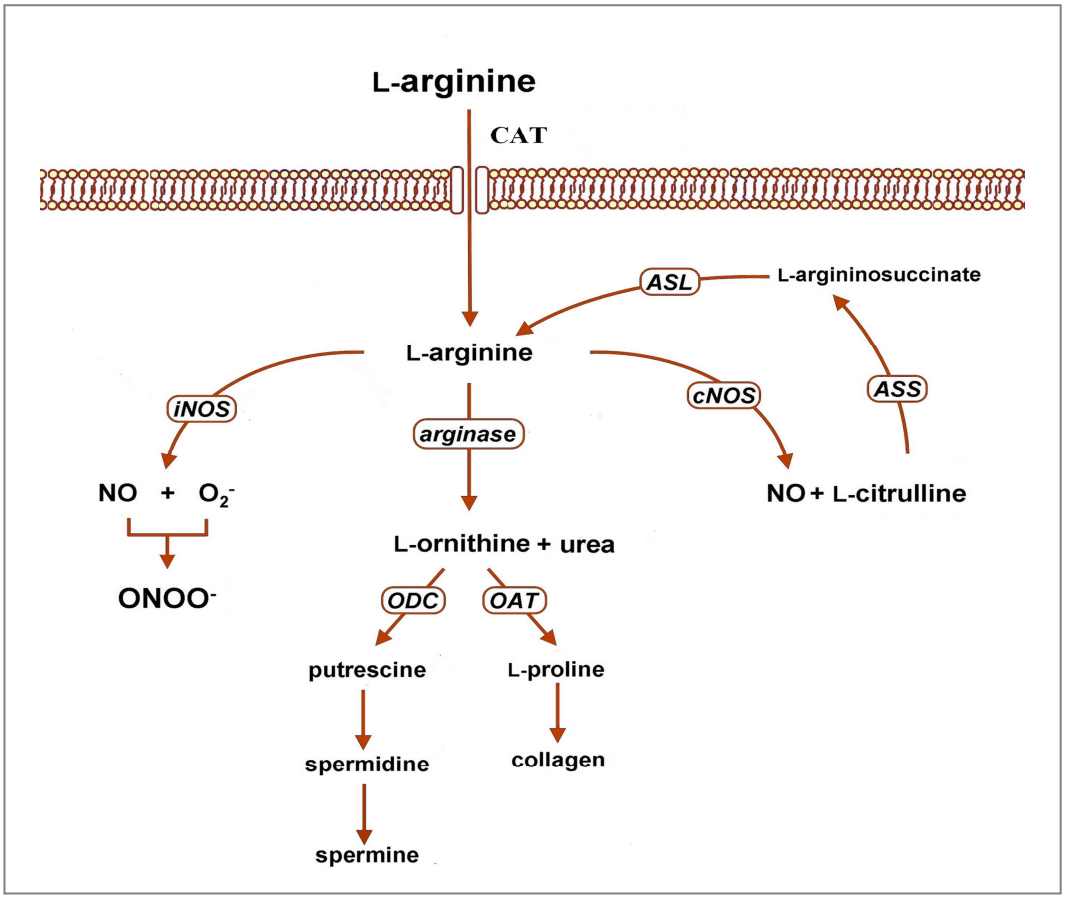

Figure 1.11 Metabolic fate of arginine in health and allergic asthma. L-Arginine is transported by specific cationic amino acid transporters (CAT) and can be metabolized by constitutive nitric oxide (cNOS) and arginase. The bioavailability of L-Arg determines the production of bronchodilating NO that regulates airway function. L-Arg bioavailability to NOS is also regulated by substrate competition. Arginase converts L-Arg into L-ornithine and urea. L-Orn is the precursor of polyamines (putrescine, spermidine and spermine) by ornithine decarboxylase (ODC) and L-proline by ornithine aminotransferase (OAT). Polyamines and L-Pro are involved in cell proliferation and collagen synthesis, respectively. L-Citrulline, the co-product in NO synthesis, can be recycled to L-Arg in two steps *via* argininosuccinate synthase (ASS) and argininosuccinate lyase (ASL) (Maarsingh *et al.*, 2008a).

1.7 Gene therapy in lung diseases

1.7.1 Introduction

Gene therapy is defined as the introduction of nucleic acids into cells for the purpose of altering the course of a medical condition or disease (Kay *et al.*, 1997). The introduced nucleic acid can replace a defective or absent gene (Kolb *et al.*, 2006). Indeed, transgenic, knockout and knockin mice can be the best available *in vivo* tool to study lung diseases models. However, generating these genetically engineered animals requires a significant amount of time, money, and effort (Dillon *et al.*, 2005). The lung represents an ideal organ for gene therapy because of its accessibility for drug delivery through both airways and vasculature. Either route of administration, or even a combination of both, might be advantageous in the targeting of lung diseases. The transfer of genes *via* the airway results in gene manipulation mainly in lung epithelial cells with minimal systemic distribution and low systemic side effects. The IV route of gene therapy transduces predominantly endothelial cells and can access primary or metastatic lung tumors. The epithelial cells of the large and small airways are usually the targets for gene therapy while entry to the parenchyma is considered to be more difficult. CF and α_1-antitrypsin deficiency, being a single gene defects diseases are the most amenable respiratory diseases for gene therapy. However, COPD, asthma, or interstitial lung diseases, being multifactorial diseases can be amenable to transient gene therapy by short-term overexpression of protective genes or the suppression of damaging genes (Kolb *et al.*, 2006). Surfactant protein B (SP-B) deficiency, an autosomal recessive pulmonary disease in neonates, which leads to lethal respiratory failure within the first year of life, might require prenatal or fetal gene therapy (Korst *et al.*, 1995).

CF has been considered the major lung disease for intervention by transfecting pulmonary cells with a functioning gene copy of the wild-type (normal) CFTR gene. The feasibility of gene replacement therapy for CF was first shown in experiments demonstrating that the introduction of normal CFTR gene into cultured CF airway epithelial cells restores normal chloride ion transport (Rich *et al.*, 1990; Drumm *et al.*, 1990). As extensively reviewed in Kolb *et al*. (2006), several problems have been identified and interfer with the restoration of human CF gene. The ideal vector system

has not yet been developed, gene transfection has been achieved the levels of expression are short-lived. Mucous plugs and local infections render gene therapy to the superficial epithelium not within reach by the aerosols. Thus, better access by the vasculature and systemic vector application can be achieved (Kolb *et al.*, 2006).

α_1-Antitrypsin (α_1 AT) deficiency is a second pulmonary disease with an underlying single gene defect and a target for gene therapy. α_1- AT protein is a serum glycoprotein that is synthesized and secreted primarily from the liver, however its major site of action is the lower respiratory tract where its passive diffusion into the alveoli protect against neutrophil elastase-mediated proteolysis (Kueppers, 1973). Still short-lived expression and not high enough protein concentration delivered are problems facing gene therapy for those patients. Intratracheal administration of adenoviral vector encoding human α_1 AT gene to rats resulted in the synthesis and secretion of human α_1 AT, detected in the lung for at least 1week (Rosenfeld *et al.*, 1991). Adenovirus-vector induces inflammation, which means that repeated adminstration would not solve the problem of transient expression. An alternative vector, liposomes, were used in New Zealand white rabbits by either aerosol or intravenous route to deliver α_1 AT cDNA, and resulted in local protein expression that last for 4 weeks without detected toxicity (Canonico *et al.*, 1994).

Gene therapy is also being considered as a rational therapeutic option for the treatment of inflammatory diseases of the lung including asthma and COPD. In these cases, disease is not the result of a single genetic defect but may be consequence of multiple factors (Kolb *et al.*, 2006). Canonico and coworkers have shown that the release of neutrophil chemoattractants from human airway epithelial cells exposed to human neutrophil elastase was prevented if the cells were transfected with the human α_1 AT cDNA prior to elastase exposure. This suggests that the general anti-inflammatory properties of antiproteases could be exploited for gene therapy in COPD (Canonico *et al.*, 1996). The mainstay treatment of asthma is inhaled corticosteroids and bronchodilators but this does not hold for all cases. Asthmatic patients who receive high doses of systemic corticosteroids or those with corticosteroid-resistant asthma can benefit from gene therapy. Both intratracheal and intravenous IFN-γ gene delivery significantly inhibit AHR and airway eosinophilia in mice with OVA-induced AHR (Dow *et al.*, 1999). In a similar study, IL-4Rα

antagonist delivered *via* recombinant adeno-associated virus vector to the airways of mice reduces AHR and airway eosinophilia triggered by either m-IL-13 or m-IL-4 (Zavorotinskaya *et al.*, 2003). In addition, the pulmonary circulation could be used to access primary or metastatic lung tumors (Kolb *et al.*, 2006). Hence, there are many lung disease states for which it might prove beneficial to deliver genes.

1.7.2 Vehicles of gene transfer

Table 1.8 Gene transfer vehicles taken from Kay *et al.*, 1997 and Kolb *et al.*, 2006

Vector	Advantages	Disadvantages
Viral ➢ Retrovirus	Integration into host DNA All viral genes removed Relatively safe	Transduction requires cell division Semi-random integration Relatively low titer
➢ Adenovirus	Higher titer Efficient transduction of nondividing cells *in vitro* and *in vivo*	Toxicity Immunological response
➢ Adeno-associated virus	All viral genes removed Safe Transduction of nondividing cells Stable expression	Small genome limits size of foreign DNA Labor-intensive production Status of genome not fully elucidated
➢ Parainfluenza virus 1 Sendai virus	RNA genome Targets apical surface of epithelium Replicates in cytoplasm	Particles are inflammatory, induce immunity
Nonviral • Liposomes	Simple, inexpensive, safe Nonimmunogenic	Inefficient gene transfer into the nucleus Lack of persistence of DNA
• Naked DNA	Simple, nonimmunogenic, inexpensive, safe	Inefficient transduction

Viral and nonviral vectors are used for gene transfer (Table 1.8). Gene transfer can be attempted by two approaches: an *ex vivo* approach where cells are removed, genetically modified, and transplanted back into the same recipient, and *in vivo* therapy adopted by direct transfer of genetic materials (Kay *et al.*, 1997).

1.7.3 RNA interference

DNA has been used for most transfections. It is more stable than RNA and can be produced in large quantities. The half-life of stable mRNA species in the mammalian cell is less than 24 hours, while unintegrated DNA can persist and function in nondividing cells for months. However, a potentially significant advantage of using RNA-encoded antigens is safety. Although RNA transfection results in low level of intact protein expression it may offer a significant advantage to decrease expected immune response (Mitchell & Nair, 2000).

RNAi is the process of sequence-specific, post-transcriptional gene silencing in animals and plants, initiated by double-stranded RNA (dsRNA) that is homologous in sequence to the silenced gene (Fire, 1999). RNAi has become a widely used simple, cheap, and powerful experimental tool to explore the function of mammalian genes, both *in vitro* and *in vivo*. RNAi can be induced by the introduction of synthetic double-stranded small interfering RNAs (siRNAs) 21–23 base pairs (bp) in length or by plasmid and viral vector systems that express double-stranded short hairpin RNAs (shRNAs) that are subsequently processed to siRNAs by the cellular machinery to specifically target a gene's product, resulting in null or hypomorphic phenotypes. RNAi is considered as an important tool not only for functional studies, but also to silence disease-associated genes in tissue culture, animal models and the development of RNAi-based reagents for clinical applications. The identification of most of the genes in the human genome generated large number of potential new drug targets that await discovery. However, the main limitation is to know which gene products are functionally involved in the pathology of a disease (target validation) (Dillon *et al.*, 2005; Leung & Whittaker, 2005).

RNAi was first observed by plant biologists in the late 1980s, but its molecular mechanism remained unclear until the paper in the late 1990s by Fire *et al*.

1998 (Fire *et al.*, 1998). The mechanism of RNAi is shown in Figure 1.12. Briefly, long double-stranded RNAs (dsRNAs; typically >200 nt) is processed to a 20-25 bp nucleotide siRNAs by an RNase III-like enzyme called Dicer (initiation step). Then, the siRNAs assemble into endoribonuclease-containing complexes known as RNA-induced silencing complex (RISC), unwinding in the process. The siRNA strands subsequently guide the RISCs to complementary RNA molecules, where they cleave and destroy the cognate RNA (effector step). Cleavage of cognate RNA takes place near the middle of the region bound by the siRNA strand. In mammalian cells, introduction of long dsRNA (>30 nt) initiates a potent antiviral response, exemplified by nonspecific inhibition of protein synthesis and RNA degradation. This mammalian antiviral response can be bypassed by the introduction or expression of siRNAs (Dykxhoorn *et al.*, 2003).

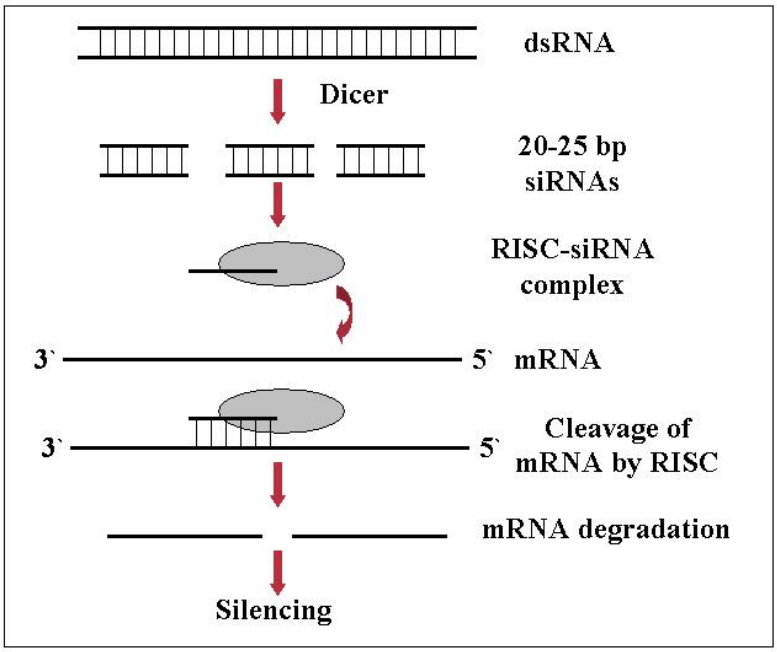

Figure 1.12 The mechanism of RNA interference. Long double-stranded RNAs (dsRNAs) is cleaved to a 20-25 bp nucleotide siRNAs by Dicer. siRNAs assemble into RNA-induced silencing complex (RISC). The siRNA strands guide the RISCs to complementary mRNA molecules to cleave the mRNA.

The functional role of individual genes using siRNA has been commonly used in different diseases as extensively reviewed in Dillon *et al.* (2005). The use of inhaled antisense oligonucleotides (Tanaka & Nyce, 2001) suggest that the delivery of siRNA molecules to the lung might be a viable approach to the treatment of respiratory diseases such as cystic fibrosis, asthma and COPD. Cell-specific targeting of siRNA is an important issue to consider during therapy. RNAi silencing specifically in rat lung alveolar epithelial type II cells using adenoviral vectors containing various shRNAs under the control of the surfactant protein C promoter was demonstrated both *in vitro* and *in vivo* (Gou *et al.*, 2004). Also, using siRNA to knock down TGF-α production diminishes mucus production in NCI-H292 human airway epithelial cells (Shao *et al.*, 2004).

Currently, developing clinical applications of siRNA in various human diseases is in the spot-light of many pharmaceutical companies (Howard, 2003; Leung & Whittaker, 2005). RNAi has the advantages of easy synthesis, low production costs (compared with protein or antibody therapies), and delivery to a wide range of organs. However, blood stability, delivery, poor intracellular uptake, and nonspecific immune stimulation still present significant challenges for the development of RNAi reagents for clinical use (Leung & Whittaker, 2005).

Off-target effects, defined as siRNAs effects on non-target genes causing change in their expression (Dillon *et al.*, 2005), can be an obstacle for usage of siRNA. Off-target effects depend on the concentration of siRNAs and similarities between the non-target genes and the 5' ends of siRNAs (Jackson *et al.*, 2003; Persengiev *et al.*, 2004). A second major limitation is an antiviral interferon response and apoptosis, however dsRNAs that are less than 30 bases in length are able to silence gene expression in a specific manner without triggering the interferon response (Elbashir *et al.*, 2001). Still some studies demonstrated that short dsRNAs trigger an interferon response (Bridge *et al.*, 2003; Sledz *et al.*, 2003). RNAi may act on dendritic cells *in vivo* by activation of Toll-like receptors, leading to unwanted immune response (Maguire *et al.*, 2008). Application of siRNA molecules as therapeutics from cells to man is still challenging. Perhaps the most significant limitation is the safe, efficient and effective delivery of RNAi reagents.

1.7.4 Recent clinical gene therapy research

Results of subretinal injections of recombinant adeno-associated virus vector contains the human RPE65 coding retinal pigment epithelial (RPE65) for inherited blindness show sight improvement, a landmark for gene therapy technology (Bainbridge *et al.*, 2008). Researchers at the National Cancer Institute (NCI), part of the National Institutes of Health, successfully re-engineer lymphocytes, to target advanced metastatic melanoma (Rosenberg *et al.*, 2008). Another progress in gene therapy technology to evaluate the safety, and efficacy of repeated intratumoral injections of adenovirus-IL-2 (TG1024) in patients with advanced solid tumors and melanoma, only injection site reactions and flu-like syndrome were noticed in those patients (Dummer *et al.*, 2008). However, leukaemia due to inadvertent vector-mediated upregulation of host cellular oncogenes is recorded in two clinical studies of gene therapy (Hacein-Bey-Abina *et al.*, 2003; Howe *et al.*, 2008). Gene therapy for CF started in 1990 with the demonstration that ion conductance could be restored by giving CF cells a normal copy of the CFTR gene. The UK cystic fibrosis gene therapy consortium announced two clinical trials were completed in 2006/2007 to measure CFTR expression and function in patients to select the most effective methods to measure changes in the lung after gene therapy. One of these studies used BAL fluid from 39 CF children and 38 respiratory disease controls and the most discriminatory biomarker found had a mass of 5.163 kDa (Macgregor *et al.*, 2008).

1.8 Aims of the study

This research is based on the finding that IL-13 is implicated as a key cytokine in the pathogenesis of allergy and asthma. Pulmonary expression of IL-13 induces an asthma-like phenotype in mice. AHR is a key sign of asthma and underlies the spontaneous airflow limitation seen in asthma. AHR characterizes a complex interaction between resident and recruited inflammatory cells at sites of injury. However, growing evidence indicate the crucial role of different resident cells to mediate AHR. One aim of this study to use an *in vitro* isolated tracheal ring model to investigate the role of resident cells in IL-13-induced hyperresponsiveness. Also, which rodent species displays the most IL-13-induced hyperresponsiveness and the

effect of murine-, rat- and human-IL-13 on two commonly used animal model species i.e. mouse and rat.

The mechanism(s) by which IL-13 induces hyperresponsiveness remains unclear. PI3K is known to play a role in inflammatory lung diseases; therefore it is an attractive target for the potential treatment of respiratory diseases. Furthermore, targeting specific PI3K isoforms that may be overexpressed or overactive may allow control for conventional drugs resistant cases. Another aim of this work to test the hypothesis that IL-13-induced hyperresponsiveness in isolated murine tracheal rings is regulated by PI3K. As mice lacking p110δ exhibit a high degree of normal development and growth, investigation of the role of p110δ can characterize the roles of this PI3K isoform in IL-13-induced hyperresponsiveness. The non-isoform-selective inhibitors wortmannin and LY294002, or the selective inhibitor of p110δ, IC87114 will be studied. To investigate further evidence for the role of p110δ in IL-13-induced hyperresponsiveness, tracheae from genetically–modified mice will be employed. The role of IL-13 in induction of arginase I as a potential mechanism of IL-13-induced hyperresponsiveness, with an assessment of the role of the epithelium, will be undertaken. Moreover, the possible link between PI3K and arginase I in IL-13-induced hyperresponsiveness will be studied.

The development of siRNA has facilitated a better understanding of the role that each member of PI3K family plays in the physiology and pathology of the respiratory system. A significant part of of this study to deliver siRNA to inhibit expression of determined target(s). For this purpose, the use of lipid based vectors for non-viral gene delivery or the employment of a reverse permeabilization technique in tracheal segments will be investigated. Determination of target(s) involved in IL-13-enhanced hyperresponsiveness will help in the development of new therapeutic strategies for the effective treatment of inflammatory lung diseases such as asthma.

Chapter Two

Methods and Materials

2.1 Organ bath experiments

2.1.1 Animals

Male CD1 mice (25-30 g, 8-10 week-old) and Wistar rats (200-300 g, 8 week-old), were used in this study (University of Bath). In another set of experiments, tissues from genetically modified mice (male or female, 6-8 week-old) expressing a catalytically inactive p110 isoform of PI3K ($p110\delta^{D910A/D910A}$) and matched DO11.10 control mice (Okkenhaug *et al.*, 2002) were kindly provided by Dr. K. Okkenhaug (Babraham Institute, Cambridge, UK). Breeding and maintenance of animals was according to UK Home Office regulations and guidelines for the care and welfare of laboratory animals, and fed with standard rodent chow and water *ad libitum*.

2.1.2 Tissue preparation and tracheal organ culture

Animals were killed by exposure to a rising concentration of CO_2. The thorax and ventral surface of the neck were opened by a mid-line longitudinal incision, and the trachea from the larynx to the carina rapidly removed. The oesophagus was carefully separated, and the trachea cleared of loose connective tissue and divided into 2-4 segments according to the subsequent experiment. Tissues were placed individually into multiwell plates containing Dulbecco's modified Eagle's medium (DMEM) containing 25 mM D-glucose, 1 mM sodium pyruvate, 100 U/ml penicillin, 100 μg/ml streptomycin, 4 mM L-glutamine, 2.5 μg/ml Fungizone, and 0.1% w/v bovine serum albumin (BSA). Tracheal segments were incubated at 37 °C in a humidified 5% CO_2 gassed incubator in the presence or absence (control) of IL-13. The effect of PI3K inhibition was assessed by treating murine tracheal rings with wortmannin (100 nM), LY294002 (10 μM), or IC87114 (10 μM) 30 min before IL-13 addition. These inhibitor concentrations were chosen based on their *in vitro* potencies Tracheal rings treated with dimethyl sulfoxide (DMSO) [0.05% (v/v)] served as vehicle controls in inhibitor experiments. In another set of experiments, tracheal segments were incubated in the presence or absence of IL-13 or an arginase inhibitor, L-norvaline (10 mM), for 24 h.

2.1.3 Isometric recording of airway smooth muscle

Trachea smooth muscle reactivity was assessed using temperature-controlled (37 °C) organ baths containing Krebs-Henseleit buffer solution (see section 9.1) continuously bubbled with 5% CO_2 and 95% O_2. Tracheal segments were mounted in organ baths between two metal hooks. One hook was connected via a loop of thread to a K30 force displacement transducer (Hugo Sachs Elektronik, March, Germany); the other hook connected to the base of displacement rod in order to be able to change the tension of the mounted segments. Murine segments were suspended under approximately 5 mN resting tension for continuous recording of isometric tension while rat tracheal segments suspended using 10 mN tension. Care was taken to mount the tracheal segments so that the membranous part of the rings was not in contact with the hook. The tissues were equilibrated in the organ bath for 1 h, during which time each tissue exposed to 60 mM KCl three times with 15 min resting period in between each addition. At the plateau of KCl induced-contraction, each preparation was washed with Krebs-Henseleit solution until active tension returned to baseline. Isometric contractile responses were recorded with a MacLab/4e and Quad bridge amplifier linked to a PC running Chart 4 software for Windows (ADInstruments Ltd, Chalgrove, Oxfordshire, UK). Cumulative concentration-response curves to carbachol (10^{-8} to 10^{-5} M) or KCl (10 to 100 mM) were determined. Relaxation response curves after contracting the tissue with a submaximal dose of CCh were recorded using isoprenaline (10^{-8} to 10^{-5} M).

2.1.4 Epithelial removal

Mechanical removal of the airway epithelial layer was achieved by gently rubbing the luminal surface of the murine tracheal segments either before or after incubation with m-IL-13 or media alone (control). Epithelium denudation was confirmed by histological examination of the segments (see section 2.4.1 & 2.4.2).

2.2 Cell lines

2.2.1 Airway epithelial cell lines

9HTEo-, A549 and BEAS-2B were used in this study. 9HTEo- are SV40 transformed human tracheal epithelial cells which retain phenotypic characteristics of epithelial cells such as chloride ion transport, keratin, microvilli, and tight junctions (Gruenert *et al.*, 1988). A549 are human alveolar epithelial cells (Giard *et al.*, 1973) obtained from the European Collection of animal cell culture while BEAS-2B are adeno 12 SV40-transformed human bronchial epithelial cells (Reddel *et al.*, 1988) obtained from American Tissue Culture Collection.

2.2.2 Thawing cell lines

Flasks used for BEAS-2B cells were precoated for at least 4 h at 37 °C with a mixture of 0.01 mg/ml fibronectin, 0.03 mg/ml bovine collagen type I and 0.01 mg/ml BSA dissolved in basal LHC medium. The fibronectin, collagen and BSA were gently mixed in basal LHC medium, not vortexed. The bottom half of the cryotube containing the cell line was placed in a 37 °C water bath until the cells were defrosted. Immediately afterwards, the cryotube was wiped with 70% ethanol and all operations from this point were carried out under aseptic conditions. The contents of the cryotube were transferred dropwise into a sterile 15 ml plastic tube containing 10 ml prewarmed media. The tube was then centrifuged for 10 min at 20 ºC. The supernatant was discarded and cells pellet thoroughly resuspended in fresh warmed media. Cell viability and number were checked using a Neubauer haemocytometer after mixing 1:1 with 0.4% trypan blue. More than 90% of the cells were viable. Cells were then seeded into 75 cm^2 tissue culture flasks containing 15 ml warm media and maintained at 37 °C in a 5% CO_2 humidified incubator. On the following day the media were replaced with fresh warm media and replaced again every 2 days. Cells reached 60-80% confluence after 4-5 days (see section 9.2 for each cell line cultured conditions).

2.2.3 Subculture

After reaching 60-80 % confluence, media were removed and the cells washed twice with warm sterile D-PBS to get rid of any serum. The flasks were incubated with 3 ml of prewarmed trypsin-EDTA for 3-10 min at 37 °C, removed from the incubator and 10 ml prewarmed media added to inhibit the effect of the trypsin. The side of the flask was tapped to dislodge any remaining adherent cells. The dislodged cells were centrifuged for 5 min at 20 °C for subsequent cell counting and seeding in 75 cm^2 tissue culture flasks for further subculture or into 12-, 96-well plates or 35 mm diameter petri dish (see section 9.2 for each cell line cultured conditions).

2.2.4 Freezing cell lines

Cells were grown to 50-60% confluence, dislodged by trypsinization and checked for viability and counted using trypan blue exclusion. Cells were resuspended at $2x10^6$ cells / ml of freezing media into sterile labelled cryotubes with the name of cell line, medium, date and passage number (see section 9.2). Cryotubes containing either 9HTEo- or A549 were gradually cooled in isopropyl alcohol at -80 °C for 16 h, and stored into liquid nitrogen tanks while cryotubes containing BEAS-2B cells were stored straightaway in liquid nitrogen vapour phase tanks.

2.3. Histology

2.3.1 Embedding and sectioning

A plastic tube, to store the tissue-mounted disks, was placed into liquid nitrogen. A glass beaker was half filled with isopentane and placed in liquid nitrogen to allow the isopentane to cool. Isopentane turns white as it solidifies on the base of the beaker. Then enough Optimum Cutting Temperature (OCT) compound was added onto the surface of a cork disk for embedding the tissue. The cork disk was held in the cold isopentane for a few seconds or until it began to solidify and then removed from the isopentane. The solution was gently removed from around the tissue about to be frozen, the tracheal ring placed into the OCT and manipulated so that the lumen is

facing upward. Air bubbles were avoided and more OCT was added if necessary so that no bare areas were observed. The disk with sample was placed back into the isopentane and stored at -80 °C until use. The samples were sectioned using a cryostat (5030 Microtome, Bright Instruments company Ltd., Huntingdon, England) to obtain 5 μm flat, thin, wrinkle-free, fully intact, frozen sections bonded to Superfrost Plus microscopic slides (VWR International).

2.3.2 Haematoxylin and eosin stain

Slides were immersed in cold acetone (4 °C) for 5 min, and then rehydrated in tap water for 5 min. From this point onwards sections were not allowed to dry out. The slides were immersed in Harris Haematoxylin (HH, diluted 1 part HH to 3 parts water) for 5 min and shaken to remove the excess. Then they were immersed in running water for 5 min, immersed in acid/alcohol (IMS with 1% v/v HCl) for up to 30 seconds and agitated gently to differentiate the stain. The slides were then rinsed in water for 5 min, immersed in eosin for 30 s, rinsed again in running water for 5 min and excess water gently removed. Dehydration was then induced by immersing the slides in IMS for 1 min. Excess IMS was shaken off and the slides were immersed again in a second bath of IMS. This, and subsequent steps were carried out in a fume hood. Sections were then cleared by immersing in xylene for 1 min twice. The transfer of water to IMS and of IMS to xylene was avoided. Sections were mounted using DePeX mounting medium, the under-surface of the slides was cleaned using tissue soaked with xylene, and slides were allowed to dry for at least an hour before microscopic examination.

2.3.3 Specimen preparation for immunohistochemistry

Mice tracheae were dissected, treated with IL-13 with or without the inhibitors or the control vehicle, and fixed in 4% paraformaldehyde (PFA) for 24 h at 4 °C. After fixation, the tissue blocks were embedded in paraffin. The embedding of paraffin blocks were carried out using Leica TP1020 automatic tissue processor (Leica Microsystems) then cut into 5 μm sections using a microtome. Sections were then transferred onto Superfrost Plus microscopic slides, left overnight to dry to

remove any water that may be trapped under the section, and stored at 4 °C until microscopic examination.

2.3.4 Preparation of 4% PFA for fixation

PFA was prepared by the addition of 4 g of PFA into 65 ml of distilled water heated up to 60 °C. The solution was stirred, maintained at 60 °C on hot plate in the fume hood and then approximately 2-4 drops of 2 M NaOH were added. The solution was removed from the heater, 21 ml of 3X PBS added and the pH then adjusted to 7.2 with 1 M aq. HCl. Deionized water was added to a final volume of 100 ml, the solution filtered and then stored at -20 °C for up to a month.

2.4 Immunoblotting

Immunoblot analysis is a technique of identifying specific proteins in a given sample of cell or tissue homogenate. It uses gel electrophoresis to separate denatured proteins according to their molecular weight. The proteins are then transferred to a nitrocellulose or polyvinylidene fluoride membrane, and detected using antibodies (primary antibodies) specific to the target protein. Afterwards, the membrane is exposed to another antibody known as secondary antibody which is commonly horseradish peroxidase-linked to catalyse a reaction that, in the presence of chemilumnescent reagents produces luminescence in proportion to the amount of protein and is detected using photosensitive film.

2.4.1 Tissue lysis

After 24 h incubation with or without IL-13 and/or inhibitors, tracheal rings were rapidly frozen and stored in liquid nitrogen until used. Then, they were broken down mechanically using PowerGen 125 homogenizer (Fisher Scientific Co., Loughborough, UK) in 200 µl cold lysis buffer (see section 9.3) per 6-8 pooled tracheal rings. Lysates were rotated at 4^{o}C for 15 min to allow inhibition of proteases, centrifuged at 15,400g for 15 min at 4 °C, and the supernatant collected.

2.4.2 Quantification of protein

Protein concentration was quantified using the Bradford assay (Bio-Rad Laboratories, Hercules, USA) (Bradford, 1976). BSA solution (1 mg/ml) was prepared and used to construct a standard curve at concentrations of 0-32 μg/ μl. Equal volumes (2 μl) of each lysate sample were added to 250 μl of Bio-Rad Bradford dye reagent (BioRad). Both the standard and lysate samples were carried out in triplicate using a 96-well microtitre plate. Protein concentration was measured at 595 nm with a microplate reader using Softmax Pro software (Molecular Devices, VERSAmax, U.S.A.).

2.4.3 Sample preparation

After determining protein concentrations, lysate samples were diluted with ice-cold lysis buffer to normalize the protein concentrations between the samples and 100 μl of each diluted sample mixed with 25 μl of 5X sodium dodecyl sulphate sample buffer (see section 9.3) to give a final protein concentration of approximately 1.5-2 μg/μl. The samples were then mixed, boiled at 100 °C for 5 min using Techne dri block DB 2A (Techne Cambridge Limited, Cambridge, UK), and transferred immediately into ice. At this point, the samples could be stored at -20 °C for subsequent Western immunoblotting.

2.4.4 Gel electrophoresis

One-dimensional polyacrylamide gels were employed which allows separation of proteins according to their molecular weight, thus smaller proteins migrate faster than proteins of higher molecular weight. The proteins of the samples were separated using Bio-Rad Mini Protean II system (Bio-Rad Labs. Hemel Hempstead, UK). The resolving and stacking recipe were prepared following the recipe described in section 9.4. The resolving gel was prepared at 10 % of acrylamide for all proteins studied. The resolving gel was pipetted between the assembled glass plates and overlaid with deionized to create a uniform surface. The resolving gel would polymerize after 40 min, the water was withdrawn and the stacking gel poured on top of the resolving gel. A gel comb (which formed the wells where prepared

samples and ladder were placed) was inserted into the stacking gel and the gel left to polymerize for another 20 min. After that, the comb was removed and the wells washed thoroughly with deionized water and then filled with running buffer (see section 9.3). With the use of a micropipette, 20 µl (~30 µg of protein per lane) of the samples were loaded into the bottom of the wells. One lane was reserved for a marker (5-10 µl), a commercially available mixture of proteins having defined molecular weights. The gels were run at 20 °C at 80 V until the bromophenol blue tracking contained in the samples entered the resolving gel, and then the voltage increased to 180 V. The gels were then run until the desired separation of bands in reference to the molecular weight markers was achieved, then gels were removed from the electrophoresis equipment and placed into semi-dry transfer buffer (see section 9.3).

2.4.5 Transfer of proteins to nitrocellulose membrane

In order to make the proteins accessible to antibody detection, they were moved from within the gel onto a membrane made of nitrocellulose using the graphite electrode of transfer apparatus (Transblot SD cell; Bio-Rad Laboratories, USA). As shown in Figure 2.1, four pieces of Whatman paper were placed on the bottom electrode followed by the nitrocellulose membrane. Then the resolving gel was placed on top of the nitrocellulose paper, followed by another four pieces of Whatman paper. Blotting and nitrocellulose papers were cut to the size of the gel and pre-soaked in the semi-dry transfer buffer before placed. The layers were pressed gently to expel any air bubbles to ensure efficient electroblotting, and then the upper negative electrode, dampened with transfer buffer, positioned. The proteins were electro-transferred from the gel on the membrane at 20 °C with the following settings, 1 h duration, at 0.8 mA current per 1 cm^2 of gel (approximately 40 mA per gel). When the transfer was completed, the nitrocellulose membrane was placed in Tris buffered saline (TBS, see section 9.3 for composition) plus 0.1% Tween 20 (TBS-Tween 20). TBS-Tween 20 was thrown away and the membrane was gently shaken in Ponceau S at 20 °C for 1-2 min to verify successful protein transfer.

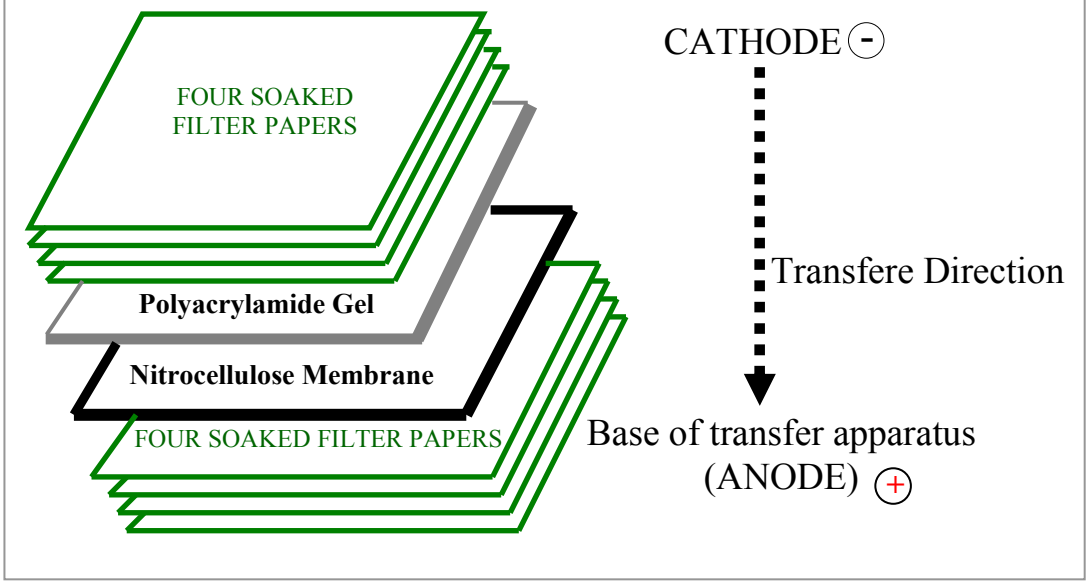

Figure 2.1 Transfer of proteins to nitrocellulose membrane.

2.4.6 Antibody probing and immunoblot developing

To block non-specific binding sites on the nitrocellulose membrane, it was incubated with 10 ml TBS-Tween 20 with 5% w/v non-fat milk and left to shake for 1 h at 20 °C. The membrane was then washed using 1x TBS-Tween 20 three times, 5 min per wash, and incubated for 16 h at 4 °C under gentle agitation with 10 ml of TBS-Tween 20 with 0.1% sodium azide and the desired concentration of the primary antibody (see section 9.5). The antibody solution was removed and kept for future use. On the following day, the membrane was washed three times in 1x TBS-Tween 20, 5 min per wash, and incubated with horseradish peroxidase-conjugated secondary antibody at the recommended concentration (see section 9.5) in 10 ml TBS-tween 20 and 1% (w/v) non-fat milk for two hours with gentle agitation at 20 °C. The membrane was again washed three times in TBS-Tween 20, 5 min per wash and bound antibody detected using Enhanced Chemiluminescent Lumigen (ECL) reagent according to the manufacturer's instruction, placed in cling film to prevent drying and exposed to photosensitive film (Fujifilm Corporation, Tokyo, Japan) using an X-ray film processor (model RGII, Fuji). The intensity of the specific bands was quantified by densitometric analysis using Labimage software (Kapelan Bio-imaging Solutions, Halle, Germany).

2.5 Immunohistochemistry (IHC)

2.5.1 Deparaffinization and rehydration of sections

The sections were dewaxed by immersing the slides into Histoclear I and then Histoclear II, for 7 min each. Then the slides were immersed twice into 100% ethanol for 1 min each and then 95%, 90%, 70% and 50% ethanol, 1 min each. The slides were rinsed in distilled H_2O for 1 min. From this point onwards the slides were not allowed to dry to avoid non-specific antibody binding that causes high background. The slides were washed twice in PBS, 5 min per wash and tracheal sections permeabilized by immersing the slides in 0.5% Triton X 100 in PBS for 30 min at 20 °C. After permeabilization, the slides were washed twice with PBS for 5 min per wash.

2.5.2 Antigen retrieval and antibody staining

Most formalin-fixed tissue requires an antigen retrieval step before immunohistochemical staining due to the formation of protein cross-links that mask the antigenic sites in tissue specimens giving weak or false negative staining. EDTA buffer was used to break the protein cross-links and unmask the antigens in formalin-fixed and paraffin embedded tissue sections.

The sections were covered with EDTA buffer and the slides placed on a holder in a humid box at 37 °C for 1 h. The slides were then washed twice with PBS with 5 min per wash. After washing, the sections were framed using PAP pen to decrease the volume of the antibody used. Peroxo-Block was added for 1-2 min to quench endogenous peroxidase activity, and sections were then washed twice with PBS for 5 min per wash. The tracheal sections were covered with 5% FBS in PBS for 20 min to block non- specific binding, then washed twice with PBS, 1 min per wash. Rabbit polyclonal anti-arginase I antibody 1:100 dilution in PBS was applied on the tracheal tissue sections and the slides placed in a moistened chamber at 4 °C for 16 h. Mouse liver tissue sections, as a positive control, and tracheal rings sections in which the primary antibody was omitted to exclude non-specific binding, as a negative control, were used. On the following day, the slides were washed twice with PBS, 5

min per wash, and then the SuperPicTure™ Polymer Detection Kit used according to the protocol provided by the manufacturer (Zymed Laboratories, Invitrogen). The slides were immersed in two separate IMS solutions for 3 min each and then two separate xylene solutions for 3 min each. The sections were mounted using DePeX mounting medium and visualised using an inverted microscope stage (Olympus 1X51).

2.6 siRNA

2.6.1 Transfection of cell lines with fluorescent siRNA

The Label IT® RNAi delivery control was used for this experiment. For the siRNA-vector complex formation, two solutions were prepared for each well of a 12-well plate, solution A (RNA) and solution B (transfecting reagents). Solution A was prepared by diluting 1.25 µl siRNA solution (10 µM) to 12.5 µl (1 µM) using 1X RNAi dilution buffer in a 1.5 ml sterile plastic tube, gently mixing and incubating for 20 min at 20 °C. Solution B was prepared by adding TransIT–TKO Transfection reagent 10 µg/ 12.5 µl of 1 µM siRNA stock, 4 µl C20/ 12.5 µl of 1 µM siRNA stock and 6 µl C22/ 12.5 µl of 1 µM siRNA stock into Opti-MEM using a 1.5 ml sterile plastic tube, which was gently mixed and incubated for 20 min at 20 °C. The complex was then prepared by gently mixing solution A and B and incubated for 20 min at 20 °C.

For transfection, $5x10^4$ cells of A549 and $1x10^5$ cells of 9HTEo- were seeded in 12-well plates in 2 ml of complete medium per well and maintained at 37 °C in a 5% CO_2 humidified incubator for 24 h to reach 50-60 % confluence. Prior to transfection, the media was replaced with 437.5 µl of Opti-MEM into which 62.5 µl of the transfection complex was added dropwise for final volume of 500 µl/well with the exception of the control cells where 500 µl of Opti-MEM was used. The plates were gently rocked back and forth and from side to side to distribute the complex evenly, then maintained at 37 °C in a 5% CO_2 humidified incubator for 24 h. After that, the media was removed, replaced with 2 ml of complete media and incubated for a further 48 h.

2.6.2 Cytotoxicity (MTT) assay of RNAi-lipospermine complex

The MTT assay is a colorimetric assay used to evaluate the metabolic activity of viable cells in which a soluble tetrazolium salt [3-(4, 5-dimethylthiazol-2-yl)-2,5-diphenyl tetrazolium bromide (MTT)] is converted into an insoluble formazan crystal (Mosmann, 1983). It was used to investigate the cytotoxic effects of lipopolyamines and lipoplexes (siRNA complexes). RNase and DNase free water was used to dilute 10X RNAi to 1X RNAi dilution buffer. Two solutions, solution A and solution B were prepared. Solution A (siRNA) was prepared by diluting 0.25 µl solution siRNA (2.5 pmoles/well) to 2.5 µl using 1X RNAi dilution buffer in a 1.5 ml sterile plastic tube, gently mixed and incubated for 20 min at 20 °C. Solution B (transfection reagents) was prepared by diluting the transfection reagents solution to the same concentrations mentioned in section 2.6.3 in a 1.5 ml sterile plastic tube with Opti-MEM, gently mixing and incubating for 20 min at 20 °C. The complex was then prepared by mixing solution A and B and incubated for 20 min at 20 °C. For the assay, 8000 cells/well were seeded in 200 µl of complete medium using 96-well plates. Cells were maintained at 37 °C in 5% CO_2 humidified incubator for 24 h to reach 50-60 % confluence. The medium was removed and replaced with 87.5 µl of complete medium to which 12.5 µl of either the transfection complex (lipoplex), the free lipopolyamine, or the free RNA (naked RNA) were added to give a final volume of 100 µl, with the exception of the control cells where 100 µl of serum Opti-MEM was added. The plates were then maintained at 37 °C in 5% CO_2 humidified incubator for 24 h. After that, the medium was removed and replaced with 200 µl of complete medium and maintained for a furthur 48 h. The medium was then replaced with 90 µl of fresh medium and 10 µl of sterile filtered MTT solution (5 mg/ml) to reach a final concentration of 0.5 mg/ml. The plates were then incubated for 4 h at 37 ^{o}C in 5% CO_2 humidified incubator. Following incubation, the media and the un-reacted dye were removed and the formed blue formazan crystals dissolved in 200 µl/well of DMSO. The colour produced was measured using a plate-reader (VERSAmax, Molecular Devices, Crawley, UK) at a wavelength of 570 nm. The percentage viability with respect to control wells containing cells without siRNA and/or lipopolyamines was calculated according to the following formula:

$$\% \ cell \ viability = \left(\frac{A_{570} \ sample}{A_{570} \ control} \right) \times 100$$ (Fischer *et al.*, 1999)

2.6.3 Preparation of cells for flow cytometry analysis

After 72 h incubation, the medium was removed and cells washed twice with PBS solution. Cells were detached using 500 µl of 0.05 % (w/v) trypsin and 0.02% (w/v) EDTA and incubated for 5 min at 37 °C in a 5% CO_2 humidified incubator. After that, the plates were gently tapped to further detach the cells. The trypsin reaction was stopped by the addition of 1 ml of complete medium into each well. The cell suspension was transferred to 1.5 ml plastic tubes and centrifuged twice with PBS at 375 g, 5 min each at 20 ºC. A cell suspension for FACS analysis was obtained by resuspending the pellet in 500 µl PBS/tube and an untransfected cell sample used as a control. Flow cytometry was performed with a FACSCanto flow cytometer and analyzed with Cell Quest pro software (Becton Dickinson, MA, USA). Prior to analysis, all samples were gated by both forward and side scatter to eliminate data interference by dead cells.

2.6.4 Transfection of tracheal segments with fluorescent siRNA

The Label IT® RNAi delivery control was needed for this experiment, which consists of fluorescein-labeled double-stranded RNA duplexes, that have the same length, charge, and configuration as standard siRNA used in RNAi studies. The 10X RNAi dilution buffer provided was adjusted to 1X RNAi dilution buffer using RNase and DNase free water. Fluorescent siRNA was diluted using 1X RNAi dilution buffer to a final concentration of 50 and 100 nM /well. TransIT–TKO transfection reagent and synthetic lipospermine transfecting reagents C20 and C22 (University of Bath) were added to 250 µl Opti-MEM without serum. The volumes of the transfection reagents used were according to positive results achieved using 9HTEo- and A549 cell lines. Diluted siRNA or different transfection reagents were then mixed gently and incubated at 20 °C for 15 min. The diluted flourescent siRNA was added to the different transfecting reagents, mixed and incubated at 20 °C for another 15 min. The transfecting reagent/fluorescent siRNA complex mixtures were then added dropwise

to the wells containing murine tracheal segments such that the final volume in the well was 1 ml. The plate was rocked gently back and forth and from side to side to distribute the complexes evenly and then incubated at 37 °C for 72 h before preparing slides as mentioned in section 2.3.1. The slides were washed three times with PBS at 20 °C, fixed with 4% PFA for 4 min at 20 °C, rewashed three times with PBS, mounted in 20 µl Vectashield, antifade mounting media, a cover slip placed onto the slides and left in the dark for 20 h before subsequent confocal microscopic examination.

2.6.5 Reverse permeabilization

Reverse permeabilisation is a method used to study the role of specific intracellular proteins in intact tissues and determining their effects on functions, such as contractility especially if it not normally measured in cultured cells due to dedifferentiation in culture to noncontracting phenotypes. Reversible membrane permeabilization depends on using high ATP concentration in divalent cation–free solutions resulting in increase in membrane permeability. This is reversed by removal of extracellular ATP and addition of high [Mg^{2+}] followed by a gradual restoration of the physiological concentrations of extracellular Mg^{2+} and Ca^{2+} (Steinberg *et al.*, 1987). Reverse permeabilization was used to introduce siRNA into murine tracheal segments based on a method described by Corteling *et al*., 2007. Isolated tracheal segments were exposed to four successive solutions (see Table 2.1) Murine tracheal segments were then placed in DMEM medium (supplemented with 100 U/ml penicillin, 100 µg/ml streptomycin, 2.5 µg/ml Fungizone, and 0.1% w/v BSA) and maintained at 37 °C in a humidified CO_2 gassed incubator for 48 h. The medium was then changed to medium with or without the presence of m-IL-13 and the segments further incubated for 24 h. The segments were subjected to organ bath experiments as described in section 2.1.3, homogenized in lysis buffer and Western blotting was carried out as previously described in section 2.4. In another set of experiments, reverse permeabilisation was carried out using different concentration of the fluorescein-labeled double-stranded RNA duplexes (20, 50 and 100 nM). The rings were then embedded in OCT and kept at -80 °C until sectioned by cryostat as previously described in section 2.3.1**.** The slides were washed with PBS three times at 20 °C, and fixed with 4% PFA for 4 min at 20 °C. After fixation, the slides were

washed three times with PBS at 20 °C, 20 µl of vectorshield antifade mounting media added on top, and a slide cover was placed onto the slide. The slides were left in the dark for 20 h before using confocal microscopy to detect the fluorescein-labeled siRNA.

Table 2.1 Solutions used in reverse permeabilisation (mM)

Solution (1)	10 EGTA, 120 KCl, 5 ATP, 2 $MgCl_2$, 20 TES (pH 6.8; 20 min, 4 °C)
Solution (2)	120 KCl, 5 ATP, 2 $MgCl_2$, and 20 TES with 20 nM siRNA (pH 6.8; 3 h, 4 °C)
Solution (3)	120 KCl, 5 ATP, 10 $MgCl_2$, and 20 TES with 20 nM siRNA (pH 6.8; 30 min, 4 °C).
Solution (4)	140 NaCl, 5 KCl, 10 $MgCl_2$, 5 glucose, and 2 MOPS (pH 7.1, 22 °C) and $[Ca^{2+}]$ was gradually increased from 0.01 to 0.1 to 1.8 mM every 15 min.

2.7 Flow cytometry

Surface expression of IL-13 Rα2 by 9HTEo-cells was analysed to determine its possible role in IL-13 treated cells. 9HTEo- cells were cultured as mentioned in section 2.2, and incubated with IL-13 (1, 10, 30 and 100 ng/ml, 24 h). After 24 h incubation, the cells were washed twice in PBS/0.1% BSA, detached by incubation of the cells with 500 µl of 0.05% trypsin and 0.02% EDTA for 5 min at 37 °C. The trypsin/EDTA reaction was stopped by the addition of 1 ml prewarmed complete media to the cultured dish and the content of the dish pipetted several times, transferred into 1.5 Plastic tubes and washed twice using cold PBS/ 0.1% BSA by centrifuging the cells at 9600 g for 1 sec. The cells were resuspended in 500 µl cold PBS/0.1% BSA then 10 µl of anti-human IL-13 Rα2 antibody was added and incubated in the dark for 30 min. The cells were rewashed twice using cold PBS/ 0.1% BSA by centrifuging the cells at 9600 g rpm for 1 s. After washing, 10 µl of

FITC-conjugated secondary antibody was added, incubated in the dark on ice for 30 min, and washed twice using cold PBS/0.1% BSA. The cells were then resuspended in 400 µl cold PBS/0.1% BSA as a final volume and transferred to flow cytometer polypropylene tubes. Flow cytometry was performed with a FACSCanto flow cytometer using wavelengths of 488 nm for excitation and 520 nm for emission and analyzed with Cell Quest Pro software (Becton Dickinson, MA, USA). Prior to measurement, all samples were gated by both forward and side scatter to eliminate data interference by dead cells.

2.8 Reverse transcription-polymerase chain reaction

To evaluate expression of IL-13 Rα1 and IL-13 Rα2 on IL-13 treated 9HTEo- cells, reverse transcription PCR for each receptor was carried out. Extracted RNA was reverse transcribed to complementary (cDNA) which was amplified to generate millions or more copies of the DNA piece.

2.8.1 RNA extraction

After culturing 2 X 10^5 9HTEo- cells in a 3.5 cm diameter dish cells with IL-13 for 24 h as mentioned in section 2.2.3, the cells were washed twice with sterile PBS. Then, 1 ml of TRIZOL reagent was added, passed several times through a pipette and incubated for 5 min at 20 °C. Chloroform (0.2 ml per 1 ml of TRIZOL reagent used) was added to the samples, vortexed and incubated at 20 °C for 2-3 min. The samples were then centrifuged at 15,400 g for 15 min at 4 °C. Following centrifugation, the mixture was separated into a lower red, phenol-chloroform phase, an interphase, and a colorless upper aqueous phase containing RNA. The aqueous phase was transferred to a sterile 1.5 ml plastic tube with the RNA being precipitated by adding 0.5 ml of isopropyl alcohol per 1 ml of TRIZOL reagent used for the initial lysis. Samples were then incubated at 20 °C for 10 min and centrifuged at 15,400g for 10 min at 4 °C where the RNA was precipitated in the form of a gel-like pellet. The supernatant was removed and the pellet washed once by adding 1 ml of 75% ethanol per 1 ml of TRIZOL reagent used, and mixed by vortex before centrifugation at 15,400g for 5 min at 4 °C. The supernatant was removed and the RNA pellet was air-dried for 5-10 min, resuspended in 50 µl of sterile water and heated to 55°C for 10

minutes to break secondary structures within the RNA and enhance its solubility. RNA concentration and purity for each sample was determined using a 1:100 dilution of the RNA and the absorbance measured at 260 nm and 280 nm using the GeneQuant II spectrophotometer (GeneQuant II, Pharmacia Biotech Ltd., Cambridge, UK). The concentration of RNA was determined using the following estimation:
Concentration of RNA (μg/ml) = dilution factor x 40* x A_{260}
* The standard consideration is that 40 μg/m1 of RNA has an absorbance of 1 at 260 nm –of ratio values of 1.8-2.0 verified acceptable RNA purity. RNA samples were then stored at -80 °C until used.

2.8.2 PCR

For cDNA synthesis, 1 μg of RNA was reverse transcribed into its DNA complement, using Omniscript RT Kit (Quiagen GmbH, Hilden, Germany) with anchored oligo dT primers (ABgene, Surrey, UK) in presence of an RNase inhibitor (RNasin Plus, Promega, Madison, WI, USA) according to the manufacturer's instructions using a Perkin Elmer GeneAmp PCR System 2400 thermal cycler with the following setup: 40°C for 60 minutes followed by 70°C for 10 minutes to inactivate the reverse-transcriptase reaction (see section 9.6 for reaction mixture). Reverse transcriptase -negative samples were also prepared to exclude any possible genomic DNA contamination within RNA samples. cDNAs produced were stored at -20°C.

PCR is an *in vitro* method for the enzymatic synthesis of specific DNA sequences, using two oligonucleotide primers that bind to opposite strands and flank the region of interest in the target DNA. Numerous cycles involving template denaturation to open the double stranded DNA, primer annealing, and the extension of the annealed primer by a DNA polymerase such as Thermus aquaticus (Taq) result in exponential accumulation of specific fragments defined by the 5' ends of the primers. The products synthesised at the end of each cycle then serve as the template in the next round, hence the number of target DNA copies double at every cycle. Refer to section 9.7 for the design and sequences of primers used in this study

All PCR reactions were carried out in 25 µl reaction volumes in thin walled PCR tubes as follows

Component	Volume (µl)
PCR Master Mix (Promega)	12.5
Sense primer (0.5 µM final)	0.5
Antisense primer (0.5 µM final)	0.5
cDNA template	1-2.5
PCR grade H_2O	to 25

At the beginning of each run, the samples were incubated at 95°C to enable activation of the thermostable recombinant Taq DNA polymerase (hot start DNA polymerase) by the removal of specific blocking groups. The cDNA was amplified using a Perkin Elmer GeneAmp PCR System 2400 thermocycler, and the amplification cycles (30 second at 94°C, and 1min each 57 and 72 ° C) for 30 cycles PCR products were then analysed by agarose gel electrophoresis.

2.8.3 Agarose gel electrophoresis

Electrophoresis grade agarose (0.5 g) was added to 50 ml of the 1 X Tris/Borate/EDTA (TBE) buffer. The agarose was heated in microwave for 1.5 min then cooled to about 50 °C in a water bath for 5 min and the volume readjusted to 50 ml using warm ultrapure water. The sides of the tray were secured using autocave tape before the agarose was poured into; the comb inserted, and the gel allowed to solidify at 4 °C. The comb was removed and the buffer solution was poured into the gel box to a level of 2-3 mm above the gel, which was sufficient to prepare a small 8-sample gel. The formed wells were loaded with 20 µl of the following a mixture: Deionzed H_2O (10 µl), 6X Track-it load buffer (3.3 µl) and DNA samples (6.7 ul). A spare well was used to load a low molecular weight DNA ladder marker. The gel was run at 80 V using a Kodac Biomax Qs 710 gel electrophoresis chamber attached to BioRad PowerPac 300 unit for approximately 1.5 h until the bands were clearly separated, as visualised by the migration of orangeG at 50 bp and bromophenol blue at 300 bp. Afterward, the gel was placed in the staining tray containing ethidium

bromide 50 µl in 100 ml TBE buffer for 10 min, rinsed twice with distilled water, illuminated at 254 nm wavelength and photographed using Gene Genius Gel Documentation System (Syngene Inc., Cambridge, UK).

2.9 Statistical analysis

Contractions evoked by KCl and CCh are expressed as mN/mg of wet weight tissue, and all values are presented as mean ± s.e.m. Nonlinear regression analysis using Prism software (version 4; GraphPad Software, San Diego, CA) was used to determine Emax. Comparisons among groups were performed by Student's paired *t*-test or ANOVA with Dunnett's or Tukey-Newman-Keuls post hoc tests as appropriate for n = 4-12 mice.

2.10 Materials

Materials	*Catalog No.*	*Company*
Absolute ethanol	E7148	Sigma-Aldrich (Poole, UK)
30% Acrylamide-Bis acrylamide solution	161-0158	Bio-rad (Hercules, USA)
Adenosine triphosphate	A7699	Sigma-Aldrich (Poole, UK)
Agarose	A5304	Sigma-Aldrich (Poole, UK)
Alpha-D(+)-Glucose	17008-0025	Fisher Scientific (Loughborough, UK)
Ammonium persulfate	327081000	Fisher Scientific (Loughborough, UK)
Anchored oligo dT	AB-1247	Abgene (Epsom, UK)
Anti-Akt1 antibody	Sc-1618	Santa Cruz Biotechnology (Santa Cruz, Ca, USA)
Anti-arginase I antibody (mouse)	610708	BD Biosciences (Oxford, UK)
Anti-arginase I antibody (rabbit)	Sc-20150	Santa Cruz Biotechnology (Santa Cruz, Ca, USA)
Anti-β-actin	4967	Cell Signaling Technology (Boston, USA)
Anti-human IL-13 Rα2	AF146	R&D Systems (Abingdon, UK)
Anti-phosphoSer^{473}-Akt antibody	9271	Cell Signaling Technology (Boston, USA)
Anti-PI3K p110δ antibody	Sc-7176	Santa Cruz Biotechnology (Santa Cruz, Ca, USA)
Aprotonin from bovine lung	A3428	Sigma-Aldrich (Poole, UK)
Bovine serum albumin	A6003	Sigma-Aldrich (Poole, UK)
Bromophenol blue	B8026	Sigma-Aldrich (Poole, UK)
Carbamoylcholine chloride	C4382	Sigma-Aldrich (Poole, UK)
Chloroform	C2432	Sigma-Aldrich (Poole, UK)
Citrate Buffer for Heat-induced Epitope Retrieval	AP-9003-050	Fisher Scientific (Loughborough, UK)
Collagen from calf skin	C9791	Sigma-Aldrich (Poole, UK)
Cork disks - 20mm x 3mm	-	Raymond Alamb (Eastbourne, UK)

Cryogenic vials	368632	Fisher Scientific (Loughborough, UK)
Custom primers	-	Invitrogen (Carlsbad, USA)
Deoxyribonuclease I from bovine pancreas	D5025	Sigma-Aldrich (Poole, UK)
DePeX mounting media	361252B	BDH (Poole, UK)
Dimethyl sulfoxide (DMSO)	D8418	Sigma-Aldrich (Poole, UK)
DNA Ladder 100 bp	N3231S	NewEngland Biolabs (Herts, UK)
Dulbecco's Modified Eagle's Medium (DMEM)	41966-029	GIBCO (Paisley, UK)
Dulbecco's Phosphate Buffered Saline (D-PBS) (10X), liquid	14200-067	GIBCO (Paisley, UK)
EDTA	ED2SS	Sigma-Aldrich (Poole, UK)
EDTA Buffer For Heat-Induced Epitope Retrieval (10X)	AP-9004-050	Fisher Scientific (Loughborough,UK)
Enhanced Chemiluminescent Lumigen (ECL) Kit for Western blotting	RPN2209	GE Healthcare (Buckinghamshire, UK)
Eosin Y solution, aqueous	HT110216	Sigma-Aldrich (Poole, UK)
Ethylene glycol-bis(2-aminoethylether)-N,N,N′,N′-tetraacetic acid	E4378	Sigma-Aldrich (Poole, UK)
Fetal bovine serum-heat inactivated	10082-147	GIBCO (Paisley, UK)
Fibronectin, Bovine Plasma	33010018	GIBCO (Paisley, UK)
FUJI Medical X-ray Film	2731261	Fisher Scientific (Loughborough, UK)
Fungizone Antimycotic liquid	15290-026	GIBCO (Paisley, UK)
Gel-Saver II Pipette Tip (1-200 µl)	NC9438173	Fisher Scientific (Loughborough,UK)
Glycerol	G5516	Sigma-Aldrich (Poole, UK)
Glycine	50046	Sigma-Aldrich (Poole, UK)
Goat anti-mouse peroxidase	P0447	DAKO (Glostrup, Denmark)

Goat anti-rabbit peroxidase	P0448	DAKO (Glostrup, Denmark)
Hematoxylin Solution, Harris Modified	HHS16	Sigma-Aldrich (Poole, UK)
Histoclear	HS-200	Fisher Scientific (Loughborough, UK)
Histoclear (II)	HS-202	Fisher Scientific (Loughborough, UK)
IC87114	-	ICOS Corporation (Bothell, USA)
Iso-Pentane	B10361-74	BDH (Poole, UK)
Isoprenaline hydrochloride	I5627	Sigma-Aldrich (Poole, UK)
The Label IT® RNAi Delivery Control	MIR 7902	Mirus (Madison, USA)
LAMB OCT embedding medium	-	Raymond Alamb (Eastbourne,UK)
Leupeptin hemisulfate salt	L8511	Sigma-Aldrich (Poole, UK)
LHC- Basal Medium (1X)	12677-019	Invitrogen (Carlsbad, USA)
LHC-9 medium (1X)	12680-013	Invitrogen (Carlsbad, USA)
Lipofectamine 2000	11668-027	Invitrogen (Carlsbad, USA)
L-Norvaline	N7627	Sigma-Aldrich (Poole, UK)
LY294002	L9908	Sigma-Aldrich (Poole, UK)
Magnesium chloride - Solution	A3888.0500	VWR International (Poole, UK
Marvel non-fat dehydrated milk	-	Sainsbury's (Bath, UK)
2-Mercaptoethanol	M3148	Sigma-Aldrich (Poole, UK)
Methanol	M/4056/17	Sigma-Aldrich (Poole, UK)
Microscopic slides, superfrost Plus	6310108	VWR International (Poole, UK)
MOPS (4-Morpholinepropanesulfonic acid)	M1254	Sigma-Aldrich (Poole, UK)
Nitrocellulose membrane (TransBlot Transfer membrane)	162-0115	Bio-Rad (Hercules, USA)
Nonidet P-40	56009	Sigma-Aldrich (Poole, UK)

Non-targeting predesigned siRNA duplex	D-001210-01	Dharmacon (Erembodegem, Belgium)
Omniscript RT Kit	205111	QIAGEN (Crawley, UK)
Opti-MEM, Reduced-Serum Medium (1X), liquid	31985-062	Invitrogen (Carlsbad, USA)
Paraformaldehyde	P6148	Sigma-Aldrich (Poole, UK)
PAP pen for immunostaining	Z377821	Sigma-Aldrich (Poole, UK)
PCR Master Mix	M7502	Promega (Southampton, UK)
Penicillin/Streptomycin	15140-122	GIBCO (Paisley, UK)
Peroxo-Block	00-2015	Zymed Laboratories, Invitrogen (Carlsbad, USA)
Pepstatin A	P5318	Sigma-Aldrich (Poole, UK)
Phenylmethanesulfonylflouride	P7626	Sigma-Aldrich (Poole, UK)
Phosphate buffered saline	P4417	Sigma-Aldrich (Poole, UK)
Pipette (serological sterile, 10 ml)	FB55484	Fisher Scientific (Loughborough, UK)
Polyvinylpyrrolidone (PVP)	P5288	Sigma-Aldrich (Poole, UK)
Potassium chloride	P/4240153	Fisher Scientific (Loughborough, UK)
Precision Plus Protein Standard (for Western blotting)	161-0373	Bio-Rad (Hercules, USA)
Predesigned siRNA duplex P110δ, human)	D-006775-05	Dharmacon (Erembodegem, Belgium)
Predesigned siRNA P110δ-(mouse)	M-041078-00	Dharmacon (Erembodegem, Belgium)
Recombinant human IL-13	200-13	Peprotech (London, UK)
Recombinant murine IL-13	210-13	Peprotech (London, UK)
Recombinant rat IL-13	400-16	Peprotech (London, UK)
RNasin Plus RNase Inhibitor	N2611	Promega (Southampton, UK)
RNeasy mini kit	74106	QIAGEN (Crawley, UK)
Sodium azide	S2360	Sigma-Aldrich (Poole, UK)
Sodium chloride	S7653	Sigma-Aldrich (Poole, UK)

Sodium dodecyl sulphate	L4390	Sigma-Aldrich (Poole, UK)
Sodium fluoride	S1504	Sigma-Aldrich (Poole, UK)
Sodium molybdate	S6646	Sigma-Aldrich (Poole, UK)
Sodium orthvanadate	S6508	Sigma-Aldrich (Poole, UK)
SuperPicTure™ Polymer Detection Kit	87-9263	Zymed Laboratories, Invitrogen (Carlsbad, USA)
Syring Filter Millex	FDR-050-071N	Fisher Scientific (Loughborough, UK)
TEMED	T9281	Sigma-Aldrich (Poole, UK)
TES (N-[Tris(hydroxymethyl)methyl]-2-aminoethanesulfonic acid)	R1375	Sigma-Aldrich (Poole, UK)
Thiazolyl Blue Tetrazolium Bromide	M5655	Sigma-Aldrich (Poole, UK)
Tissue culture 48-well plate	137101	NUNC (Roskilde, Denmark)
Tissue culture 6-well plate	140675	NUNC (Roskilde, Denmark)
Tissue culture dish 35x10	153066	NUNC (Roskilde, Denmark)
Tissue culture flask 25 cm^2	690175	Greinerbio-one (Stonehouse, UK)
Tissue culture flask 75 cm^2	658175	Greinerbio-one (Stonehouse, UK)
TransIT-TKO® Transfection Reagent	MIR 2150	Mirus (Madison, USA)
Trizma base	T87602	Sigma-Aldrich (Poole, UK)
Trypan blue	T6146	Sigma-Aldrich (Poole, UK)
Trypsin, 0.05% (1X) /EDTA	25300 -.054	GIBCO (Paisley, UK)
Trypsin inhibitor from Glycine max (soybean)	T9003	Sigma-Aldrich (Poole, UK)
Tween-20	P1379	Sigma-Aldrich (Poole, UK)
UltraPure TBE Buffer (10X)	15581-044	Invitrogen (Carlsbad, USA)
Vectashield mounting medium	H-1000	Vector Laboratories (Peterborough, UK)
Wortmannin	W1628	Sigma-Aldrich (Poole, UK)

Chapter Three

IL-13-induced hyperresponsiveness of ASM

3.1 Introduction

The importance of using animal models of many human diseases is central to the drug discovery process. Each of the animal models currently used has advantages and disadvantages. Mouse and rat are by far the most widely used experimental models for human diseases and biology. Mice have been extensively used for genetic studies. However, rat is often the model of choice for physiological studies due to its large size (Gill, *et al.*, 1989). The most commonly used experimental animal, the mouse, has some important advantages including the well-studied immune system, the wide range of tools e.g. antibodies available for characterizing the cells and cytokines, the potential for development of genetic knockouts and transgenic animals, the resemblance of the mouse Th2/Th1 system to that believed to be involved in human asthma, and the relatively low cost of the animals and their maintenance. The available tools for studies in rats are less than that of mice and even fewer of the required tools are available for the guinea pig, although the guinea pig has a robust bronchoconstriction response that is lacking in the other rodents. In order to gain more insight in the mechanisms of human lung diseases and potential beneficial therapeutic agents, adequate models are needed. (Hulsmann & de Jongste, 1993).

Although several Th2 cytokines have been implicated in antigen-induced AHR, IL-13 seems to play a pre-eminent role in AHR, a definite feature of asthma. Targeted deletion of IL-13 prevents expression of AHR in allergen-challenged mice, despite maintenance of elevated IL-4 and IL-5 release (Walter *et al.*, 2001). Likewise, neutralization of IL-13 using IL-13 receptor constructs or antibodies reduces AHR (Grunig *et al.*, 1998; Eum *et al.*, 2005).

The aim of studies represented in the present chapter is to demonstrate the responsiveness of ASM by pre-incubation with IL-13 *in vitro*. It was also necessary to identify which species to be used in this study. Isometric tension was recorded in isolated tracheal ring preparations and comparative studies using both rat and mouse isolated tracheal rings were investigated. The effects of mouse, rat or human IL-13 on tracheal contractility of both species were compared.

3.2 The effect of m-IL-13 on mice tracheal smooth muscle

As shown in Table 3.1 and Figure 3.1 A and B, initial experiments were carried out using isolated murine tracheae. m-IL-13 potentiated KCl (10-100 mM) and CCh (10^{-8}–10^{-5} M)-induced contractions in which the agonist E_{max} of the concentration response curve was significantly higher in murine rings pretreated with m-IL-13 (10 or 100 ng/ml) compared with controls, with E_{max} values for KCl and CCh increased approximately 1.6- to 2-fold (Table 3.1). While m-IL-13 elevated the maximal response, limited changes in EC_{50} values were observed (Table 3.1), indicating that m-IL-13 seemed to increase smooth-muscle contractility rather than induce increased sensitivity to low concentrations of contractile agents.

Table 3.1 Effect of IL-13 induced contractions in isolated murine tracheal rings. Tissues isolated from CD1 mice and were incubated with media alone (controls, n = 24) or IL-13 (10 and 100 ng/ml, n = 12 per group) for 24 h prior to assessment of contractile responses to KCl or CCh. Values are mean ± s.e.m. of E_{max} values or pEC_{50} values.

	KCl		CCh	
	E_{max}	pEC_{50}	E_{max}	pEC_{50}
Control	mN/mg tissue 1.2 ± 0.1	-log[M] 1.43 ± 0.03	mN/mg tissue 2.0 ± 0.2	-log[M] 6.53 ± 0.09
IL-13 (10 ng/ml)	2.2 ± 0.3[a]	1.44 ± 0.03	3.8 ± 0.5[a]	6.54 ± 0.10
IL-13 (100 ng/ml)	2.7 ± 0.4[a]	1.44 ± 0.03	3.8 ± 0.5[a]	6.53 ± 0.09

[a]$p < 0.01$ compared with matched control segments.

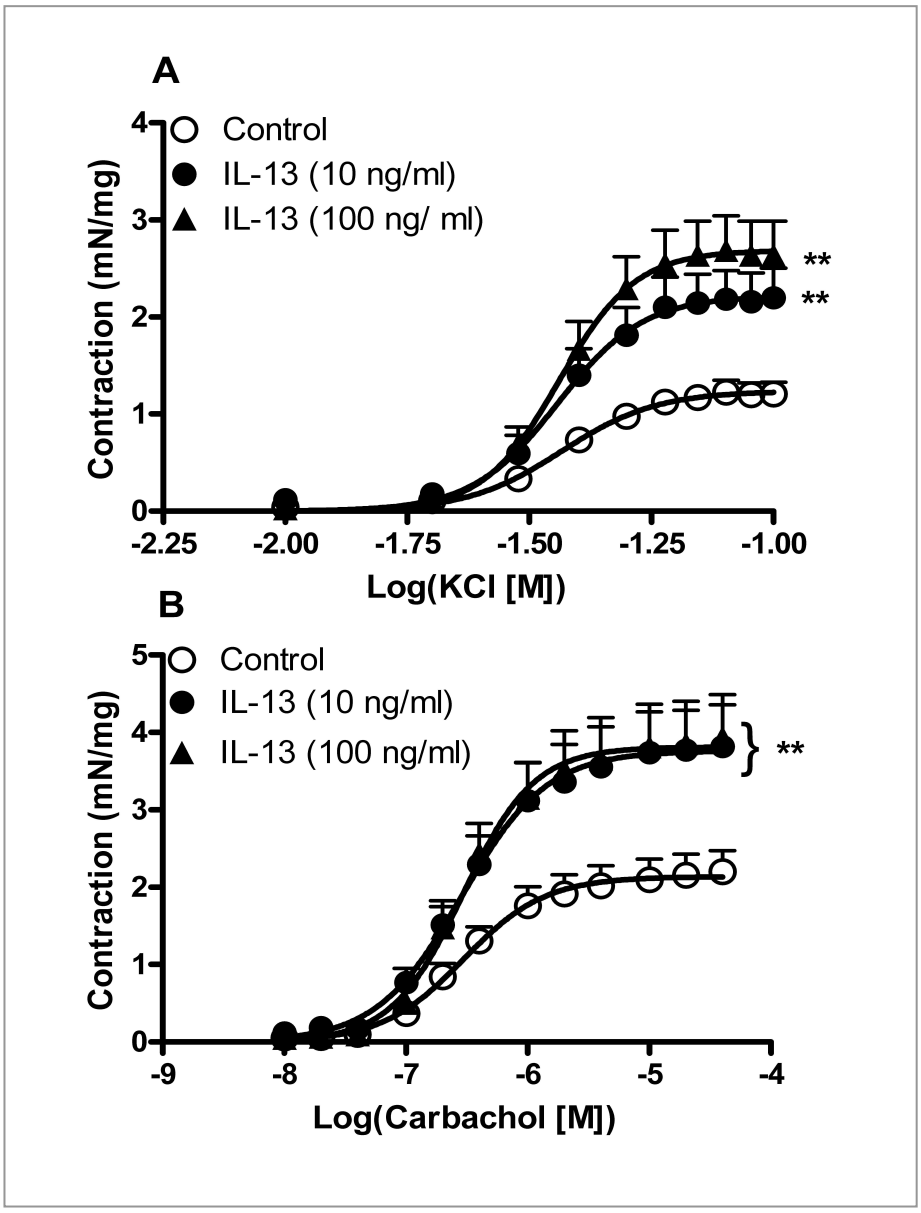

Figure 3.1 m-IL-13 enhanced KCl- and CCh-induced contraction of murine tracheal rings. Male, 8- to-10 weeks old, CD1 strain mice were used to obtain the tracheae, which were cut into two segments. Cumulative concentration-response curves to KCl (A) and CCh (B) in the absence or presence of m-IL-13 (10 or 100 ng/ml, 24 h). Data were expressed as mean mN per mg of tissue (wet weight) ± s.e.m. One-way ANOVA followed by Dunnett's test were performed to determine the statistical significance of differences between E_{max} values of control and IL-13-treated tissues. **, $p < 0.01$ compared with non IL-13 treated tissue, n = 12.

3.3 The effect of r-IL-13 on rat tracheal smooth muscle

To determine whether r-IL-13 would affect rat airway smooth muscle response after 24 h incubation, cumulative concentration response curve to KCl (10-100 mM) or CCh (10^{-8} -10^{-5}) were carried out. From Table 3.2 and Figure 3.2, although the contractile responses (in mN/mg) to KCl and CCh were apparently increased there was no statistically significant difference observed between r-IL-13 treated segments and control. There was also no difference in sensitivity between the control group and r-IL-13 treated group for both concentrations as shown by EC_{50} values (Table 3.2).

Table 3.2 Effect of r-IL-13 in isolated rat tracheal rings. Tissues isolated from Wistar rats were incubated with media alone (controls, n = 16), r-IL-13 (10 ng/ml, n = 10) or r-IL-13 (100 ng/ml, n = 6) for 24 h prior to assessment of contractile responses to KCl or CCh. Values are mean ± s.e.m. of E_{max} values or pEC_{50} values.

	KCl		CCh	
	E_{max}	pEC_{50}	E_{max}	pEC_{50}
Control	mN/mg tissue 1.6 ± 0.2	-log[M] 1.59 ± 0.06	mN/mg tissue 2.3 ± 0.1	-log[M] 6.44 ± 0.07
r-IL-13 (10 ng/ml)	1.9 ± 0.2	1.54 ± 0.08	2.8 ± 0.1	6.58 ± 0.05
r-IL-13 (100 ng/ml)	2.4 ± 0.3	1.55 ± 0.06	2.9 ± 0.3	6.32 ± 0.05

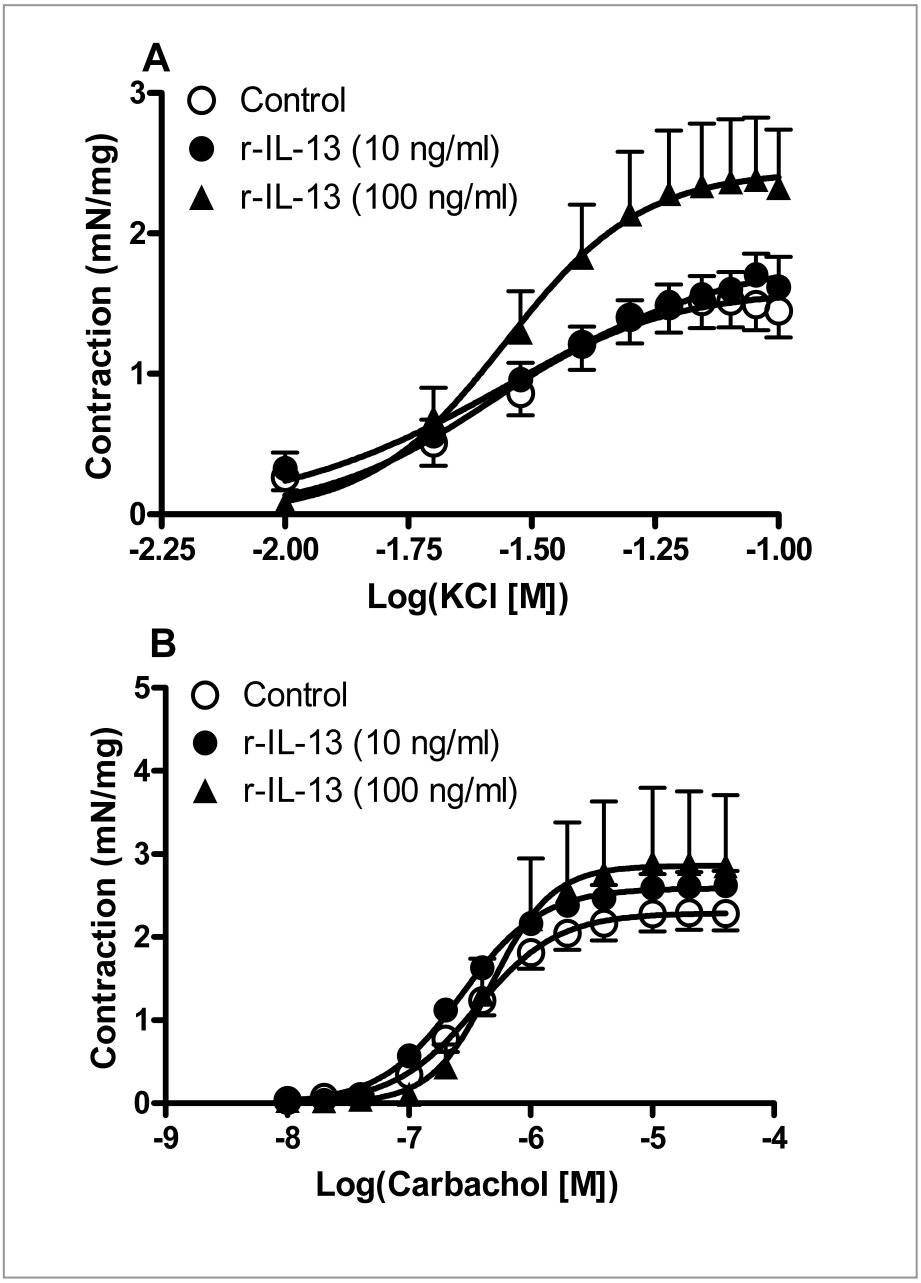

Figure 3.2 r-IL-13 did not enhance KCl- and CCh-induced contraction of rat tracheal rings. Male, 8 weeks old, Wistar strain rats were used to obtain the tracheae which were cut into 4-6 segments. Cumulative concentration-response curves to KCl (A) and CCh (B) in the absence or presence of r-IL-13 (10 or 100 ng/ml, 24 h). Data were expressed as mean mN per mg of tissue (wet weight) ± s.e.m. One-way ANOVA followed by Dunnett's test were performed to determine the statistical significance of differences between E_{max} values of control and IL-13-treated tissues, n = 6-10.

3.4 Time course study of IL-13 enhanced contraction

As seen in Figure 3.1 m-IL-13 enhanced both KCl and CCh-induced contraction at both concentrations examined, however, m-IL-13 (100 ng/ml) was chosen, being more effective, for subsequent experiments. To investigate further the m-IL-13 induced enhancement of mice tracheal segments contraction, responsiveness was assessed after 1, 4, or 8 h incubation with m-IL-13 (100 ng/ml). There were no significant differences in IL-13 treated tracheal segments compared with control groups both to KCl and CCh at these times of incubation (Figure 3.3).

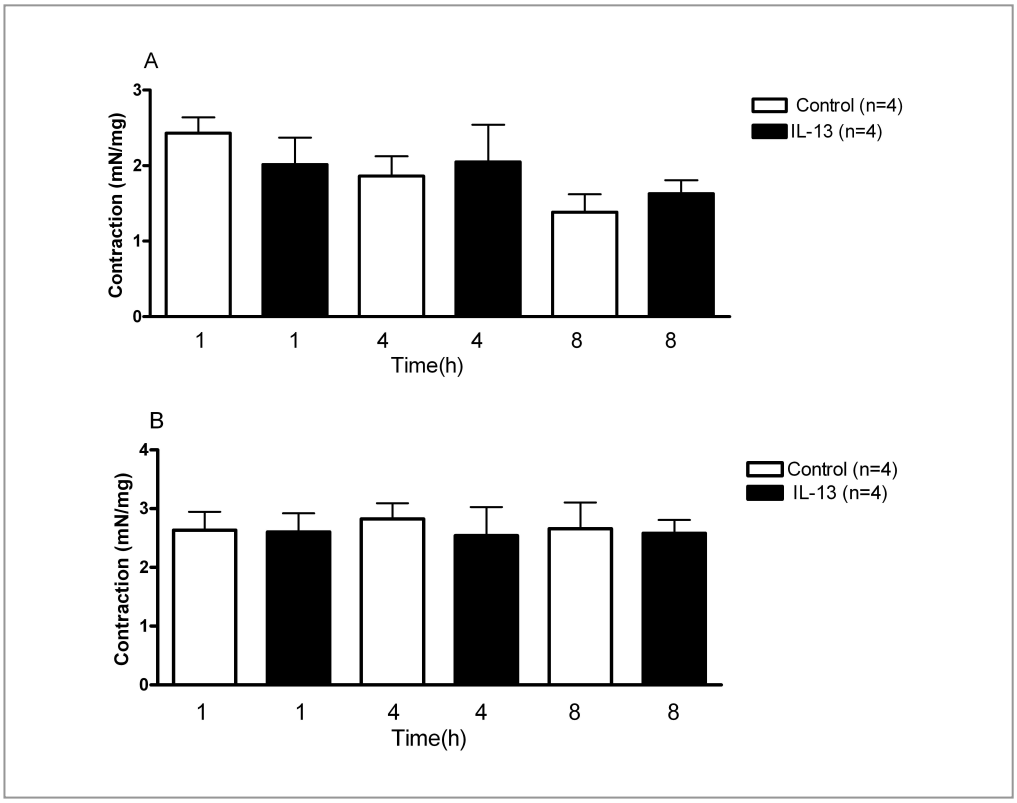

Figure 3.3 Time course response of murine trachea after IL-13 treatment. Male, 8-to-10 weeks old, CD1 strain mice were used to obtain the tracheae, which were cut into two segments. Response to KCl (A) and CCh (B) in the absence or presence of IL-13 (100 ng/ml) 1, 4 and 8 h expressed as mean mN per mg of tissue (wet weight) ± s.e.m. Student's paired *t*-test was performed to determine the statistical significance of differences between control and IL-13-treated tissues for n = 4.

3.5 Effect of KCl or CCh in fresh and cultured tracheal segments

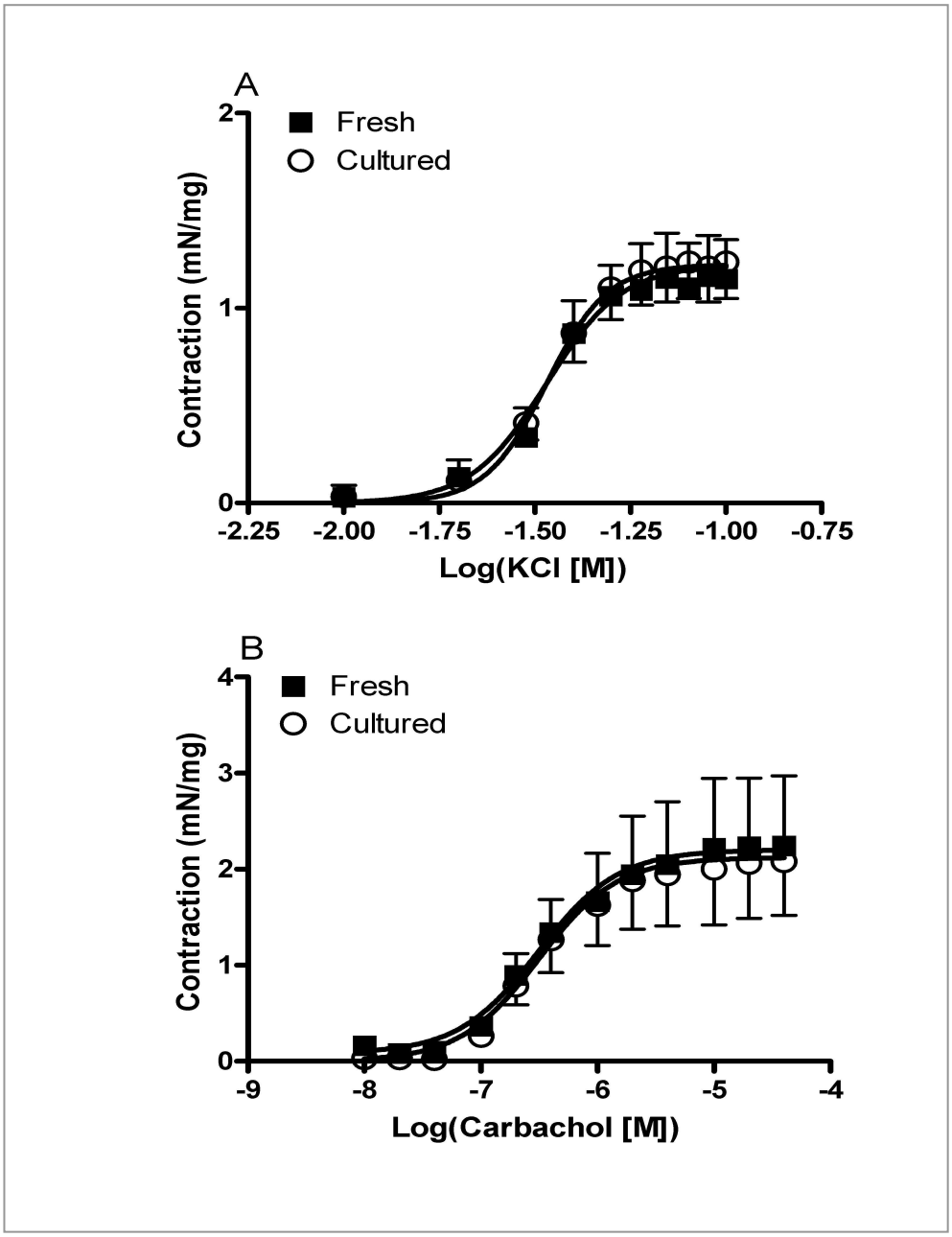

Figure 3.4 The effect of KCl and CCh on isolated mice tracheal segments, fresh and cultured for 24 h. Concentration-effect curves of KCl (A) and CCh (B) obtained on fresh and cultured murine tracheal segments (24 h) expressed as mean mN per mg of tissue (wet weight) ± s.e.m. Student's paired *t*-test was performed to determine the statistical significance of differences between fresh and cultured tissues for n = 4.

In control experiments, fresh murine tracheal segments and segments cultured for 24 h in the absence of IL-13 contracted similarly upon addition of KCl and CCh. The potency and maximal contraction of fresh and 24 h-cultured segments were not significantly different (Figure 3.4). KCl E_{max} values of fresh and cultured segments were 1.1 ± 0.1 and 1.2 ± 0.1 mN/mg respectively while CCh gave E_{max} values of 2.2 ± 0.3 and 1.8 ± 0.1 mN/mg for fresh and cultured segments respectively. The calculated pEC_{50} for KCl of fresh and cultured segments were 1.47 ± 0.03 and 1.47 ±0.03 mN/mg, respectively while those of CCh were 6.49 ± 0.22 and 6.46 ± 0.1 mN/mg for fresh and cultured segments respectively. Those non-significant results were similar for both agonist used except for a relatively small nonsignificant degree of lower contraction following culture observed with CCh dose response curve.

3.6 The effect of IL-13 on the relaxant response of isoprenaline

The effect of IL-13 on the relaxant response induced by isoprenaline was studied. A sustained contraction of the tracheal rings obtained using submaximal dose of CCh (1 μM) determined from prior construction of a CCh dose response curve was established. Then, cumulative concentration-response relaxant curves to isoprenaline (10^{-8} to 10^{-5} M) were carried out. Expressing results as a percentage of the pre-determined submaximal CCh concentration normalized the obtained relaxation responses. As shown in Figure 3.5 A the effect of m-IL-13 on the isoprenaline relaxant response using murine tracheal rings was investigated. The concentration-response relaxant curve to isoprenaline was unaffected by m-IL-13 (100 ng/ml) with maximal relaxant responses (as % of preconstriction) of 47 ± 8 % in the control rings and 43 ± 9 % in m-IL-13 treated rings (n = 12).

In another set of experiments relaxation of rat tracheal rings pretreated with r-IL-13 (10 and 100 ng/ml respectively) were not different from control groups given a maximal relaxant response of 36 ± 2 % in control group versus 34 ± 3 % in r-IL-13 (10 ng/ml) treated group and a maximal relaxant response of 30 ± 2 % in control group versus 34 ± 2 % in r-IL-13 (100 ng/ml) treated group (Figure 3.5 B and C respectively).

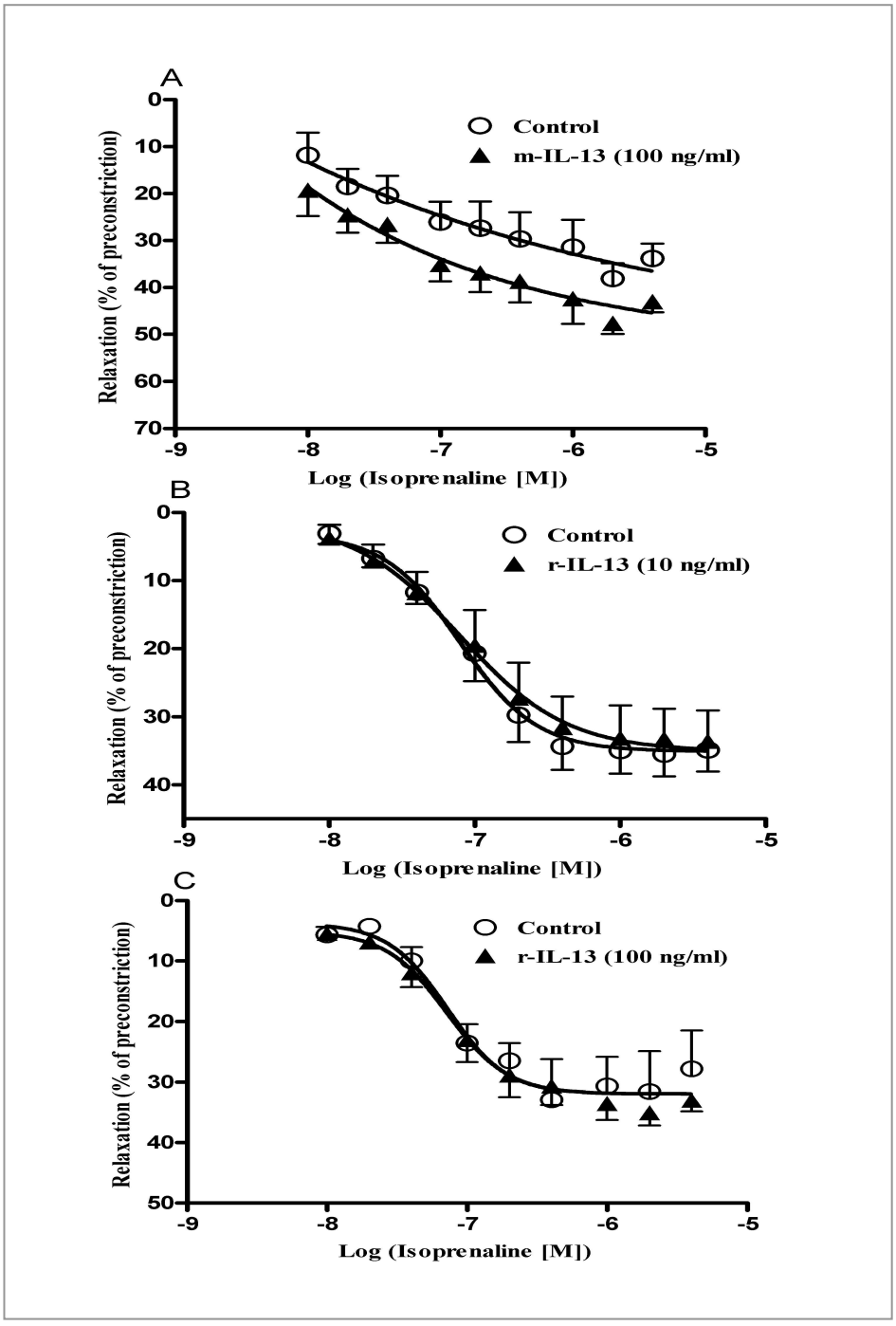

Figure 3.5 The effect of IL-13 on the relaxant response of isoprenaline. Following pre-contraction with CCh (75% of maximal contraction, 1 μM), (A) cumulative concentration- response curves to isoprenaline (10^{-8} to 10^{-5} M) obtained on mice tracheal rings preincubated for 24 h with m-IL-13 (100 ng/ml, n = 12), (B) rat tracheal rings preincubated for 24 h with r-IL-13 (10 ng/ml, n = 10) and (C) r-IL-13 (100 ng/ml, n = 5). All tension measurements from different groups are expressed as mean percentage of maximal contraction induced by CCh ± s.e.m.

3.7 Cross-species studies

Previous investigators have reported enhanced airway responsiveness to various mediators in various species, as reviewed by Shore & Moore (2002). Different studies used human isolated bronchial strips or segments (Pype *et al.*, 2001) or mice isolated tracheal segments (Chen *et al.*, 2003; Tliba *et al.*, 2003; Bryborn *et al.*, 2004; Moffatt *et al.*, 2004; Walker *et al.*, 2004; Bachar *et al.*, 2005), however isolated tissues from other species were used such as rat tracheae, bronchi or bronchiol, (Koto *et al.*, 1996; Van & Joos, 1998; Chiba *et al.*, 2000; Liu *et al.*, 2003; Sakai *et al.*, 2004), rabbit tracheae (Hakonarson *et al.*, 1996; Grunstein *et al.*, 2002) and guinea pig tracheae (Wills-Karp *et al.*, 1993). To examine species differences, response to m-IL-13 or r-IL-13 in rats or mice tracheal segments respectively was investigated. A significant response was only detected to CCh in rat tracheal rings incubated with m-IL-13 (100 ng/ml) (Figure 3.6) while the contractile effect of KCl was not significantly increased in either species (Figure 3.6 & 3.7).

A comparison of the effect of h-IL-13 on mice or rat isolated tracheal rings to determine the role of h-IL-13 in hyperreactivity was carried out. Therefore, murine or rat tracheal rings were cultured with h-IL-13 (100 ng/ml) for 24 h. A significant h-IL-13 enhanced contraction to KCl was demonstrated in both isolated rat and murine tracheal rings (Figure 3.8 A and 3.9 A). None of the pre-treatments with h-IL-13 altered the cumulative dose response curves for CCh of the tracheae isolated from mice or rats as compared with control segments (Figure 3.8 B and 3.9 B).

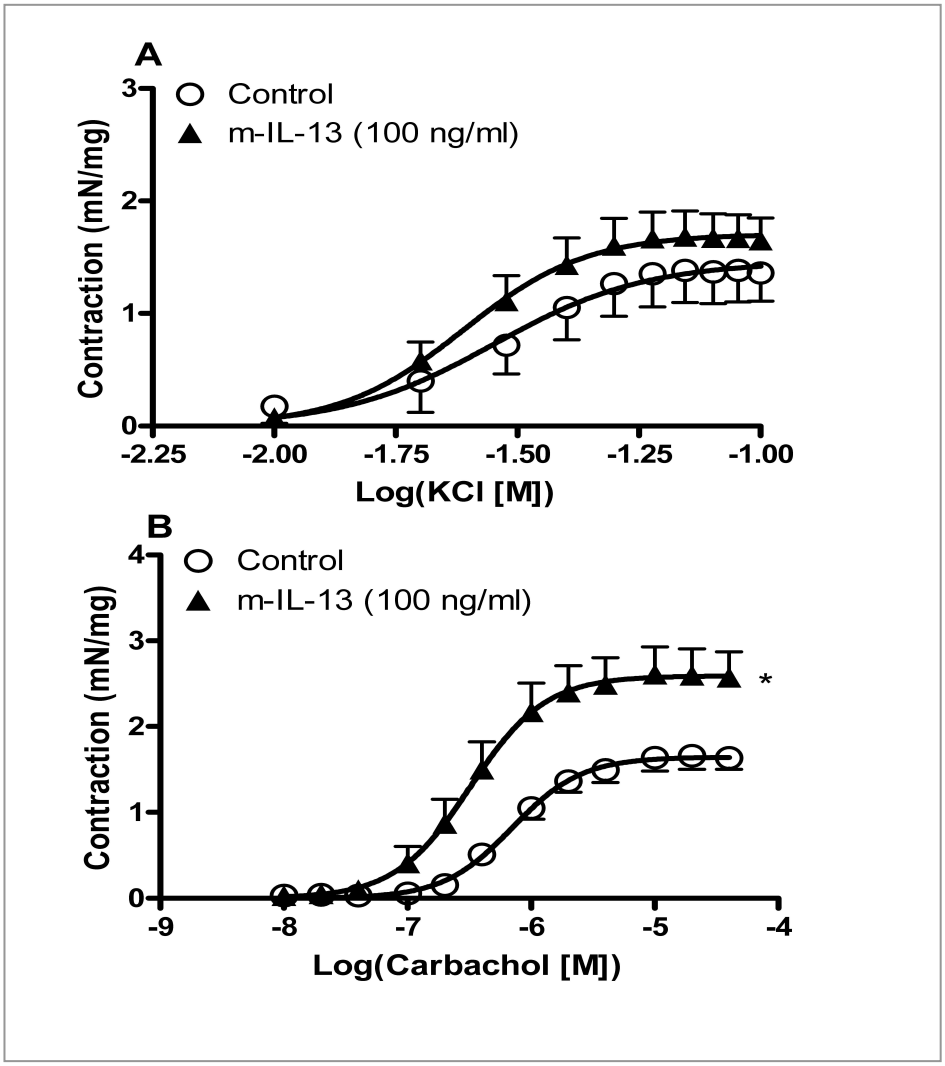

Figure 3.6 Effect of m-IL-13 on rat tracheal smooth muscle contraction. Male, 8 weeks old, Wistar strain rat were used to obtain the tracheae which were cut into 4-6 segments. Cumulative concentration-response curves to KCl (A) and CCh (B) in the absence or presence of m-IL-13 (100 ng/ml, 24 h). Data were expressed as mean mN per mg of tissue (wet weight) ± s.e.m. Student's paired *t*-test was performed to determine the statistical significance of differences between E_{max} values of control and IL-13-treated tissues for n = 7.

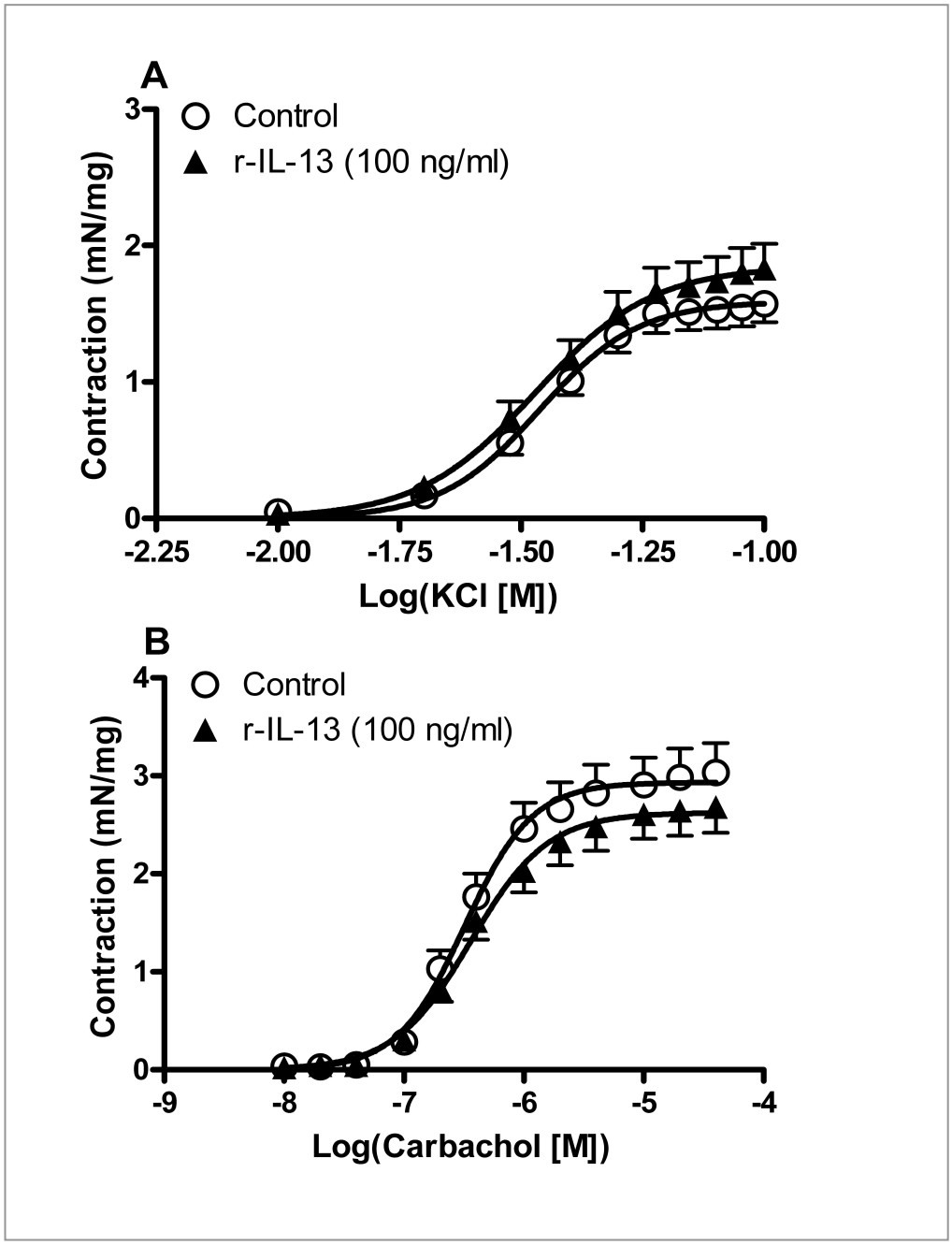

Figure 3.7 Effect of r-IL-13 on murine tracheal smooth muscle contraction. Male, 8-to-10 weeks old, CD1 strain mice were used to obtain the tracheae which were cut into two segments. Cumulative concentration-response curves to KCl (A) and CCh (B) in the absence or presence of r-IL-13 (100 ng/ml, 24 h). Data were expressed as mean mN per mg of tissue (wet weight) ± s.e.m. Student's paired *t*-test was performed to determine the statistical significance of differences between E_{max} values of control and IL-13-treated tissues for n = 12.

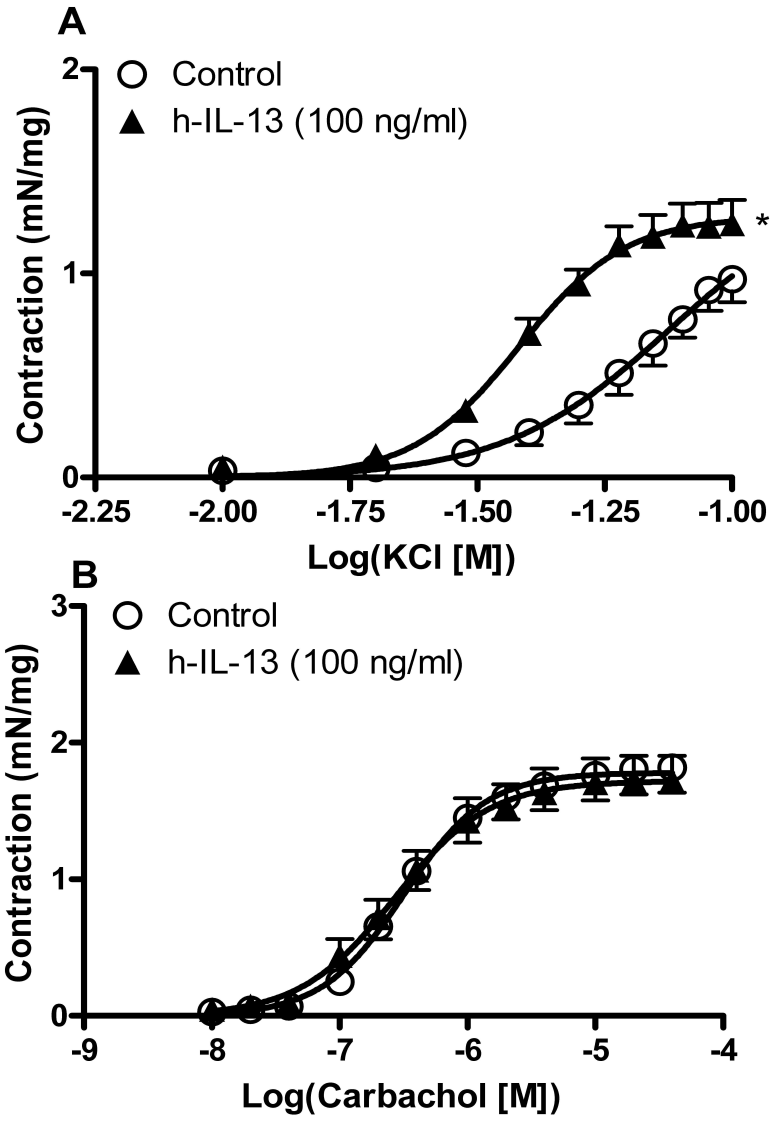

Figure 3.8 Effect of h-IL-13 on murine tracheal smooth muscle contraction. Male, 8-to-10 weeks old, CD1 strain mice were used to obtain the tracheae which were cut into two segments. Cumulative concentration-response curves to KCl (A) and CCh (B) in the absence or presence of h-IL-13 (100 ng/ml, 24 h). Data were expressed as mean mN per mg of tissue (wet weight) ± s.e.m. Student's paired *t*-test was performed to determine the statistical significance of differences between E_{max} values of control and IL-13-treated tissues for n = 12.

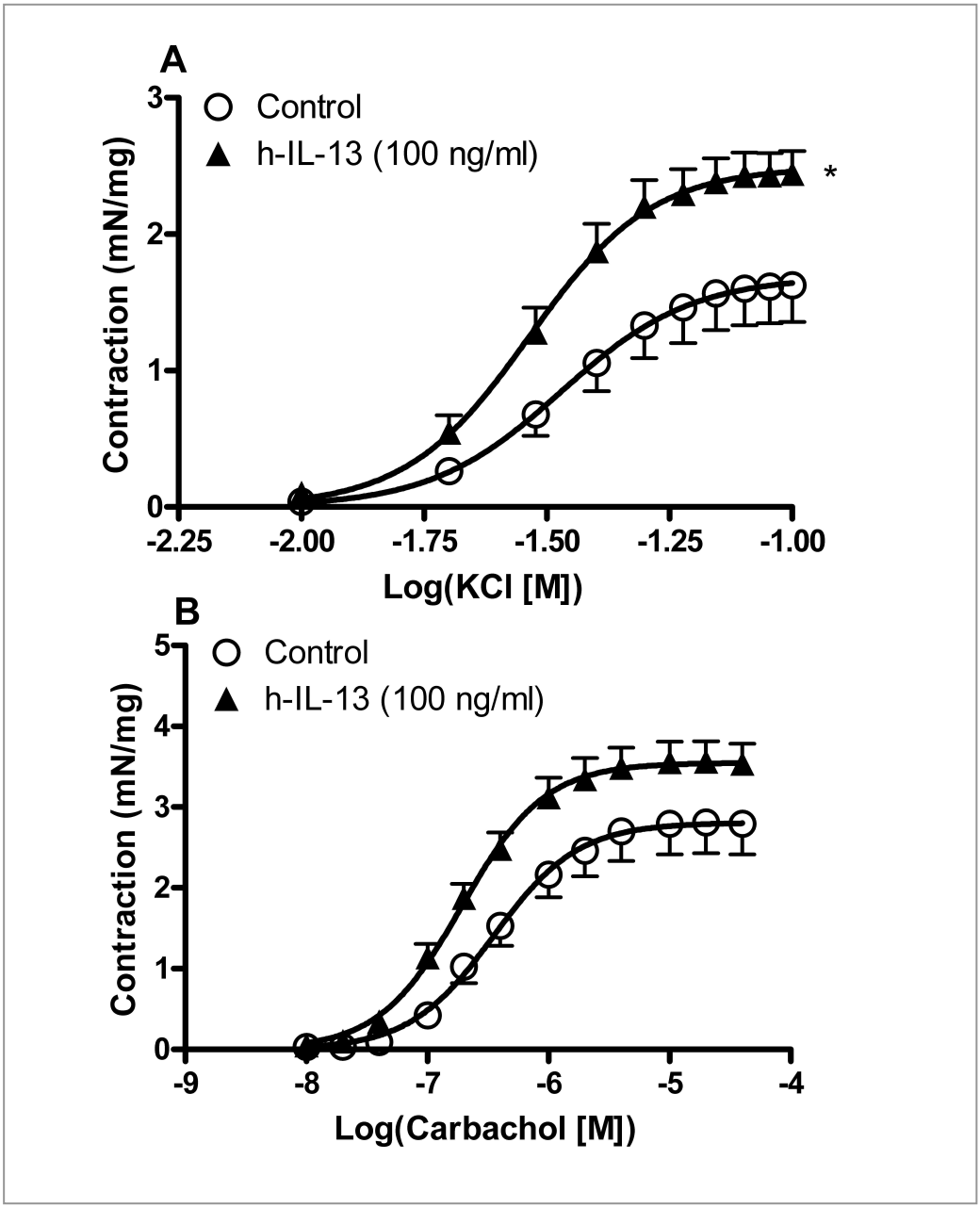

Figure 3.9 Effect of h-IL-13 on rat tracheal smooth muscle contraction. Male, 8 weeks old, Wistar strain rat were used to obtain the tracheae which were cut into 4-6 segments. Cumulative concentration-response curves to KCl (A) and CCh (B) in the absence or presence of m-IL-13 (100 ng/ml, 24 h). Data were expressed as mean mN per mg of tissue (wet weight) ± s.e.m. Student's paired *t*-test was performed to determine the statistical significance of differences between E_{max} values of control and IL-13-treated tissues for n = 8.

3.8 Discussion

Mice and rat airways are widely used as an experimental model to investigate airway smooth muscle contraction *in vitro* (Van & Joos, 1998; Bryborn *et al.*, 2004; Moffatt *et al.*, 2004; Barrio *et al.*, 2006). Thus, the response of isolated tracheal rings from both species to IL-13, a key cytokine implicated in the pathogenesis of asthma, was studied. The selection of the species was studied. A review to demonstrate species differences in adenosine receptor-mediated bronchoconstrictor responses showed that Brown Norway rat provides a close model to the response of adenosine in human asthma when compared with guinea pig and rabbit (Fozard & Hannon, 2000). In another study undertaken to clarify smooth muscle-stimulating effects of neuromedin U peptide in rats, mice and guinea pigs tracheal rings, it was demonstrated that neuromedin U peptide has no effect on trachea of any species. (Prendergast *et al.*, 2006). These data demonstrate a marked variation in response among different species even for the same agonist.

In isolated murine tracheal rings, incubation with m-IL-13 resulted in consistent and significantly enhanced responsiveness compared with the control group. As contractile responses to both KCl and CCh (which act via voltage gated ion channel-dependent and G-protein coupled receptor-dependent mechanisms respectively) were influenced to a similar extent by IL-13, it appears likely that the modulation is at the level of the smooth muscle contractile apparatus, rather than influencing receptor density or transduction. Fredberg (2004) defined the hyperreactivity component of airway hyperresponsiveness, represented by E_{max}, as the ability of the airways to narrow excessively and added that it accounts for the morbidity and mortality associated with asthma. These results demonstrated that the effects of IL-13 on contractility were principally to increase E_{max}, and no significant changes in EC_{50} were observed. A similar conclusion was demonstrated from an earlier *in vitro* study showing that cultured murine tracheal rings in the presence of IL-13 (100 ng/ml) resulted in enhanced KCl and CCh-induced contraction without changes in receptor affinity (Tliba *et al*., 2003).

It was expected that r-IL-13 would enhance KCl and CCh induced contraction in Wistar rat tracheal segments, but it was observed that there was no significant

difference between KCl or CCh induced contraction in r-IL-13 (10 or 100 ng/ml)-treated tissues compared with the control group. Previous work has demonstrated that bronchus isolated from male Wistar rats with TNF-α (300 ng/ml) for 24 h enhanced acetylcholine induced contraction compared with controls (Sakai *et al.*, 2004). This discrepancy might be due to different responses of different airway tissues or different cytokine. However, no significant differences in relative contraction in response to CCh were found between the trachea, main bronchi and bronchioles of Fisher 344 rats (Van & Joos, 1998). Also no difference in sensitivity to acetylcholine was found between isolated trachea strips and small intrapulmonary bronchioles (Russell, 1978; Van & Joos, 1998). Results concerning insignificant r-IL-13 enhanced responsiveness using rat isolated tracheal rings may also suggest different functions of r-IL-13 in rats other than enhanced smooth muscle contraction. It was shown that rat B cells were able to bind IL-13 and proliferate when cultured with CD40 ligand and IL-13, but the administration of IL-13 does not enhance IgE production *in vivo* (Pierrot *et al*., 2001). Furthermore, it was found that mouse IL-13 does not have an effect on B cells, in contrast to human IL-13, supporting the different functions of IL-13 in different species (Izuhara & Arima, 2004).

The current study demonstrated an evaluation of the short term-effects of culturing murine tracheal segments with m-IL-13. Isolated segments cultured for 1, 4 or 8 h in the presence of m-IL-13 showed no significant difference from control segments. It is apparent that more than 8 h incubation with IL-13 is needed for enhanced hyperresponsiveness. It was shown in primary fibroblasts cultured from asthmatic subjects and normal controls that an increase in eotaxin protein expression was not observed above the detection limit until 6 h incubation with IL-13 (30 ng/ml) with significant increase at 24 h, and 48 h (Wenzel *et al.*, 2002). Another study reported no significant difference in contraction to electric field stimulation or CCh at 24 h in Brown-Norway rats tracheal strips and bronchial rings between control and IL-1β treated tissue (Koto *et al.*, 1996). Absence of a 24 h response in their study might be due to species-dependent differences and using a different cytokine.

The effect of culture period of murine tracheal segments on KCl and CCh was evaluated by comparing 24 h-incubated rings with fresh segments. There was no significant difference in cultured tissue in response to KCl and CCh compared with

fresh segments. These data are in agreement with a study (Adner *et al.*, 2002) using murine tracheal segments isolated from BALB/cJ mice showing that the maximal contraction was increased insignificantly for the first two days of culture compared with fresh segments and maximal contraction decreased to 40 and 70 % of initial contraction for KCl and CCh respectively by day 8 (Adner *et al.*, 2002). However, a similar study using BALB/cJ strain mice showed no significant difference in response to CCh between fresh segments and segments cultured for 1, 2, 4 and 8 days (Bryborn *et al.*, 2004). These studies support the use of 24 h as culture period as tissues were shown to maintain their contractile phenotype during culture.

This study demonstrated that exposure of murine tracheal segments to m-IL-13 (100 ng/ml) did not modulate the relaxant responses to isoprenaline. These results are the opposite of what would be expected, but it may be due to high concentration used. Also, r-IL13 (10 or 100 ng/ml) did not modulate relaxant responses to isoprenaline would support different function of r-IL-13. It was studied in isolated human tracheal smooth muscle cell that the response to isoprenaline was significantly reduced in IL-13 (50 ng/ml)-treated cells (Laporte *et al.*, 2001).

Despite the fact that mouse and rat are closely related rodents (Scalzi & Hozier, 1998), an apparent variation in IL-13 enhanced contraction between species was demonstrated in this study. Cross-reactivity study using rat isolated tracheal rings incubated with m-IL-13 showed no significant difference in KCl induced contraction, but m-IL-13 significantly enhanced contraction to CCh. These findings suggest that functional homology exists between mouse and rat at the receptor level rather than at the IL-13 protein level. Furthermore, it was demonstrated that r-IL-13 did not enhance murine tracheal contraction to KCl and CCh, which might support a different function of r-IL-13 rather than hyperresponsiveness. These findings are consistent with the findings of other investigators in a guinea pig model. They demonstrated that a single exposure to nebulized m-IL-13 induces a significant increase in AHR with increased inflammatory cells in BAL fluid 24 h after exposure (Morse *et al.*, 2002).

Although this chapter emphasizes the differences in response to IL-13 across animal species, it was important to investigate the responsiveness to h-IL-13 in both species, which may provide a suitable and useful replacement to human tissue to

screen IL-13 enhanced contraction. This study showed that h-IL-13 enhanced contraction to KCl in tracheal rings isolated from both rat and mice but did not enhance contraction to CCh. This may suggest that h-IL-13 may not be able to enhance rat or mouse muscarinic receptors activity. In accordance with the present study, it was shown that pretreatment of guinea pig tracheal rings with h-TNFα, h-IL-1β or h-IL-2 for 18 h had no effect on CCh-induced contraction (Wills-Karp *et al.*, 1993). However, these workers extended their study to test the effect of these human proinflammatory cytokines on the relaxant effect of isoprenaline. They demonstrated that h-TNFα, or h-IL-1β, but not h-IL-2 affect the relaxation elicited by isoprenaline (Wills-Karp *et al.*, 1993). In a further study, it was demonstrated that incubation of guinea pigs tracheal strips with human TNFα for 30 min significantly increased the maximum response to methacholine, and this was completely inhibited by a specific TNFα antagonist i.e. rh-soluble TNF-receptor-p80 (Pennings *et al.*, 1998). Although an anti-inflammatory effect of h-IL-13 was shown in a guinea pig model of eosinophilic inflammation induced by TNF-α (Watson *et al.*, 1999), their study also supports cross reactivity between h-IL-13 and tissues or cells isolated from different species. A recent study showed that incubation of bovine tracheal smooth muscle cells incubated with h-IL-13 (20 ng/ml) for 6 h, but not h-IL-4, induced augmentation of the ATP-induced gel contraction (Ohta *et al.*, 2008). Although different experimental design and cytokines were used in these previous studies, cross reactivity interactions were demonstrated.

3.9 Summary

From this chapter, it can be concluded that:

- isolated murine tracheal rings incubated with m-IL-13 are a suitable model to further study IL-13-enhanced contraction;
- culturing murine tracheal segments did not affect their contractile phenotype;
- IL-13-enhanced contraction was not detected until overnight incubation with IL-13;
- cross species studies may also signify different pharmacological function(s) of IL-13 from different species.

Chapter Four

PI3K involvement in IL-13-induced ASM contraction

4.1 Introduction

One of the aims of this work was to examine the mechanism(s) involved in IL-13-enhanced responsiveness of murine tracheal segments. Although most IL-13 signalling studies have concentrated on the Janus kinase/signal transducers and activators of transcription-6 pathway, IL-13 also activates PI3K and downstream effector molecules (Wright *et al.*, 1997; Ceponis *et al.*, 2000; Hershey, 2003). PI3K signalling and its putative roles in lung disease have been extensively reviewed (Vanhaesebroeck *et al.*, 2001; Medina-Tato *et al.*, 2007; Ito *et al.*, 2007). PI3K may contribute to the pathogenesis of asthma by effecting the recruitment, activation, and apoptosis of inflammatory cells. PI3K signalling is also important in the regulation of resident smooth muscle cells which play critical roles in airway inflammation and airway hyperresponsiveness (Halayko & Amrani, 2003). In smooth muscle, PI3K is implicated in the enhancement of agonist-induced contraction, as evidenced by the ability of pharmacological inhibitors or molecular manipulations of PI3K to reduce agonist-stimulated contraction of tissue from hypertensive rats (Northcott *et al.*, 2005) or insulin-treated airway smooth muscle (Schaafsma *et al.*, 2007).

Two commercially available broad-spectrum inhibitors of PI3K, wortmannin and LY294002, contribute greatly to our knowledge of the biological role of PI3K in lung inflammation. Administration of wortmannin or LY294002 attenuates inflammation in murine models of allergic asthma (Ezeamuzie *et al.*, 2001; Kwak *et al.*, 2003). Intratracheal administration of LY294002 significantly inhibits most of the pathological characteristics of the mouse asthma model, including increased eosinophil counts and eotaxin, IL-5, and IL-13 levels in bronchoalveolar lavage fluid. Furthermore, lung tissue eosinophilia, airway mucus production, and AHR to inhaled methacholine are all significantly suppressed (Duan *et al.*, 2005). Furthermore, PI3K inhibitors can be delivered locally to minimize systemic exposure to the drugs and optimise their dosage (Finan & Thomas, 2004).

Although these studies with broad-spectrum inhibitors provide good evidence for a role for PI3K in allergic airway dysfunction, these inhibitors do not distinguish among the four class I PI3K isoforms (Davies *et al.*, 2000). The development of isoform selective inhibitors, as well as genetically modified mice, allow the

characterization of the different roles of individual PI3K isoforms in airway disease. As reviewed in Medina-Tato *et al.* (2007), a wide variety of therapeutic options are available for respiratory diseases but better drugs are required. Furthermore, a p110δ-specific inhibitor seems to offer the most potential as a therapeutic target in respiratory disease. Such an inhibitor could offer the opportunity of reducing Th2 responses without severely affecting Th1-mediated immunity, which would prove highly beneficial to the allergic patient. In addition, the effects of p110δ silencing on mucus production, mast cell degranulation and leucocyte recruitment are all very positive effects that an inhibitor could have in the clinic.

The present section of this study examines the role of the PI3K signalling pathway in IL-13-induced hyperresponsiveness of murine tracheal smooth muscle. Evidence is provided that a PI3Kδ-dependent mechanism plays a key role in IL-13-enhanced responsiveness.

4.2 IL-13 induced Akt phosphorylation in tracheal lysate

As discussed in chapter three, it was necessary first to identify the species to be used. Initial experiments presented in chapter 3 revealed consistent results with the use of murine tracheal segments. The ability of IL-13 to activate PI3K signalling in murine tracheal tissue was next investigated by assessing the phosphorylation of Akt, a downstream target of PI3K. This phosphorylation is dependent on PI3K activity. For these experiments, an antibody specific for Ser^{473} phosphorylated Akt, as well as an antiAkt antibody to act as the loading control was used. Time-course studies were carried out using m-IL-13 (100 ng/ml). Rapid phosphorylation of Akt Ser^{473} in murine tracheal tissue was detected after 2 min, which continued for 1 h and returned close to the basal level after 4 h stimulation. No significant changes in total Akt protein levels were observed in any of the group tested (Figures 4.1 and 4.2).

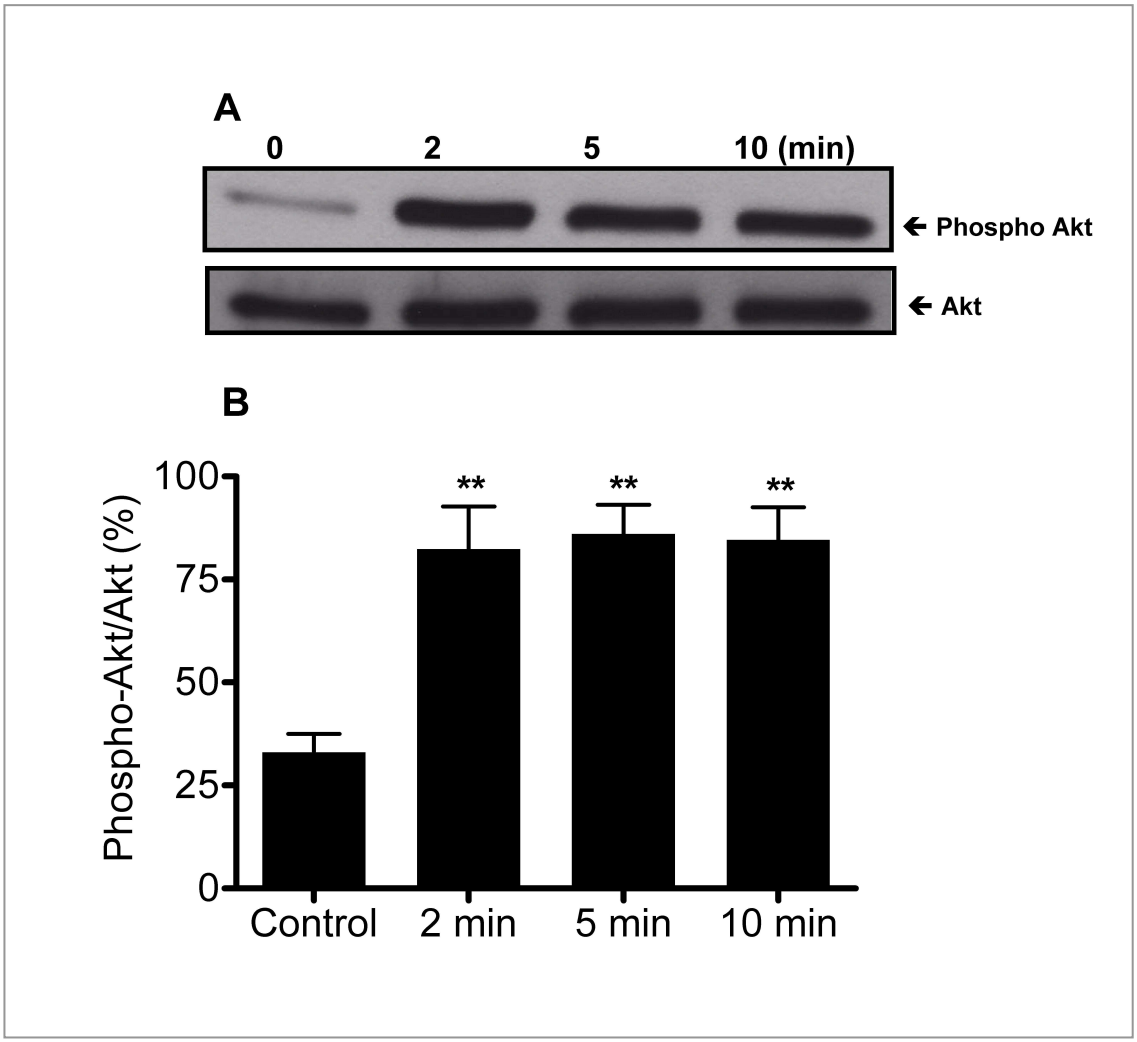

Figure 4.1 Effect of IL-13 on Akt phosphorylation at 2, 5 and 10 min. Tracheal rings from 8 CD1 mice treated with IL-13 (100 ng/ml) for 2 to 10 min were homogenized in ice-cold lysis buffer. Proteins (30 µg per lane) were separated by SDS-PAGE and probed with anti-phospho-Akt and anti-Akt antibodies before detection by enhanced chemiluminescence. A, immunoblot from one experiment representative of three. After probing for phospho-Akt, blots were reprobed for Akt to determine equal loading. B, densitometric analysis of phospho-Akt expression. Results are expressed as percentage phospho-Akt compared with total Akt, as determined using LabImage software (Lapelan Bio-imaging Solution, Halle, Germany). Bars indicate the mean density ratio ± s.e.m. from three independent experiments. **, $p < 0.01$, significant difference from control.

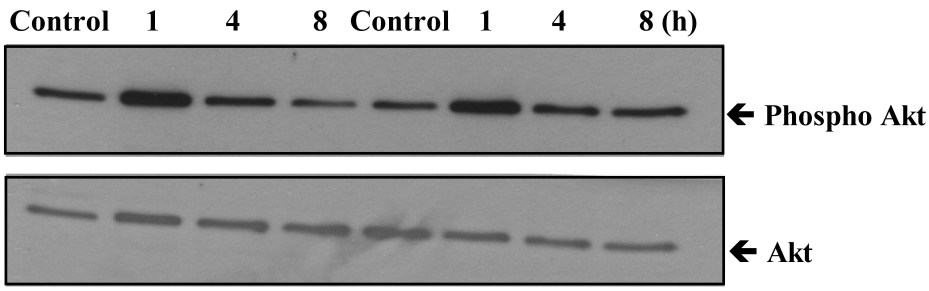

Figure 4.2 Effect of IL-13 on Akt phosphorylation at 1, 4 and 8 h. Tracheal rings from 8 CD1 mice treated with IL-13 (100 ng/ml) for 1 to 8 h were homogenized in ice-cold lysis buffer. Proteins (33 μg per lane) were separated by SDS-PAGE and probed with anti-phospho-Akt and anti-Akt antibodies before detection by enhanced chemiluminescence. The immunoblot shows samples prepared in two separate experiments. After probing for phospho-Akt, blots were reprobed for Akt to determine equal loading.

4.3 PI3K and IL-13-induced hyperresponsiveness

To examine the potential role of PI3K in IL-13-induced hyperresponsiveness in murine tracheal segments, the effects of two structurally distinct non–isoform-selective PI3K inhibitors, wortmannin (100 nM) and LY29402 (10 μM) were assessed. Addition of either inhibitor 30 min before IL-13 prevented the induction of ASM hyperresponsiveness, reducing E_{max} values for both KCl and CCh to that of drug vehicle-treated control tissues (Figure 4.3 and Table 4.1). Under the conditions used, neither wortmannin nor LY29402 had any effect on the contractility of murine tracheal smooth muscle in tissues not pretreated with IL-13 (Table 4.1).

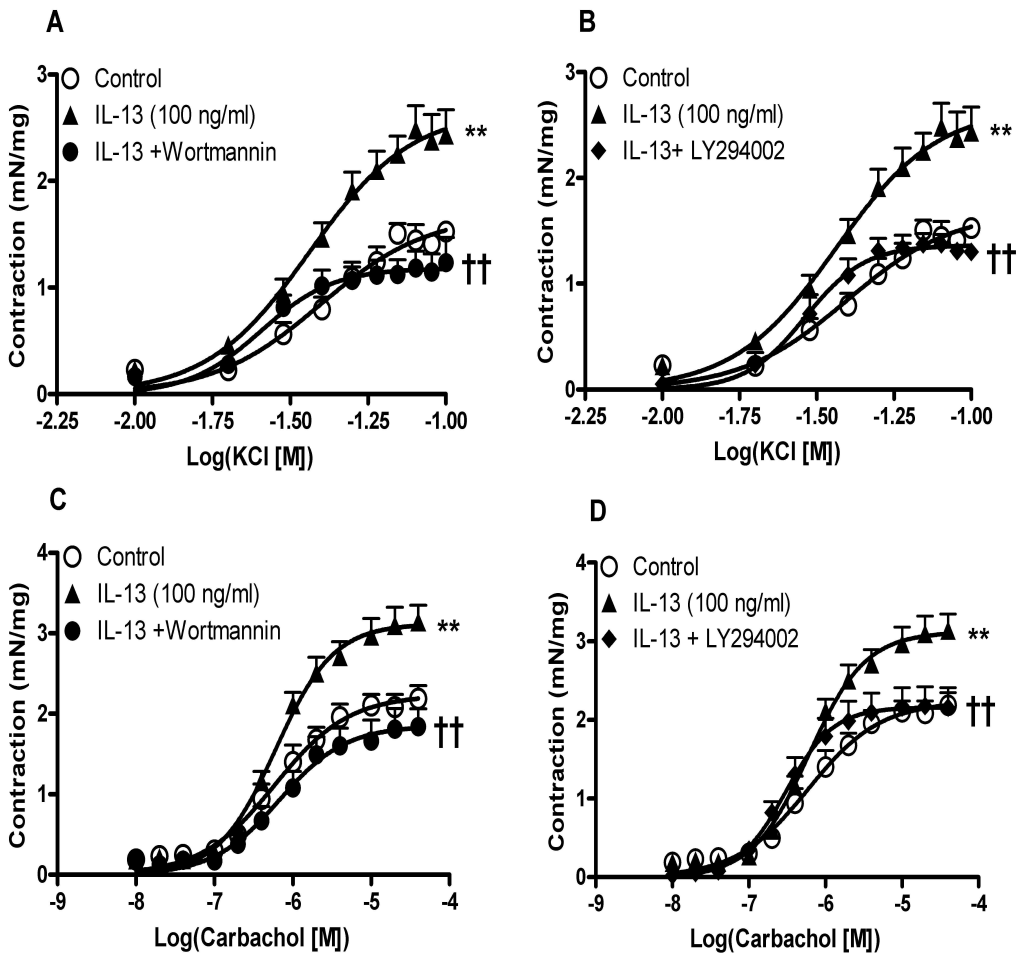

Figure 4.3 Effect of PI3K inhibitors on IL-13-enhanced contraction. Tissues were incubated for 30 min with drug vehicle (Control), wortmannin (100 nM), or LY294002 (10 μM) before exposure to murine IL-13 (100 ng/ml) for 24 h before assessing tissue responses to contractile agents KCl (A and B) and CCh (C and D). Data from groups are expressed as mean mN per mg of tissue (wet weight) ± s.e.m. One-way ANOVA followed by Dunnett's test were performed to determine the statistical significance of differences between E_{max} values. **, $p < 0.01$ compared with control; †† $p < 0.01$ compared with IL-13-treated tissue.

Table 4.1 Effect of broad-spectrum PI3K inhibitors on IL-13-induced contraction in isolated tracheal rings. Tissues were preincubated for 30 min with drug vehicle (Control, DMSO, 0.05% v/v), wortmannin (100 nM) or LY-249002 (10 μM). Media or IL-13 (100 ng/ml) was then added for a further 24 h before assessing contractility responses to KCl and CCh. Data are expressed as mean E_{max} ± s.e.m for n = 5 - 7 rings from different animals.

	KCl	CCh
	mN /mg tissue	
Control	1.7 ± 0.1	2.2 ± 0.1
Wortmannin	1.4 ± 0.2	1.8 ± 0.2
LY294002	1.9 ± 0.4	2.5 ± 0.4
IL-13	2.8 ± 0.3[a]	3.1 ± 0.2[b]
IL-13 + Wortmannin	1.3 ± 0.2[c]	1.8 ± 0.3[c]
IL-13 + LY294002	1.4 ± 0.1[c]	2.2 ± 0.3[d]

[a] $P < 0.05$ compared with control.

[b] $P < 0.01$ compared with control.

[c] $P < 0.05$ compared with tissues treated with IL-13 alone.

[d] $P < 0.05$ compared with tissues treated with IL-13 alone.

4.4 Effect of wortmannin on murine tracheal contraction

Control experiments were performed to investigate the effect of wortmannin at concentrations ranging from 10 - 100 nM. For these experiments, each murine trachea was split into two segments. One segment was incubated with wortmannin and the other segment was incubated with wortmannin 30 min before m-IL-13 (100 ng/ml) addition. Responses to KCl and CCh did not show any significant difference from vehicle control (DMSO). Mean KCl E_{max} values expressed in mN/mg for DMSO, wortmannin 10, 30 or 100 nM were 1.7 ± 0.1, 1.7 ± 0.3, 1.3 ± 0.1 and 1.3 ±

0.2 respectively and CCh mean values were 2.2 ± 0.1, 2.6 ± 0.3, 1.9 ± 0.2 and 1.8 ± 0.2 in the same order (Figure 4.4).

In another set of control experiments to examine the effect of wortmannin on KCl- or CCh- induced contraction, the same protocol was carried out with the exception that one segment was incubated with vehicle control and the other segment was incubated with m-IL-13 (100 ng/ml) for 24 h. After incubation and mounting the tissue in the organ bath, wortmannin (100 nM) was added 30 min before determining the KCl and CCh dose response curves. As seen in Figure 4.5, significant hyperresponsiveness was still observed, resulting in E_{max} values for KCl and CCh of 2.8 ± 0.3 ($p < 0.05$) and 4.1 ± 0.4 ($p < 0.001$, n = 6) compared with control values of 1.7. ± 0.1 and 2.2 ± 0.1 (n = 7) respectively.

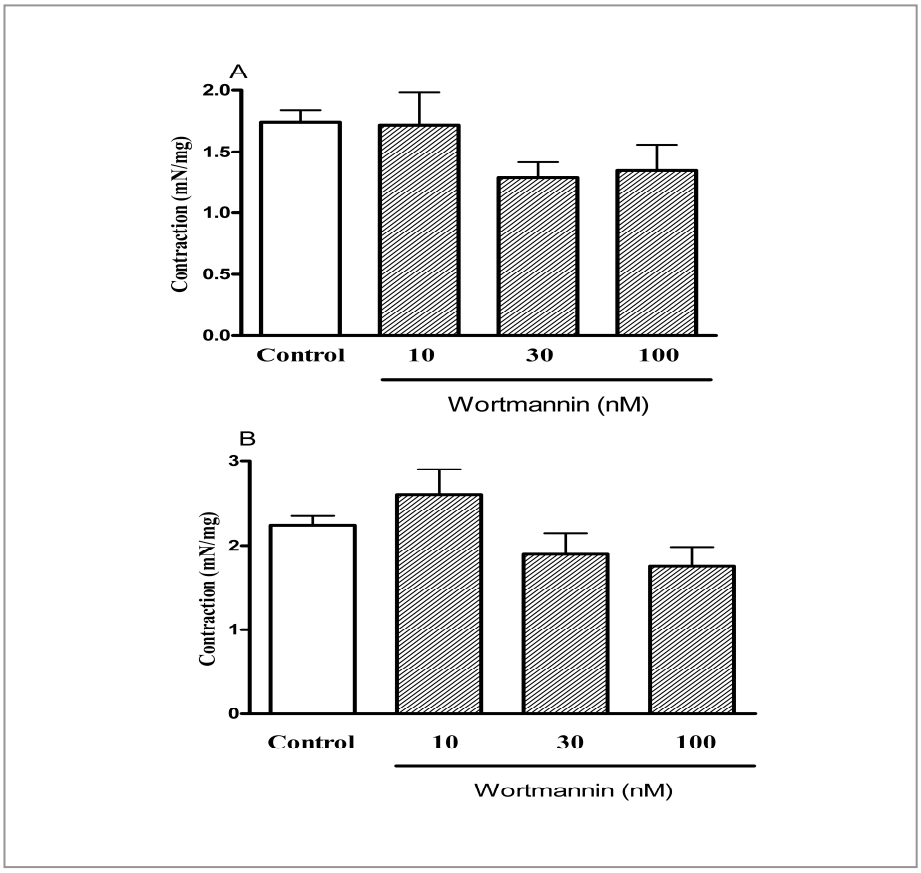

Figure 4.4 Effect of wortmannin on isolated murine tracheal rings. Isolated murine tracheal segments were exposed to wortmannin (10 –100 nM) for 24 h. Data are mean ± s.e.m. n = 4-7. Wortmannin did not significantly affect KCl (A) or CCh (B) induced contraction compared with vehicle control.

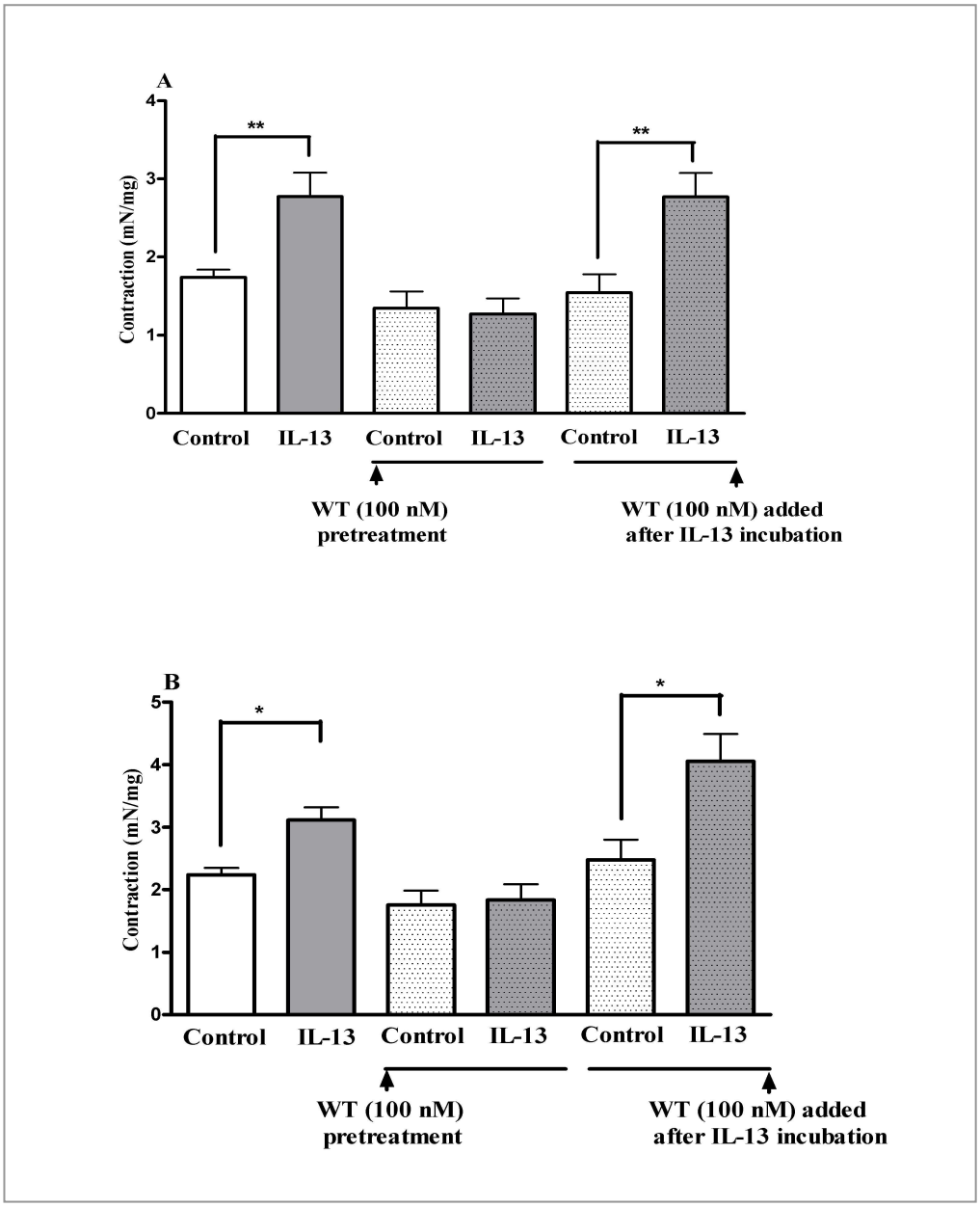

Figure 4.5 Effect of wortmannin (WT) addition before or after IL-13 incubation. Wortmannin (100 nM) was added to isolated murine tracheal rings 30 min before m-IL-13 (100 ng/ml, 24 h) incubation; or 30 min after incubation with m-IL-13 (100 ng/ml, 24 h) before assessing tissue responses to KCl (A) and CCh (B). Control (non-IL-13-treated) tissues were incubated in parallel cultures for each protocol (light shaded bars). Data from groups are expressed as mean mN per mg of tissue (wet weight) ± s.e.m. Student's paired *t*-test was performed to determine the statistical significance of differences between responses of control and IL-13-treated tissues * $P < 0.05$; ** $P < 0.01$; n = 6-7**.**

4.5 Role of PI3Kδ in IL-13-enhanced contraction

The previous results showed that the non–isoform-selective PI3K inhibitors, wortmannin and LY29402, prevented IL-13-induced hyperresponsiveness in isolated murine tracheal rings, however both inhibitors act on all four-class I PI3K isoforms. Recent *in vivo* studies support a major role for PI3K p110δ for IL-13-induced hyperresponsiveness (Lee *et al.*, 2006a; Nashed *et al.*, 2007), however these *in vivo* studies related the detected hyperresponsiveness to qualitatively altered immune responses, rather than alterations in structural cells. Therefore, tissues were treated with the selective PI3Kδ inhibitor IC87114 30 min before IL-13 addition (Figure 4.6).

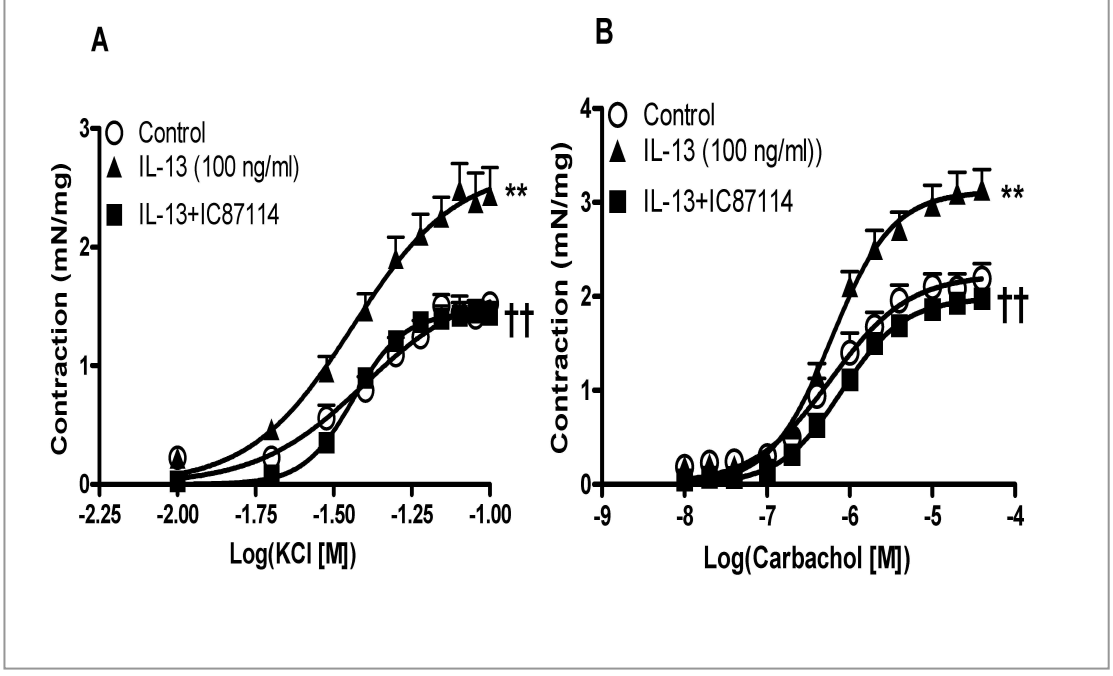

Figure 4.6 IC87114 prevents IL-13-enhanced contraction. Isolated murine tracheal segments were treated for 30 min with vehicle (control) or with IC87114 (10 μM) then incubated for a further 24 h in the absence or presence of IL-13 (100 ng/ml). Dose response curves to KCl (A) or CCh (B) were studied. Data points indicate mean ± s.e.m. for n = 5-7 animals. One-way ANOVA followed by Dunnett's test were performed to determine the statistical significance of differences between E_{max} values; **, significantly different compared with control, $p < 0.01$; ††, significantly different compared with tissues treated with IL-13 alone, $p < 0.01$.

IC87114 (10 μM) was able to inhibit completely the ability of IL-13 to elicit hyperresponsiveness to either KCl or CCh. In control experiments, this compound did not reduce tracheal smooth muscle contractility in the absence of IL-13 treatment, giving E_{max} values for KCl and CCh of 1.7 ± 0.3 and 2.6 ± 0.5, respectively, compared with 1.7 ± 0.2 and 2.2 ± 0.1 in vehicle-control treated tissues.

4.6 Effects of IL-13 using tracheal rings from p110δ$^{D910A/D910A}$ mice

To investigate further the role of PI3Kδ in IL-13-induced contraction, tracheal rings were obtained from mice expressing p110δ$^{D910A/D910A}$, a catalytically inactive form of p110δ (Okkenhaug *et al.*, 2002). These mice were generated by point mutation instead of deletion to prevent changes in the expression levels of the other PI3K catalytic and regulatory subunits. IL-13 was unable to enhance contraction in rings isolated from p110δ$^{D910A/D910A}$ mice compared with control rings isolated from same mice (Table 4.2 and Figure 4.7). However, IL-13 did elicit enhanced contraction in response to KCl and CCh in tracheal rings isolated from control DO11-10 mice (Table 4.2 and Figure 4.6).

Table 4.2 Effect of IL-13 on KCl- and CCh-induced contractions in isolated murine tracheal rings of p110δ$^{D910A/D910A}$ and DO11-10 mice. Data are expressed as mean E_{max} ± s.e.m. for n = 6 pairs of tracheal rings.

	KCl		CCh	
	Control	IL-13	Control	IL-13
	mN/mg tissue			
DO11-10 control mice	1.8 ± 0.2	2.9 ± 0.2[a]	2.5 ± 0.3	3.7 ± 0.3[a]
p110δ$^{D910A/D910A}$ mice	1.9 ± 0.3	1.8 ± 0.4	2.8 ± 0.3	2.4 ± 0.2

[a] $P < 0.01$ compared with non-IL-13 treated control mice.

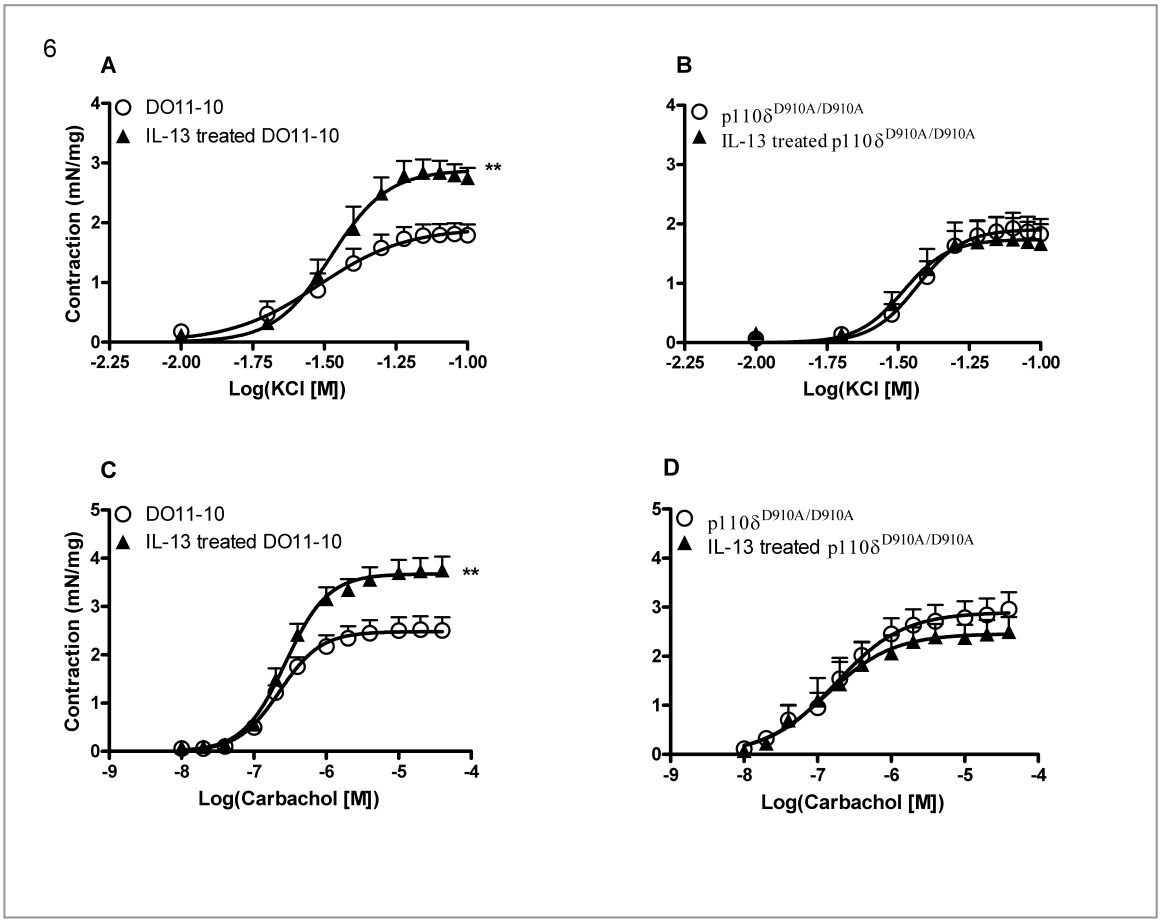

Figure 4.7 Effect of IL-13 on responsiveness of tissues from p110δ$^{D910A/D910A}$ mice. Isolated murine tracheal segments from DO11-10 control or p110δ$^{D910A/D910A}$ kinase-dead mice were incubated with IL-13 (100 ng/ml, 24 h) before assessment of responsiveness to KCl (A) or CCh (B). Data indicate mean ± s.e.m. for n = 6 mice. **, $p < 0.01$ compared with matched tissue not treated with IL-13, Student's paired *t*-test.

4.7 Discussion

4.7.1 PI3K in IL-13 enhanced contraction

After determining IL-13 enhanced contraction in murine tracheal segments, the mechanism by which IL-13 induces ASM hyperresponsiveness was characterized. Several lines of evidence in this study implicate PI3K signalling in IL-

13-induced hyperresponsiveness. IL-13-treated tracheal segments express phosphorylated Akt. However, immunoblot analysis showed IL-13 induced a very early (after 2 min, as assessed by PI3K-dependent phosphorylation of Akt) activation of PI3K, while increased responsiveness was not observed until overnight incubation. These findings support an earlier study in which human alveolar macrophages obtained from normal non-smoking volunteers cultured with IL-13 (10 ng/ml) for 1 min - 6 h showed phosphorylation of Akt at 5 min – 3 h (Monick *et al.*, 2002). In an *in vivo* allergen challenge model, other research group noted Akt phosphorylation at 1, 24, 48, and 72 h after OVA inhalation, likely as a consequence of an ongoing inflammatory response and persistent local cytokine production (Lee *et al.*, 2006a). Furthermore, intratracheal administration of LY294002 significantly inhibits OVA-induced increases in total cell counts, eosinophil counts, and IL-5, IL-13, and eotaxin levels in bronchoalveolar lavage fluid, and dramatically inhibited OVA-induced tissue eosinophilia and airway mucus production. This is associated with a significant suppression of OVA-induced AHR to inhaled methacholine (Duan *et al.*, 2005). It is noteworthy that the study by Duan and co-workers showed that LY294002 markedly attenuated OVA-induced serine phosphorylation of Akt. Their findings support studies showing attenuated eosinophilic airway inflammation and AHR by LY294002 and wortmannin in asthma models (Ezeamuzie *et al.*, 2001; Kwak *et al.*, 2003) connecting PI3K and the immune system in hyperresponsiveness observed in these models.

In this study using the isolated segments provide functional evidence for the role of PI3K in the regulation of IL-13-induced hyperresponsiveness to KCl and CCh, established by pharmacological blockade of PI3K activity using wortmannin and LY294002. These non–isoform-selective inhibitors prevented IL-13-induced hyperresponsiveness in isolated murine tracheal rings.

4.7.2 Effect of wortmannin on murine tracheal contraction

Results of this study demonstrated that wortmannin could be used to inhibit IL-13-enhanced contraction to both KCl and CCh. Wortmannin (10, 30 or 100 nM) did not suppress the maximum responses for either KCl or CCh, although a non-significant decrease was observed with 30 and 100 nM wortmannin concentrations. It

was previously reported that wortmannin (0.3-3 μM) added for 5 or 30 min inhibited the contraction in rat aortic rings stimulated with KCl (Nakanishi *et al.*, 1992). In a following study using male pig tracheal smooth muscle, it was demonstrated that the PI3K stimulating effect of acetylcholine (1 μM) was blocked by wortmannin (1μM) or LY294002 (10 μM), detected by the blocking of PI3K-induced incorporation of [^{32}P] into the D-3 position on phosphatidylinositols (Mamoon *et al.*, 2001) and wortmannin also blocked the phosphorylation of p110 in a concentration-dependent manner (10 nM - 1 μM). Although these previous studies demonstrated an inhibitory effect of wortmannin on acetylcholine and KCl responses, they used a higher concentration of wortmannin and implicated myosin light chain kinase inhibition for the wortmannin effect. A recent study supported a PI3K stimulating effect of IL-13 (20 ng/ml) using wortmannin by testing contractions of collagen gels containing bovine tracheal smooth muscle cells (Ohta *et al.*, 2008). This inhibition was detected with high (1 μM) wortmannin, but not seen at 100 nM, which indicate non- selective effect of wortmannin.

An important question is whether IL-13 enhanced KCL and CCh contractions reflect a difference between pre-treatment and post-treatment with wortmannin (100 nM). Therefore the effect of wortmannin added prior to or after incubation with IL-13 was examined. Treatment of tissues with wortmannin after 24 h exposure to IL-13 was unable to reduce the enhanced responsiveness, suggesting a role for PI3K in the development of hyper-contractility, rather than in the contraction response per se. Thus, it seems reasonable to conclude that the inhibitory effect of wortmannin is indicative of effect on IL-13 signalling rather than an effect on KCl or CCh action.

4.7.3 PI3K p110δ in IL-13 enhanced contraction

Recent *in vivo* studies support a role for PI3K p110δ for IL-13-induced AHR. Lee *et al*. (2006a) demonstrated that p110δ is the main component of class I PI3K-dependent, allergen-induced Akt activation and inflammation in the lung and IC87114 significantly suppresses OVA-induced AHR to methacholine *in vivo*. It was also established that AHR to inhaled methacholine is markedly attenuated in p110δ-inactivated mice after allergen challenge (Nashed *et al.*, 2007). Using isolated tracheal rings treated with the p110δ-selective inhibitor, as well as tissue from

animals expressing the catalytically inactive PI3K subunit p110δ$^{D910A/D910A}$, this chapter shows a crucial role of p110δ in inflammation-independent induction of hyperresponsiveness by IL-13. Hence, whereas previous studies implicate the involvement of the PI3K p110δ isoform in the inflammatory component of AHR, this work indicates an important role in IL-13-induced ASM contraction independent of effects mediated by infiltrating immune cells. These dual actions of IL-13-stimulated p110δ activity, both in airway inflammation, and in the direct effects on structural cells shown in the present study, point to p110δ as an attractive target for the treatment of airway disease. An important feature of this study is that PI3K was involved only in IL-13-enhanced contractility, because contractility of control tissues treated with inhibitors, or tissue expressing p110δ$^{D910A/D910A}$, had responsiveness similar to that of normal tissues.

4.8 Summary

In summary, in the present chapter the following was demonstrated:

- IL-13 induced early Akt phosphorylation;
- the non–isoform-selective PI3K inhibitors, wortmannin and LY29402, inhibited IL-13-enhanced contraction;
- IC87114 selectively inhibited the p110δ isoform required for IL-13-induced tracheal smooth muscle contraction;
- tissue from p110δ$^{D910A/D910A}$ kinase-dead mice had responsiveness similar to that of normal tissues;
- IL-13-enhanced contraction is due to an effect of p110δ activation in resident airway cells.

Chapter Five

Effect of PI3K inhibition on IL-13–induced arginase I expression

5.1 Introduction

Arginase is a key enzyme of the urea cycle in the liver. It exists as two distinct isoenzymes, arginase I, and II, which are encoded by different genes. Arginase I is expressed in the liver, as well as other tissues, including the airway epithelium (Cederbaum *et al.*, 2004; Bergeron *et al.*, 2007). Arginase I hydrolyzes L-arginine to urea and L-ornithine, precursors of polyamines and L-proline involved in smooth muscle cell growth and collagen synthesis respectively (Maarsingh *et al.*, 2008a). Arginase I expression is upregulated by Th2 cells and their cytokines (Munder *et al.*, 1999). A potential mechanism of IL-13-induced hyperresponsiveness is the induction of arginase, which can compete with nitric oxide synthase (NOS) for the common substrate arginine, and remove the modulatory effects of NO on airway smooth muscle contraction (Meurs *et al.*, 2003). Furthermore, attenuation of IL-13-induced airway hyperresponsiveness was observed *in vivo* using RNA interference towards arginase I (Yang *et al.*, 2006). Microarray analysis in two distinct models of experimental asthma, as well as in the lungs of asthma patients, revealed up-regulation of three genes involved in arginine metabolism, arginase I, arginase II, and the cationic amino acid transporter 2. Of particular note is that arginase I is up-regulated in perivascular and peribronchial pockets of inflammation within the lungs of asthmatic mice (Zimmermann *et al.*, 2003). Zimmermann and co-workers also demonstrated that up-regulation of arginase occurs in response not only to allergens but also in response to IL-4 and IL-13. The development of AHR has also been linked to the regulation of L-arginine catabolism by arginase I (Meurs *et al.*, 2002; Yang *et al.*, 2006). In chapter four of this study it was demonstrated that IL-13-induced hyperresponsiveness depends on PI3K activity. However, IL-13 induced a very early activation of PI3K, whereas increased responsiveness was not observed until overnight incubation denoting further downstream effector molecule(s).

This study was extended to investigate the role of IL-13-induced hyperresponsiveness and arginase I protein expression in murine tracheal segments. A number of reports have shown that IL-13 may exert its deleterious effects in asthma by directly acting on airway resident cells, including epithelial cells and airway smooth muscle cells (Kuperman *et al.*, 2002; Tliba *et al.*, 2003). This section of

results also investigated the role of epithelium in IL-13-enhanced contraction as well as the effect of epithelial denudation on IL-13-induced expression of arginase I.

5.2 Effect of L-norvaline on IL-13 enhanced contraction

The results in chapter 4 show that IL-13 treatment of tracheal tissue is associated with an early activation of PI3K, as assessed by phosphorylation of Akt, (after 2 min, using immunoblot analysis) whereas increased responsiveness is not observed until overnight incubation. Hence, the mechanism by which IL-13-induced contraction remains unclear. For this purpose this chapter investigates a further downstream effector molecule of IL-13-induced contraction mechanism. A potential mechanism of IL-13-induced hyperresponsiveness is the induction of arginase, which can compete with nitric oxide synthase for the common substrate arginine, and remove the modulatory effects of NO on airway smooth muscle contraction and could be involved in the regulation of cholinergic airway reactivity. Therefore, the role of arginase I was investigated in IL-13 induced hyperresponsiveness.

As previously observed, incubation of murine tracheal rings with m-IL-13 for 24 h potentiated KCl (10-100 mM) and CCh (10^{-8} – 10^{-5} M)-induced contractions (Figure 5.1). The agonist E_{max} of the concentration response curve was significantly higher in rings pretreated with m-IL-13 (100 ng/ml) compared with controls, with E_{max} values for KCl and CCh increased approximately 1.6-fold (Table 5.1). Addition of L-norvaline before IL-13 prevented the enhanced contraction, reducing E_{max} values for both KCl and CCh to that of drug vehicle-treated control tissues (Figure 5.1, Table 5.1). Under the conditions used, L-norvaline had no effect on the contractility of murine tracheal smooth muscle in tissues not pretreated with IL-13 (Table 5.1).

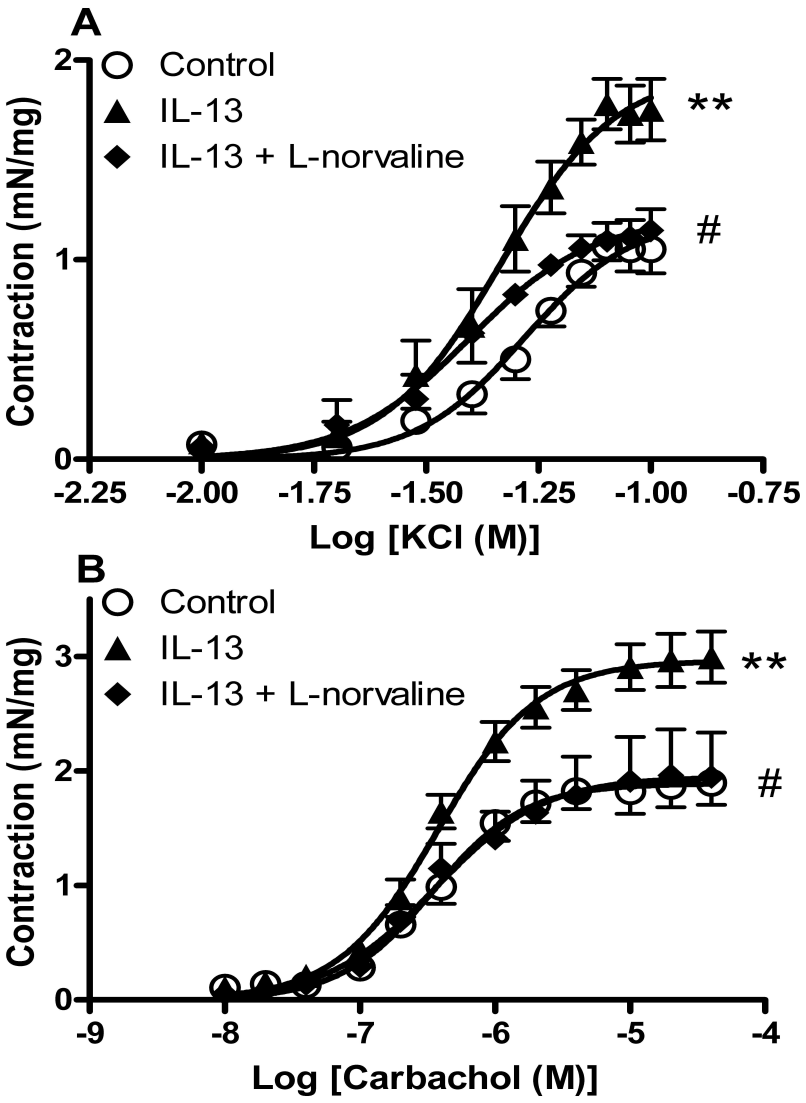

Figure 5.1 Effect of L-norvaline on IL-13-induced hyperresponsiveness to KCl (A) and CCh (B). Exposure of tracheal rings to IL-13 (100 ng/ml, 24h) resulted in enhanced responsiveness to KCl and CCh compared with control (n = 8), whereas responsiveness was reduced when contraction was assessed in the presence of L-norvaline (10 mM) (n = 4). Tissues were incubated without IL-13 (Control), with IL-13, with L-norvaline (10 mM) before exposure to murine IL-13, or with L-norvaline alone for 24 h, before assessing tissue responses to contractile agents. Data from groups were expressed as mean mN per milligram of tissue (wet weight) ± s.e.m. One-way ANOVA followed by Dunnett's test were performed to determine the statistical significance of differences between E_{max} values. **, $p < 0.01$ compared with control; #, $p < 0.05$ compared with IL-13-treated tissue.

Table 5.1 Effect of L-norvaline on responsiveness to KCl and carbachol of IL-13 incubated murine tracheal segments

	KCl	CCh
	E_{max} (mN / mg)	
Control	1.2 ± 0.1	1.9 ± 0.1
L-norvaline	1.3 ± 0.1	1.7 ± 0.04
IL-13	1.9 ± 0.2[a]	3.0 ± 0.1[a]
IL-13 + L-norvaline	1.2 ± 0.1[b]	1.9 ± 0.1[b]

[a]$p < 0.01$ compared with matched control. [b]$p < 0.05$ compared with tissues treated with IL-13 alone (n = 4).

5.3 Detection of arginase I protein expression

5.3.1 Western blotting of tracheal homogenates

To correlate IL-13-enhanced contraction detected after 24 h and IL-13-induced arginase I protein expression, it was necessary to examine the concentration- and time-dependent effect of m-IL-13 on arginase I protein expression. Arginase I protein expression was determined after incubating murine tracheal rings with various concentrations (10-100 ng/ml) of m-IL-13 for 24 h. Figure 5. 2 A shows that mice tracheae exhibits a low resting level of arginase I in the absence of IL-13. Arginase I protein expression was increased by m-IL13 at the different concentrations tested with the largest increase seen at 100 ng/ml. The time-dependent study of arginase I protein expression in murine tracheal segments treated with 100 ng/ml is shown in Figure 5.2 B. Arginase I protein expression was not detected at 1 and 4 h but was first observed to increase 8 h after the addition of IL-13. Densitometric analysis of arginase I protein expression after treating the rings with m-IL-13 (100 ng/ml) for 24 h is shown in Figure 5.3. As ascertain from these immunoblotting results, IL-13-induced arginase I protein expression coincided with the organ bath results showing hyperresponsiveness in response to m-IL-13 (10 and 100 ng/ml, 24 h).

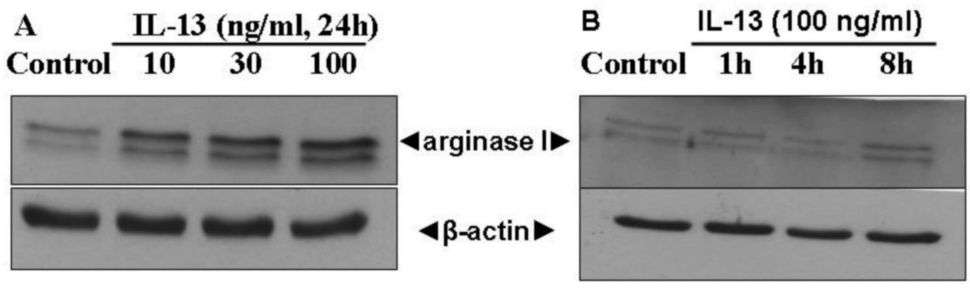

Figure 5.2 Induction of arginase I by IL-13. Tissues were treated with IL-13 (10-100 ng/ml, 24h) (A) or IL-13 (100 ng/ml) for 1, 4, 8h (B). The lysates were subjected to immunoblotting against arginase I (probed with mouse monoclonal anti-arginase I). IL-13-induced arginase I protein expression was observed when tissues were treated with different concentrations of IL-13 for 24 h, but not at earlier incubation times.

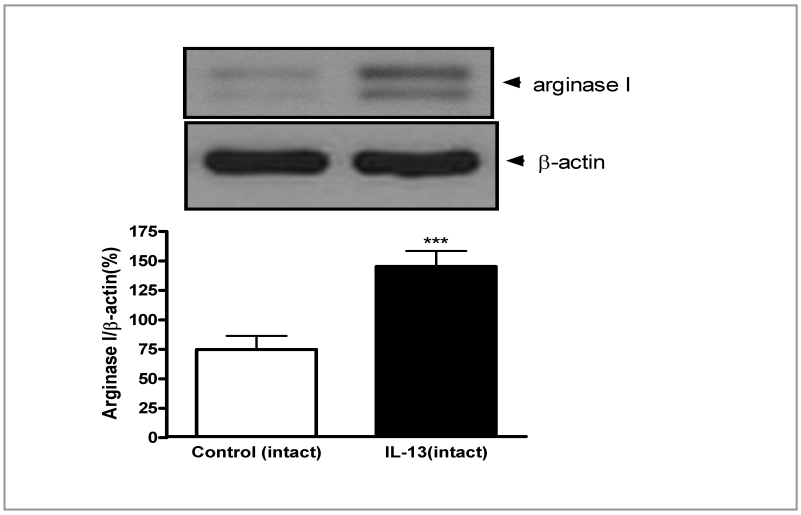

Figure 5.3 Effect of IL-13 on arginase I protein expression in tracheal rings. Tracheal rings from 6 CD1 mice treated with IL-13 (100 ng/ml) for 24 h were homogenized in ice-cold lysis buffer. Proteins (30 μg per lane) were separated by SDS-PAGE and probed with mouse monoclonal anti-arginase I and anti-β-actin antibodies before detection by enhanced chemiluminescence. After probing for arginase I, blots were reprobed for β-actin to determine equal loading. Densitometric analysis of arginase I protein expression was determined using Labimage software (Lapelan Bio-imaging Solution, Halle, Germany) and were expressed as percentage arginase I compared with β-actin. Bars indicate the mean density ratio ± s.e.m from four independent experiments. ***, $p < 0.001$, significant difference from control.

5.3.2 IHC detection of arginase I in murine tracheal rings

To determine the cellular source of the IL-13-induced arginase I protein expression demonstrated by Western blotting, IHC staining of arginase I in murine tracheal segments was carried out. It was necessary to validate the method used in this system, therefore the murine liver served as a positive control, since it is established that arginase I is highly expressed in the liver (a synonymous name of arginase I is liver arginase). Validity of this method using the liver as a positive control was confirmed by the perivenular absence of arginase I expression (Figure 5.4 A). A negative control in which the rabbit polyclonal anti-arginase I antibody was omitted showed no background staining (Figure 5.4 B).

To examine the expression and localization of arginase I in murine tracheal segments incubated for 24 h with m-IL-13 (100 ng/ml), paraffin-embedded sections were immunostained with rabbit polyclonal anti-arginase I antibody. Strong immunostaining for arginase I protein was observed in both epithelium and smooth muscle (Figure 5.4 D) compared with control (Figure 5.4 C).

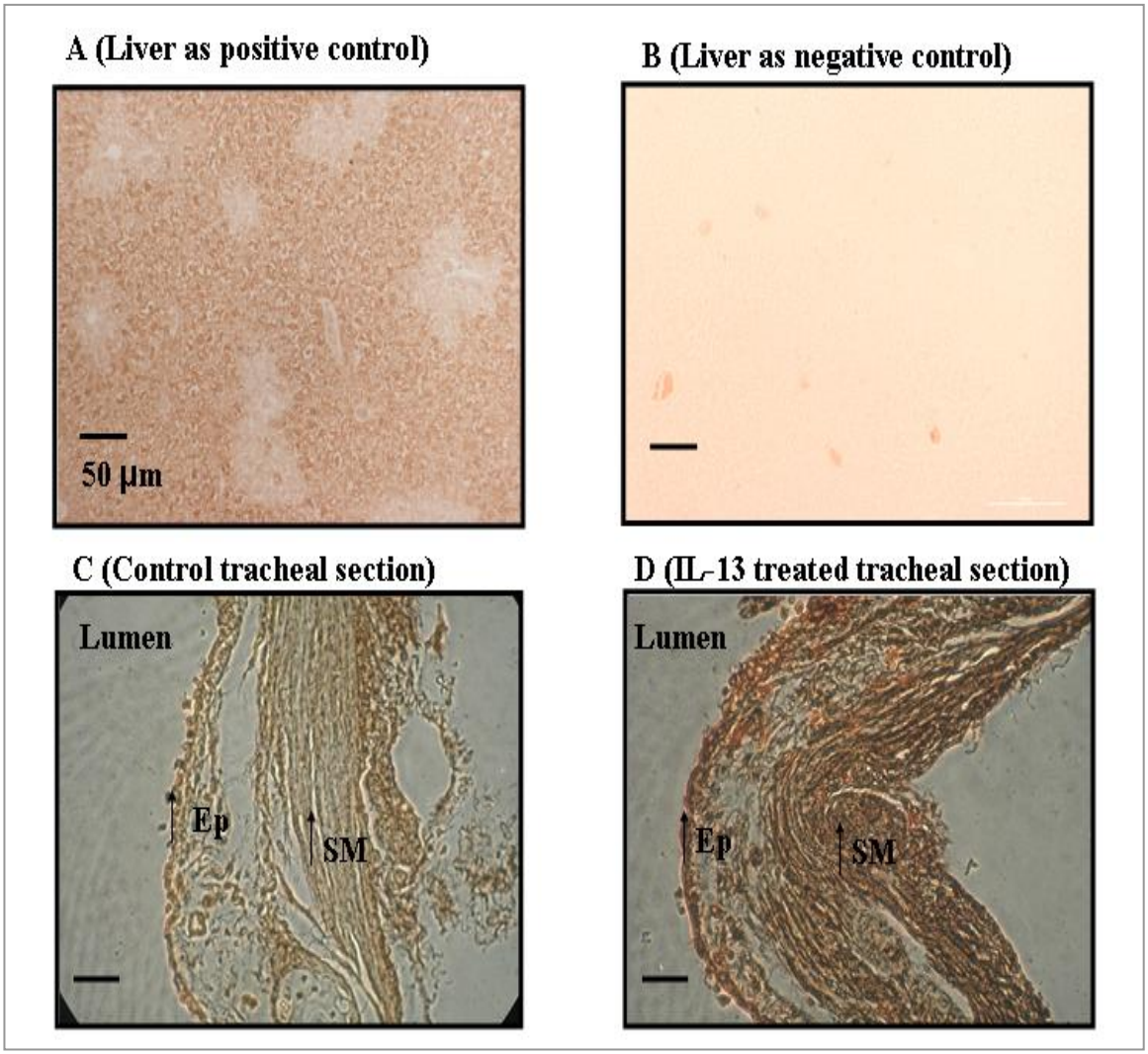

Figure 5.4 IHC analysis of arginase I in IL-13 treated segments. Murine Liver served as positive control (A) showed expression of arginase I probed with rabbit polyclonal anti-arginase I antibody in hepatocyte with perivenular absence of arginase I. No staining was observed in control Liver section (B). Increased expression of arginase I in both epithelium (Ep) and smooth muscle (SM) compared with control (C & D). Positive staining is indicated by the brown colour. Images are representative of experiments with 3 mice with positive staining indicated by the brown colour. X 400 magnification.

5.4 PI3K and IL-13-induced arginase I protein expression

To examine further the potential role of PI3K in IL-13-induced arginase I protein expression, the effects of two structurally distinct non–isoform-selective PI3K inhibitors, wortmannin (100 nM) and LY29402 (10 µM), were assessed. LY294002 clearly inhibited IL-13 induced arginase I protein expression in murine tracheal rings

(Figure 5.5). Additionally, IHC analysis using LY29402 established increased expression of arginase I in IL-13 treated segments in both epithelium and smooth muscle (Figure 5.6 B) compared with control (Figure 5.6 A), and inhibited by prior treatment with LY294002 30 min before addition of m-IL-13 (Figure 5.6 C). Similarly increased expression of arginase I in both epithelium and smooth muscle was seen in IL-13 treated segments (Figure 5.6 E) compared with control (Figure 5.6 D), and this was also inhibited by prior treatment with wortmannin 30 min before addition of m-IL-13 (Figure 5.6 F). These results obtained from immunoblotting and IHC established a link between PI3K activity and IL-13 induced-arginase I protein expression.

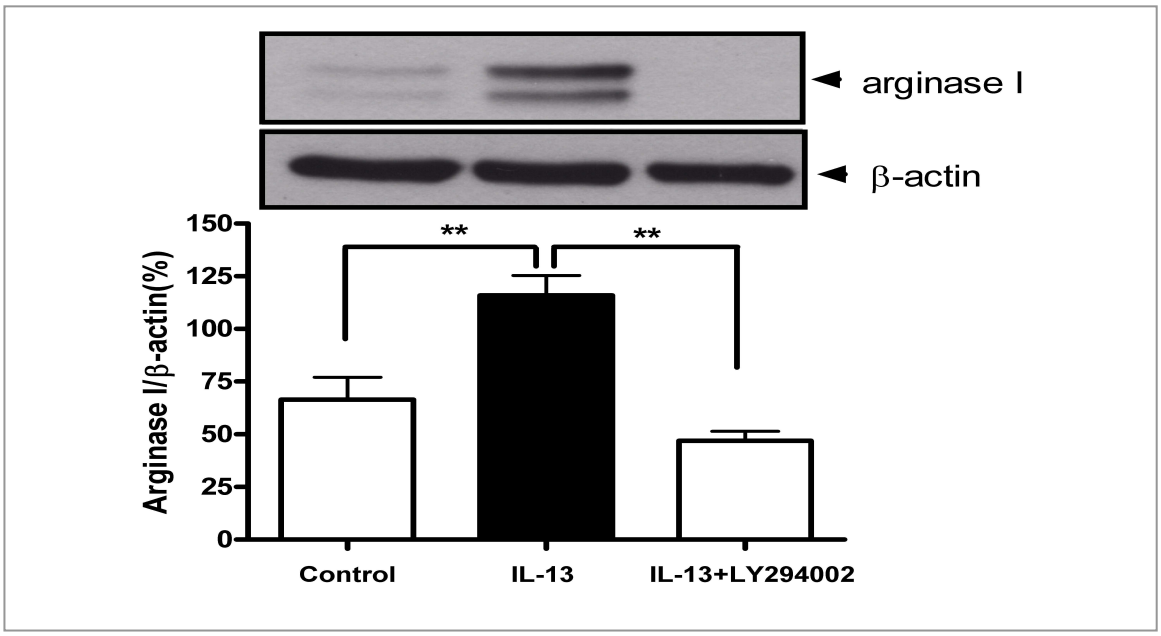

Figure 5.5 LY294002 inhibits IL-13–induced arginase I protein expression in murine tracheal rings. Tracheal rings from 8 CD1 mice treated with LY294002 (10 μM) for 30 min before exposure to IL-13 (100 ng/ml) for 24 h were homogenized in ice-cold lysis buffer. Proteins (30 μg per lane) were separated by SDS-PAGE and probed with mouse monoclonal anti-arginase I antibody before detection by enhanced chemiluminescence. After probing for arginase I, blots were reprobed for β-actin to determine equal loading. Densitometric analysis of arginase I protein expression are expressed as percentage arginase I compared with β-actin, determined using Labimage software (Lapelan Bio-imaging Solution, Halle, Germany). Bars indicate the mean density ratio ± s.e.m. from three independent experiments. **, $p < 0.01$, significant difference from IL-13-treated tissue.

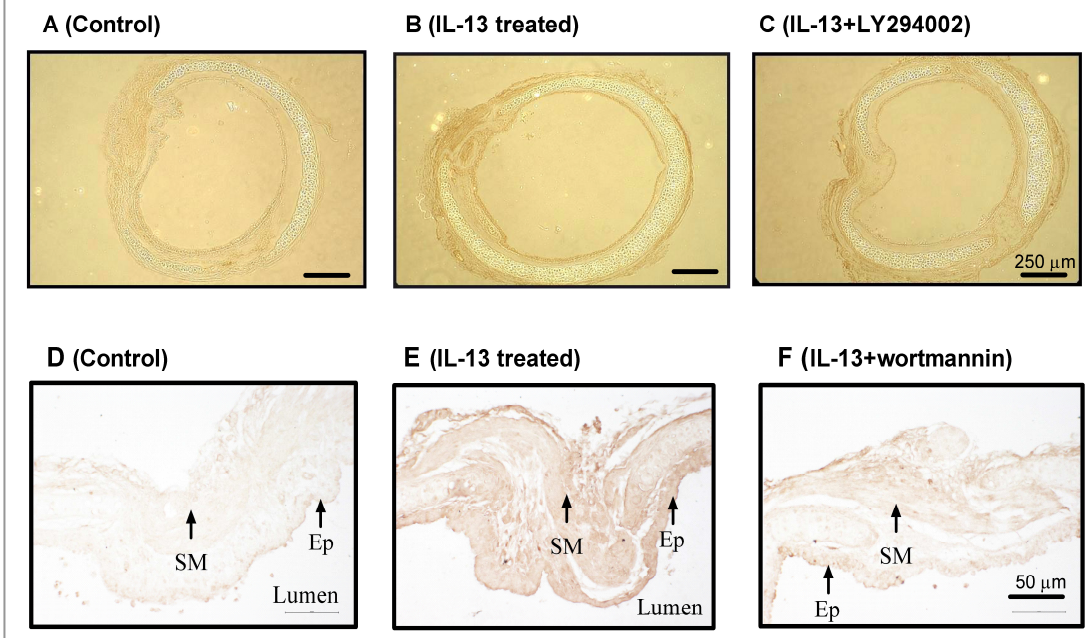

Figure 5.6 LY294002 or wortmannin inhibited IL-13–induced arginase I protein expression in murine tracheal rings. Tracheal rings from CD1 mice were treated with or without LY294002 (10 µM), upper panels, or wortmannin (100 nM) lower panels for 30 min before exposure to m-IL-13 (100 ng/ml) for 24 h and subjected to IHC analysis. Increased expression of arginase I (probed with rabbit polyclonal anti-arginase I antibody) in both epithelium and smooth muscle of IL-13 treated segments (B & E for LY294002 or wortmannin respectively) compared with control (A & D for LY294002 or wortmannin respectively). IL-13 induced arginase I protein expression was inhibited by pretreatment with LY294002 or wortmannin (C & F respectively). The graphs are representative of experiments with 3 mice for each inhibitor, with positive staining indicated by the brown colour.

5.5 p110δ and IL-13-induced arginase I protein expression

It has been demonstrated in chapter 4 of this study that IL-13-induced smooth muscle contraction in isolated murine tracheal rings depends on PI3Kδ activity, the role of PI3Kδ on IL-13–induced arginase I protein expression was investigated by Western blot analysis and IHC. Western blot analysis revealed that the PI3K p110δ

selective inhibitor IC87114 (10 μM) added 30 min before m-IL-13 addition did not inhibit IL-13 induced arginase I protein expression (Figure 5.7). IHC analysis of tracheal segments treated with m-IL-13 showed expression of arginase I (Figure 5.8 B) compared with control sections (Figure 5.8 A). However, Arginase I expression was decreased in tracheal segments pretreated with IC87114 below basal expression in control tracheal segments (Figure 5.8 C).

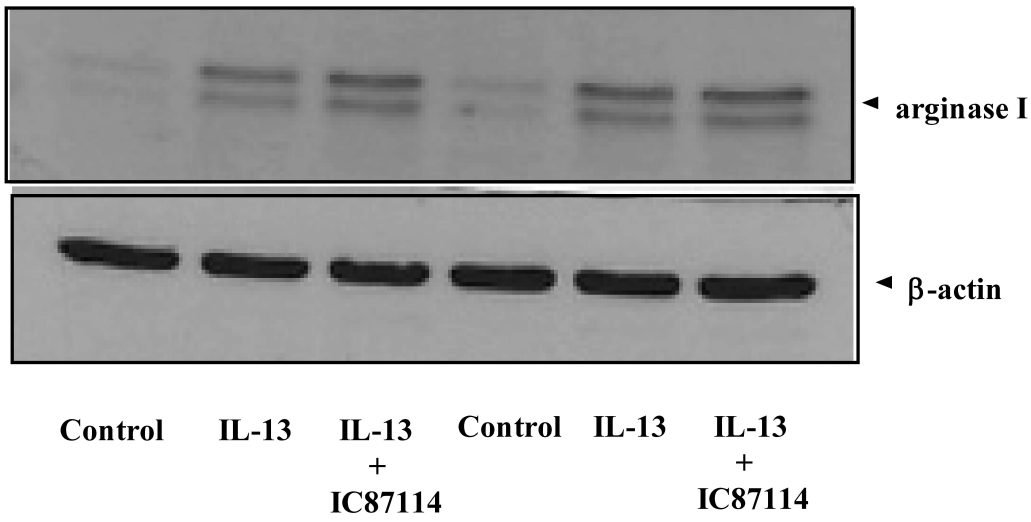

Figure 5.7 IC87114 did not inhibit IL-13–induced arginase I protein expression in murine tracheal rings. Tracheal rings from 6 CD1 mice treated with IC87114 (10 μM) for 30 min before exposure to m-IL-13 (100 ng/ml) for 24 h were homogenized in ice-cold lysis buffer. Proteins (30 μg per lane) were separated by SDS-PAGE and probed with mouse monoclonal anti-arginase I antibody before detection by enhanced chemiluminescence. After probing for arginase I, blots were reprobed for β-actin to determine equal loading. The blot shows bands from two independent experiments, and was confirmed in further independent experiment.

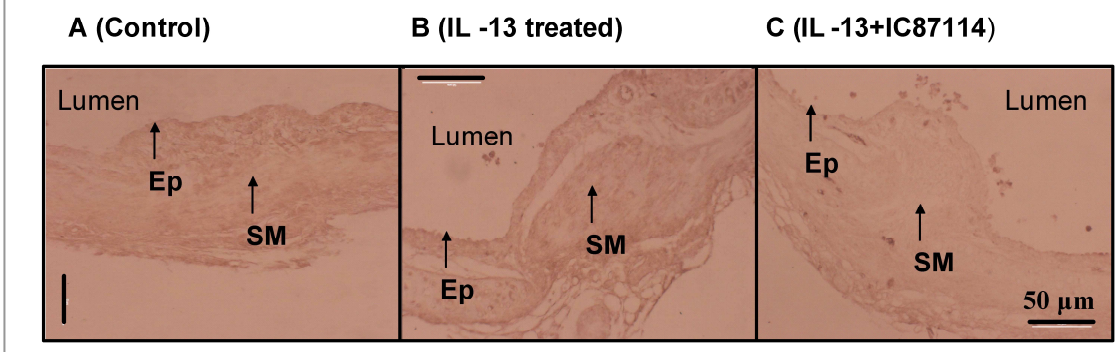

Figure 5.8 Effect of IC87114 on m-IL-13–induced arginase I protein expression by IHC analysis. Tracheal rings from CD1 mice treated with IC87114 (10 µM) for 30 min before exposure to m-IL-13 (100 ng/ml) for 24 h were subjected to IHC analysis. Increased expression of arginase I was seen in both epithelium and smooth muscle of IL-13 treated segments (B) compared with control (A). IL-13 induced arginase I protein expression was decreased below control level by prior treatment with IC87114 (C). The graphs are representative of 2 experiments out of 3 with positive staining indicated by the brown colour.

5.6 Role of epithelium in IL-13 enhanced contraction

To elucidate the role played by the epithelium in IL-13 enhanced contraction using isolated murine tracheal rings, two sets of experiments were carried out. Firstly, in experiments in which the epithelium was denuded before incubation with m-IL-13 (100 ng/ml, 24 h) resulted in E_{max} values of 1.4 ± 0.1 and 1.8 ± 0.1 compared with control values of 1.2 ± 0.0 and 2.0 ± 0.1 for KCl and CCh respectively. Secondary, in experiments in which the epithelium was denuded after 24 h incubation with IL-13, significant hyperresponsiveness was still observed, resulting in E_{max} values for KCl and CCh of 1.6 ± 0.2 and 2.2 ± 0.1 compared with control values of 1.0 ± 0.2 and 1.4 ± 0.2 respectively (*$p < 0.05$, **$p < 0.01$, $n = 6$) (Figure 5.9). Denudation of the epithelium was confirmed by histological examination of sections of tracheal ring (Figure 5.10). Organ bath results obtained from segments with retained or partially denuded epithelium were excluded. Epithelial denudation did not appear to damage submucosal tissue or the underlying trachealis muscle.

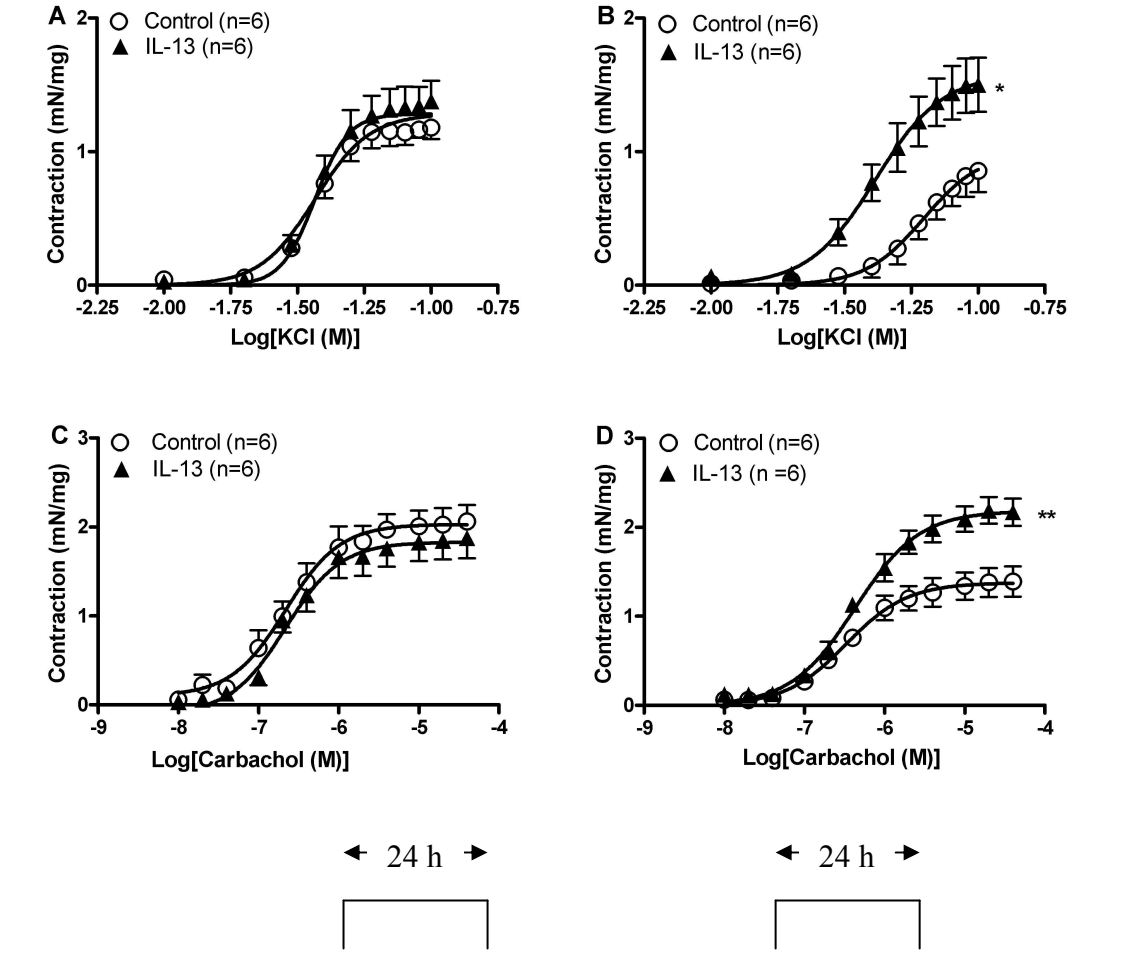

Figure 5.9 IL-13-induced contraction in isolated murine tracheal rings requires epithelium. Cumulative concentration-response curves to KCl (A&B) and CCh (C&D) in the absence (control) or presence of IL-13 (100 ng/ml, 24 h). Data are expressed as mean mN per milligram of tissue (wet weight) ± s.e.m. for n = 6. *, $p< 0.05$; **, $p< 0.001$ compared with control, Student's paired *t*-test. Murine tracheal hyperresponsiveness was lost when epithelium was denuded before incubation with IL-13 (100 ng/ml) (A&C) and was maintained when epithelium was denuded after incubation with IL-13 (100 ng/ml) (B&D).

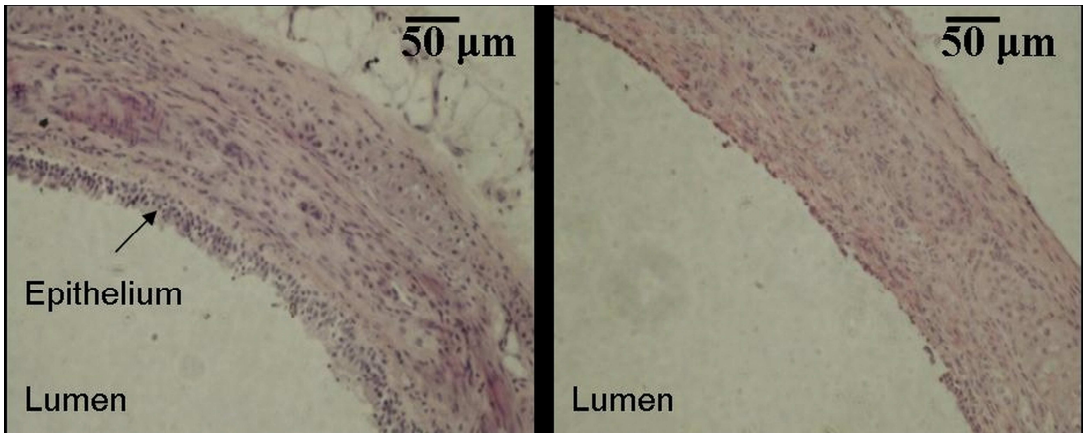

Figure 5.10 Haematoxylin and eosin-stained murine tracheal segments. H.& E stain of histological sections of tracheal segments before (left panel) and after (right panel) removal of the epithelium, X400 magnification.

5.7 The epithelium and IL-13-induced arginase I expression

To investigate the role of epithelium in IL-13 induced arginase I protein expression, the dissected mouse trachea was cut into four segments. One segment, with intact epithelium was incubated with m-IL-13 (100 ng/ml). Another segment with still intact epithelium was employed as a control. The epithelium was denuded in the remaining two segments and the segments were incubated with or without m-IL-13. Arginase I protein expression was induced significantly in IL-13 treated tracheal segments as detected by Western blot analysis compared with control in both intact and denuded tissues (Figure 5.11). Although IL-13-induced arginase I protein expression in the airway smooth muscle was still observed, arginase I protein expression in IL-13 treated, epithelium-intact segments was significantly higher than IL-13 treated, epithelium-denuded segments. These data implicate the involvement of epithelium in IL-13 induced arginase I induction.

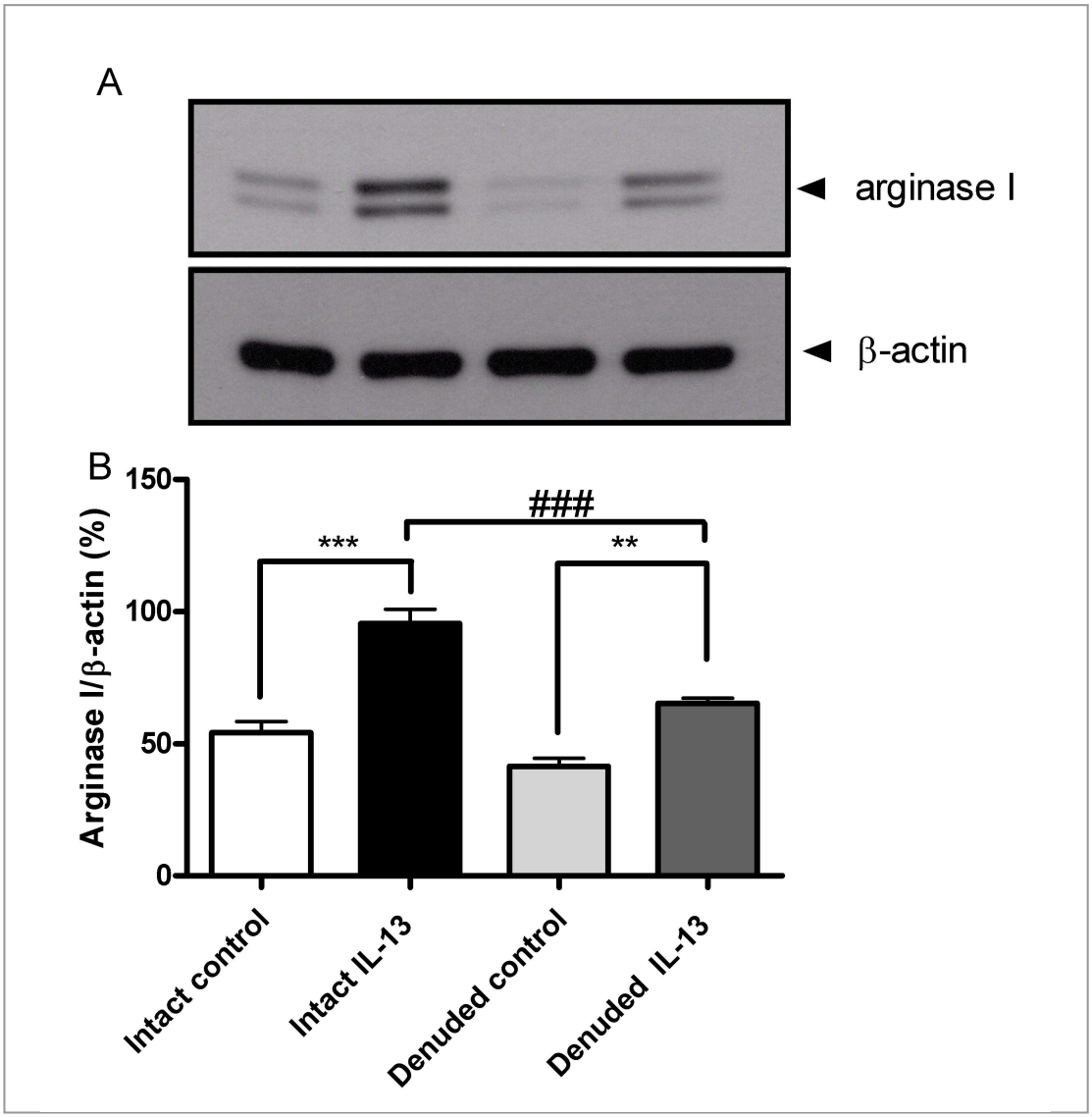

Figure 5.11 IL-13 induces arginase I in epithelium intact and denuded tissue. Removal of the epithelium was associated with a decrease in the amount of arginase I protein expression. Tracheal rings from 8 CD1 mice were homogenized in ice-cold lysis buffer. Proteins (30 μg per lane) were separated by SDS-PAGE and probed with arginase I and β-actin antibodies before detection by enhanced chemiluminescence. After probing with mouse monoclonal anti-arginase I antibody, blots were reprobed for β-actin to determine equal loading. Densitometric analysis of arginase I protein expression are expressed as percentage arginase I compared with β-actin, was determined using Labimage software (Lapelan Bio-imaging Solution, Halle, Germany). Bars indicate the mean density ratio ± s.e.m. from three independent experiments. **, $p < 0.01$, ***, $p < 0.001$ significant difference from control, ### significant difference between intact and denuded tissue expression levels, $p < 0.001$, $n = 3$, each using tissue from 8 mice.

5.8 Discussion

5.8.1 L-Norvaline inhibits IL-13 enhanced contraction

To investigate of the role of arginase in IL-13-induced hyperresponsiveness, the effect of L-norvaline, an arginase inhibitor, was assessed using murine tracheal segments. Although L-norvaline has low potency, it was used in this study because it does not affect NOS activity (Chang *et al.*, 1998). A study by the same group (using the murine macrophage cell line J774A.1) demonstrated that both actinomycin D and cycloheximide completely inhibited the increase in arginase activity and hence is a result of inhibition of de novo synthesis of arginase I mRNA and protein (Chang *et al.*, 2000). They also showed that IL-13 (5 ng/ml)-inhibited LPS-induced NO production was restored by about 70 % when L-norvaline (20 mM) was added for 18 h, which indicates the contribution of IL-13-induced arginase activity in inhibition of NO production. In the present study, the results obtained by modulating arginase activity by L-norvaline showed that IL-13 is a potent arginase inducer, which contributes significantly to IL-13-enhanced contraction. Similar observations were made in mice that had received IL-13 to induce AHR (Yang *et al.*, 2006). In their study AHR to methacholine was completely inhibited by arginase I targeted RNAi. Moreover, in a recent study conducted in a guinea pig model of asthma, pretreatment with the non-selective arginase inhibitor ABH reversed ovalbumin-induced AHR (Maarsingh *et al.*, 2008b).

5.8.2 IL-13 induced arginase I protein expression

Once the inhibitory profile of L-norvaline had been investigated, the study was continued by immunoblot analysis at various IL-13 concentrations and times of treatment. Arginase I is expressed constitutively in murine tracheae, which was induced by exposure to m-IL-13 at different concentrations. Notably, changes in the expression of arginase I correlate with IL-13 enhanced responsiveness to KCl and CCh detected in chapter 3 in this study. Arginase I protein was detected in murine tracheal tissue lysate as two immunoreactive bands. These are believed to result from translational initiation from two different methionine codons (Ohtake *et al.*, 1988; Akiba *et al.*, 2002). A comparable study to this current investigation showed that rat

aortic smooth muscle cells contain basal arginase I protein that is elevated at 12 h, peaks at 24-48 h and starts to decline at 72 h after the addition of IL-13 (10 ng/ml) (Wei *et al.*, 2000). Exposure of rat airway fibroblast to 10 ng/ml of either IL-4 or IL-13 causes a time-dependent increase in arginase activity, and increased concentration of either cytokines does not cause larger effects (Lindemann & Racke, 2003).

Arginase I was investigated in this study. It has been previously studied that arginase I but not arginase II is the induced isoform both i*n vitro (in* cultured rat peritoneal cells) and in *vivo* (in rat lung) after LPS treatment (Sonoki *et al.*, 1997). IL-4 and IL-13 are major arginase inducers since schistosome egg-induced granuloma arginase I expression and activity are reduced in IL-13-deficient and nearly completely eliminated in double IL-4/IL-13-deficient mice (Hesse *et al.*, 2001). This is in agreement with studies using murine dendritic cells (Munder *et al.*, 1999) and rat aortic smooth muscle cells (Wei *et al.*, 2000) where IL-4 and IL-13 specifically induce arginase I but not arginase II mRNA and protein. However, Yang *et al.* (2006) stated that IL-13 alone was sufficient for the induction of AHR, and shRNAi inhibition of arginase I results in marked attenuation of IL-13-induced AHR. Their study also demonstrated enhanced expression of arginase I, but not arginase II, which was directly correlated with the presence of IL-13-induced AHR while the recruitment of eosinophils and induction of mucus production persisted after the resolution of AHR (Yang *et al.*, 2006).

IHC analysis was carried out and the 24 h time-point was selected to support immunoblotting results obtained in this current study. After validation of the technique using the liver as a positive control as described by (Multhaupt *et al.*, 1987), it was demonstrated that murine tracheal segments express a basal level of arginase I detected in both epithelium and smooth muscle cells which was notably increased after 24 h incubation with m-IL-13.

5.8.3 PI3K role in IL-13-induced arginase I protein expression

To test the hypothesis that IL-13-induced arginase I depends on PI3K activation, and that is the key mechanism required for IL-13 enhanced

hyperresponsiveness, additional immunoblotting and IHC studies were carried out. Pretreatment of murine tracheal segments with LY294002 before IL-13 addition resulted in inhibition of IL-13 induced arginase I protein expression below basal levels of expression. Comparing results obtained from Western blotting with those from IHC analysis, similar results were obtained in murine tracheal section pretreated with LY294002. These results were confirmed using another non-selective inhibitor wortmannin. The link between PI3K and arginase was studied previously in peritoneal or bone marrow-derived macrophages (Rauh *et al.*, 2003; Sakai *et al.*, 2006; MacKinnon *et al.*, 2008). It was demonstrated that both IL-4 and IL-13 increase arginase activity in bone marrow-derived macrophages and that LY294002 blocks IL-4-stimulated arginase activity (MacKinnon *et al.*, 2008). These findings support studies showing increased arginase I protein expression in the $SHIP^{-/-}$ macrophages (Rauh *et al.*, 2003), although an increase in arginase activity was not detected in PI3K-deficient macrophages (Sakai *et al.*, 2006).

To test the hypothesis of selective PI3K p110δ involvement in IL-13 induced arginase I protein induction, in these experiments IC87114 was added to murine tracheal segments before m-IL-13 and p110δ expression assessed by Western blotting did not inhibit IL-13-induced arginase I protein expression. However, IL-13-induced expression was decreased below control level by prior treatment with IC87114 in two out of three experiments demonstrated by IHC. This discrepancy between Western blotting and IHC results maybe due to regional differences or inconsistent decrease of p110δ. The findings obtained using IC87114 question the role of p110δ in IL-13-induced arginase I and its link to IL-13-enhanced responsiveness. Taken together, these results suggest that PI3K plays a role in IL-13- induced-arginase I protein expression, but the role of p110δ is not clear.

5.8.4 Epithelial role in IL-13 enhanced ASM contraction

This work demonstrates the role of the epithelium in IL-13-enhanced hyperresponsiveness in murine tracheal segments. When the epithelium was denuded before incubation with IL-13 hyperresponsiveness was lost, suggesting that the potential mechanism of IL-13 to promote hyperresponsiveness is epithelial dependent. However, when the epithelium was denuded after incubation with

m-IL-13, the increased contractile responses to KCl and carbachol compared with control is still observed. Epithelium removal can be carried out mechanically or chemically (reviewed in Hulsmann & de Jongste, 1993), however mechanical removal was chosen because chemical removal of epithelium necessitates the use of the entire length of the trachea since it decreases the maximal contractile force (Moffatt *et al.*, 2004). Mechanical removal was verified by histological examination of the sections. Mechanical removal of the epithelium could have influenced tracheal smooth muscle contraction but, on comparing responses obtained from epithelium-denuded control with epithelium -intact control segments, the obtained tensions were not different. *In vivo* results obtained by Kuperman *et al*. (2002) demonstrated that reconstitution of STAT6 expression in airway epithelial cells in transgenic mice expressing murine IL-13 was sufficient for complete restoration of IL-13-induced AHR to methacholine and acetylcholine.

Airway epithelium is a major location of polyamines in the asthmatic lung, but they can be found in other cell types in the lung such as smooth muscle cells and macrophages (Hoet & Nemery, 2000). As discussed above, the epithelium is needed in IL-13-induced hyperresponsiveness. Therefore, the site(s) of IL-13-induced arginase I expression were studied. A previous study demonstrated that the respiratory epithelium, mononuclear cells with macrophage morphology, and some granulocytes isolated from bronchoalveolar lavage fluid stained positive for arginase I protein in allergic asthmatic patients (Zimmermann *et al.*, 2003). Current findings show IL-13-induced arginase I in both epithelium-intact and denuded tracheal segments. However, there was still a significant difference between IL-13-treated denuded epithelium segments and IL-13- treated intact epithelium segments pointing to the involvement of other cells beside the epithelium in IL-13-induced arginase and hyperresponsiveness. Although arginase I expression is reported to be induced by Th2 cells and their cytokines (Yang *et al.*, 2006), a recent study using human bronchial epithelial cells demonstrated that IL-13 (10 ng/ml) decreases arginase I protein compared with the control group (Chibana *et al.*, 2008). Their group also shows that arginase II is constitutively expressed and is not affected by IL-13 treatment at mRNA or protein levels. However, this discrepancy may be due to the use of human epithelial cells after 10 days of culture (Chibana *et al.*, 2008).

5.9 Summary

- IL-13-induced hyperresponsiveness is reduced by the arginase inhibitor, L-norvaline, which may point to arginase induction as downstream mediator of IL-13-enhanced hyperresponsiveness;
- concentration and time-course studies correlated IL-13-induced arginase I protein expression with hyperresponsiveness;
- IHC analysis confirmed 24 h as the time point for maximal IL-13 induced arginase I protein expression;
- inhibition of PI3K signalling prevents IL-13-induced arginase I expression in isolated tracheal rings detected by both Western blotting and IHC analysis;
- the epithelium is needed for IL-13-induced hyperresponsiveness;
- IL-13 upregulates epithelial and smooth muscle arginase I expression but the epithelium has a key role in IL-13 induced hyperresponsiveness.

Chapter Six

Inhibition of IL-13-induced hyperresponsiveness by PI3Kδ-targeted siRNA

6.1 Introduction

An aim of many smooth muscle studies is directed towards investigating the biophysical factors governing muscle properties and molecular biology including the roles of different genes. Currently DNA or RNA transfer is a common method used in many studies. An efficient and safe method of delivery of genetic material is a continuing problem. The development of methods suitable for efficient intracellular targeting of genetic material in intact tissues is very important for therapeutic use and the determination of affected function (s), such as contractility, that are not normally expressed and/or readily measured in cultured cells

Nonviral transfection strategies include chemical and physical approaches. The chemical methods include the use of cationic liposomes (lipoplex), polymers (polyplex), combinations of the two (lipopolyplex), calcium phosphate, and diethylaminoethyl-dextran. In almost all of these chemical methods the reagents promote transfection by complexing with the genetic material to neutralize the charge. The condensed DNA or RNA will then interact with the cell membrane and enter the cell via endocytosis.

Cationic lipid-mediated gene transfer can use cationic lipids alone but are often formulated with a noncharged phospholipid or cholesterol to form liposomes, which condense genetic material into small stable particles called lipoplexes. Lipoplexes enter the cells and release the genetic material before reaching destructive lysosomal compartments (Felgner *et al.*, 1987). Many cationic lipids show good transfection activity in cell culture. Once administered *in vivo*, lipoplexes undergo marked changes in size, surface charge, and lipid composition due to interaction with negatively charged blood components and formation of large aggregates which prevent their access into the intended target (Li *et al.*, 1999; Simberg *et al.*, 2003). Intravenous (Thierry *et al.*, 1995; Templeton *et al.*, 1997) and airway (Hyde *et al.*, 2000; Bragonzi *et al.*, 2000) gene delivery of lipoplexes to the lung have been studied. One of the obstacles that face lipoplex-based gene delivery to the airways is that a negatively charged and viscous mucus layer that traps and neutralizes lipoplexes covers upper airway epithelial cells. Furthermore, in CF patients the epithelial cells are also covered with a thick sputum layer that contains DNA released

from dead cells and bacteria that increase the negativity state. The presence of several phospholipids and surfactant proteins can also inhibit the transfection activity of lipoplexes. In addition, well-differentiated upper airway epithelial cells are less active in taking up lipoplexes (Duncan *et al.*, 1997; Rosenecker *et al.*, 2003). Toxicity related to gene transfer by lipoplexes has been reported especially with systemic delivery in the form of induction of proinflammatory cytokines, leukopenia, thrombocytopenia, and liver injury with elevated serum transaminase (Tousignant *et al.*, 2003). Improved chemical design of lipids with increased biodegradability can decrease lipoplex toxicity (Tang & Hughes, 1999).

Cationic polymer-mediated gene transfer is another approach, which is similar to lipoplex in action and toxicity. Cationic polymer condenses genetic material into small particles to facilitate endocytosis. Airway gene delivery of low-dose polyplex by aerosols shows efficient lung delivery with no evidence of acute inflammation (Gautam *et al.*, 2000). Lipopolyplex is a combination of lipoplex and polyplex. Linear poly-L-lysine, protamine, histone, and several synthetic polypeptides have been used to condense DNA; the polyplexes formed are then coated with a lipid layer. Better protection and more efficiency are achieved with this approach (Gao & Huang, 1996).

Physical methods allow the direct entry of uncomplexed genetic material into cells by transient defects on cell membranes, so that the gene enters the cells by diffusion. Physical methods include gene transfer by gene gun, electroporation, ultrasonic gene transfer and hydrodynamic gene transfer. Needle injection of naked genetic material is simple and safe but leads to low level gene expression (Meyer *et al.*, 1995). DNA-attached gold particles accelerated by pressurized gas and expelled onto cells or a tissue is the principle of the “gene gun” method. It is simple and efficient method but only suitable for exposed tissues as skin and mucosa (O'Brien & Lummis, 2002). Electroporation is a physical method in which a pair of electrodes is inserted on the target tissue. Although electroporation is efficient method (Molnar *et al.*, 2004) it needs surgical procedures for non-topical applications and the associated high voltage applied to tissues can result in tissue damage (Durieux *et al.*, 2004). Ultrasound-facilitated gene transfer creates membrane pores and facilitates gene transfer by passive diffusion. Although it has the advantage of site-specific gene

delivery, low efficiency is a major problem which might be solved by complexing DNA and cationic lipids (Koch *et al.*, 2000). Hydrodynamic gene delivery introduces genes into cells of highly perfused internal organs, for example the liver. Although simple it is effective in small animals (Liu *et al.*, 1999), although surgical procedure may be needed for localized gene delivery (Eastman *et al.*, 2002). The real barrier for gene transfer by the hydrodynamic method is the very large volume of fluid required for delivery to humans.

Reverse permeabilization is a method originally used to introduce fluorescent heparin and the calcium indicator aequorin into smooth and cardiac muscle respectively (Morgan *et al.*, 1984; Kobayashi *et al.*, 1989). The mechanism of reversible permeabilization is not established but it depends on adding ATP in high concentration in divalent cation–free solutions. ATP binds to cell surface receptors and removes membrane-associated divalent cations, which leads to increased membrane permeability. The induced membrane permeability is then reversed by removal of extracellular ATP and addition of high Mg^{2+} followed by graded restoration of the physiological concentrations of extracellular Mg^{2+} and Ca^{2+} (Steinberg *et al.*, 1987). Although the introduction of high molecular weight molecules could restrict the use of this technique (Lesh *et al.*, 1995), the possibility of introducing siRNA into intact tissue, combined with survival of these preparations in organ culture for long periods, suggest that the application of this technique may be promising for studying the effects of genetic manipulation on smooth muscle contractility.

The objective of investigations represented in this final part of the study is to deliver PI3K p110δ-targeted siRNA into IL-13-treated murine tracheal segments and assess contractility of smooth muscle rings containing siRNA after organ culture. C20 and C22 are new synthesized lipospermines in our department that efficiently deliver siRNA in both primary and cancer cell lines (Ghonaim *et al.*, 2008). The ability of C20 or C22 to deliver fluorescein-tagged nonselective RNA into 9HTEo- and A549 epithelial cell lines and murine tracheal segments was investigated, to compare efficiency with a commercially available transfecting agent, TransIT-TKO.

6.2 p110δ-targeted siRNA delivery into BEAS-2B cell line

Isolation of primary murine tracheal epithelium was attempted using method described in (Davidson *et al.*, 2004) but insufficient isolated epithelial cell was demonstrated. Isolation of murine smooth muscle was also attempted (Figure 6.1) and elevation in intracellular calcium was measured in response to different agonists CCh (10, 30, 100 μM and 1 mM), KCl (100 mM) and ATP (1 or 10 mM). However, none of the tested agonists had an effect on intracellular calcium. This raised the question if those isolated ASM were functioning cells and were not investigated further. Therefore human epithelia cell lines were employed in this study

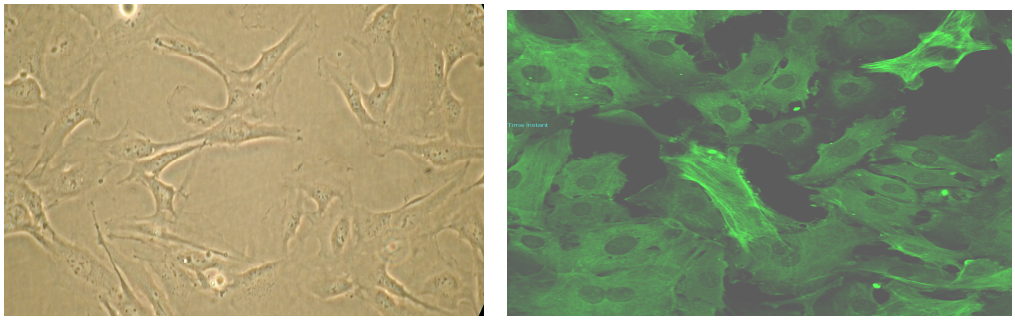

Figure 6.1 Murine tracheal smooth muscle express muscle specific α-actin. Isolation of primary murine smooth muscle from enzymatically digested tracheae (left panel). Immunocytochemical analysis of isolated murine tracheal smooth muscle cells demonstrates α-actin smooth muscle immunopositive staining (right panel).

BEAS-2B is a human bronchial epithelial cell line transformed with adenovirus 12-SV40 virus. For transfection 4×10^5 cells per well were seeded in a 6-well plate and incubated overnight to reach 50–70% confluency. Cells were transfected with 100 nM p110δ-targeted siRNA in the presence of 10 μl Lipofectamine 2000. Lysis of cells was carried out after 72 h of culture. Western blot analysis of total cell lysates (Figure 6.2) demonstrated a strong reduction of p110δ protein in the siRNA-treated samples. Transfections without siRNA or with scrambled siRNA served as a control.

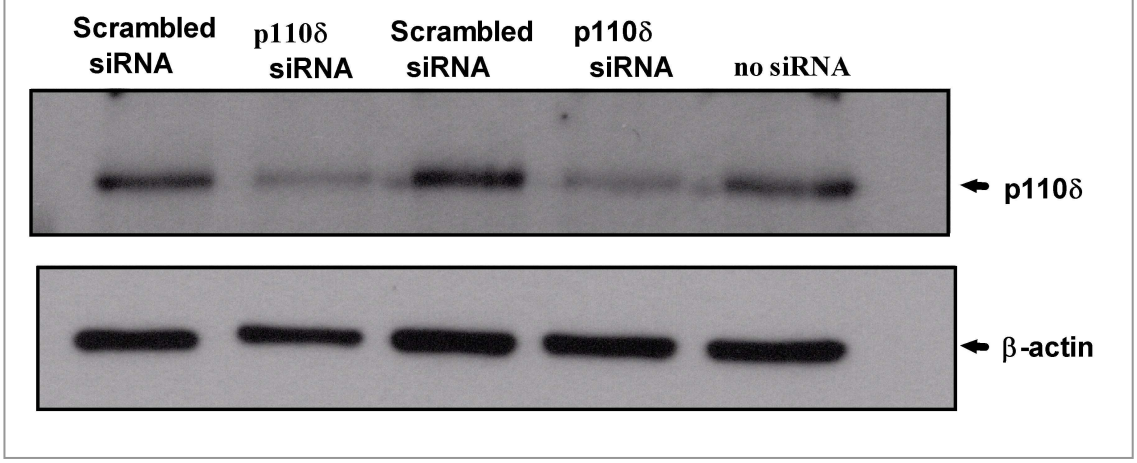

Figure 6.2 Effect of p110δ-targeted siRNA in BEAS-2B cells. BEAS-2B cells were transfected with p110δ-targeted siRNA in the presence of Lipofectamine 2000. After 72 h, the cells were lysed and p110δ expression assessed by Western blotting and detection with specific antibodies for p110δ. β-actin served as equal loading control. Representative of 2 experiments.

6.3 Expression of IL-13 receptors in human tracheal 9HTEo- cells

As described in chapter 5 the epithelium has a key role in IL-13 enhanced hyperresponsiveness, and additionally plays a role in IL-13-induced arginase I protein expression. 9HTEo- are a transformed human tracheal epithelial cell line (Gruenert *et al.*, 1988). To assess the suitability of 9HTEo- in siRNA experiments and study the role of IL-13 on human epithelium, the expression of IL-13Rα1 and IL-13Rα2 was examined in unstimulated 9HTEo-. As shown in Figure 6.3 and 6.4, IL-13 Rα1 and IL-13 Rα2 mRNA were detected by PCR in unstimulated 9HTEo-. To study the effect of IL-13 on IL-13 Rα2 gene expression in 9HTEo-, the cells were incubated with h-IL-13 (10 or 100 ng/ml, concentrations previously used in the organ bath experiments). The level of IL-13 Rα2 mRNA was not altered in IL-13 (10 ng/ml)-treated cells compared with unstimulated 9HTEo- cells (Figure 6.4). In contrast, a decrease in IL-13 Rα2 mRNA was seen when 9HTEo- cells were incubated with IL-13 (100 ng/ml) (Figure 6.4). The cell surface expression of IL-13 Rα2 was also investigated by flow cytometry following treatment with h-IL-13 (1,

10, 30 and 100 ng/ml) in 9HTEo-cells. Basal expression of IL-13 Rα2 protein was detected on the cell surface of non-stimulated 9HTEo- cells, and similar levels of IL-13 Rα2 expression were observed in 9HTEo- cells when different IL-13 concentrations were investigated (Figure 6.5). Again, a small decrease in IL-13 Rα2 protein expression was suggested in IL-13 (30 or 100 ng/ml) stimulated cells.

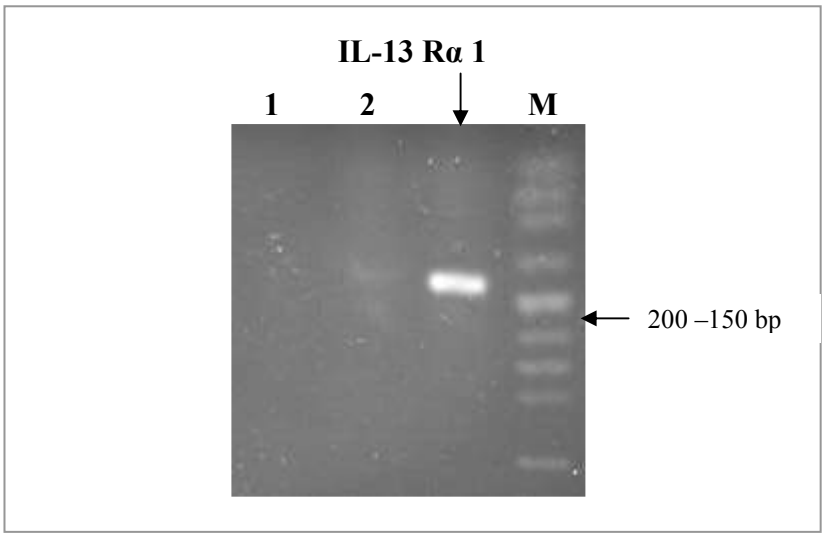

Figure 6.3 Detection of IL-13-Rα 1 mRNA in 9HTEo- cell line. Gel was stained with ethidium bromide and visualized under U.V. light. Lane 1: no template (negative) control; Lane 2: negative control where reverse transcriptase was omitted from the reaction; Lane M: DNA molecular marker. Representative of 2 experiments.

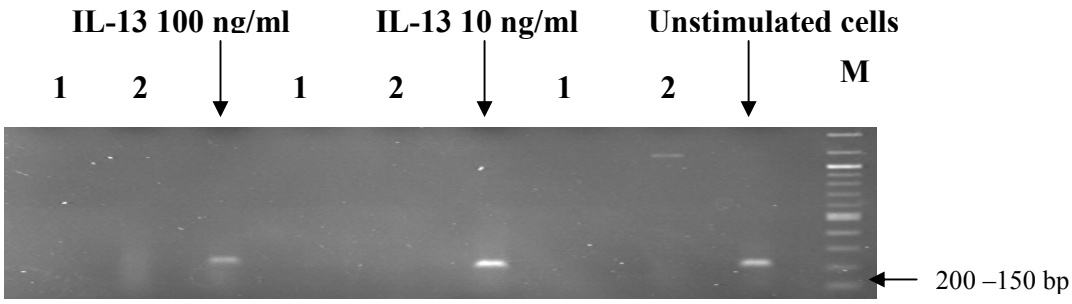

Figure 6.4 Effect of IL-13 (10 or 100 ng/ml) on IL-13 Rα2 expression in 9HTEo- cell line. Gel was stained with ethidium bromide and visualized under U.V. light. Lane 1: no template (negative) control; Lane 2: negative control where reverse transcriptase was omitted from the reaction; Lane M: DNA molecular marker. Representative of 2 experiments.

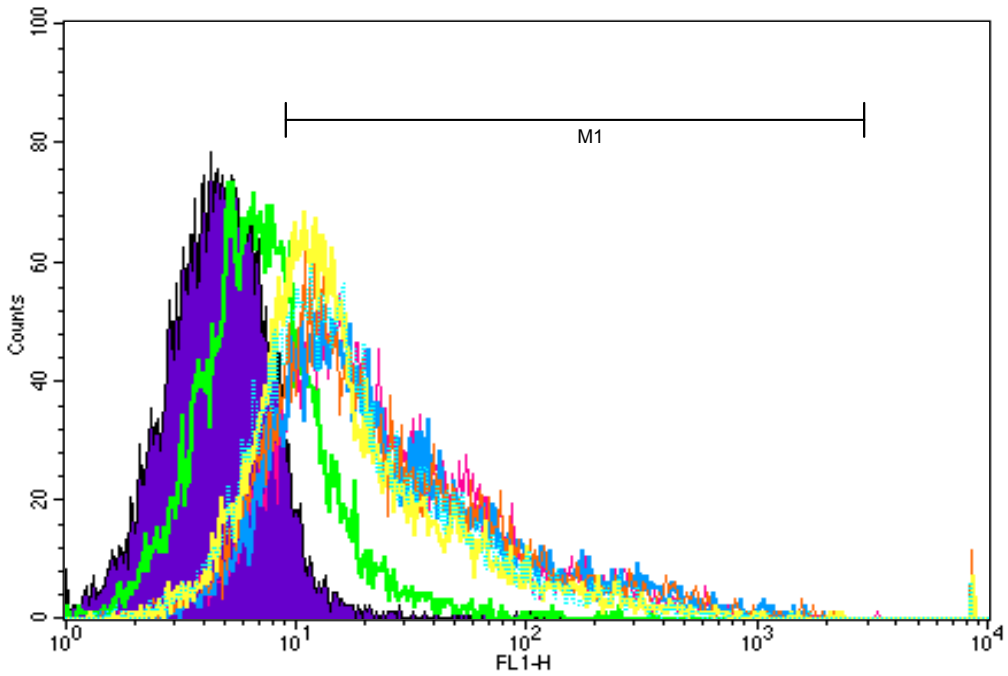

Effect of h-IL-13 on IL-13R alpha 2 expression in 9-HTEo- cells by flow cytometry

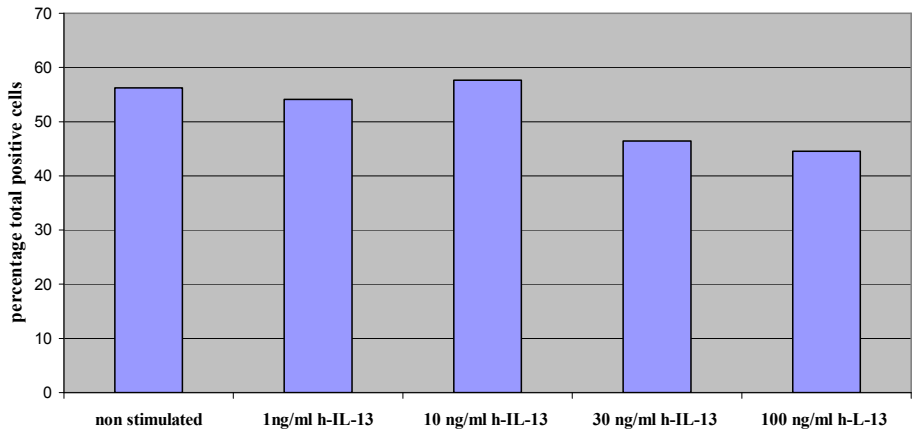

Figure 6.5 Expression of IL-13 Rα2 in 9HTEo- cell line. 9HTEo- cells were cultured without or with IL-13 (1, 10, 30 or 100 ng/ml) for 24 h and flow cytometric analysis was performed using antihuman IL-13 Rα2 antibodies or isotype control to detect surface expression of IL-13Rα2. No Ab —, an isotype control —, non-stimulated cells —, IL-13 (1ng/ml)-stimulated cells —, IL-13 (10 ng/ml)-stimulated cells —, IL-13 (30 ng/ml)-stimulated cells —, (100 ng/ml)-stimulated cells —. Linear graphs in the top figure are % total positive cells. Each bar in the lower graph is % total positive cells of indicated treated cells after subtraction of isotype control % total positive cells. The histogram data is a mean of two different experiments. M1 is live gate during acquisition.

6.4 RNA delivery into 9HTEo- and A549 cell lines

The transfection of fluorescein-tagged RNA (RNAi Delivery Control, Mirus) into 9HTEo- and A549 cell lines was investigated and compared with a market leader TransIT-TKO (Mirus). A fluorescein-labelled RNA duplex has the same length, charge, and configuration as standard siRNA was used. C20 (eicosenoyl) and C22 (erucoyl) are novel nonviral lipospermines, which were chosen according to their high transfection efficiency (Ghonaim *et al.*, 2008). The fluorescein-tagged RNA transfection efficiency experiments, carried out in triplicate on three separate occasions demonstrated that the transfection ability of C20 or C22 were comparable to the results of TransIT-TKO in both cell lines (Figure 6.6 A). Also, the cell viability (MTT assay) results demonstrated that there was no significant difference in the viability of A549 and 9HTEo- cells exposed to the commercially available TransIT-TKO or lipospermines (Figure 6.6 B).

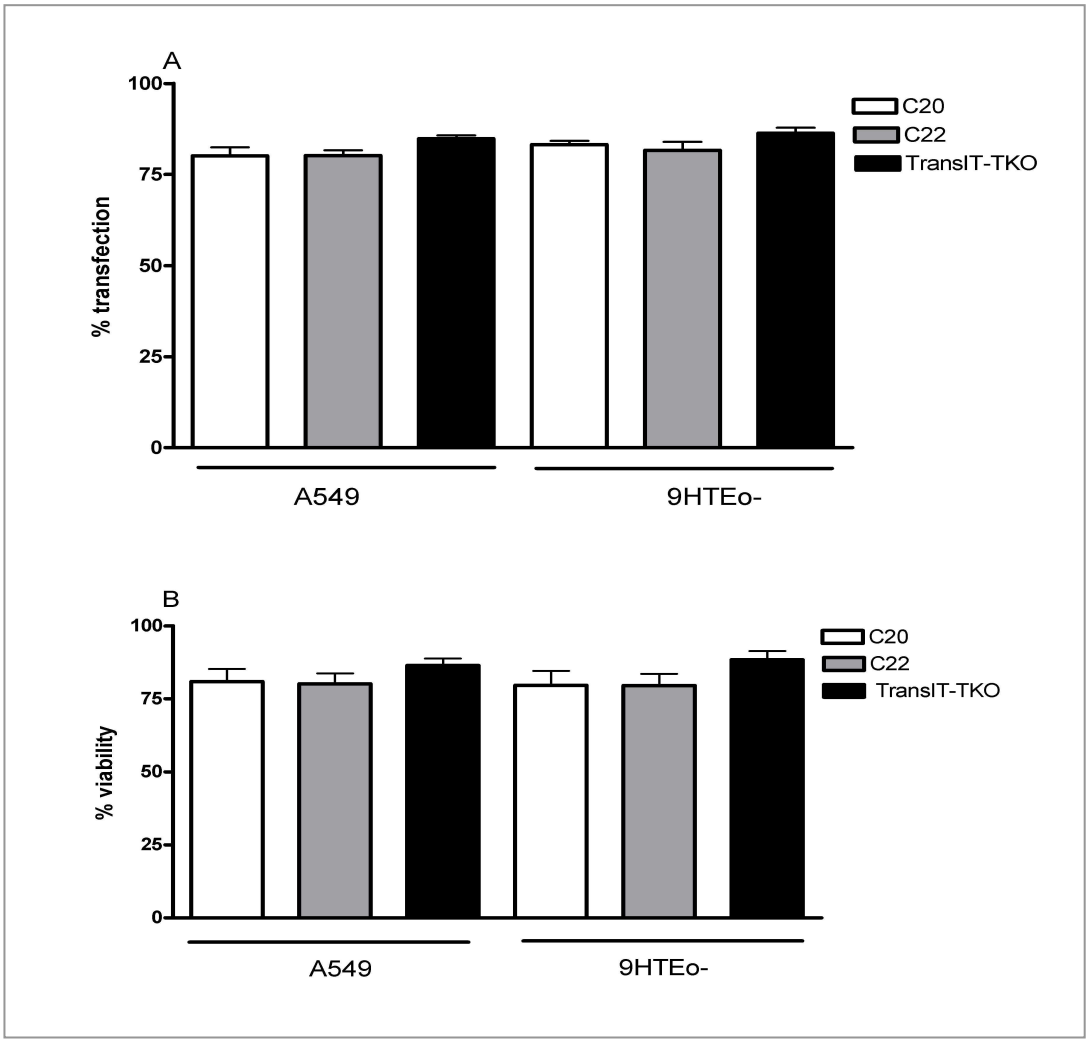

Figure 6.6 Lipofection and cytotoxicity effects of fluorescein-tagged RNA complexed with C20, C22 or TransIT-TKO on 9HTEo- and A549 cell lines.

(A) % of transfected cells, bars represent the mean ± s.e.m of 3 experiments, each performed in triplicate. (B) % of viable cells, bars represent the mean ± s.e.m of 3 experiments. One-way ANOVA was performed to determine any statistical significance of differences between mean values.

6.5 Assessment of siRNA uptake

The transfection of fluorescein-tagged RNA into murine tracheal rings was also investigated with the use of two newly synthesized lipospermines in our department, N^4,N^9-dieicosenoyl spermine (eicosenoyl or C20), N^4,N^9-dierucoyl spermine (erucoyl or C22). The transfection efficiency of C20 or C22 was compared with TransIT-TKO (Mirus), a commercially available transfection agent. (Figure 6.7) The fluorescein-tagged RNA has the same length, charge, and configuration as standard siRNA. It is a 21 nucleotide "target" sequence with UG-3′ overhangs:

GAGGCGCAACUGGCUGACCUG
GUCUCCGAGUUGACCGACUGG

The sequence of the duplex (above) is inert and not known to affect any cellular events. The concentrations for the tested transfecting agents were previously determined (Ghonaim *et al.*, 2008). Also to validate siRNA uptake using the reverse permeabilization technique the fluorescein-tagged RNA was introduced into isolated murine tracheal rings at different concentrations (20, 50, and 100 nM). Lipospermine, TransIT-TKO and reversibly permeabilized treated segments were subsequently cultured for 72 h. After tissue embedding, sectioning and fixation (see section 2.4.1, 2.4.4), the intracellular localization and efficacy of fluorescein-tagged RNA incorporation was determined by confocal microscopy. In control experiments, in which murine tracheal rings were incubated without being reversibly permeabilized (Control 1) or reversible permeabilized in the absence of fluorescein-tagged RNA (Control 2), only minimal epithelial fluorescence was detected by confocal microscopy (Figure 6.8) The transfection of fluorescein-tagged RNA (50 or 100 nM) by C20, C22 or TransIT-TKO (Figure 6.7) showed the same fluorescence compared with controls seen in Figure 6.8.This indicates low efficiency of those transfecting substances; there was a mild increase in fluorescence with the use of TransIT-TKO, which may enabled transfection with 100 nM fluorescein-tagged RNA (Figure 6.7 F). As demonstrated in Figure 6.8 reverse permeabilization enabled the influx of fluorescein-tagged RNA (50 and 100 nM) into murine tracheal rings. The lining epithelium was more brightly fluorescent following treatment with 50 and 100 nM than with 20 nM concentration of fluorescein-tagged RNA. There was

minimal fluorescence in controls and segments reversibly permeabilized and treated with 20 nM fluorescein-tagged RNA.

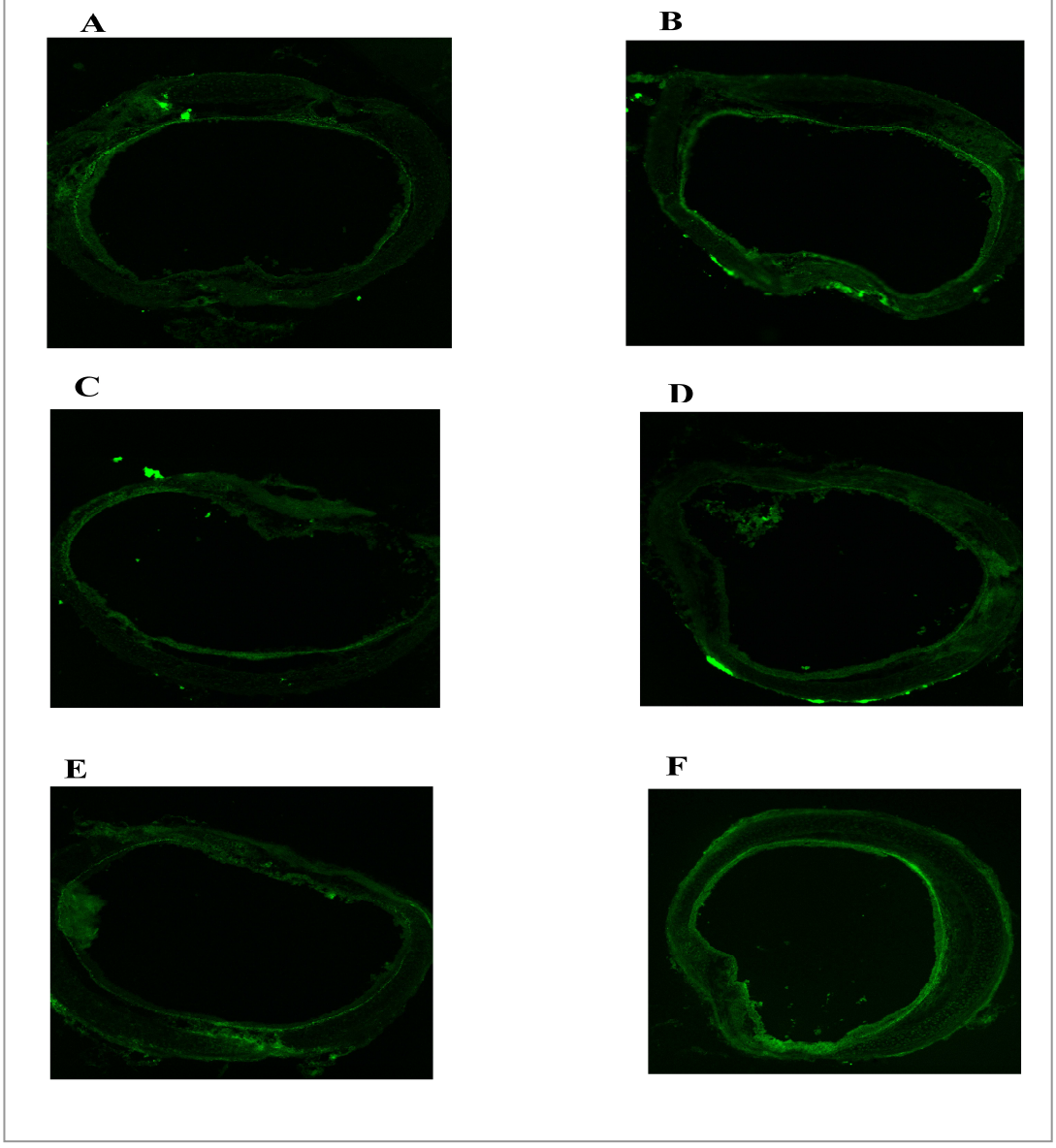

Figure 6.7 Confocal images of lipoplex-treated murine tracheal segments. Confocal microscopy of murine tracheal segments showing the absence of an increased fluorescent signal at either 50 or 100 nM RNA concentrations tested. A is C20 / fluorescein-tagged RNA 50 nM, B is C20 /100 nM fluorescein-tagged RNA, C is C22 /50 nM fluorescein-tagged RNA, D is C22 /100 nM fluorescein-tagged RNA, E is TransIT-TKO/ 50 nM and F is TransIT-TKO/ 100 nM fluorescein-tagged RNA. Sections are representative of 2 independent experiments.

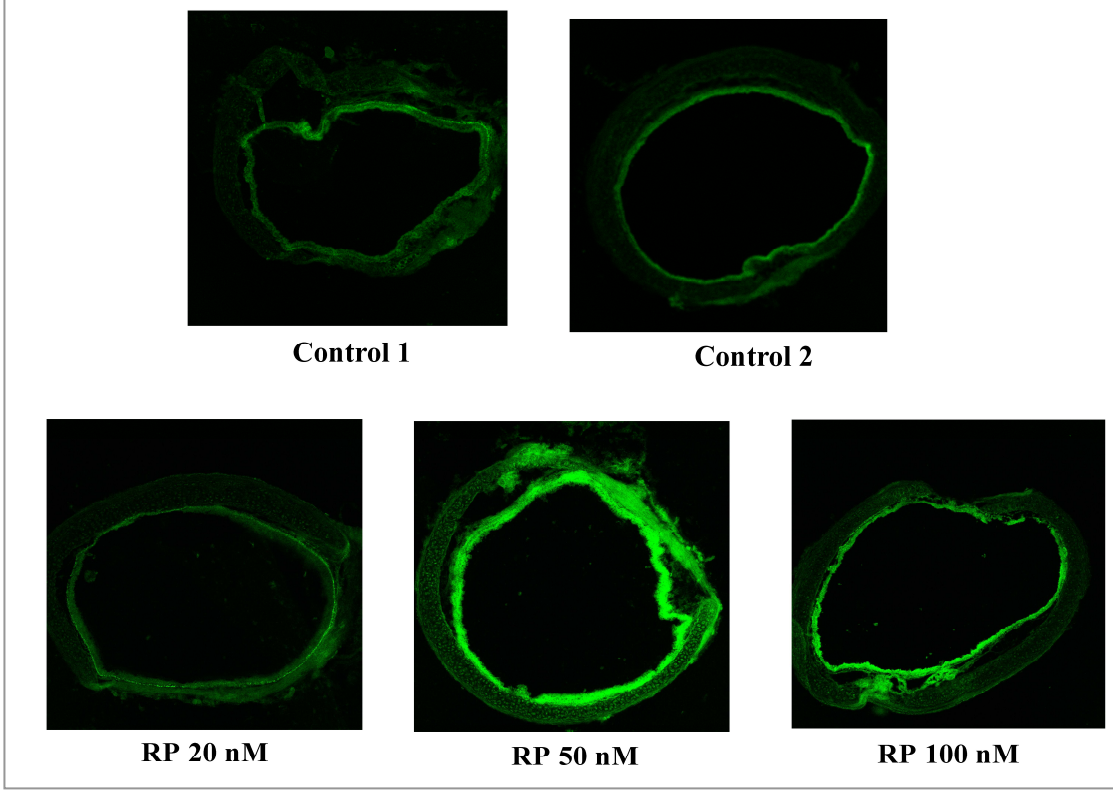

Figure 6.8 Confocal images of reversibly-permeabilized tracheal rings. Murine tracheal segments were reversibly permeabilized (RP) and exposed to fluorescein-tagged RNA at concentrations 20, 50 and 100 nM. Confocal microscopy 72 h after reversible permeabilization shows the presence of fluorescent signal mainly in the lining epithelium of tissues treated with 50 and 100 nM concentrations of RNA. For control experiments to exclude autofluorescence, the tracheal ring was exposed to culture media (Control 1) or to the reversible permeabilization protocol without addition of fluorescein-tagged RNA siRNA (Control 2). Sections are representative of 2 independent experiments.

6.6 PI3Kδ-targeted siRNA attenuates IL-13-enhanced contraction

To confirm the role of p110δ in the IL-13-enhanced responsiveness studied in chapter 4, contraction response in tissues treated with p110δ-targeted siRNA delivered by reverse permeabilization was assessed. Controls with or without the introduction of scrambled siRNA were also studied. Segments were reversibly permeabilized without siRNA, with p110δ-targeted siRNA or with scrambled siRNA then cultured for 2 days. m-IL-13 (100 ng/ml) was then added to all three groups for an additional 24 h before measurement of isometric force. There was no significant difference between murine tracheal segments that were reversibly permeabilized with or without the introduction of scrambled siRNA. KCl E_{max} values of control and scrambled siRNA-treated segments were 1.0 ± 0.15 and 1.1 ± 0.17 mN/mg respectively (Figure 6.9 A) while CCh gave E_{max} values of 1.8 ± 0.26 and 2.0 ± 0.14 mN/mg for control and scrambled siRNA-treated segments respectively (Figure 6.9 B). KCl (Figure 6.9 C) and CCh (Figure 6.9 D) responses in IL-13-treated segments reversibly permeabilized and treated with p110δ-targeted siRNA were significantly reduced compared with tissues reversibly permeabilized in the absence of siRNA or in the presence of scrambled siRNA.

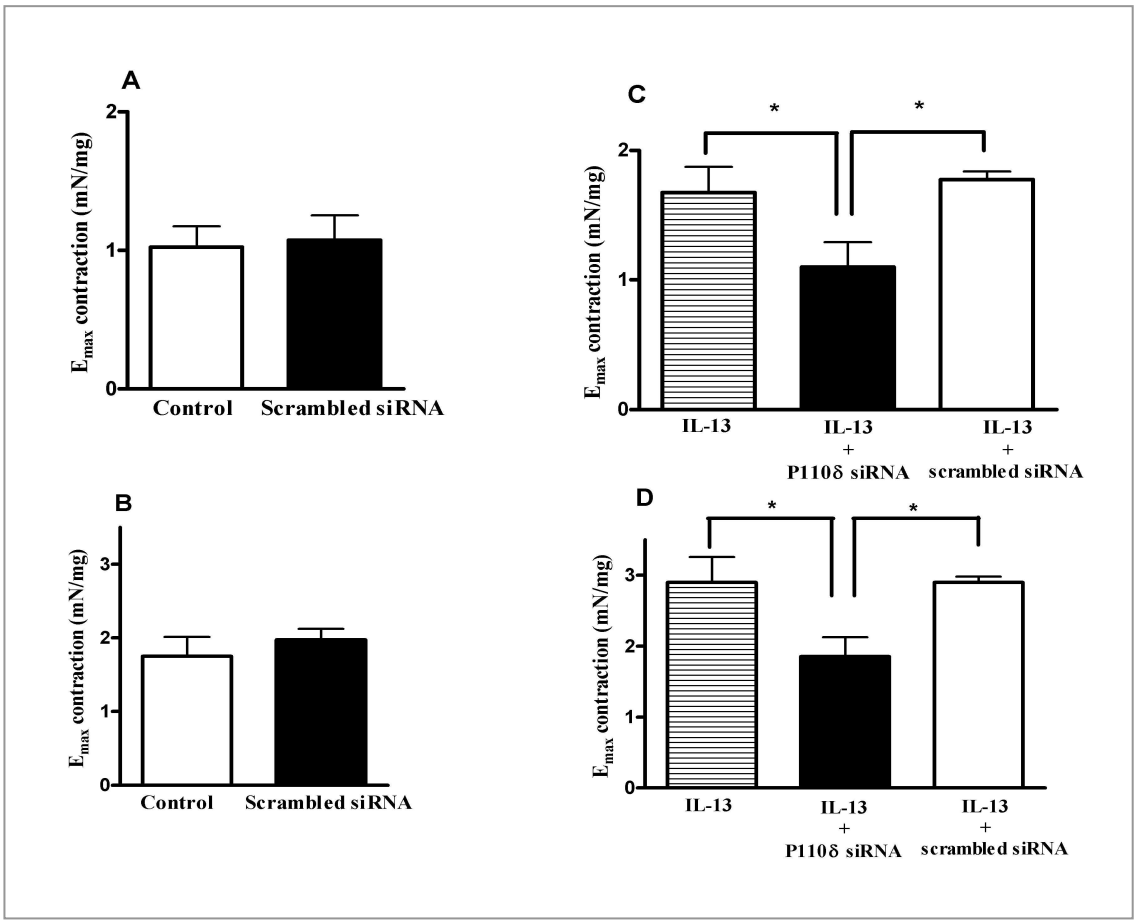

Figure 6.9 p110δ-targeted siRNA prevents IL-13-enhanced contraction in response to KCl and CCh. Isolated murine tracheal segments were reversibly permeabilized in absence of siRNA (control) or in the presence of scrambled siRNA (20 nM) then incubated for 72 h before determining E_{max} for KCl (A) or CCh (B). Reverse permeabilization in the absence of siRNA or presence of p110δ siRNA (20 nM) or presence of scrambled siRNA (20 nM) then cultured for 48 h. IL-13 (100 ng/ml) was then added to the three groups and the tissue were cultured for additional 24 h followed by determination of KCl (C) or CCh (D) E_{max} values. Data indicate mean E_{max} tension (mN/mg) ± s.e.m. for n = 4 animals. Student's paired *t*-test was performed to determine the statistical significance of differences between control and scrambled siRNA-treated tissues for n = 4. One-way ANOVA followed by Dunnett's test were performed to determine the statistical significance of differences between E_{max} values of IL-13 treated tissues; *, significantly different compared with p110δ-targeted tissue, $p < 0.05$.

6.7 PI3Kδ-targeted siRNA downregulates p110δ protein

Murine tracheal segments employed for tension measurements in section 6.6 were rapidly transferred into liquid nitrogen prior to preparation of samples for Western blot analysis for the detection of p110δ. For these experiments, an antibody specific for p110δ as well as β-actin antibody to act as the loading control was used. There was no difference between scrambled-siRNA treated tissue and control, but p110δ-targeted siRNA in IL-13 treated segments showed lower p110δ protein levels compared with segments treated with scrambled siRNA or IL-13 alone (Figure 6.10). The same membrane was reprobed with an antibody specific for arginase I. Arginase I protein expression was increased in IL-13-treated murine tracheal segments compared with controls, and was not reduced by p110δ-targeted siRNA. These findings demonstrated an absence of a link between p110δ and arginase I. No changes in β-actin were observed, demonstrating that p110δ is downregulated as a result of p110δ-targeted siRNA (Figure 6.10).

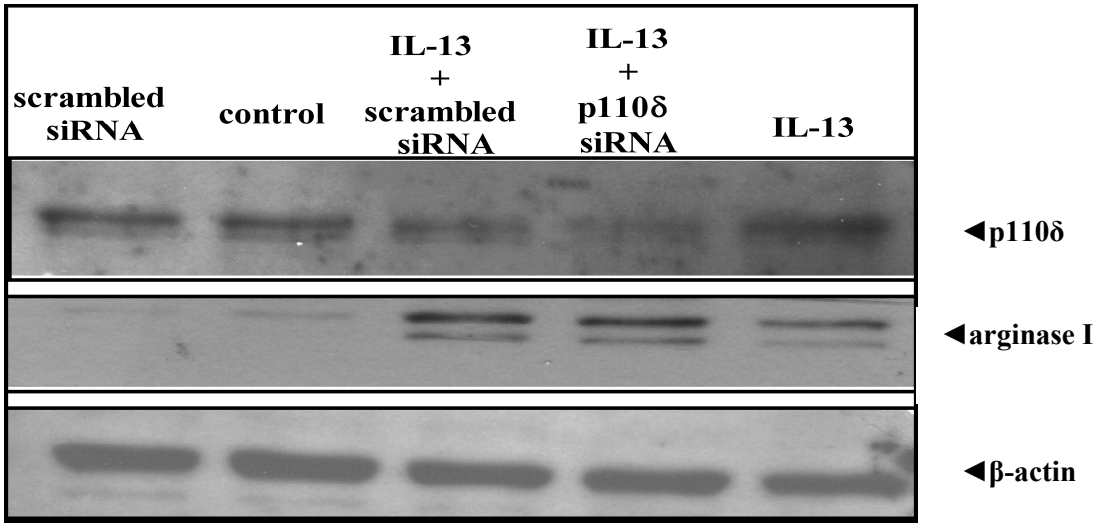

Figure 6.10 p110δ knock-down in tracheal rings by reverse permeabilization. Tracheal rings from 4 mice were reversibly permeabilized in the presence or absence of scrambled siRNA and cultured for 72 h. Tracheal rings from another 4 mice were reversibly permeabilized in the absence or presence of p110 δ-targeted siRNA or the presence of scrambled siRNA and cultured for 48 h. IL-13 (100 ng/ml) was added to the intended groups, then recultured for additional 24 h. Western blotting analysis was carried out with anti-p110δ, and mouse monoclonal anti-arginase I antibodies before detection by enhanced chemiluminescence. The β-actin band shown in the lower blot was used to ensure equal loading. Immunoblot from one experiment is a representative of two.

6.8 Discussion

RNAi so far has been used mainly as a functional rather than a therapeutic tool. It faces many challenges to step from cell culture and preclinical *in vivo* models to the clinic. Delivery to the right cell type, in the right organ, at the right time with no or minimal nonspecific, including immunological, effects are obstacles to be overcome (Caplen, 2004).

In order to assess the delivery of siRNA epithelial cell lines were examined. The knock-down of p110δ was demonstrated in the human bronchial epithelial cell line BEAS-2B. p110δ-targeted siRNA treated cells showed lower protein levels

compared with cells treated with scrambled siRNA or untreated cells. In a similar study it was demonstrated that STAT6 knock down by siRNA results in decreased eotaxin-3 level in BEAS-2B (Rippmann *et al.*, 2005).

Further experiments were carried out with human tracheal epithelial cell line 9HTEo-. Work shown in this chapter demonstrates that unstimulated 9HTEo- express both IL-13Rα1 and IL-13Rα2 and flow cytometric analysis revealed similar levels of IL-13 Rα2 in IL-13-stimulated 9HTEo-cells. These findings encouraged the application of 9HTEo- for siRNA studies.

C20 and C22 were found to be efficiently delivery vectors to both 9HTEo- and A549 cell lines, which were comparable to the results obtained with TransIT-TKO, C20 and C22, novel very long chain lipopolyamines. A549 cell line viability was 80.9 % and 80.1 % for C20 and C22 respectively, which was similar to TransIT-TKO recorded viability of 86.4 %. A recent study to deliver enhanced green fluorescence protein siRNA to A549 using polyplex was both efficient and safe and the delivery of shRNA efficiently silenced Akt1, confirmed by Western blot analysis (Jere *et al*., 2008).

Both C20 and C22 effectively transduce fluorescein-tagged RNA into 9HTEo-, and similar viability was observed compared with TransIT-TKO. In a similar study to test cytotoxic effects of polyplexes in A549 and 9HTEo- cells by measuring the release of lactate dehydrogenase (LDH), A549 cell cytotoxicity was not increased by transfecting substance but 9HTEo- showed a slight increase (Carrabino *et al.*, 2005) which may indicate the vulnerability of 9HTEo-. Another study showed that 9HTEo- were transfected with nanospheres contain DNA encoding the CFTR gene resulted in CFTR expression in about 50%-60% of the cells (Truong-Le *et al*., 1999).

C20 or C22, the lipospermines, were tested as well as TransIT-TKO in murine tracheal segments with the use of two different concentrations of fluorescein-tagged RNA (50 or 100 nM). The level of fluorescence in tested murine tracheal segments was comparable to that of control segments denoting low efficiency entry of the tested lipospermines. The use of siRNA for respiratory system delivery has

focused on direct delivery of siRNA to lung epithelial cells through intratracheal or intranasal route and most reported successful studies have used simple saline formulations (reviewed in de Fougerolles & Novobrantseva, 2008). Although the cationic lipid GL has been utilized in human clinical trials, GL-formulated siRNA was found in alveolar macrophages while protein levels of β-galactosidase (as a functional tool to test siRNA targeting) was not decreased in murine airway epithelial cells (Griesenbach *et al.*, 2006). Many factors can account for the failure of lipoplexes to efficiently transfect airways (see section 6.1), but it was recently demonstrated that IL-13-targeted siRNA complexed with a polyethylenimine derivative jetPEI delivered via the tail vein of OVA-sensitized mice resulted in reduced lung resistance in response to inhaled methacholine compared with controls (Lively *et al.*, 2008).

Fluorescein-tagged nonselective RNA was used also to assess siRNA uptake into murine tracheal segments by the reverse permeabilization technique. Fluorescein-tagged RNA was introduced into the epithelial lining of murine tracheal segments as assessed by confocal microscopy, which also showed higher fluorescence with the use of higher concentrations, a result consistent with other reports demonstrating accumulation of FITC-labelled oligodeoxynucleotides into rat ileum smooth muscle cells (Lesh *et al.*, 1995), and FITC-conjugated nonselective siRNA into rat isolated aortic smooth muscle cells (Corteling *et al.*, 2007). It was demonstrated that fluorescein-tagged nonselective RNA showed higher fluorescence when applied at 50 nM compared with 100 nM, which maybe due to a saturation effect. Fluorescence detected in the epithelium is consistent with role of epithelium as a site of IL-13 enhanced hyperresponsiveness demonstrated earlier in this study.

RNAi can be used as means to induce transient loss of function of molecules involved in respiratory diseases. Efficient introduction of siRNAs into cells in intact tissue and the maintenance of normal contractility of smooth muscle rings containing siRNA for at least 3 days in organ culture are major obstacles. The reverse permeabilization method to deliver p110δ-targeted siRNA was carried out. The tension of control murine tracheal segments exposed to reverse permeabilization solutions and recorded after three days of culture was maintained compared with previously recorded tension in control segments cultured for 24 h. This is consistent

with a previous siRNA reverse permeabilization approach for intact cerebral arteries in which siRNA effectively decreased Gq and RhoA mRNA levels over a 5-day period of organ culture, and importantly RhoA siRNA-targeted arteries did not constrict to UTP after 4 days of organ culture. The main objective of these studies was to deliver siRNA or antisense oligodeoxynucleotides into smooth muscle cells (Lesh *et al.*, 1995; Corteling *et al.*, 2007; Smolock *et al.*, 2007). In the current study, epithelium-intact murine tracheal segments were investigated to simulate in vivo conditions. These data using p110 δ-targeted siRNA support the results shown in chapter 4 that demonstrated an essential role of p110δ using the p110δ–selective inhibitor, as well as tracheal segments from animals expressing the catalytically inactive PI3K subunit $p110\delta^{D910A/D910A}$. In the current chapter p110δ-targeted siRNA-treated tissue no longer demonstrates IL-13-enhanced responsiveness to KCl or CCh compared with scrambled siRNA-treated segments. Studies carried out with denuded rat cerebral or swine carotid arteries showed decreased contraction after RhoA or casin kinase 2-targeted siRNA respectively, which were delivered by reverse permeabilization (Corteling *et al.*, 2007; Smolock *et al.*, 2007). Although fluorescein-tagged nonselective RNA (20 nM) did not indicate transfection, the functional study using this concentration of p110δ-targeted siRNA revealed loss of IL-13 enhanced responsiveness. This can be explained by decreased fluorescence after 3 days incubation at 20 nM concentration.

Reversibly permeabilized murine tracheal rings that were studied for isometric tension contraction were processed for measurements of p110δ protein content. Although there were small differences between p110δ content in controls (segments with or without scrambled siRNA) and IL-13-treated segments, this is likely due to animal-to animal variation. Because it was difficult to dissect more than 2 rings to study isometric contraction, control and IL-13-treated segments were obtained from two different groups. However, it was demonstrated that the introduction of p110δ-targeted siRNA into murine tracheal rings downregulated p110δ protein content and scrambled siRNA had no effect on p110δ level. No significant changes in β-actin (used for equal loading) were observed and p110δ downregulation was a result p110δ-targeted siRNA. Yang *et al*. (2006) showed that arginase I expression correlated with the development, persistence and resolution of IL-13-induced AHR and silencing arginase I in murine lung by RNAi resulted in

marked attenuation of IL-13-induced AHR to methacholine. Although the results presented in this chapter indicate that IL-13 upregulates arginase I protein expression, the possibility that PI3K p110δ contributes to IL-13-induced arginase I-protein expression is not supported by the data shown in this chapter and other signalling mechanism (s) such as STAT6 may be involved. In STAT6-deficient mice, Yang *et al.* (2006) showed that STAT-6 regulates arginase I protein expression in response to IL-13.

Delivery of p110δ-targeted siRNA by reverse permeabilization into murine tracheal segments followed by functional evaluation seems to be a step forward to assess the delivery of RNAi. This method was evaluated both by functional loss of IL-13-enhanced hyperresponsiveness and detection of fluorescein-tagged nonselective RNA in tissue. However, the lipospermines C20 and C22 investigated were not suitable to deliver siRNA into tissue, although these can be efficiently delivered to cell lines and can serve to further elucidate signalling mechanisms. Efficient delivery and viability of tissues or cell lines following siRNA delivery are important to evaluate the methods used.

6.9 Summary

- p110δ- was knocked down in BEAS-2B cell line;
- human tracheal 9HTEo- cells express IL-13 receptors;
- RNA was efficiently delivered into 9HTEo- and A549 cell lines by novel lipospermines;
- PI3Kδ-targeted siRNA attenuates IL-13-enhanced contraction using reverse permeabilization method.

Chapter Seven

General conclusions

IL-13 has a range of effector functions, with key roles in asthma. Although IL-13 potentially contributes to the effector phase of the allergic response for example recruitment of inflammatory cells into the airway spaces, IgE production and airway remodelling, it is likely that some effects of IL-13 maybe through its action on resident cells such as epithelial cells, fibroblasts, and smooth muscle cells (Wills-Karp, 2004). AHR is a hallmark of asthma and IL-13 can induce AHR in the absence of inflammatory cells (Grunig *et al.*, 1998).

The main objective of this project was to identify and characterize pharmacological target(s) for the treatment of altered lung function seen in inflammatory lung disease. Although a disadvantage of using airway strips and ring preparations is the inability to stimulate the mucosal or the serosal side selectively (Hulsmann & de Jongste, 1993) tracheal rings were selected over tracheal strips because the configuration of the ASM bundles is largely preserved in this arrangement, and their contraction is directly related to *in vivo* airway narrowing. Animal models of inflammatory lung disease can reflect short-term or acute inflammation seen in human chronic airway diseases. At the start of this project, comparison of the responses using smooth muscle preparations from two common laboratory animals (rat and mice) to investigate IL-13-induced hyperresponsiveness was carried out. It was observed that murine tracheal segments produced consistent and significant enhanced responsiveness to both KCl and CCh after incubation with m-IL-13. These findings, added to the availability of a wide range of tools of mice genetics, provided support for the use of isolated murine tracheal segments in the following experiments. A 24 h incubation period also proved to be important in m-IL-13 enhanced hyperresponsiveness. This period was most probably needed for protein synthesis for IL-13 enhanced contraction. As shown in chapter three, the 24 h culture period had no effect on murine tracheal segments contraction as demonstrated by insignificant difference between fresh and cultured rings. However, it was determined that rat tracheal rings incubated with r-IL-13 at different concentration were not significantly different from control group. It was anticipated that IL-13 might attenuate the relaxant responses to isoprenaline, but this was not detected in either rat or mice isolated tracheal segments. Cross-reactivity studies demonstrated that m-IL-13 significantly enhanced contraction to CCh in rat tissue while r-IL-13 did not enhance contraction to either KCl or CCh. This may imply a different

function of r-IL-13 rather than induction of hyperresponsiveness. While r- and m-IL-13 represent a much more homologous system for rat and mice isolated tracheal segments respectively, it was important to test h-IL-13 on both rat and murine tracheal segments. h-IL-13 enhanced contraction to KCl in tracheal rings isolated from both rat and mice, but did not enhance contraction to CCh which may indicate that h-IL-13 does not enhance rat or mice muscarinic receptors activation.

The next part of this study involved investigating the mechanism(s) by which IL-13 induces hyperresponsiveness. Previous studies have focused on the Janus kinase/signal transducers and activators of transcription-6 pathway (Kuperman *et al.*, 1998; Roy *et al.*, 2002; Kuperman *et al.*, 2002), although IL-13 was shown to activate PI3K and downstream effector molecules in a range of other systems (Wright *et al.*, 1997; Ceponis *et al.*, 2000; Hershey, 2003). The role of PI3K p110δ in IL-13-induced hyperresponsiveness was recently studied (Lee *et al.*, 2006a; Nashed *et al.*, 2007). Work presented in this thesis provides several lines of evidence that implicate PI3K signalling in IL-13-induced hyperresponsiveness. IL-13 induced a very early (after 2 min) PI3K-dependent phosphorylation of Akt. Wortmannin and LY294002, non-isoform-selective PI3K inhibitors, prevented IL-13-induced hyperresponsiveness in isolated murine tracheal rings. When studying wortmannin at different concentrations, it did not suppress the maximum tension elicited for either KCl or CCh. Moreover, the enhanced responsiveness was maintained when the segments were treated with wortmannin after 24 h exposure to IL-13. Isolated tracheal rings treated with IC87114, p110δ-selective inhibitor, as well as segments isolated from animals expressing the catalytically inactive PI3K subunit $p110\delta^{D910A/D910A}$, had responsiveness similar to that of normal tissues. These findings indicate an important role of IL-13-induced ASM contraction independent of effects mediated by infiltrating immune cells.

Akt phosphorylation downstream of IL-13 signalling was detected early, whereas increased responsiveness was not observed until overnight incubation, which suggested further downstream effector molecule (s) involved in IL-13-induced contraction. A potential mechanism of IL-13-induced hyperresponsiveness is the induction of arginase (Maarsingh *et al.*, 2008b). The next finding in this study was inhibition of IL-13 enhanced contraction by L-norvaline, an arginase inhibitor,

implying a role for arginase in this system. Arginase I protein expression as detected by Western blotting was induced by m-IL-13 after 24 h, but not at earlier times tested, which correlated with IL-13 enhanced hyperresponsiveness. IHC analysis supported IL-13-induced arginase I protein expression after 24 h treatment with IL-13. Therefore, is there a link between PI3K and arginase I in IL-13-enhanced responsiveness? IL-13-induced arginase I protein expression was inhibited by wortmannin and LY294002 as determined by Western blot analysis and IHC suggesting a role of PI3K. Surprisingly, IL-13-induced arginase I protein expression remained unchanged when murine tracheal segments were pretreated with the p110δ-selective inhibitor IC87114. Although these findings imply a role for PI3K in IL-13-induced arginase I induction, p110 δ does not appear to be the important isoform. This contrasts with the role of p110δ in IL-13-enhanced responsiveness shown earlier in this study. The reason for this discrepancy could be multiple signalling pathways related to IL-13-enhanced contraction. The first pathway could be IL-13/p110δ enhanced hyperresponsiveness. Another pathway could be IL-13/ PI3K/arginase I enhanced responsiveness. Moreover, off-target effects of LY294002 on other PI3K-related or PI3K-unrelated kinases have been reported (Gharbi *et al.,* 2007), including mTOR (mammalian target of rapamycin), DNA-PK (DNA-dependent protein kinase) and casein kinase 2 (reviewed in Kong & Yamori, 2008). PI3K-independent inhibition of signalling via Ca^{2+} and transcription factors such as NF-κB have also been reported for LY294002 (Tolloczko *et al.,* 2004; Kim *et al.,* 2005). Based on these previous studies, it is possible that PI3K-independent effects contribute in the current study to LY294002-induced inhibition of arginase I protein expression.

A key finding of this thesis is the role of epithelium in IL-13-enhanced hyperresponsiveness. To elucidate the action of IL-13 on airway epithelial cells, the epithelium was denuded before incubation with IL-13. IL-13-induced hyperresponsiveness was lost suggesting that the potential mechanism of IL-13 to promote hyperresponsiveness is epithelial-dependent. The lack of response was not a consequence of mechanical trauma to the muscle as the obtained tension in epithelium-denuded control was not different from that obtained in epithelium -intact control segments. When the epithelium was denuded after incubation with m-IL-13, the increased contractile responses to KCl and CCh compared with control were maintained. IL-13-enhanced contraction is epithelial dependent, therefore, the site(s)

of IL-13-induced arginase I expression were studied. IL-13 induced arginase I in both epithelium-intact and denuded murine tracheal segments.

Throughout the course of this research a key aim was to find target(s) by which IL-13 induced hyperresponsiveness and find a method to inhibit those targets while retaining functionality of murine tracheal segments. Gene silencing by siRNA can be not only a research tool, but also a therapeutic drug. Efficient introduction of siRNA into cells in intact tissue and the maintenance of normal contractility of smooth muscle rings containing siRNA for at least 3 days in organ culture were essential in this study. Thus, a reverse permeabilization method to deliver p110δ-targeted siRNA was carried out. Recorded tension in response to KCl and CCh in control murine tracheal segments exposed to reverse permeabilization solutions was not significantly different compared with recorded tension in control segments. Hence reverse permeabilization appeared to be a suitable method to deliver siRNA as it did not affect measured tension. p110δ-targeted siRNA inhibited IL-13-enhanced responsiveness and Western blot analysis of the same segments showed that introduction of p110 δ-targeted siRNA downregulated p110δ protein content with no observed effect of inactive siRNA on p110δ level.

To assess siRNA uptake into murine tracheal segments after reverse permeabilization, the delivery of fluorescein-tagged nonselective RNA was studied. It was demonstrated that fluorescence in the epithelial lining of murine tracheal segments as assessed by confocal microscopy increased with the use of higher concentrations of fluorescein-tagged nonselective RNA, although no uptake was demonstrated at low (20 nM) concentration.

To test another method to deliver siRNA into intact tissue, two lipospermines (C20 or C22) synthesized in our department were compared with a commercially available transfecting agent, TransIT-TKO, as delivery agents for fluorescein-tagged nonselective RNA. 9HTEo- and A549 epithelial cell lines were used to test C20, C22 or TransIT-TKO delivery of fluorescein-tagged nonselective RNA. All tested fluorescein-tagged nonselective RNA-lipospermine complexes were efficiently delivered to both 9HTEo- and A549 cell lines. Viability of A549 and 9HTEo cell lines with the use of C20 or C22 was similar to that of TransIT-TKO. When delivery

to tracheal segments was attempted it was not possible to demonstrate any increased fluorescence compared with control segments, which may denote low efficiency entry or the need to test earlier time points for efficient delivery.

The results of this research demonstrate that PI3K p110δ is the main isoform involved in IL-13-induced hyperresponsiveness in isolated murine tracheal rings and its inhibition using different pharmacological and genetic tools (selective inhibitor, p110δ kinase-dead mice and p110δ-targeted siRNA) leads to inhibition of IL-13-induced hyperresponsiveness. PI3K is also important in IL-13 induced arginase I induction and IL-13-induced hyperresponsiveness is epithelial dependent. Gene therapy and especially the knock-down of p110δ by RNAi techniques may be important in future research in this important topic, pharmacological targets in inflammatory lung diseases.

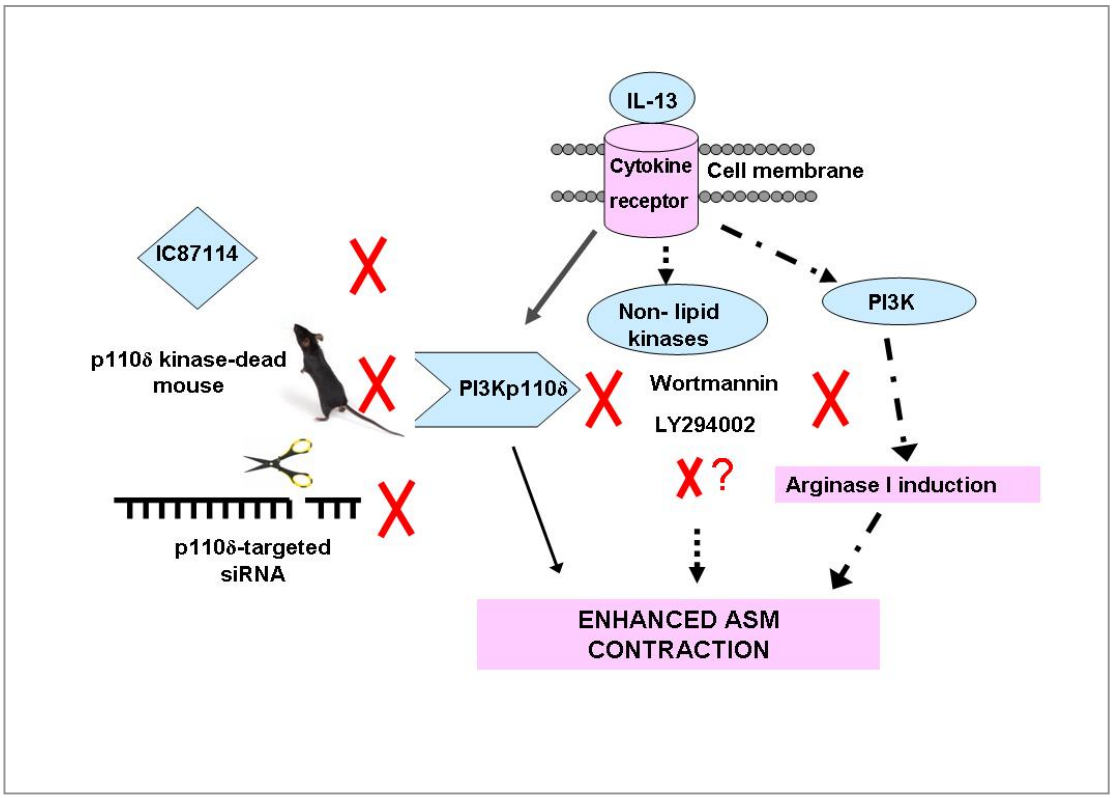

Figure 7.1 Mechanism(s) of IL-13 enhanced contraction in murine ASM. The work carried out in this thesis demonstrates the role of PI3Kp110δ in IL-13-induced hyperresponsiveness in murine tracheal segments. Inhibition of p110δ, using the selective inhibitor (IC87114), tracheal segments isolated from mice expressing a catalytically inactive p110δ isoform of PI3K, or p110δ-targeted siRNA, resulted in inhibition of IL-13-enhanced hyperresponsiveness. PI3K is also important in IL-13-induced arginase I protein expression which was inhibited by the non-selective inhibitors wortmannin and LY294002. Other kinases e.g. CK2, mTOR may be implicated in IL-13-enhanced contraction.

Chapter Eight

References

Adner M, Rose AC, Zhang YP, Sward K, Benson M, Uddman R, Shankley NP, Cardell LO (2002). An assay to evaluate the long-term effects of inflammatory mediators on murine airway smooth muscle: evidence that TNF alpha up-regulates 5-HT2A-mediated contraction. *Br J Pharmacol*, **137:** 971-982.

Aït-Khaled N, Enarson D, Bousquet J (2001). Chronic respiratory diseases in developing countries: the burden and strategies for prevention and management. *Bull World Health Organ*, **79:** 971-979.

Akaiwa M, Yu B, Umeshita-Suyama R, Terada N, Suto H, Koga T, Arima K, Matsushita S, Saito H, Ogawa H, Furue M, Hamasaki N, Ohshima K, Izuhara K (2001). Localization of human interleukin 13 receptor in non-haematopoietic cells. *Cytokine*, **13:** 75-84.

Akbari O, Stock P, Meyer E, Kronenberg M, Sidobre S, Nakayama T, Taniguchi M, Grusby MJ, DeKruyff RH, Umetsu DT (2003). Essential role of NKT cells producing IL-4 and IL-13 in the development of allergen-induced airway hyperreactivity. *Nat Med*, **9:** 582-588.

Akiba T, Kuroiwa N, Atsuko SY, Iwase K, Hiwasa T, Yokoe H, Kubosawa H, Kageyama R, Darlington GJ, Mori M, Tanzawa H, Takiguchi M (2002). Expression and regulation of the gene for arginase I in mouse salivary glands: Requirement of CCAAT/enhancer-binding protein alpha for the expression in the parotid gland. *J Biochem*, **132:** 621-627.

Ammit AJ, Armour CL, Black JL (2000). Smooth-muscle myosin light-chain kinase content is increased in human sensitized airways. *Am J Respir Crit Care Med*, **161:** 257-263.

Amrani Y, Panettieri RA (2003). Airway smooth muscle: contraction and beyond. *Int J Biochem Cell Biol*, **35:** 272-276.

Andrews AL, Bucchieri F, Arima K, Izuhara K, Holgate ST, Davies DE, Holloway JW (2007). Effect of IL-13 receptor alpha 2 levels on the biological activity of IL-13 variant R110Q. *J Allergy Clin Immunol*, **120:** 91-97.

Andrews AL, Holloway JW, Holgate ST, Davies DE (2006). IL-4 receptor alpha is an important modulator of IL-4 and IL-13 receptor binding: implications for the development of therapeutic targets. *J Immunol*, **176:** 7456-7461.

Arcaro A, Volinia S, Zvelebil MJ, Stein R, Watton SJ, Layton MJ, Gout I, Ahmadi K, Downward J, Waterfield MD (1998). Human phosphoinositide 3-kinase C2beta, the role of calcium and the C2 domain in enzyme activity. *J Biol Chem*, **273:** 33082-33090.

Arcaro A, Zvelebil MJ, Wallasch C, Ullrich A, Waterfield MD, Domin J (2000). Class II phosphoinositide 3-kinases are downstream targets of activated polypeptide growth factor receptors. *Mol Cell Biol*, **20:** 3817-3830.

Arima K, Sato K, Tanaka G, Kanaji S, Terada T, Honjo E, Kuroki R, Matsuo Y, Izuhara K (2005). Characterization of the interaction between interleukin-13 and interleukin-13 receptors. *J Biol Chem*, **280:** 24915-24922.

Ash DE (2004). Structure and function of arginases. *J Nutr*, **134:** 2760S-2764S.

Babu KS, Arshad SH, Holgate ST (2001). Anti-IgE treatment: an update. *Allergy*, **56:** 1121-1128.

Bachar O, Rose AC, Adner M, Wang XD, Prendergast CE, Kempf A, Shankley NP, Cardell LO (2005). TNF alpha reduces tachykinin, PGE(2)-dependent, relaxation of the cultured mouse trachea by increasing the activity of COX-2. *Br J Pharmacol*, **144:** 220-230.

Bainbridge JW, Smith AJ, Barker SS, Robbie S, Henderson R, Balaggan K, Viswanathan A, Holder GE, Stockman A, Tyler N, Petersen-Jones S, Bhattacharya SS, Thrasher AJ, Fitzke FW, Carter BJ, Rubin GS, Moore AT, Ali RR (2008). Effect of gene therapy on visual function in Leber's congenital amaurosis. *N Engl J Med*, **358:** 2231-2239.

Barksdale AR, Bernard AC, Maley ME, Gellin GL, Kearney PA, Boulanger BR, Tsuei BJ, Ochoa JB (2004). Regulation of arginase expression by T-helper II cytokines and isoproterenol. *Surgery*, **135:** 527-535.

Barnes PJ (2008). Immunology of asthma and chronic obstructive pulmonary disease. *Nat Rev Immunol*, **8:** 183-192.

Barnes PJ (2000). Mechanisms in COPD: differences from asthma. *Chest*, **117:** 10S-14S.

Barrio J, Cortijo J, Milara J, Mata M, Guijarro R, Blasco P, Morcillo EJ (2006). In vitro tracheal hyperresponsiveness to muscarinic receptor stimulation by carbachol in a rat model of bleomycin-induced pulmonary fibrosis. *Auton Autacoid Pharmacol*, **26:** 327-333.

Bergeron C, Boulet LP, Page N, Laviolette M, Zimmermann N, Rothenberg ME, Hamid Q (2007). Influence of cigarette smoke on the arginine pathway in asthmatic airways: Increased expression of arginase I. *J Allergy Clin Immunol*, **119:** 391-397.

Bloemen K, Verstraelen S, Van Den HR, Witters H, Nelissen I, Schoeters G (2007). The allergic cascade: review of the most important molecules in the asthmatic lung. *Immunol Lett*, **113:** 6-18.

Booij-Noord H, Orie NG, de VK (1971). Immediate and late bronchial obstructive reactions to inhalation of house dust and protective effects of disodium cromoglycate and prednisolone. *J Allergy Clin Immunol*, **48:** 344-354.

Boulet LP, Turcotte H, Boutet M, Montminy L, Laviolette M (1993). Influence of Natural Antigenic Exposure on Expiratory Flows, Methacholine Responsiveness, and Airway Inflammation in Mild Allergic-Asthma. *J Allergy Clin Immunol*, **91:** 883-893.

Boutard V, Havouis R, Fouqueray B, Philippe C, Moulinoux JP, Baud L (1995). Transforming growth factor-beta stimulates arginase activity in macrophages. Implications for the regulation of macrophage cytotoxicity. *J Immunol*, **155:** 2077-2084.

Bradford MM (1976). A rapid and sensitive method for the quantitation of microgram quantities of protein utilizing the principle of protein-dye binding. *Anal Biochem*, **72:** 248-254.

Bragonzi A, Dina G, Villa A, Calori G, Biffi A, Bordignon C, Assael BM, Conese M (2000). Biodistribution and transgene expression with nonviral cationic vector/DNA complexes in the lungs. *Gene Ther*, **7:** 1753-1760.

Bridge AJ, Pebernard S, Ducraux A, Nicoulaz AL, Iggo R (2003). Induction of an interferon response by RNAi vectors in mammalian cells. *Nat Genet*, **34:** 263-264.

Brightling CE, Bradding P, Symon FA, Holgate ST, Wardlaw AJ, Pavord ID (2002). Mast-cell infiltration of airway smooth muscle in asthma. *N Engl J Med*, **346:** 1699-1705.

Brown RA, Domin J, Arcaro A, Waterfield MD, Shepherd PR (1999). Insulin activates the alpha isoform of class II phosphoinositide 3-kinase. *J Biol Chem*, **274:** 14529-14532.

Brusselle G, Kips J, Joos G, Bluethmann H, Pauwels R (1995). Allergen-induced airway inflammation and bronchial responsiveness in wild-type and interleukin-4-deficient mice. *Am J Respir Cell Mol Biol*, **12:** 254-259.

Bryborn M, Adner M, Cardell LO (2004). Interleukin-4 increases murine airway response to kinins, via up-regulation of bradykinin B-1-receptors and altered signalling along mitogen-activated protein kinase pathways. *Clin Exp Allergy*, **34:** 1291-1298.

Bucala R, Spiegel LA, Chesney J, Hogan M, Cerami A (1994). Circulating fibrocytes define a new leukocyte subpopulation that mediates tissue repair. *Mol Med*, **1:** 71-81.

Canonico AE, Brigham KL, Carmichael LC, Plitman JD, King GA, Blackwell TR, Christman JW (1996). Plasmid-liposome transfer of the alpha 1 antitrypsin gene to cystic fibrosis bronchial epithelial cells prevents elastase-induced cell detachment and cytokine release. *Am J Respir Cell Mol Biol*, **14:** 348-355.

Canonico AE, Plitman JD, Conary JT, Meyrick BO, Brigham KL (1994). No lung toxicity after repeated aerosol or intravenous delivery of plasmid-cationic liposome complexes. *J Appl Physiol*, **77:** 415-419.

Caplen NJ (2004). Gene therapy progress and prospects. Downregulating gene expression: the impact of RNA interference. *Gene Ther*, **11:** 1241-1248.

Caput D, Laurent P, Kaghad M, Lelias JM, Lefort S, Vita N, Ferrara P (1996). Cloning and characterization of a specific interleukin (IL)-13 binding protein structurally related to the IL-5 receptor alpha chain. *J Biol Chem*, **271:** 16921-16926.

Carrabino S, Di GS, Copreni E, Conese M (2005). Serum albumin enhances polyethylenimine-mediated gene delivery to human respiratory epithelial cells. *J Gene Med*, **7:** 1555-1564.

Cash E, Minty A, Ferrara P, Caput D, Fradelizi D, Rott O (1994). Macrophage-inactivating IL-13 suppresses experimental autoimmune encephalomyelitis in rats. *J Immunol*, **153:** 4258-4267.

Cederbaum SD, Yu H, Grody WW, Kern RM, Yoo P, Iyer RK (2004). Arginases I and II: do their functions overlap? *Mol Genet Metab*, **81:** S38-S44.

Ceponis PJM, Botelho F, Richards CD, Mckay DM (2000). Interleukins 4 and 13 increase intestinal epithelial permeability by a phosphatidylinositol 3-kinase pathway - Lack of evidence for STAT 6 involvement. *J Biol Chem*, **275:** 29132-29137.

Chamley-Campbell J, Campbell GR, Ross R (1979). The smooth muscle cell in culture. *Physiol Rev*, **59:** 1-61.

Chanez P, Vignola AM, O'Shaugnessy T, Enander I, Li D, Jeffery PK, Bousquet J (1997). Corticosteroid reversibility in COPD is related to features of asthma. *Am J Respir Crit Care Med*, **155:** 1529-1534.

Chang CI, Liao JC, Kuo L (1998). Arginase modulates nitric oxide production in activated macrophages. *Am J Physiol*, **274:** H342-H348.

Chang CI, Zoghi B, Liao JC, Kuo L (2000). The involvement of tyrosine kinases, cyclic AMP/protein kinase A, and p38 mitogen-activated protein kinase in IL-13-mediated arginase I induction in macrophages: its implications in IL-13-inhibited nitric oxide production. *J Immunol*, **165:** 2134-2141.

Chang J, Mosenifar Z (2007). Differentiating COPD from asthma in clinical practice. *J Intensive Care Med*, **22:** 300-309.

Chen H, Tliba O, Van Besien CR, Panettieri RA, Amrani Y (2003). Selected contribution: TNF-alpha modulates murine tracheal rings responsiveness to G-protein-coupled receptor agonists and KC1. *J Appl Physiol*, **95:** 864-872.

Chen W, Ericksen MB, Levin LS, Khurana Hershey GK (2004). Functional effect of the R110Q IL13 genetic variant alone and in combination with IL4RA genetic variants. *J Allergy Clin Immunol*, **114:** 553-560.

Chen XP, Losman JA, Rothman P (2000). SOCS proteins, regulators of intracellular signaling. *Immunity*, **13:** 287-290.

Cherwinski HM, Schumacher JH, Brown KD, Mosmann TR (1987). Two types of mouse helper T cell clone. III. Further differences in lymphokine synthesis between Th1 and Th2 clones revealed by RNA hybridization, functionally monospecific bioassays, and monoclonal antibodies. *J Exp Med*, **166:** 1229-1244.

Chiba Y, Takada Y, Sakai H, Takeyama H, Misawa M (2000). Acetylcholine-induced smooth muscle contraction of intrapulmonary small bronchi is augmented in antigen-induced airway hyperresponsive rats. *Jpn J Pharmacol*, **84:** 221-224.

Chibana K, Trudeau JB, Mustovitch AT, Hu H, Zhao J, Balzar S, Chu HW, Wenzel SE (2008). IL-13 induced increases in nitrite levels are primarily driven by increases

in inducible nitric oxide synthase as compared with effects on arginases in human primary bronchial epithelial cells. *Clin Exp Allergy*, **38:** 1409.

Cho JY, Miller M, Baek KJ, Han JW, Nayar J, Lee SY, McElwain K, McElwain S, Friedman S, Broide DH (2004). Inhibition of airway remodeling in IL-5-deficient mice. *J Clin Invest*, **113:** 551-560.

Christianson DW (2005). Arginase: structure, mechanism, and physiological role in male and female sexual arousal. *Acc Chem Res*, **38:** 191-201.

Chu EK, Drazen JM (2005). Asthma: one hundred years of treatment and onward. *Am J Respir Crit Care Med*, **171:** 1202-1208.

Chung KF (2000). Airway smooth muscle cells: contributing to and regulating airway mucosal inflammation? *Eur Respir J*, **15:** 961-968.

Ckless K, van d, V, Janssen-Heininger Y (2007). Oxidative-nitrosative stress and post-translational protein modifications: implications to lung structure-function relations. Arginase modulates NF-kappaB activity via a nitric oxide-dependent mechanism. *Am J Respir Cell Mol Biol*, **36:** 645-653.

Cockcroft DW, Davis BE (2006). Mechanisms of airway hyperresponsiveness. *J Allergy Clin Immunol*, **118:** 551-559.

Cohen SG (1992). Asthma in antiquity: the Ebers Papyrus. *Allergy Proc*, **13:** 147-154.

Cohn L, Tepper JS, Bottomly K (1998). IL-4-independent induction of airway hyperresponsiveness by Th2, but not Th1, cells. *J Immunol*, **161:** 3813-3816.

Colleluori DM, Ash DE (2001). Classical and slow-binding inhibitors of human type II arginase. *Biochemistry*, **40:** 9356-9362.

Corne J, Chupp G, Lee CG, Homer RJ, Zhu Z, Chen Q, Ma B, Du Y, Roux F, McArdle J, Waxman AB, Elias JA (2000). IL-13 stimulates vascular endothelial cell growth factor and protects against hyperoxic acute lung injury. *J Clin Invest*, **106:** 783-791.

Corraliza IM, Soler G, Eichmann K, Modolell M (1995). Arginase induction by suppressors of nitric oxide synthesis (IL-4, IL-10 and PGE2) in murine bone-marrow-derived macrophages. *Biochem Biophys Res Commun*, **206:** 667-673.

Corry DB, Folkesson HG, Warnock ML, Erle DJ, Matthay MA, Wiener-Kronish JP, Locksley RM (1996). Interleukin 4, but not interleukin 5 or eosinophils, is required in a murine model of acute airway hyperreactivity. *J Exp Med*, **183:** 109-117.

Corteling RL, Brett SE, Yin H, Zheng XL, Walsh MP, Welsh DG (2007). The functional consequence of RhoA knockdown by RNA interference in rat cerebral arteries. *Am J Physiol Heart Circ Physiol*, **293:** H440-H447.

Cox JD, Cama E, Colleluori DM, Pethe S, Boucher JL, Mansuy D, Ash DE, Christianson DW (2001). Mechanistic and metabolic inferences from the binding of substrate analogues and products to arginase. *Biochemistry*, **40:** 2689-2701.

D'Amato G (2003). Therapy of allergic bronchial asthma with omalizumab - an anti-IgE monoclonal antibody. *Expert Opin Biol Ther*, **3:** 371-376.

D'Amico G, Bianchi G, Bernasconi S, Bersani L, Piemonti L, Sozzani S, Mantovani A, Allavena P (1998). Adhesion, transendothelial migration, and reverse transmigration of in vitro cultured dendritic cells. *Blood*, **92:** 207-214.

Daines MO, Hershey GKK (2002). A novel mechanism by which interferon-gamma can regulate interleukin (IL)-13 responses - Evidence for intracellular stores of IL-13 receptor alpha-2 and their rapid mobilization by interferon-gamma. *J Biol Chem*, **277:** 10387-10393.

Davidson DJ, Gray MA, Kilanowski FM, Tarran R, Randell SH, Sheppard DN, Argent BE, Dorin JR (2004). Murine epithelial cells: isolation and culture. *J Cyst Fibros*, **3** Suppl 2**:** 59-62.

Davies SP, Reddy H, Caivano M, Cohen P (2000). Specificity and mechanism of action of some commonly used protein kinase inhibitors. *Biochem J*, **351:** 95-105.

de Gouw HW, Verbruggen MB, Twiss IM, Sterk PJ (1999). Effect of oral L-arginine on airway hyperresponsiveness to histamine in asthma. *Thorax*, **54:** 1033-1035.

de Fougerolles A, Novobrantseva T (2008). siRNA and the lung: research tool or therapeutic drug? *Curr Opin Pharmacol*, **8:** 280-285.

Defrance T, Carayon P, Billian G, Guillemot JC, Minty A, Caput D, Ferrara P (1994). Interleukin 13 is a B cell stimulating factor. *J Exp Med*, **179:** 135-143.

Delmas P, Coste B, Gamper N, Shapiro MS (2005). Phosphoinositide lipid second messengers: new paradigms for calcium channel modulation. *Neuron*, **47:** 179-182.

Deshpande DA, Dogan S, Walseth TF, Miller SM, Amrani Y, Panettieri RA, Kannan MS (2004). Modulation of calcium signaling by interleukin-13 in human airway smooth muscle: role of CD38/cyclic adenosine diphosphate ribose pathway. *Am J Respir Cell Mol Biol*, **31:** 36-42.

Dillon CP, Sandy P, Nencioni A, Kissler S, Rubinson DA, Van PL (2005). Rnai as an experimental and therapeutic tool to study and regulate physiological and disease processes. *Annu Rev Physiol*, **67:** 147-173.

Djukanovic R, Wilson SJ, Kraft M, Jarjour NN, Steel M, Chung KF, Bao W, Fowler-Taylor A, Matthews J, Busse WW, Holgate ST, Fahy JV (2004). Effects of treatment with anti-immunoglobulin E antibody omalizumab on airway inflammation in allergic asthma. *Am J Respir Crit Care Med*, **170:** 583-593.

Domin J, Pages F, Volinia S, Rittenhouse SE, Zvelebil MJ, Stein RC, Waterfield MD (1997). Cloning of a human phosphoinositide 3-kinase with a C2 domain that

displays reduced sensitivity to the inhibitor wortmannin. *Biochem J*, **326** (Pt 1): 139-147.

Donaldson DD, Whitters MJ, Fitz LJ, Neben TY, Finnerty H, Henderson SL, O'Hara RM, Beier DR, Turner KJ, Wood CR, Collins M (1998). The murine IL-13 receptor alpha 2: Molecular cloning, characterization, and comparison with marine IL-13 receptor. *J Immunol*, **161:** 2317-2324.

Donnelly LE, Rogers DF (2008). Novel targets and drugs in inflammatory lung disease. *Curr Opin Pharmacol*, **8:** 219-221.

Dow SW, Schwarze J, Heath TD, Potter TA, Gelfand EW (1999). Systemic and local interferon gamma gene delivery to the lungs for treatment of allergen-induced airway hyperresponsiveness in mice. *Hum Gene Ther*, **10:** 1905-1914.

Drumm ML, Pope HA, Cliff WH, Rommens JM, Marvin SA, Tsui LC, Collins FS, Frizzell RA, Wilson JM (1990). Correction of the cystic fibrosis defect in vitro by retrovirus-mediated gene transfer. *Cell*, **62:** 1227-1233.

Duan W, Datiles AMKA, Leung BP, Vlahos CJ, Wong WSF (2005). An anti-inflammatory role for a phosphoinositide 3-kinase inhibitor LY294002 in a mouse asthma model. *Int Immunopharmacol*, **5:** 495-502.

Dummer R, Rochlitz C, Velu T, Acres B, Limacher JM, Bleuzen P, Lacoste G, Slos P, Romero P, Urosevic M (2008). Intralesional adenovirus-mediated interleukin-2 gene transfer for advanced solid cancers and melanoma. *Mol Ther*, **16:** 985-994.

Duncan JE, Whitsett JA, Horowitz AD (1997). Pulmonary surfactant inhibits cationic liposome-mediated gene delivery to respiratory epithelial cells in vitro. *Hum Gene Ther*, **8:** 431-438.

Durante W, Johnson FK, Johnson RA (2007). Arginase: a critical regulator of nitric oxide synthesis and vascular function. *Clin Exp Pharmacol Physiol*, **34:** 906-911.

Durieux AC, Bonnefoy R, Busso T, Freyssenet D (2004). In vivo gene electrotransfer into skeletal muscle: effects of plasmid DNA on the occurrence and extent of muscle damage. *J Gene Med*, **6:** 809-816.

Dykxhoorn DM, Novina CD, Sharp PA (2003). Killing the messenger: short RNAs that silence gene expression. *Nat Rev Mol Cell Biol*, **4:** 457-467.

Eastman SJ, Baskin KM, Hodges BL, Chu Q, Gates A, Dreusicke R, Anderson S, Scheule RK (2002). Development of catheter-based procedures for transducing the isolated rabbit liver with plasmid DNA. *Hum Gene Ther*, **13:** 2065-2077.

Economides AN, Carpenter LR, Rudge JS, Wong V, Koehler-Stec EM, Hartnett C, Pyles EA, Xu X, Daly TJ, Young MR, Fandl JP, Lee F, Carver S, McNay J, Bailey K, Ramakanth S, Hutabarat R, Huang TT, Radziejewski C, Yancopoulos GD, Stahl N (2003). Cytokine traps: multi-component, high-affinity blockers of cytokine action. *Nat Med*, **9:** 47-52.

Edwards AM, Howell JB (2000). The chromones: history, chemistry and clinical development. A tribute to the work of Dr R. E. C. Altounyan. *Clin Exp Allergy*, **30:** 756-774.

Elbashir SM, Harborth J, Lendeckel W, Yalcin A, Weber K, Tuschl T (2001). Duplexes of 21-nucleotide RNAs mediate RNA interference in cultured mammalian cells. *Nature*, **411:** 494-498.

Elias J (2004). The relationship between asthma and COPD. Lessons from transgenic mice. *Chest*, **126:** 111S-116S.

Endo M, Oyadomari S, Terasaki Y, Takeya M, Suga M, Mori M, Gotoh T (2003). Induction of arginase I and II in bleomycin-induced fibrosis of mouse lung. *Am J Physiol Lung Cell Mol Physiol*, **285:** L313-L321.

Endo T, Ogushi F, Sone S (1996). LPS-dependent cyclooxygenase-2 induction in human monocytes is down-regulated by IL-13, but not by IFN-gamma. *J Immunol*, **156:** 2240-2246.

Erdely A, Kepka-Lenhart D, Clark M, Zeidler-Erdely P, Poljakovic M, Calhoun WJ, Morris SM, Jr. (2006). Inhibition of phosphodiesterase 4 amplifies cytokine-dependent induction of arginase in macrophages. *Am J Physiol Lung Cell Mol Physiol*, **290:** L534-L539.

Eum SY, Maghni K, Tolloczko B, Eidelman DH, Martin JG (2005). IL-13 may mediate allergen-induced hyperresponsiveness independently of IL-5 or eotaxin by effects on airway smooth muscle. *Am J Physiol Lung Cell Mol Physiol*, **288:** L576-L584.

Ezeamuzie CI, Sukumaran J, Philips E (2001). Effect of wortmannin on human eosinophil responses in vitro and on bronchial inflammation and airway hyperresponsiveness in guinea pigs in vivo. *Am J Respir Crit Care Med*, **164:** 1633-1639.

Fallon PG, Emson CL, Smith P, McKenzie AN (2001). IL-13 overexpression predisposes to anaphylaxis following antigen sensitization. *J Immunol*, **166:** 2712-2716.

Felgner PL, Gadek TR, Holm M, Roman R, Chan HW, Wenz M, Northrop JP, Ringold GM, Danielsen M (1987). Lipofection: a highly efficient, lipid-mediated DNA-transfection procedure. *Proc Natl Acad Sci U S A*, **84:** 7413-7417.

Finan PM, Thomas MJ (2004). PI 3-kinase inhibition: a therapeutic target for respiratory disease. *Biochem Soc Trans*, **32:** 378-382.

Fire A (1999). RNA-triggered gene silencing. *Trends Genet*, **15:** 358-363.

Fire A, Xu S, Montgomery MK, Kostas SA, Driver SE, Mello CC (1998). Potent and specific genetic interference by double-stranded RNA in Caenorhabditis elegans. *Nature*, **391:** 806-811.

Fischer A, Folkerts G, Geppetti P, Groneberg DA (2002). Mediators of asthma: nitric oxide. *Pulm Pharmacol Ther*, **15:** 73-81.

Fischer D, Bieber T, Li YX, Elsasser HP, Kissel T (1999). A novel non-viral vector for DNA delivery based on low molecular weight, branched polyethylenimine: Effect of molecular weight on transfection efficiency and cytotoxicity. *Pharm Res*, **16:** 1273-1279.

Flood-Page P, Menzies-Gow A, Phipps S, Ying S, Wangoo A, Ludwig MS, Barnes N, Robinson D, Kay AB (2003). Anti-IL-5 treatment reduces deposition of ECM proteins in the bronchial subepithelial basement membrane of mild atopic asthmatics. *J Clin Invest*, **112:** 1029-1036.

Flood-Page P, Swenson C, Faiferman I, Matthews J, Williams M, Brannick L, Robinson D, Wenzel S, Busse W, Hansel TT, Barnes NC; International Mepolizumab Study Group (2007). A study to evaluate safety and efficacy of mepolizumab in patients with moderate persistent asthma. *Am J Respir Crit Care Med*, **176:** 1062-1071.

Fort MM, Cheung J, Yen D, Li J, Zurawski SM, Lo S, Menon S, Clifford T, Hunte B, Lesley R, Muchamuel T, Hurst SD, Zurawski G, Leach MW, Gorman DM, Rennick DM (2001). IL-25 induces IL-4, IL-5, and IL-13 and Th2-associated pathologies in vivo. *Immunity*, **15:** 985-995.

Foster PS, Webb DC, Yang M, Herbert C, Kumar RK (2003). Dissociation of T helper type 2 cytokine-dependent airway lesions from signal transducer and activator of transcription 6 signalling in experimental chronic asthma. *Clin Exp Allergy*, **33:** 688-695.

Fozard JR, Hannon JP (2000). Species differences in adenosine receptor-mediated bronchoconstrictor responses. *Clin Exp Allergy*, **30:** 1213-1220.
Fredberg JJ (2004). Bronchospasm and its biophysical basis in airway smooth muscle. *Respir Res*, **5:** 2-17.

Gao X, Huang L (1996). Potentiation of cationic liposome-mediated gene delivery by polycations. *Biochemistry*, **35:** 1027-1036.

Gautam A, Densmore CL, Xu B, Waldrep JC (2000). Enhanced gene expression in mouse lung after PEI-DNA aerosol delivery. *Mol Ther*, **2:** 63-70.

Gharbi SI, Zvelebil MJ, Shuttleworth SJ, Hancox T, Saghir N, Timms JF, Waterfield MD (2007). Exploring the specificity of the PI3K family inhibitor LY294002. *Biochem J,* **404:** 15-21.

Ghonaim HM, Li S, Blagbrough IS (2009). Very long chain N^4,N^9-diacyl spermines: Non-viral lipopolyamine vectors for efficient plasmid DNA and siRNA delivery. *Pharm Res*, **26:** 19-31.

Giard DJ, Aaronson SA, Todaro GJ, Arnstein P, Kersey JH, Dosik H, Parks WP (1973). In vitro cultivation of human tumors: establishment of cell lines derived from a series of solid tumors. *J Natl Cancer Inst*, **51:** 1417-1423.

Gill TJ, III, Smith GJ, Wissler RW, Kunz HW (1989). The rat as an experimental animal. *Science*, **245:** 269-276.

Gonzales ML, Anderson RA (2006). Nuclear phosphoinositide kinases and inositol phospholipids. *J Cell Biochem*, **97:** 252-260.

Gotoh T, Araki M, Mori M (1997). Chromosomal localization of the human arginase II gene and tissue distribution of its mRNA. *Biochem Biophys Res Commun*, **233:** 487-491.

Gou D, Narasaraju T, Chintagari NR, Jin N, Wang P, Liu L (2004). Gene silencing in alveolar type II cells using cell-specific promoter in vitro and in vivo. *Nucleic Acids Res*, **32:** e134.

Griesenbach U, Kitson C, Escudero GS, Farley R, Singh C, Somerton L, Painter H, Smith RL, Gill DR, Hyde SC, Chow YH, Hu J, Gray M, Edbrooke M, Ogilvie V, Macgregor G, Scheule RK, Cheng SH, Caplen NJ, Alton EW (2006). Inefficient cationic lipid-mediated siRNA and antisense oligonucleotide transfer to airway epithelial cells in vivo. *Respir Res*, **7:** 26.

Gruenert DC, Basbaum CB, Welsh MJ, Li M, Finkbeiner WE, Nadel JA (1988). Characterization of human tracheal epithelial cells transformed by an origin-defective simian virus 40. *Proc Natl Acad Sci U S A*, **85:** 5951-5955.

Grunig G, Warnock M, Wakil AE, Venkayya R, Brombacher F, Rennick DM, Sheppard D, Mohrs M, Donaldson DD, Locksley RM, Corry DB (1998). Requirement for IL-13 independently of IL-4 in experimental asthma. *Science*, **282:** 2261-2263.

Grunig G, Warnock M, Wakil AE, Venkayya R, Brombacher F, Rennick DM, Sheppard D, Mohrs M, Donaldson DD, Locksley RM, Corry DB (1999). Requirement for IL-13 independently of IL-4 in experimental asthma. *FASEB J*, **13:** A318.

Grunstein MM, Hakonarson H, Leiter J, Chen M, Whelan R, Grunstein JS, Chuang S (2002). IL-13-dependent autocrine signaling mediates altered responsiveness of IgE-sensitized airway smooth muscle. *Am J Physiol Lung Cell Mol Physiol*, **282:** L520-L528.

Hacein-Bey-Abina S, von KC, Schmidt M, Le DF, Wulffraat N, McIntyre E, Radford I, Villeval JL, Fraser CC, Cavazzana-Calvo M, Fischer A (2003). A serious adverse event after successful gene therapy for X-linked severe combined immunodeficiency. *N Engl J Med*, **348:** 255-256.

Hajoui O, Janani R, Tulic M, Joubert P, Ronis T, Hamid Q, Zheng H, Mazer BD (2004). Synthesis of IL-13 by human B lymphocytes: Regulation and role in IgE production. *J Allergy Clin Immunol*, **114:** 657-663.

Hakonarson H, Herrick DJ, Serrano PG, Grunstein MM (1996). Mechanism of cytokine-induced modulation of beta-adrenoceptor responsiveness in airway smooth muscle. *J Clin Invest*, **97:** 2593-2600.

Halayko AJ, Amrani Y (2003). Mechanisms of inflammation-mediated airway smooth muscle plasticity and airways remodeling in asthma. *Respir Physiol Neurobiol*, **137:** 209-222.

Halayko AJ, Camoretti-Mercado B, Forsythe SM, Vieira JE, Mitchell RW, Wylam ME, Hershenson MB, Solway J (1999). Divergent differentiation paths in airway smooth muscle culture: induction of functionally contractile myocytes. *Am J Physiol*, **276:** L197-L206.

Halayko AJ, Salari H, MA X, Stephens NL (1996). Markers of airway smooth muscle cell phenotype. *Am J Physiol*, **270:** L1040-L1051.

Hammermann R, Hey C, Schafer N, Racke K (2000). Phosphodiesterase inhibitors and forskolin Up-regulate arginase activity in rabbit alveolar macrophages. *Pulm Pharmacol Ther*, **13:** 141-147.

Haque SJ, Harbor P, Tabrizi M, Yi T, Williams BR (1998). Protein-tyrosine phosphatase Shp-1 is a negative regulator of IL-4- and IL-13-dependent signal transduction. *J Biol Chem*, **273:** 33893-33896.

Harrop M (2007). Psychosocial impact of cystic fibrosis in adolescence. *Paediatr Nurs*, **19:** 41-45.

Hart PH, Bonder CS, Balogh J, Dickensheets HL, Vazquez N, Davies KV, Finlay-Jones JJ, Donnelly RP (1999). Diminished responses to IL-13 by human monocytes differentiated in vitro: role of the IL-13Ralpha1 chain and STAT6. *Eur J Immunol*, **29:** 2087-2097.

Hashimoto S, Gon Y, Takeshita I, Maruoka S, Horie T (2001). IL-4 and IL-13 induce myofibroblastic phenotype of human lung fibroblasts through c-Jun NH2-terminal kinase-dependent pathway. *J Allergy Clin Immunol*, **107:** 1001-1008.

Hebenstreit D, Luft P, Schmiedlechner A, Regl G, Frischauf AM, Aberger F, Duschl A, Horejs-Hoeck J (2003). IL-4 and IL-13 induce SOCS-1 gene expression in A549 cells by three functional STAT6-binding motifs located upstream of the transcription initiation site. *J Immunol*, **171:** 5901-5907.

Heck JN, Mellman DL, Ling K, Sun Y, Wagoner MR, Schill NJ, Anderson RA (2007). A conspicuous connection: Structure defines function for the phosphatidylinositol-phosphate kinase family. *Crit Rev Biochem Mol Biol*, **42:** 15-39.

Heller NM, Matsukura S, Georas SN, Boothby MR, Rothman PB, Stellato C, Schleimer RP (2004). Interferon-gamma inhibits STAT6 signal transduction and gene expression in human airway epithelial cells. *Am J Respir Cell Mol Biol*, **31:** 573-582.

Hershey GKK (2003). IL-13 receptors and signaling pathways: An evolving web. *J Allergy Clin Immunol*, **111:** 677-690.

Hesse M, Modolell M, La Flamme AC, Schito M, Fuentes JM, Cheever AW, Pearce EJ, Wynn TA (2001). Differential regulation of nitric oxide synthase-2 and arginase-

1 by type 1/type 2 cytokines in vivo: Granulomatous pathology is shaped by the pattern of L-arginine metabolism. *J Immunol*, **167:** 6533-6544.

Hilton DJ, Zhang JG, Metcalf D, Alexander WS, Nicola NA, Willson TA (1996). Cloning and characterization of a binding subunit of the interleukin 13 receptor that is also a component of the interleukin 4 receptor. *Proc Natl Acad Sci U S A*, **93:** 497-501.

Hirst SJ (1996). Airway smooth muscle cell culture: application to studies of airway wall remodelling and phenotype plasticity in asthma. *Eur Respir J*, **9:** 808-820.

Hobbs CA, Gilmour SK (2000). High levels of intracellular polyamines promote histone acetyltransferase activity resulting in chromatin hyperacetylation. *J Cell Biochem*, **77:** 345-360.

Hoet PH, Nemery B (2000). Polyamines in the lung: polyamine uptake and polyamine-linked pathological or toxicological conditions. *Am J Physiol Lung Cell Mol Physiol*, **278:** L417-L433.

Hokin MR, Hokin LE (1953). Enzyme secretion and the incorporation of P32 into phospholipides of pancreas slices. *J Biol Chem*, **203:** 967-977.

Holgate S, Casale T, Wenzel S, Bousquet J, Deniz Y, Reisner C (2005). The anti-inflammatory effects of omalizumab confirm the central role of IgE in allergic inflammation. *J Allergy Clin Immunol*, **115:** 459-465.

Holgate ST, Polosa R (2006). The mechanisms, diagnosis, and management of severe asthma in adults. *Lancet*, **368:** 780-793.

Holgate ST, Polosa R (2008). Treatment strategies for allergy and asthma. *Nat Rev Immunol*, **8:** 218-230.

Holtta E, Pohjanpelto P (1982). Polyamine dependence of Chinese hamster ovary cells in serum-free culture is due to deficient arginase activity. *Biochim Biophys Acta*, **721:** 321-327.

Howard K (2003). Unlocking the money-making potential of RNAi. *Nat Biotechnol*, **21:** 1441-1446.

Howard TD, Whittaker PA, Zaiman AL, Koppelman GH, Xu J, Hanley MT, Meyers DA, Postma DS, Bleecker ER (2001). Identification and association of polymorphisms in the interleukin-13 gene with asthma and atopy in a Dutch population. *Am J Respir Cell Mol Biol*, **25:** 377-384.

Howe SJ, Mansour MR, Schwarzwaelder K, Bartholomae C, Hubank M, Kempski H, Brugman MH, Pike-Overzet K, Chatters SJ, de RD, Gilmour KC, Adams S, Thornhill SI, Parsley KL, Staal FJ, Gale RE, Linch DC, Bayford J, Brown L, Quaye M, Kinnon C, Ancliff P, Webb DK, Schmidt M, von KC, Gaspar HB, Thrasher AJ (2008). Insertional mutagenesis combined with acquired somatic mutations causes leukemogenesis following gene therapy of SCID-X1 patients. *J Clin Invest*, **118:** 3143-3150.

Huang HY, Lee CC, Chiang BL (2008). Small interfering RNA against interleukin-5 decreases airway eosinophilia and hyper-responsiveness. *Gene Ther*, **15:** 660-667.

Hubbard R (2006). The burden of lung disease. *Thorax*, **61:** 557-558.

Hulsmann AR, de Jongste JC (1993). Studies of human airways in vitro: a review of the methodology. *J Pharmacol Toxicol Methods*, **30:** 117-132.

Humbert M, Menz G, Ying S, Corrigan CJ, Robinson DS, Durham SR, Kay AB (1999). The immunopathology of extrinsic (atopic) and intrinsic (non-atopic) asthma: more similarities than differences. *Immunol Today*, **20:** 528-533.

Hurwitz SH (1955). Nonallergic asthma; differential diagnosis and treatment. *Calif Med*, **83:** 61-67.

Hyde SC, Southern KW, Gileadi U, Fitzjohn EM, Mofford KA, Waddell BE, Gooi HC, Goddard CA, Hannavy K, Smyth SE, Egan JJ, Sorgi FL, Huang L, Cuthbert AW, Evans MJ, Colledge WH, Higgins CF, Webb AK, Gill DR (2000). Repeat administration of DNA/liposomes to the nasal epithelium of patients with cystic fibrosis. *Gene Ther*, **7:** 1156-1165.

Ignarro LJ, Buga GM, Wei LH, Bauer PM, Wu G, del SP (2001). Role of the arginine-nitric oxide pathway in the regulation of vascular smooth muscle cell proliferation. *Proc Natl Acad Sci U S A*, **98:** 4202-4208.

Ito K, Caramori G, Adcock IM (2007). Therapeutic potential of phosphatidylinositol 3-kinase inhibitors in inflammatory respiratory disease. *J Pharmacol Exp Ther*, **321:** 1-8.

Izuhara K (2003). The role of interleukin-4 and interleukin-13 in the non-immunologic aspects of asthma pathogenesis. *Clin Chem Lab Med*, **41:** 860-864.

Izuhara K, Arima K (2004). Signal transduction of IL-13 and its role in the pathogenesis of bronchial asthma. *Drug News Perspect*, **17:** 91-98.

Jackson AL, Bartz SR, Schelter J, Kobayashi SV, Burchard J, Mao M, Li B, Cavet G, Linsley PS (2003). Expression profiling reveals off-target gene regulation by RNAi. *Nat Biotechnol*, **21:** 635-637.

Jaffar Z, Roberts K, Pandit A, Linsley P, Djukanovic R, Holgate S (1999). B7 costimulation is required for IL-5 and IL-13 secretion by bronchial biopsy tissue of atopic asthmatic subjects in response to allergen stimulation. *Am J Respir Cell Mol Biol*, **20:** 153-162.

Janmey PA (1994). Phosphoinositides and calcium as regulators of cellular actin assembly and disassembly. *Annu Rev Physiol*, **56:** 169-191.

Jenkinson CP, Grody WW, Cederbaum SD (1996). Comparative properties of arginases. *Comp Biochem Physiol B Biochem Mol Biol*, **114:** 107-132.

Jere D, Xu CX, Arote R, Yun CH, Cho MH, Cho CS (2008). Poly(beta-amino ester) as a carrier for si/shRNA delivery in lung cancer cells. *Biomaterials*, **29:** 2535-2547.

Jiang H, Harris MB, Rothman P (2000). IL-4/IL-13 signaling beyond JAK/STAT. *J Allergy Clin Immunol*, **105:** 1063-1070.

Jiang H, Rao K, Liu X, Liu G, Stephens NL (1995). Increased Ca2+ and myosin phosphorylation, but not calmodulin activity in sensitized airway smooth muscles. *Am J Physiol*, **268:** L739-L746.

Kamachi A, Munakata M, Nasuhara Y, Nishimura M, Ohtsuka Y, Amishima M, Takahashi T, Homma Y, Kawakami Y (2001). Enhancement of goblet cell hyperplasia and airway hyperresponsiveness by salbutamol in a rat model of atopic asthma. *Thorax*, **56:** 19-24.

Kashiwada M, Giallourakis CC, Pan PY, Rothman PB (2001). Immunoreceptor tyrosine-based inhibitory motif of the IL-4 receptor associates with SH2-containing phosphatases and regulates IL-4-induced proliferation. *J Immunol*, **167:** 6382-6387.

Katso R, Okkenhaug K, Ahmadi K, White S, Timms J, Waterfield MD (2001). Cellular function of phosphoinositide 3-kinases: implications for development, homeostasis, and cancer. *Annu Rev Cell Dev Biol*, **17:** 615-675.

Kawakami K, Kawakami M, Snoy PJ, Husain SR, Puri RK (2001a). In vivo overexpression of IL-13 receptor alpha 2 chain inhibits tumorigenicity of human breast and pancreatic tumors in immunodeficient mice. *J Exp Med*, **194:** 1743-1754.

Kawakami K, Takeshita F, Puri RK (2001b). Identification of distinct roles for a dileucine and a tyrosine internalization motif in the interleukin (IL)-13 binding component IL-13 receptor alpha 2 chain. *J Biol Chem*, **276:** 25114-25120.

Kay MA, Liu D, Hoogerbrugge PM (1997). Gene therapy. *Proc Natl Acad Sci U S A*, **94:** 12744-12746.

Keegan AD, Nelms K, White M, Wang LM, Pierce JH, Paul WE (1994). An IL-4 receptor region containing an insulin receptor motif is important for IL-4-mediated IRS-1 phosphorylation and cell growth. *Cell*, **76:** 811-820.

Kim YH, Choi KH, Park JW, Kwon TK (2005). LY294002 inhibits LPS-induced NO production through a inhibition of NF-κB activation: independent mechanism of phosphatidylinositol 3-kinase. *Immunol Lett*, **99:** 45–50.

Kips JC (2001). Cytokines in asthma. *Eur Respir J Suppl*, **34:** 24s-33s.

Kips JC, O'Connor BJ, Langley SJ, Woodcock A, Kerstjens HA, Postma DS, Danzig M, Cuss F, Pauwels RA (2003). Effect of SCH55700, a humanized anti-human interleukin-5 antibody, in severe persistent asthma: a pilot study. *Am J Respir Crit Care Med*, **167:** 1655-1659.

Klasen S, Hammermann R, Fuhrmann M, Lindemann D, Beck KF, Pfeilschifter J, Racke K (2001). Glucocorticoids inhibit lipopolysaccharide-induced up-regulation of arginase in rat alveolar macrophages. *Br J Pharmacol*, **132:** 1349-1357.

Klingmuller U, Lorenz U, Cantley LC, Neel BG, Lodish HF (1995). Specific recruitment of SH-PTP1 to the erythropoietin receptor causes inactivation of JAK2 and termination of proliferative signals. *Cell*, **80:** 729-738.

Kobayashi S, Kitazawa T, Somlyo AV, Somlyo AP (1989). Cytosolic heparin inhibits muscarinic and alpha-adrenergic Ca2+ release in smooth muscle. Physiological role of inositol 1,4,5-trisphosphate in pharmacomechanical coupling. *J Biol Chem*, **264:** 17997-18004.

Koch S, Pohl P, Cobet U, Rainov NG (2000). Ultrasound enhancement of liposome-mediated cell transfection is caused by cavitation effects. *Ultrasound Med Biol*, **26:** 897-903.

Kolb M, Martin G, Medina M, Ask K, Gauldie J (2006). Gene therapy for pulmonary diseases. *Chest*, **130:** 879-884.

Kondo M, Tamaoki J, Takeyama K, Nakata J, Nagai A (2002). Interleukin-13 induces goblet cell differentiation in primary cell culture from guinea pig tracheal epithelium. *Am J Respir Cell Mol Biol*, **27:** 536-541.

Kong D, Yamori T, (2008). Phosphatidylinositol 3-kinase inhibitors: promising drug candidates for cancer therapy. *Cancer Sci*, **99:** 1734-1740.

Konstantinidis AK, Barton SJ, Sayers I, Yang IA, Lordan JL, Rorke S, Clough JB, Holgate ST, Holloway JW (2007). Genetic association studies of interleukin-13 receptor alpha1 subunit gene polymorphisms in asthma and atopy. *Eur Respir J*, **30:** 40-47.

Korst RJ, Bewig B, Crystal RG (1995). In vitro and in vivo transfer and expression of human surfactant SP-A- and SP-B-associated protein cDNAs mediated by replication-deficient, recombinant adenoviral vectors. *Hum Gene Ther*, **6:** 277-287.

Koto H, Mak JC, Haddad EB, Xu WB, Salmon M, Barnes PJ, Chung KF (1996). Mechanisms of impaired beta-adrenoceptor-induced airway relaxation by interleukin-1beta in vivo in the rat. *J Clin Invest*, **98:** 1780-1787.

Koyasu S (2003). The role of PI3K in immune cells. *Nat Immunol*, **4:** 313-319.

Kroegel C, Julius P, Matthys H, Virchow JC, Jr., Luttmann W (1996). Endobronchial secretion of interleukin-13 following local allergen challenge in atopic asthma: relationship to interleukin-4 and eosinophil counts. *Eur Respir J*, **9:** 899-904.

Krugmann S, Hawkins PT, Pryer N, Braselmann S (1999). Characterizing the interactions between the two subunits of the p101/p110gamma phosphoinositide 3-kinase and their role in the activation of this enzyme by G beta gamma subunits. *J Biol Chem*, **274:** 17152-17158.

Krymskaya VP, Ammit AJ, Hoffman RK, Eszterhas AJ, Panettieri RA, Jr. (2001). Activation of class IA PI3K stimulates DNA synthesis in human airway smooth muscle cells. *Am J Physiol Lung Cell Mol Physiol*, **280:** L1009-L1018.

Kueppers F (1973). Alpha1-antitrypsin. *Am J Hum Genet*, **25:** 677-686.

Kumar RK, Herbert C, Yang M, Koskinen AML, McKenzie ANJ, Foster PS (2002). Role of interleukin-13 in eosinophil accumulation and airway remodelling in a mouse model of chronic asthma. *Clin Exp Allergy*, **32:** 1104-1111.

Kuperman D, Schofield B, Wills-Karp M, Grusby MJ (1998). Signal transducer and activator of transcription factor 6 (Stat6)-deficient mice are protected from antigen-induced airway hyperresponsiveness and mucus production. *J Exp Med*, **187:** 939-948.

Kuperman DA, Huang XZ, Koth LL, Chang GH, Dolganov GM, Zhu Z, Elias JA, Sheppard D, Erle DJ (2002). Direct effects of interleukin-13 on epithelial cells cause airway hyperreactivity and mucus overproduction in asthma. *Nat Med*, **8:** 885-889.

Kwak YG, Song CH, Yi HK, Hwang PH, Kim JS, Lee KS, Lee YC (2003). Involvement of PTEN in airway hyperresponsiveness and inflammation in bronchial asthma. *J Clin Invest*, **111:** 1083-1092.

Lanone S, Zheng T, Zhu Z, Liu W, Lee CG, Ma B, Chen QS, Homer RJ, Wang JM, Rabach LA, Rabach ME, Shipley JM, Shapiro SD, Senior RM, Elias JA (2002). Overlapping and enzyme-specific contributions of matrix metalloproteinases-9 and-12 in IL-13-induced inflammation and remodeling. *J Clin Invest*, **110:** 463-474.

Laoukili J, Perret E, Willems T, Minty A, Parthoens E, Houcine O, Coste A, Jorissen M, Marano F, Caput D, Tournier F (2001). IL-13 alters mucociliary differentiation and ciliary beating of human respiratory epithelial cells. *J Clin Invest*, **108:** 1817-1824.

Laporte JC, Moore PE, Baraldo S, Jouvin MH, Church TL, Schwartzman IN, Panettieri RA, Kinet JP, Shore SA (2001). Direct effects of interleukin-13 on signaling pathways for physiological responses in cultured human airway smooth muscle cells. *Am J Respir Crit Care Med*, **164:** 141-148.

Leckie MJ, ten Brinke A, Khan J, Diamant Z, O'Connor BJ, Walls CM, Mathur AK, Cowley HC, Chung KF, Djukanovic R, Hansel TT, Holgate ST, Sterk PJ, Barnes PJ (2000). Effects of an interleukin-5 blocking monoclonal antibody on eosinophils, airway hyper-responsiveness, and the late asthmatic response. *Lancet,* **356:** 2144–2148.

Lee JH, Kaminski N, Dolganov G, Grunig G, Koth L, Solomon C, Erle DJ, Sheppard D (2001). Interleukin-13 induces dramatically different transcriptional programs in three human airway cell types. *Am J Respir Cell Mol Biol*, **25:** 474-485.

Lee KS, Lee HK, Hayflick JS, Lee YC, Puri KD (2006a). Inhibition of phosphoinositide 3-kinase delta attenuates allergic airway inflammation and hyperresponsiveness in murine asthma model. *FASEB J*, **20:** 455-465.

Lee KS, Park SJ, Kim SR, Min KH, Jin SM, Puri KD, Lee YC (2006b). Phosphoinositide 3-kinase-delta inhibitor reduces vascular permeability in a murine model of asthma. *J Allergy Clin Immunol*, **118:** 403-409.

Leonard WJ, Lin JX (2000). Cytokine receptor signaling pathways. *J Allergy Clin Immunol*, **105:** 877-888.

Lesh RE, Somlyo AP, Owens GK, Somlyo AV (1995). Reversible permeabilization. A novel technique for the intracellular introduction of antisense oligodeoxynucleotides into intact smooth muscle. *Circ Res*, **77:** 220-230.

Leung RK, Whittaker PA (2005). RNA interference: from gene silencing to gene-specific therapeutics. *Pharmacol Ther*, **107:** 222-239.

Levy F, Kristofic C, Heusser C, Brinkmann V (1997). Role of IL-13 in CD4 T cell-dependent IgE production in atopy. *Int Arch Allergy Immunol*, **112:** 49-58.

Li S, Tseng WC, Stolz DB, Wu SP, Watkins SC, Huang L (1999). Dynamic changes in the characteristics of cationic lipidic vectors after exposure to mouse serum: implications for intravenous lipofection. *Gene Ther*, **6:** 585-594.

Li Z, Jiang H, Xie W, Zhang Z, Smrcka AV, Wu D (2000). Roles of PLC-beta2 and -beta3 and PI3Kgamma in chemoattractant-mediated signal transduction. *Science*, **287:** 1046-1049.

Lindemann D, Racke K (2003). Glucocorticoid inhibition of interleukin-4 (IL-4) and interleukin-13 (IL-13) induced up-regulation of arginase in rat airway fibroblasts. *Naunyn Schmiedebergs Arch Pharmacol*, **368:** 546-550.

Liu F, Song Y, Liu D (1999). Hydrodynamics-based transfection in animals by systemic administration of plasmid DNA. *Gene Ther*, **6:** 1258-1266.

Liu XS, Xu YJ, Zhang ZX, Li CQ, Yang DL, Zhang N, Ni W (2003). Isoprenaline and aminophylline relax bronchial smooth muscle by cAMP-induced stimulation of large-conductance Ca2+-activated K+ channels. *Acta Pharmacol Sin*, **24:** 408-414.

Lively TN, Kossen K, Balhorn A, Koya T, Zinnen S, Takeda K, Lucas JJ, Polisky B, Richards IM, Gelfand EW (2008). Effect of chemically modified IL-13 short interfering RNA on development of airway hyperresponsiveness in mice. *J Allergy Clin Immunol*, **121:** 88-94.

Lopez AD, Murray CC (1998). The global burden of disease, 1990-2020. *Nat Med*, **4:** 1241-1243.

Lordan JL, Bucchieri F, Richter A, Konstantinidis A, Holloway JW, Thornber M, Puddicombe SM, Buchanan D, Wilson SJ, Djukanovic R, Holgate ST, Davies DE (2002). Cooperative effects of Th2 cytokines and allergen on normal and asthmatic bronchial epithelial cells. *J Immunol*, **169:** 407-414.

Louis CA, Reichner JS, Henry WL, Jr., Mastrofrancesco B, Gotoh T, Mori M, Albina JE (1998). Distinct arginase isoforms expressed in primary and transformed macrophages: regulation by oxygen tension. *Am J Physiol*, **274:** R775-R782.

Loyaga-Rendon RY, Sakamoto S, Beppu M, Aso T, Ishizaka M, Takahashi R, Azuma H (2005). Accumulated endogenous nitric oxide synthase inhibitors, enhanced arginase activity, attenuated dimethylarginine dimethylaminohydrolase activity and intimal hyperplasia in premenopausal human uterine arteries. *Atherosclerosis*, **178:** 231-239.

Maarsingh H, Zaagsma J, Meurs H (2008a). Arginine homeostasis in allergic asthma. *Eur J Pharmacol*, **585:** 375-384.

Maarsingh H, Zuidhof AB, Bos IS, van DM, Boucher JL, Zaagsma J, Meurs H (2008b). Arginase inhibition protects against allergen-induced airway obstruction, hyperresponsiveness, and inflammation. *Am J Respir Crit Care Med*, **178:** 565-573.

Macgregor G, Gray RD, Hilliard TN, Imrie M, Boyd AC, Alton EW, Bush A, Davies JC, Innes JA, Porteous DJ, Greening AP (2008). Biomarkers for cystic fibrosis lung disease: Application of SELDI-TOF mass spectrometry to BAL fluid. *J Cyst Fibros*, **7:** 352-358.

MacKinnon AC, Farnworth SL, Hodkinson PS, Henderson NC, Atkinson KM, Leffler H, Nilsson UJ, Haslett C, Forbes SJ, Sethi T (2008). Regulation of alternative macrophage activation by galectin-3. *J Immunol*, **180:** 2650-2658.

Maguire AM, Simonelli F, Pierce EA, Pugh EN, Jr., Mingozzi F, Bennicelli J, Banfi S, Marshall KA, Testa F, Surace EM, Rossi S, Lyubarsky A, Arruda VR, Konkle B, Stone E, Sun J, Jacobs J, Dell'Osso L, Hertle R, Ma JX, Redmond TM, Zhu X, Hauck B, Zelenaia O, Shindler KS, Maguire MG, Wright JF, Volpe NJ, McDonnell JW, Auricchio A, High KA, Bennett J (2008). Safety and efficacy of gene transfer for Leber's congenital amaurosis. *N Engl J Med*, **358:** 2240-2248.

Mamoon AM, Baker RC, Farley JM (2001). Activation of phospholipase D in porcine tracheal smooth muscle: role of phosphatidylinositol 3-kinase and RhoA activation. *Eur J Pharmacol*, **433:** 7-16.

Marone R, Cmiljanovic V, Giese B, Wymann MP (2008). Targeting phosphoinositide 3-kinase: moving towards therapy. *Biochim Biophys Acta*, **1784:** 159-185.

Martin JG, Duguet A, Eidelman DH (2000). The contribution of airway smooth muscle to airway narrowing and airway hyperresponsiveness in disease. *Eur Respir J*, **16:** 349-354.

Martin TF (2001). PI(4,5)P(2) regulation of surface membrane traffic. *Curr Opin Cell Biol*, **13:** 493-499.

Masoli M, Fabian D, Holt S, Beasley R (2004). The global burden of asthma: executive summary of the GINA Dissemination Committee report. *Allergy*, **59:** 469-478.

Mattes J, Yang M, Mahalingam S, Kuehr J, Webb DC, Simson L, Hogan SP, Koskinen A, McKenzie AN, Dent LA, Rothenberg ME, Matthaei KI, Young IG, Foster PS (2002). Intrinsic defect in T cell production of interleukin (IL)-13 in the absence of both IL-5 and eotaxin precludes the development of eosinophilia and airways hyperreactivity in experimental asthma. *J Exp Med*, **195:** 1433-1444.

McAnulty RJ (2007). Fibroblasts and myofibroblasts: their source, function and role in disease. *Int J Biochem Cell Biol*, **39:** 666-671.

McAnulty RJ, Campa JS, Cambrey AD, Laurent GJ (1991). The effect of transforming growth factor beta on rates of procollagen synthesis and degradation in vitro. *Biochim Biophys Acta*, **1091:** 231-235.

McKenzie AN, Culpepper JA, de Waal MR, Briere F, Punnonen J, Aversa G, Sato A, Dang W, Cocks BG, Menon S, (1993a). Interleukin 13, a T-cell-derived cytokine that regulates human monocyte and B-cell function. *Proc Natl Acad Sci U S A*, **90:** 3735-3739.

McKenzie AN, Li X, Largaespada DA, Sato A, Kaneda A, Zurawski SM, Doyle EL, Milatovich A, Francke U, Copeland NG, (1993b). Structural comparison and chromosomal localization of the human and mouse IL-13 genes. *J Immunol*, **150:** 5436-5444.

Medina-Tato DA, Ward SG, Watson ML (2007). Phosphoinositide 3-kinase signalling in lung disease: leucocytes and beyond. *Immunology*, **121:** 448-461.

Medina-Tato DA, Watson ML, Ward SG (2006). Leukocyte navigation mechanisms as targets in airway diseases. *Drug Discov Today*, **11:** 866-879.

Messeri D, Hammermann R, Mossner J, Gothert M, Racke K (2000). In rat alveolar macrophages lipopolysaccharides exert divergent effects on the transport of the cationic amino acids L-arginine and L-ornithine. *Naunyn Schmiedebergs Arch Pharmacol*, **361:** 621-628.

Meurs H, Maarsingh H, Zaagsma J (2003). Arginase and asthma: novel insights into nitric oxide homeostasis and airway hyperresponsiveness. *Trends Pharmacol Sci*, **24:** 450-455.

Meurs H, Mckay S, Maarsingh H, Hamer MAM, Macic L, Molendijk N, Zaagsma J (2002). Increased arginase activity underlies allergen-induced deficiency of cNOS-derived nitric oxide and airway hyperresponsiveness. *Br J Pharmacol*, **136:** 391-398.

Meyer KB, Thompson MM, Levy MY, Barron LG, Szoka FC, Jr. (1995). Intratracheal gene delivery to the mouse airway: characterization of plasmid DNA expression and pharmacokinetics. *Gene Ther*, **2:** 450-460.

Meyts I, Hellings PW, Hens G, Vanaudenaerde BM, Verbinnen B, Heremans H, Matthys P, Bullens DM, Overbergh L, Mathieu C, De BK, Ceuppens JL (2006). IL-12 contributes to allergen-induced airway inflammation in experimental asthma. *J Immunol*, **177:** 6460-6470.

Minty A, Chalon P, Derocq JM, Dumont X, Guillemot JC, Kaghad M, Labit C, Leplatois P, Liauzun P, Miloux B, (1993). Interleukin-13 is a new human lymphokine regulating inflammatory and immune responses. *Nature*, **362:** 248-250.

Minty AJ (1997). Interleukin-13. In: Remick DG & Friedland JS (ed). *Cytokines in health and disease.* Marcel Dekker: NewYork, pp 185-197.

Misson J, Clark W, Kendall MJ (1999). Therapeutic advances: leukotriene antagonists for the treatment of asthma. *J Clin Pharm Ther*, **24:** 17-22.

Mitchell DA, Nair SK (2000). RNA-transfected dendritic cells in cancer immunotherapy. *J Clin Invest*, **106:** 1065-1069.

Modolell M, Corraliza IM, Link F, Soler G, Eichmann K (1995). Reciprocal regulation of the nitric oxide synthase/arginase balance in mouse bone marrow-derived macrophages by TH1 and TH2 cytokines. *Eur J Immunol*, **25:** 1101-1104.

Moffatt JD, Cocks TM, Page CP (2004). Role of the epithelium and acetylcholine in mediating the contraction to 5-hydroxytryptamine in the mouse isolated trachea. *Br J Pharmacol*, **141:** 1159-1166.

Molnar MJ, Gilbert R, Lu Y, Liu AB, Guo A, Larochelle N, Orlopp K, Lochmuller H, Petrof BJ, Nalbantoglu J, Karpati G (2004). Factors influencing the efficacy, longevity, and safety of electroporation-assisted plasmid-based gene transfer into mouse muscles. *Mol Ther*, **10:** 447-455.

Monick MM, Robeff PK, Butler NS, Flaherty DM, Carter AB, Peterson MW, Hunninghake GW (2002). Phosphatidylinositol 3-kinase activity negatively regulates stability of cyclooxygenase 2 mRNA. *J Biol Chem*, **277:** 32992-33000.

Morgan JG, Dolganov GM, Robbins SE, Hinton LM, Lovett M (1992). The selective isolation of novel cDNAs encoded by the regions surrounding the human interleukin 4 and 5 genes. *Nucleic Acids Res*, **20:** 5173-5179.

Morgan JP, DeFeo TT, Morgan KG (1984). A chemical procedure for loading the calcium indicator acquorin into mammalian working myocardium. *Pflugers Arch*, **400:** 338-340.

Morris SM, Jr. (2002). Regulation of enzymes of the urea cycle and arginine metabolism. *Annu Rev Nutr*, **22:** 87-105.

Morris SM, Bhamidipati D, KepkaLenhart D (1997). Human type II arginase: Sequence analysis and tissue-specific expression. *Gene*, **193:** 157-161.

Morse B, Sypek JP, Donaldson DD, Haley KJ, Lilly CM (2002). Effects of IL-13 on airway responses in the guinea pig. *Am J Physiol Lung Cell Mol Physiol*, **282:** L44-L49.

Mosmann T (1983). Rapid colorimetric assay for cellular growth and survival - application to proliferation and cytotoxicity assays. *J Immunol Methods*, **65:** 55-63.

Multhaupt H, Fritz P, Schumacher K (1987). Immunohistochemical localisation of arginase in human liver using monoclonal antibodies against human liver arginase. *Histochemistry*, **87:** 465-470.

Munder M, Eichmann K, Moran JM, Centeno F, Soler G, Modolell M (1999). Th1/Th2-regulated expression of arginase isoforms in murine macrophages and dendritic cells. *J Immunol*, **163:** 3771-3777.

Munitz A, Brandt EB, Mingler M, Finkelman FD, Rothenberg ME (2008). Distinct roles for IL-13 and IL-4 via IL-13 receptor alpha1 and the type II IL-4 receptor in asthma pathogenesis. *Proc Natl Acad Sci U S A*, **105:** 7240-7245.

Myers MG, Jr., Wang LM, Sun XJ, Zhang Y, Yenush L, Schlessinger J, Pierce JH, White MF (1994). Role of IRS-1-GRB-2 complexes in insulin signaling. *Mol Cell Biol*, **14:** 3577-3587.

Nakanishi S, Kakita S, Takahashi I, Kawahara K, Tsukuda E, Sano T, Yamada K, Yoshida M, Kase H, Matsuda Y, . (1992). Wortmannin, a microbial product inhibitor of myosin light chain kinase. *J Biol Chem*, **267:** 2157-2163.

Nashed BF, Zhang TT, Al-Alwan M, Srinivasan G, Halayko AJ, Okkenhaug K, Vanhaesebroecks B, HayGlass KT, Marshall AJ (2007). Role of the phosphoinositide 3-kinase p110 delta in generation of type 2 cytokine responses and allergic airway inflammation. *Eur J Immunol*, **37:** 416-424.

Nelms K, Keegan AD, Zamorano J, Ryan JJ, Paul WE (1999). The IL-4 receptor: signaling mechanisms and biologic functions. *Annu Rev Immunol*, **17:** 701-738.

Niimi A, Matsumoto H, Takemura M, Ueda T, Chin K, Mishima M (2003). Relationship of airway wall thickness to airway sensitivity and airway reactivity in asthma. *Am J Respir Crit Care Med*, **168:** 983-988.

Northcott CA, Hayflick J, Watts SW (2005). Upregulated function of phosphatidylinositol-3-kinase in genetically hypertensive rats: A moderator of arterial hypercontractility. *Clin Exp Pharmacol Physiol*, **32:** 851-858.

O'Brien J, Lummis SC (2002). An improved method of preparing microcarriers for biolistic transfection. *Brain Res Brain Res Protoc*, **10:** 12-15.

O'Byrne PM, Inman MD (2003). Airway hyperresponsiveness. *Chest*, **123:** 411S-416S.

Obiri NI, Debinski W, Leonard WJ, Puri RK (1995). Receptor for interleukin 13. Interaction with interleukin 4 by a mechanism that does not involve the common gamma chain shared by receptors for interleukins 2, 4, 7, 9, and 15. *J Biol Chem*, **270:** 8797-8804.

Oddera S, Silvestri M, Penna R, Galeazzi G, Crimi E, Rossi GA (1998). Airway eosinophilic inflammation and bronchial hyperresponsiveness after allergen inhalation challenge in asthma. *Lung*, **176:** 237-247.

Ohshima M, Yokoyama A, Ohnishi H, Hamada H, Kohno N, Higaki J, Naka T (2007). Overexpression of suppressor of cytokine signalling-5 augments eosinophilic airway inflammation in mice. *Clin Exp Allergy*, **37:** 735-742.

Ohta Y, Hayashi M, Kanemaru T, Abe K, Ito Y, Oike M (2008). Dual modulation of airway smooth muscle contraction by Th2 cytokines via matrix metalloproteinase-1 production. *J Immunol*, **180:** 4191-4199.

Ohtake A, Takiguchi M, Shigeto Y, Amaya Y, Kawamoto S, Mori M (1988). Structural Organization of the Gene for Rat Liver-Type Arginase. *J Biol Chem*, **263:** 2245-2249.

Okkenhaug K, Bilancio A, Farjot G, Priddle H, Sancho S, Peskett E, Pearce W, Meek SE, Salpekar A, Waterfield MD, Smith AJH, Vanhaesebroeck B (2002). Impaired B and T cell antigen receptor signaling in p110 delta PI 3-kinase mutant mice. *Science*, **297:** 1031-1034.

Orie NG (2000). The Dutch hypothesis. *Chest*, **117:** 299S.

Oyoshi MK, Bryce P, Goya S, Pichavant M, Umetsu DT, Oettgen HC, Tsitsikov EN (2008). TNF receptor-associated factor 1 expressed in resident lung cells is required for the development of allergic lung inflammation. *J Immunol*, **180:** 1878-1885.

Parameswaran K, Janssen LJ, O'Byrne PM (2002). Airway hyperresponsiveness and calcium handling by smooth muscle: a "deeper look". *Chest*, **121:** 621-624.

Partridge MR (2007). Asthma: 1987-2007. What have we achieved and what are the persisting challenges? *Prim Care Respir J*, **16:** 145-148.

Pennings HJ, Kramer K, Bast A, Buurman WA, Wouters EF (1998). Tumour necrosis factor-alpha induces hyperreactivity in tracheal smooth muscle of the guinea-pig in vitro. *Eur Respir J*, **12:** 45-49.

Persengiev SP, Zhu X, Green MR (2004). Nonspecific, concentration-dependent stimulation and repression of mammalian gene expression by small interfering RNAs (siRNAs). *RNA*, **10:** 12-18.

Pierrot C, Beniguel L, Begue A, Khalife J (2001). Expression of a functional IL-13Ralpha1 by rat B cells. *Biochem Biophys Res Commun*, **287:** 969-976.

Pope SM, Brandt EB, Mishra A, Hogan SP, Zimmermann N, Matthaei KI, Foster PS, Rothenberg ME (2001). IL-13 induces eosinophil recruitment into the lung by an IL-5- and eotaxin-dependent mechanism. *J Allergy Clin Immunol*, **108:** 594-601.

Pope SM, Fulkerson PC, Blanchard C, Akei HS, Nikolaidis NM, Zimmermann N, Molkentin JD, Rothenberg ME (2005). Identification of a cooperative mechanism involving interleukin-13 and eotaxin-2 in experimental allergic lung inflammation. *J Biol Chem*, **280:** 13952-13961.

Prendergast CE, Morton MF, Figueroa KW, Wu X, Shankley NP (2006). Species-dependent smooth muscle contraction to Neuromedin U and determination of the receptor subtypes mediating contraction using NMU1 receptor knockout mice. *Br J Pharmacol*, **147:** 886-896.

Puddicombe SM, Torres-Lozano C, Richter A, Bucchieri F, Lordan JL, Howarth PH, Vrugt B, Albers R, Djukanovic R, Holgate ST, Wilson SJ, Davies DE (2003). Increased expression of p21(waf) cyclin-dependent kinase inhibitor in asthmatic bronchial epithelium. *Am J Respir Cell Mol Biol*, **28:** 61-68.

Pype JL, Xu H, Schuermans M, Dupont LJ, Wuyts W, Mak JC, Barnes PJ, Demedts MG, Verleden GM (2001). Mechanisms of interleukin 1beta-induced human airway smooth muscle hyporesponsiveness to histamine. Involvement of p38 MAPK NF-kappaB. *Am J Respir Crit Care Med*, **163:** 1010-1017.

Quan TE, Cowper S, Wu SP, Bockenstedt LK, Bucala R (2004). Circulating fibrocytes: collagen-secreting cells of the peripheral blood. *Int J Biochem Cell Biol*, **36:** 598-606.

Que LG, Kantrow SP, Jenkinson CP, Piantadosi CA, Huang YCT (1998). Induction of arginase isoforms in the lung during hyperoxia. *Am J Physiol Lung Cell Mol Physiol*, **19:** L96-L102.

Rameh LE, Cantley LC (1999). The role of phosphoinositide 3-kinase lipid products in cell function. *J Biol Chem*, **274:** 8347-8350.

Rauh MJ, Kalesnikoff J, Hughes M, Sly L, Lam V, Krystal G (2003). Role of Src homology 2-containing-inositol 5 '-phosphatase (SHIP) in mast cells and macrophages. *Biochem Soc Trans*, **31:** 286-291.

Reddel RR, Ke Y, Gerwin BI, McMenamin MG, Lechner JF, Su RT, Brash DE, Park JB, Rhim JS, Harris CC (1988). Transformation of human bronchial epithelial cells by infection with SV40 or adenovirus-12 SV40 hybrid virus, or transfection via strontium phosphate coprecipitation with a plasmid containing SV40 early region genes. *Cancer Res*, **48:** 1904-1909.

Rich DP, Anderson MP, Gregory RJ, Cheng SH, Paul S, Jefferson DM, McCann JD, Klinger KW, Smith AE, Welsh MJ (1990). Expression of cystic fibrosis transmembrane conductance regulator corrects defective chloride channel regulation in cystic fibrosis airway epithelial cells. *Nature*, **347:** 358-363.

Rippmann JF, Schnapp A, Weith A, Hobbie S (2005). Gene silencing with STAT6 specific siRNAs blocks eotaxin release in IL-4/TNFalpha stimulated human epithelial cells. *FEBS Lett*, **579:** 173-178.

Rogers DF (2004). Airway mucus hypersecretion in asthma: an undervalued pathology? *Curr Opin Pharmacol*, **4:** 241-250.

Ronchetti R, Villa MP, Barreto M, Rota R, Pagani J, Martella S, Falasca C, Paggi B, Guglielmi F, Ciofetta G (2001). Is the increase in childhood asthma coming to an end? Findings from three surveys of schoolchildren in Rome, Italy. *Eur Respir J*, **17:** 881-886.

Rosenberg SA, Restifo NP, Yang JC, Morgan RA, Dudley ME (2008). Adoptive cell transfer: a clinical path to effective cancer immunotherapy. *Nat Rev Cancer*, **8:** 299-308.

Rosenecker J, Naundorf S, Gersting SW, Hauck RW, Gessner A, Nicklaus P, Muller RH, Rudolph C (2003). Interaction of bronchoalveolar lavage fluid with polyplexes and lipoplexes: analysing the role of proteins and glycoproteins. *J Gene Med*, **5:** 49-60.

Rosenfeld MA, Siegfried W, Yoshimura K, Yoneyama K, Fukayama M, Stier LE, Paakko PK, Gilardi P, Stratford-Perricaudet LD, Perricaudet M, (1991). Adenovirus-mediated transfer of a recombinant alpha 1-antitrypsin gene to the lung epithelium in vivo. *Science*, **252:** 431-434.

Roy B, Bhattacharjee A, Xu B, Ford D, Maizel AL, Cathcart MK (2002). IL-13 signal transduction in human monocytes: phosphorylation of receptor components, association with Jaks, and phosphorylation/activation of Stats. *J Leukoc Biol*, **72:** 580-589.

Russell JA (1978). Responses of isolated canine airways to electric stimulation and acetylcholine. *J Appl Physiol*, **45:** 690-698.

Sakai H, Otogoto S, Chiba Y, Abe K, Misawa M (2004). TNF-alpha augments the expression of RhoA in the rat bronchus. *J Smooth Muscle Res*, **40:** 25-34.

Sakai K, Suzuki H, Oda H, Akaike T, Azuma Y, Murakami T, Sugi K, Ito T, Ichinose H, Koyasu S, Shirai M (2006). Phosphoinositide 3-kinase in nitric oxide synthesis in macrophage - Critical dimerization of inducible nitric-oxide synthase. *J Biol Chem*, **281:** 17736-17742.

Salagianni M, Wong KL, Thomas MJ, Noble A, Kemeny DM (2007). An essential role for IL-18 in CD8 T cell-mediated suppression of IgE responses. *J Immunol*, **178:** 4771-4778.

Sasaki T, Irie-Sasaki J, Horie Y, Bachmaier K, Fata JE, Li M, Suzuki A, Bouchard D, Ho A, Redston M, Gallinger S, Khokha R, Mak TW, Hawkins PT, Stephens L, Scherer SW, Tsao M, Penninger JM (2000). Colorectal carcinomas in mice lacking the catalytic subunit of PI(3)Kgamma. *Nature*, **406:** 897-902.

Scalzi JM, Hozier JC (1998). Comparative genome mapping: mouse and rat homologies revealed by fluorescence in situ hybridization. *Genomics*, **47:** 44-51.

Schaafsma D, McNeill KD, Stelmack GL, Gosens R, Baarsma HA, Dekkers BGJ, Frohwerk E, Penninks JM, Sharma P, Ens KM, Nelemans SA, Zaagsma J, Halayko AJ, Meurs H (2007). Insulin increases the expression of contractile phenotypic markers in airway smooth muscle. *Am J Physiol Cell Physiol*, **293:** C429-C439.

Schu PV, Takegawa K, Fry MJ, Stack JH, Waterfield MD, Emr SD (1993). Phosphatidylinositol 3-kinase encoded by yeast VPS34 gene essential for protein sorting. *Science*, **260:** 88-91.

Shao MX, Nakanaga T, Nadel JA (2004). Cigarette smoke induces MUC5AC mucin overproduction via tumor necrosis factor-alpha-converting enzyme in human airway epithelial (NCI-H292) cells. *Am J Physiol Lung Cell Mol Physiol*, **287:** L420-L427.

Shore SA, Moore PE (2002). Effects of cytokines on contractile and dilator responses of airway smooth muscle. *Clin Exp Pharmacol Physiol*, **29:** 859-866.

Siddiqui S, Sutcliffe A, Shikotra A, Woodman L, Doe C, McKenna S, Wardlaw A, Bradding P, Pavord I, Brightling C (2007). Vascular remodeling is a feature of asthma and nonasthmatic eosinophilic bronchitis. *J Allergy Clin Immunol*, **120:** 813-819.

Simberg D, Weisman S, Talmon Y, Faerman A, Shoshani T, Barenholz Y (2003). The role of organ vascularization and lipoplex-serum initial contact in intravenous murine lipofection. *J Biol Chem*, **278:** 39858-39865.

Sledz CA, Holko M, de Veer MJ, Silverman RH, Williams BR (2003). Activation of the interferon system by short-interfering RNAs. *Nat Cell Biol*, **5:** 834-839.

Sluiter HJ, Koeter GH, de Monchy JG, Postma DS, de VK, Orie NG (1991). The Dutch hypothesis (chronic non-specific lung disease) revisited. *Eur Respir J*, **4:** 479-489.

Smolock EM, Wang T, Nolt JK, Moreland RS (2007). siRNA knock down of casein kinase 2 increases force and cross-bridge cycling rates in vascular smooth muscle. *Am J Physiol Cell Physiol*, **292:** C876-C885.

Sonoki T, Nagasaki A, Gotoh T, Takiguchi M, Takeya M, Matsuzaki H, Mori M (1997). Coinduction of nitric-oxide synthase and arginase I in cultured rat peritoneal macrophages and rat tissues in vivo by lipopolysaccharide. *J Biol Chem*, **272:** 3689-3693.

Sparkes RS, Dizikes GJ, Klisak I, Grody WW, Mohandas T, Heinzmann C, Zollman S, Lusis AJ, Cederbaum SD (1986). The gene for human liver arginase (ARG1) is assigned to chromosome band 6q23. *Am J Hum Genet*, **39:** 186-193.

Spina D, Page CP (1992). The pharmacology of the respiratory epithelium. *Pharmacol Res*, **26:** 17-32.

Spina D, Shah S, Harrison S (1998). Modulation of sensory nerve function in the airways. *Trends Pharmacol Sci*, **19:** 460-466.

Stahl N, Farruggella TJ, Boulton TG, Zhong Z, Darnell JE, Jr., Yancopoulos GD (1995). Choice of STATs and other substrates specified by modular tyrosine-based motifs in cytokine receptors. *Science*, **267:** 1349-1353.

Steinberg TH, Newman AS, Swanson JA, Silverstein SC (1987). ATP^{4-} permeabilizes the plasma membrane of mouse macrophages to fluorescent dyes. *J Biol Chem*, **262:** 8884-8888.

Stephens LR, Eguinoa A, Erdjument-Bromage H, Lui M, Cooke F, Coadwell J, Smrcka AS, Thelen M, Cadwallader K, Tempst P, Hawkins PT (1997). The G beta gamma sensitivity of a PI3K is dependent upon a tightly associated adaptor, p101. *Cell*, **89:** 105-114.

Sterk PJ, Bel EH (1989). Bronchial Hyperresponsiveness - the Need for A Distinction Between Hypersensitivity and Excessive Airway Narrowing. *Eur Respir J*, **2:** 267-274.

Stirling RG, Chung KF (2001). Severe asthma: definition and mechanisms. *Allergy*, **56:** 825-840.

Stokoe D (2005). The phosphoinositide 3-kinase pathway and cancer. *Expert Rev Mol Med*, **7:** 1-22.

Stoyanov B, Volinia S, Hanck T, Rubio I, Loubtchenkov M, Malek D, Stoyanova S, Vanhaesebroeck B, Dhand R, Nurnberg B, . (1995). Cloning and characterization of a G protein-activated human phosphoinositide-3 kinase. *Science*, **269:** 690-693.

Suh BC, Hille B (2005). Regulation of ion channels by phosphatidylinositol 4,5-bisphosphate. *Curr Opin Neurobiol*, **15:** 370-378.

Suire S, Condliffe AM, Ferguson GJ, Ellson CD, Guillou H, Davidson K, Welch H, Coadwell J, Turner M, Chilvers ER, Hawkins PT, Stephens L (2006). Gbetagammas and the Ras binding domain of p110gamma are both important regulators of PI(3)Kgamma signalling in neutrophils. *Nat Cell Biol*, **8:** 1303-1309.

Syed F, Panettieri RA, Tliba O, Huang C, Li K, Bracht M, Amegadzie B, Griswold D, Li L, Amrani Y (2005). The effect of IL-13 and IL-13R130Q, a naturally occurring IL-13 polymorphism, on the gene expression of human airway smooth muscle cells. *Respir Res*, **6**.

Takeda K, Kamanaka M, Tanaka T, Kishimoto T, Akira S (1996). Impaired IL-13-mediated functions of macrophages in STAT6-deficient mice. *J Immunol*, **157:** 3220-3222.

Takemoto K, Ogino K, Shibamori M, Gondo T, Hitomi Y, Takigawa T, Wang DH, Takaki J, Ichimura H, Fujikura Y, Ishiyama H (2007). Transiently, paralleled upregulation of arginase and nitric oxide synthase and the effect of both enzymes on the pathology of asthma. *Am J Physiol Lung Cell Mol Physiol*, **293:** L1419-L1426.

Tanaka M, Nyce JW (2001). Respirable antisense oligonucleotides: a new drug class for respiratory disease. *Respir Res*, **2:** 5-9.

Tang F, Hughes JA (1999). Use of dithiodiglycolic acid as a tether for cationic lipids decreases the cytotoxicity and increases transgene expression of plasmid DNA in vitro. *Bioconjug Chem*, **10:** 791-796.

Tarazona-Santos E, Tishkoff SA (2005). Divergent patterns of linkage disequilibrium and haplotype structure across global populations at the interleukin-13 (IL13) locus. *Genes Immun*, **6:** 53-65.

Temann UA, Laouar Y, Eynon EE, Homer R, Flavell RA (2007). IL9 leads to airway inflammation by inducing IL13 expression in airway epithelial cells. *Int Immunol*, **19:** 1-10.

Templeton NS, Lasic DD, Frederik PM, Strey HH, Roberts DD, Pavlakis GN (1997). Improved DNA: liposome complexes for increased systemic delivery and gene expression. *Nat Biotechnol*, **15:** 647-652.

Thierry AR, Lunardi-Iskandar Y, Bryant JL, Rabinovich P, Gallo RC, Mahan LC (1995). Systemic gene therapy: biodistribution and long-term expression of a transgene in mice. *Proc Natl Acad Sci U S A*, **92:** 9742-9746.

Thomas MJ, Noble A, Sawicka E, Askenase PW, Kemeny DM (2002). CD8 T cells inhibit IgE via dendritic cell IL-12 induction that promotes Th1 T cell counter-regulation. *J Immunol*, **168:** 216-223.

Tliba O, Deshpande D, Chen H, Van Besien C, Kannan M, Panettieri RA, Amrani Y (2003). IL-13 enhances agonist-evoked calcium signals and contractile responses in airway smooth muscle. *Br J Pharmacol*, **140:** 1159-1162.

Tolloczko B, Turkewitsch P, Al Chalabi M, Martin JG (2004). LY-294002 [2-(4-morpholinyl)-8-phenyl-4H-1-benzopyran-4-one] affects calcium signaling in airway smooth muscle cells independently of phosphoinositide 3-kinase inhibition. *J Pharmacol Exp Ther,* **311:** 787–793.

Tousignant JD, Zhao H, Yew NS, Cheng SH, Eastman SJ, Scheule RK (2003). DNA sequences in cationic lipid:pDNA-mediated systemic toxicities. *Hum Gene Ther*, **14:** 203-214.

Truong-Le VL, Walsh SM, Schweibert E, Mao HQ, Guggino WB, August JT, Leong KW (1999). Gene transfer by DNA-gelatin nanospheres. *Arch Biochem Biophys*, **361:** 47-56.

Turner SJ, Domin J, Waterfield MD, Ward SG, Westwick J (1998). The CC chemokine monocyte chemotactic peptide-1 activates both the class I p85/p110 phosphatidylinositol 3-kinase and the class II PI3K-C2alpha. *J Biol Chem*, **273:** 25987-25995.

Ulrik CS, Backer V (1999). Nonreversible airflow obstruction in life-long nonsmokers with moderate to severe asthma. *Eur Respir J*, **14:** 892-896.

Usacheva A, Sandoval R, Domanski P, Kotenko SV, Nelms K, Goldsmith MA, Colamonici OR.(2002). Contribution of the Box 1 and Box 2 motifs of cytokine receptors to Jak1 association and activation. *J Biol Chem,* **277:** 48220-48226

van der Pouw Kraan TC, van VA, Boeije LC, van Tuyl SA, de Groot ER, Stapel SO, Bakker A, Verweij CL, Aarden LA, van der Zee JS (1999). An IL-13 promoter polymorphism associated with increased risk of allergic asthma. *Genes Immun*, **1:** 61-65.

Van Schoor J, Pauwels R, Joos G (2005). Indirect bronchial hyper-responsiveness: the coming of age of a specific group of bronchial challenges. *Clin Exp Allergy*, **35:** 250-261.

Van d, V, Joos G (1998). Regionally different influence of contractile agonists on isolated rat airway segments. *Respir Physiol*, **112:** 185-194.

Vanhaesebroeck B, Leevers SJ, Ahmadi K, Timms J, Katso R, Driscoll PC, Woscholski R, Parker PJ, Waterfield MD (2001). Synthesis and function of 3-phosphorylated inositol lipids. *Annu Rev Biochem*, **70:** 535-602.

Wakabayashi Y, Yamada E, Yoshida T, Takahashi H (1994). Arginine becomes an essential amino acid after massive resection of rat small intestine. *J Biol Chem*, **269:** 32667-32671.

Walker JK, Gainetdinov RR, Feldman DS, McFawn PK, Caron MG, Lefkowitz RJ, Premont RT, Fisher JT (2004). G protein-coupled receptor kinase 5 regulates airway responses induced by muscarinic receptor activation. *Am J Physiol Lung Cell Mol Physiol*, **286:** L312-L319.

Walter DM, McIntire JJ, Berry G, McKenzie ANJ, Donaldson DD, DeKruyff RH, Umetsu DT (2001). Critical role for IL-13 in the development of allergen-induced airway hyperreactivity. *J Immunol*, **167:** 4668-4675.

Wang WW, Jenkinson CP, Griscavage JM, Kern RM, Arabolos NS, Byrns RE, Cederbaum SD, Ignarro LJ (1995). Co-induction of arginase and nitric oxide synthase in murine macrophages activated by lipopolysaccharide. *Biochem Biophys Res Commun*, **210:** 1009-1016.

Wang Z, Zheng T, Zhu Z, Homer RJ, Riese RJ, Chapman HA, Jr., Shapiro SD, Elias JA (2000). Interferon gamma induction of pulmonary emphysema in the adult murine lung. *J Exp Med*, **192:** 1587-1600.

Ward SG, Finan P (2003). Isoform-specific phosphoinositide 3-kinase inhibitors as therapeutic agents. *Curr Opin Pharmacol*, **3:** 426-434.

Watson ML, White AM, Campbell EM, Smith AW, Uddin J, Yoshimura T, Westwick J (1999). Anti-inflammatory actions of interleukin-13 - Suppression of tumor necrosis factor-alpha and antigen-induced leukocyte accumulation in the guinea pig lung. *Am J Respir Cell Mol Biol*, **20:** 1007-1012.

Wei LH, Jacobs AT, Morris SM, Ignarro LJ (2000). IL-4 and IL-13 upregulate arginase I expression by cAMP and JAK/STAT6 pathways in vascular smooth muscle cells. *Am J Physiol Cell Physiol*, **279:** C248-C256.

Welte T, Groneberg DA (2006). Asthma and COPD. *Exp Toxicol Pathol*, **57:** 35-40.

Wenk MR, De CP (2004). Protein-lipid interactions and phosphoinositide metabolism in membrane traffic: insights from vesicle recycling in nerve terminals. *Proc Natl Acad Sci U S A*, **101:** 8262-8269.

Wenzel SE, Trudeau JB, Barnes S, Zhou X, Cundall M, Westcott JY, McCord K, Chu HW (2002). TGF-beta and IL-13 synergistically increase eotaxin-1 production in human airway fibroblasts. *J Immunol*, **169:** 4613-4619.

White MF (1985). The transport of cationic amino acids across the plasma membrane of mammalian cells. *Biochim Biophys Acta*, **822:** 355-374.

White MF (1998). The IRS-signaling system: a network of docking proteins that mediate insulin and cytokine action. *Recent Prog Horm Res*, **53:** 119-138.

Wills-Karp M (2004). Interleukin-13 in asthma pathogenesis. *Immunol Rev*, **202:** 175-190.

Wills-Karp M, Chiaramonte M (2003). Interleukin-13 in asthma. *Curr Opin Pulm Med*, **9:** 21-27.

Wills-Karp M, Luyimbazi J, Xu XY, Schofield B, Neben TY, Karp CL, Donaldson DD (1998). Interleukin-13: Central mediator of allergic asthma. *Science*, **282:** 2258-2261.

Wills-Karp M, Uchida Y, Lee JY, Jinot J, Hirata A, Hirata F (1993). Organ culture with proinflammatory cytokines reproduces impairment of the beta-adrenoceptor-mediated relaxation in tracheas of a guinea pig antigen model. *Am J Respir Cell Mol Biol*, **8:** 153-159.

Woolcock AJ, Salome CM, Yan K (1984). The shape of the dose-response curve to histamine in asthmatic and normal subjects. *Am Rev Respir Dis*, **130:** 71-75.

Wright K, Ward SG, Kolios G, Westwick J (1997). Activation of phosphatidylinositol δ-kinase by interleukin-13 - An inhibitory signal for inducible nitric-oxide synthase expression in epithelial, cell line HT-29. *J Biol Chem*, **272:** 12626-12633.

Wu AH, Low WC (2002). Molecular cloning of the rat IL-13 alpha 2 receptor cDNA and its expression in rat tissues. *J Neurooncol*, **59:** 99-105.

Wu C, Yang G, Bermudez-Humaran LG, Pang Q, Zeng Y, Wang J, Gao X (2006). Immunomodulatory effects of IL-12 secreted by Lactococcus lactis on Th1/Th2 balance in ovalbumin (OVA)-induced asthma model mice. *Int Immunopharmacol*, **6:** 610-615.

Wu GY, Morris SM (1998). Arginine metabolism: nitric oxide and beyond. *Biochem J*, **336:** 1-17.

Wynn TA (2003). IL-13 effector functions. *Annu Rev Immunol*, **21:** 425-456.

Yang GY, Li L, Volk A, Emmell E, Petley T, Giles-Komar J, Rafferty P, Lakshminarayanan M, Griswold DE, Bugelski PJ, Das AM (2005). Therapeutic dosing with anti-interleukin-13 monoclonal antibody inhibits asthma progression in mice. *J Pharmacol Exp Ther*, **313:** 8-15.

Yang GY, Volk A, Petley T, Emmell E, Giles-Komar J, Shang XZ, Li J, Das AM, Shealy D, Griswold DE, Li L (2004). Anti-IL-13 monoclonal antibody inhibits airway hyperresponsiveness, inflammation and airway remodeling. *Cytokine*, **28:** 224-232.

Yang M, Hogan SP, Henry PJ, Matthaei KI, McKenzie ANJ, Young IG, Rothenberg ME, Foster PS (2001). Interleukin-13 mediates airways hyperreactivity through the IL-4 receptor-alpha chain and STAT-6 independently of IL-5 and eotaxin. *Am J Respir Cell Mol Biol*, **25:** 522-530.

Yang M, Rangasamy D, Matthaei KI, Frew AJ, Zimmmermann N, Mahalingam S, Webb DC, Tremethick DJ, Thompson PJ, Hogan SP, Rothenberg ME, Cowden WB, Foster PS (2006). Inhibition of arginase I activity by RNA interference attenuates IL-13-induced airways hyperresponsiveness. *J Immunol*, **177:** 5595-5603.

Yasunaga S, Yuyama N, Arima K, Tanaka H, Toda S, Maeda M, Matsui K, Goda C, Yang Q, Sugita Y, Nagai H, Izuhara K (2003). The negative-feedback regulation of the IL-13 signal by the IL-13 receptor alpha 2 chain in bronchial epithelial cells. *Cytokine*, **24:** 293-303.

Yin HL, Janmey PA (2003). Phosphoinositide regulation of the actin cytoskeleton. *Annu Rev Physiol*, **65:** 761-789.

Yoshikawa M, Nakajima T, Tsukidate T, Matsumoto K, Iida M, Otori N, Haruna S, Moriyama H, Saito H (2003). TNF-alpha and IL-4 regulate expression of IL-13 receptor alpha 2 on human fibroblasts. *Biochem Biophys Res Commun*, **312:** 1248-1255.

Yoshisue H, Hasegawa K (2004). Effect of MMP/ADAM inhibitors on goblet cell hyperplasia in cultured human bronchial epithelial cells. *Biosci Biotechnol Biochem*, **68:** 2024-2031.

Zavorotinskaya T, Tomkinson A, Murphy JE (2003). Treatment of experimental asthma by long-term gene therapy directed against IL-4 and IL-13. *Mol Ther*, **7:** 155-162.

Zhang JG, Hilton DJ, Willson TA, McFarlane C, Roberts BA, Moritz RL, Simpson RJ, Alexander WS, Metcalf D, Nicola NA (1997). Identification, purification, and characterization of a soluble interleukin (IL)-13-binding protein. Evidence that it is distinct from the cloned Il-13 receptor and Il-4 receptor alpha-chains. *J Biol Chem*, **272:** 9474-9480.

Zheng T, Liu W, Oh SY, Zhu Z, Hu B, Homer RJ, Cohn L, Grusby MJ, Elias JA (2008). IL-13 receptor alpha2 selectively inhibits IL-13-induced responses in the murine lung. *J Immunol*, **180:** 522-529.

Zheng T, Zhu Z, Liu W, Lee CG, Chen QS, Homer RJ, Elias JA (2003). Cytokine regulation of IL-13R alpha 2 and IL-13R alpha 1 in vivo and in vitro. *J Allergy Clin Immunol*, **111:** 720-728.

Zheng T, Zhu Z, Wang Z, Homer RJ, Ma B, Riese RJ, Jr., Chapman HA, Jr., Shapiro SD, Elias JA (2000). Inducible targeting of IL-13 to the adult lung causes matrix metalloproteinase- and cathepsin-dependent emphysema. *J Clin Invest*, **106:** 1081-1093.

Zhu Z, Homer RJ, Wang Z, Chen Q, Geba GP, Wang J, Zhang Y, Elias JA (1999). Pulmonary expression of interleukin-13 causes inflammation, mucus hypersecretion, subepithelial fibrosis, physiologic abnormalities, and eotaxin production. *J Clin Invest*, **103:** 779-788.

Zimmermann N, King NE, Laporte J, Yang M, Mishra A, Pope SM, Muntel EE, Witte DP, Pegg AA, Foster PS, Hamid Q, Rothenberg ME (2003). Dissection of experimental asthma with DNA microarray analysis identifies arginase in asthma pathogenesis. *J Clin Invest*, **111:** 1863-1874.

Zurawski SM, Vega F, Jr., Huyghe B, Zurawski G (1993). Receptors for interleukin-13 and interleukin-4 are complex and share a novel component that functions in signal transduction. *EMBO J*, **12:** 2663-2670.

Chapter Nine

Appendix

9.1 Solution used in organ bath studies

Krebs-Henseleit buffer solution	
Components	Concentration (mM)
NaCl	118
KCl	4.7
$CaCl_2$	2.5
$MgSO_4$	1.2
$NaHCO_3$	25
KH_2PO_4	1.2
glucose	11.1

9.2 Conditions used for 9HTEo-, A549 and BEAS-2B cells

Cell line	Thawing/subculture media	Freezing media	Centrifugation (g)	Cell Seeding value	Trypsin/ EDTA
9HTEo-	Complete media (DMEM + 10% FBS + 100 U/ml penicillin + 100 µg/ml streptomycin + 2 mM glutamine)	10% DMSO, 40% FBS and 50% complete media.	375	$5x10^4$ cells/ml	0.05% Trypsin 0.02% EDTA
A549	Complete media	10% DMSO, 40% FBS and 50% complete media.	375	$3x10^4$ cells/ml	0.05% Trypsin 0.02% EDTA
BEAS-2B	LHC-9 medium	LHC-9 with 1% PVP and 7.5% DMSO	125	1.5 $X10^4$ cells/ml	0.25% Trypsin-0.02 % EDTA) containing 0.5% PVP

9.3 Immunoblot buffers

Lysis buffer	(50 mM Tris-HCl, pH 7.5, 150 mM NaCl, 5 mM EDTA, 1% (v/v) Nonidet P40, 1 mM Na3VO4, 1 mM Na2MoO4, 10 mM NaF, 10 µg/ml leupeptin, 10 µg/ml aprotinin, 10 µg/ml soybean trypsin inhibitor, 1 mM phenylmethylsulfonyl fluoride, and 1 µg/ml pepstatin A) with 10% (v/v) glycerol
Sample buffer	10% sodium dodecyl sulphate, 50% glycerol, 200 mM Tris-HCl pH 6.8, 0.01% bromophenol blue and 5% 2-mercaptoethanol to be added freshly to the sample buffer
Running buffer	192 mM glycine, 25 mM Trizma base, 0.1% (w/v) SDS, MilliQ-filtered water)
Semi-dry transfer buffer	39 mM glycine, 48 mM Trizma base, 0.0375% SDS, 20% (v/v) methanol, MilliQ-filtered water
Tris-buffered saline (TBS)	20 mM Tris-HCl pH 7.5, 150 mM NaCl and deionized water

9.4 Basic recipe for gel electrophoresis

	Resolving gel (20 ml)						Stacking Gels (12 ml)
	5%	7.5%	10%	12%	14%	15%	5%
MilliQ-filtered H2O (ml)	11.51	9.84	8.17	6.84	5.51	4.84	6.85
Resolving gel buffer , pH 8.8 (ml)	5.0	5.0	5.0	5.0	5.0	5.0	Stacking gel buffer, pH 6.8 (3.0 ml)
30% Acrylamide-Bis acrylamide Solution (ml)	3.33	5.0	6.67	8.0	9.33	10	2.0
AMPS (µl)	150	150	150	150	150	150	150
TEMD (µl)	15	15	15	15	15	15	15

*AMPS (10% w/v) and TEMED are added to resolving or stacking gel mixtures just before pouring into the gel cassettes.

9.5 Immunoblotting conditions

Protein targeted by primary antibody	Primary antibody species	Molecular weight (kDa)	Blocking buffer[a]	Primary antibody concentration [b]	Secondary antibody concentration[c]
Akt1	Goat	60	5%	1 : 1000	1 : 10000
phosphoSer^{473}-Akt	Rabbit	60	5%	1 : 700	1 : 7000
PI3K p110δ	Rabbit	110	5%	1 : 700	1 : 7000
Arginase I	mouse	35	5%	1 : 1000	1 : 5000
Arginase I	Rabbit	35	5%	1 : 1000	1 : 5000
β-actin	Rabbit	45	5%	1 : 1000	1 : 5000

[a] Expressed as percentage (w/v) non-fat milk diluted w/v in TBS-Tween 20

[b] Diluted v:v in 0.01% (w/v) sodium azide TBS-Tween 20

[c] Diluted v:v in 0.01% (w/v) sodium azide TBS-Tween 20

9.6 Reverse transcriptase (RT) reaction mixture

Component	Volume (µl)
10X RT buffer	2
dNTP (5 mM)	2
Anchored oligo dT primers (500 ng / ml)	2
RNasin plus	0.25
Reverse transcriptase (RT)	1
RNA template	1-12
PCR grade H_2O	to 20

9.7 Primers used in this study

Primer*		Sequence
IL-13 Rα1	Forward	GTCCCTGGGTGTTCTTCCTGA
	Reverse	CGACGATGACTGGAACAAGT
IL-13 Rα2	Forward	TCCCTATTTGGAGGCATCAG
	Reverse	GAAACCCTGGATAAGGTCGT

*Primers were designed using Primer3 (Whitehead Institute for Biomedical Research) and ProbeFinder Version 2.04 (Roche Applied Science, Mannheim, Germany), after retrieving gene specific sequences and intron-exon information from Pubmed (Entrez Gene) and Ensembl v37 (Homo sapiens genome). Primers were analysed by NetPrimer software (PREMIER Biosoft International) to detect any primer-dimer, haipins or other secondary structures. Each primer was then blasted on Pubmed/Ensembl to ensure its specificity to the gene required. All primers were intron spanning to avoid amplification of any genomic DNA and their product sizes are approximately 200 bp, which is optimal size for PCR.

9.8 Paper published from this study